EVALUATION OF FLOW MODELS AND POLLUTANT RETENTION ISOTHERMS FOR THEIR APPLICATION TO RAIN GARDEN BIORETENTION

Ruth Quinn

A thesis submitted in partial fulfilment of the requirements of the University of Greenwich for the Degree of Doctor of Philosophy

DECLARATION

"I certify that this work has not been accepted in substance for any degree, and is not concurrently being submitted for any degree other than that of Doctor of Philosophy being studied at the University of Greenwich. I also declare that this work is the result of my own investigations except where otherwise identified by references and that I have not plagiarised the work of others".

_____

Ruth Quinn

Candidate

Supported by

_____

Peter Kyberd

Head of Engineering Science

ACKNOWLEDGEMENTS

Firstly, I would like to express my gratitude to my supervisor Dr. Alejandro Dussaillant for his contributions to my research. I also wish to thank my second supervisor Prof Amir Alani for his advice and support during my Ph.D. study.

Besides my advisors, I would like to thank my thesis committee: Prof Sue Charlesworth and Prof Colin Hills for their suggestions, encouragement and support.

My sincere thanks also goes to the staff at the school of engineering especially the laboratory staff and technicians: Ian Cakebread, Tony Stevens, Bruce Hassan, Colin Gordon and Matthew Bunting whose help and assistance was invaluable. Without their support it would not have been possible to conduct this research.

I would also like to thank the head of Engineering and Deputy Pro-Vice Chancellor Prof Simeon Keates for his advice and understanding.

Last but not least, I would like to thank my parents, Peter and Elizabeth, my brother, Cillian, my boyfriend Jeff and all of my friends for supporting me throughout writing this thesis and my life in general.

ABSTRACT

The primary aims of this research was firstly to develop a computer modelling tool which could predict pollution retention in a rain garden and secondly to use the model and additional experiments to examine various aspects of rain garden design with respect to pollutant retention.

Initially, the behaviour of all contaminants in urban runoff was examined including their retention and possible modelling methods. Heavy metals were then identified as the main focus of this project as this choice was the most beneficial addition to current research. The main factors affecting their retention were found to be macropore flow, pore water velocity, soil moisture content and soil characteristics and the primary method of modelling capture was identified as a sorption isotherm. Thus a dual-permeability heavy metal sorption model was developed; this was based on an intensive literature review of current best practice in both hydrological modelling and pollutant retention fields with respect to rain garden devices.

The kinematic wave equation was chosen to model water movement in both the matrix and macropore regions as this provided a simpler alternative to more complex equations while still maintaining good accuracy. With regards to the modelling of heavy metal retention three isotherms were chosen: the linear, Langmuir and Freundlich equations as these were found from previous research to be the most accurate. These isotherms were incorporated into a one dimensional advection-dispersion-adsorption equation in order to model both transport and retention together.

This model was tested against the appropriate literature and accurate comparisons were obtained thus validating it.

Column experiments were designed to both provide a unique contribution to rain garden research and further validate the model. This was achieved by analysing past experiments and identifying an area where research is lacking; this area was the effect of macropore flow on heavy metal retention in rain garden systems under typical English climatic conditions. The findings of these experiments indicated that although macropore flow did not impact the hydraulic performance of the columns, retention of the most mobile of heavy metals, copper, was decreased slightly in one case. The overall retention of the columns was still high however at a value in excess of 99% for copper, lead and zinc. The results of the experiments were also used to further validate the model.

The model was then applied to the development of a rain garden device for a planned roundabout in Kent, U.K. Preliminary design considered an upper root zone layer with organic soil and a sandy storage sublayer each 30 cm thick, for a rain garden area of 5 and 10% the size of the contributing impervious surface. Two scenarios were examined; the accumulation and movement of metals without macropores and the possibility of groundwater contamination due to preferential flow. It was shown that levels of lead can build up in the upper layers of the system, but only constituted a health hazard after 10 years. Simulations showed that copper was successfully retained (no significant concentrations below 50 cm of rain garden soil depth). Finally given concerns of preferential flow bypassing sustainable drainage systems, macropore flow was examined; results indicated that due to site conditions it was not a threat to groundwater at this location for the time frame considered.

These actions successfully completed the objectives of this project and it was deemed successful.

CONTENTS

LIST OF FIGURES

LIST OF TABLES

LIST OF SYMBOLS

A	Area Ratio (%)
a_F	Freundlich Exponent (Dimensionless)
a_{LF}	Langmuir-Freundlich Exponent (Dimensionless)
a_m	Macropore Exponent (Dimensionless)
A_{rg}	Area of Rain Garden (cm^2)
b_m	Conductance of Macropores (cm/s)
c	Kinematic Wave Celerity (cm/s)
C	Dissolved Pollutant Concentration (mg/L)
CA	Cross Sectional Area (m^2)
c_D	Drainage Celerity (cm/s)
C_e	Effluent Metal Level (mg/L)
c_m	Macropore Celerity (cm/s)
C_{ma}	Pollutant Concentration in Macropore (mg/L)
C_{mi}	Pollutant Concentration in Matrix (mg/L)
C_o	Influent Metal Level (mg/L)
C_s	Media-sorbed Pollutant (mg/kg)
c_w	Wetting Front Celerity (cm/s)
D	Dispersion Coefficient (cm^2/s)
d	Dispersity (cm)
D_e	Effective Diffusion Coefficient (cm^2/s)
D_m	Mechanical Dispersion (cm^2/s)
D_o	Binary Diffusion Coefficient (cm^2/s)
d_p	Effective ‘Diffusion’ Pathlength (cm)
d_r	Drainage Rate (cm/s)
E_{actual}	Actual Evaporation (cm/s)

e_e	Molecular Diffusion (cm^2/s)
E_p	Potential Evaporation (cm)
E_s	Potential Soil Evaporation (cm/s)
F	Infiltration (cm)
G	Soil Heat Density (W/m^2)
G_f	Geometry Factor (Dimensionless)
h	Pressure Head (cm)
h_b	Head at Bottom Boundary (cm)
h_d	Depression Depth of Rain Garden (cm)
h_f	Pressure Head in the Macropore (cm)
h_m	Pressure Head in the Matrix (cm)
h_s	Ponded Depth (cm)
h_t	Pressure Head at Time t (cm)
h_{wf}	Average Capillary Suction Head of the Wetting Front (cm)
i	Water Supply Intensity (cm/s)
i_{mat}	Infiltration into Soil Matrix (cm/s)
K	Unsaturated Hydraulic Conductivity (cm/s)
K_d	Distribution Coefficient (L/kg)
K_F	Freundlich Constant (L/kg)
K_L	Langmuir Isotherm Coefficient (L/kg)
K_{LF}	Langmuir-Freundlich Isotherm Constant (L/kg)
k_r	Relative Hydraulic Conductivity (Dimensionless)
K_s	Saturated Hydraulic Conductivity (cm/s)
L	Specified Depth in Soil (cm)
LAI	Leaf Area Index (Dimensionless)
M	Moisture Capacity Function
M_{Acc}	Total Metal Accumulation (mg)

MDA	Macropore Drainage Area (cm^2)
m_{vg}	van Genuchten Parameter (Dimensionless)
n_{LF}	Langmuir-Freundlich Exponent (Dimensionless)
n_{mac}	Macropore Density ($1/cm^2$)
n_{vg}	van Genuchten Parameter (Dimensionless)
P	Pollutant Transfer (mg/L)
$Q_{evaporation}$	Evaporation from Rain Garden (m^3/s)
Q	Flow (m^3/s)
q	Water Flow Rate (cm/s)
q_f	Maximum Infiltration Rate of Water into Soil (cm/s)
q_{in}	Maximum Infiltration Rate into Macropores (cm/s)
$Q_{infiltration}$	Infiltration into Rain Garden (m^3/s)
q_{int}	Water Transfer from Macropores to Matrix (cm/s)
Q_{rain}	Input from Rain Directly on Rain Garden Surface Area (m^3/s)
Q_{runon}	Flow Input from the Surrounding Catchment (m^3/s)
r	Rainfall Rate (cm/s)
R	Retardation Coefficient (kg/m^3)
R^2	Coefficient of Determination (Dimensionless)
R_n	Net Radiation (W/m^2)
S	Plant Transpiration Rate (cm/s)
S_e^f	Effective Fluid of Macropores (m^3/m^3)
S_e^m	Effective Fluid of Matrix (m^3/m^3)
S_{max}	Total Concentration of Sorption Sites Available (mg/kg)
t	Time (s)
T_{ACTUAL}	Actual Plant Transpiration (cm/s)
t_D	Time of Arrival of Drainage Front (s)
t_s	Timestep

T_p	Potential Plant Transpiration (cm/s)
t_w	Time of Arrival of Wetting Front (s)
U	Sink Term for Pollutants (mg/L)
U_w	Sink Term for Water (1/s)
V	Water Volume (L)
v	Average Pore Velocity (cm/s)
v_e	Exponent (cm/s)
V_s	Volume which Moves Past a Specified Point (cm^3)
w	Mobile Moisture Content in the Macropore (m^3/m^3)
x	Horizontal Distance (cm)
y	Radial Distance of Wetting Front (cm)
Z	Specified Depth Point (cm)
z	Vertical depth of Soil (cm)
α	Ratio of Actual to Equilibrium Evaporation (Dimensionless)
α_{vg}	van Genuchten Parameter (1/cm)
α_w	First Order Mass Transfer Coefficient for Water (1/s)
β	Attenuation Coefficient (Dimensionless)
Γ_w	Water Transfer Term (cm/s)
γ	Psychrometric Constant (1/^{o}C)
Δ	Slope of the Saturation Vapour Pressure Curve (Dimensionless)
$\boldsymbol{\Theta}$	Relative Water Content (Dimensionless)
θ	Soil Moisture Content (m^3/m^3)
θ_{ini}	Initial Soil Moisture Content (m^3/m^3)
θ_m	Soil Moisture Content of Matrix (m^3/m^3)
θ_{mat}	Matrix Soil Moisture Content (m^3/m^3)
θ_{res}	Residual Soil Water Content (m^3/m^3)

θ_{sat}	Saturated Soil Water Content (m^3/m^3)
θ_s	Change Soil Water Content Over a Given Time Step (m^3/m^3)
λ	Latent Heat of Vaporization (^oC)
ρ	Bulk Mass Density (kg/m^3)
τ	Transmissivity Coefficient (Dimensionless)
τ_o	Tortuosity (Dimensionless)
ω	First Order Rate Coefficient (cm/s)

ACROYNMS

ADE	Advection Dispersion Equation
ANOVA	Analysis of Variance
CPU	Central Processing Unit
CTRW	Continuous-time Random Walk
erfc	Error Function
FADE	Fractional Advective-Dispersion Equation
KWE	Kinematic Wave Equation
PDE	Partial Differential Equation
RSME	Root Square Mean Error
RZWQM	Root Zone Water Quality Model
SuDS	Sustainable Drainage Systems
TDR	Time Domain Reflectometry
UK	United Kingdom
USA	United States of America
WMP	Water Matric Potential

1 INTRODUCTION

1.1 Background to Research

Urbanisation is an ever growing invasive and rapid form of land use change. In the United Kingdom alone more than 90% of the population inhabit cities and it has been predicted that 60% of the global populace will live in urban areas by the year 2030 (The Guardian, 2009).

Urbanisation has been linked to hydrological problems such as diminished groundwater recharge and impaired quality of water sources (Leopold, 1968; Klein, 1979; Pan, et al., 2011). The decrease in groundwater recharge is caused by the rise in impervious surfaces which prevent rainfall from percolating into the ground and replenishing aquifers. This is of major concern especially in the South-East of England where aquifers are the primary source of public water supply and drought has become increasingly common (British Geological Survey, 2012).

In addition, the effects of increased urbanisation on the quality of water are visible in many lakes and waterways throughout the United Kingdom with 11% of the total pollution in Scottish rivers attributed to urban runoff. In the United States, urban runoff is second only to agriculture as a source of river pollution (Ellis & Mitchell, 2006). This pollution occurs as contaminants present in urban storm water, such as nutrients, hydrocarbons and heavy metals, are transferred through storm drains and pipes into local waterways. Needless to say these contaminants are extremely harmful to the environment with nutrients causing noticeable problems such as eutrophication. Heavy metals also impact on the health of humans; copper (Cu) and cadmium (Cd) can cause liver and kidney damage (Brown, et al., 2000).

In order to prevent these detrimental effects, methods which enhance infiltration, evaporation and recharge have been proposed. These methods involve the use of Sustainable Drainage Systems (SuDS) which provide several benefits including increased groundwater recharge and improved water quality through mechanisms such as filtering, adsorption and biological processes (Klein, 1979). The motivation behind SuDS is to replicate natural systems that use cost effective solutions with low environmental impact to drain away urban runoff through collection, storage, and cleaning before allowing it to be released slowly back into the environment.

Regarding the long-term water balance, in mild climates such as that of the South-East of England the majority of rainfall is associated with relatively common events. For example, at

Heathrow, Greater London more than 90% of yearly rainfall falls in events of intensity less than 10 mm/h (**Figure 1.1**). This diagram was created from data gathered from the MIDAS weather database (http://badc.nerc.ac.uk/data/ukmo-midas/).

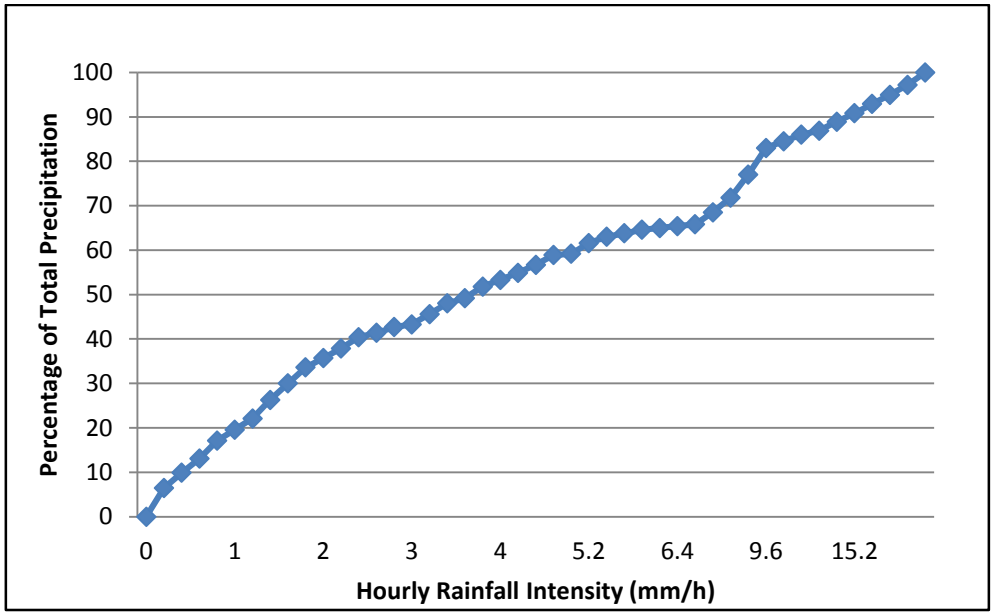

Figure 1.1 Hourly Rainfall Intensity as a Percentage of Total Precipitation at Heathrow Airport

Infiltration practices are better equipped to handle smaller events and thus should perform well in these conditions. One of the best infiltration methods has proven to be rain gardens (Dietz & Clausen, 2005).

A rain garden is a vegetated depression that has been specifically designed to collect and infiltrate the storm water running off impervious areas such as car parks, roofs and pavements (**Figure 1.2**). They are usually shallow depressions (less than 20 cm in depth) and much smaller than the impervious surface from which they receive storm water (Dussaillant, 2002). Rain gardens consist of vegetation, a high permeability upper layer and lower storage zone, an underdrain may also be present to prevent overflow in cases of heavy precipitation.

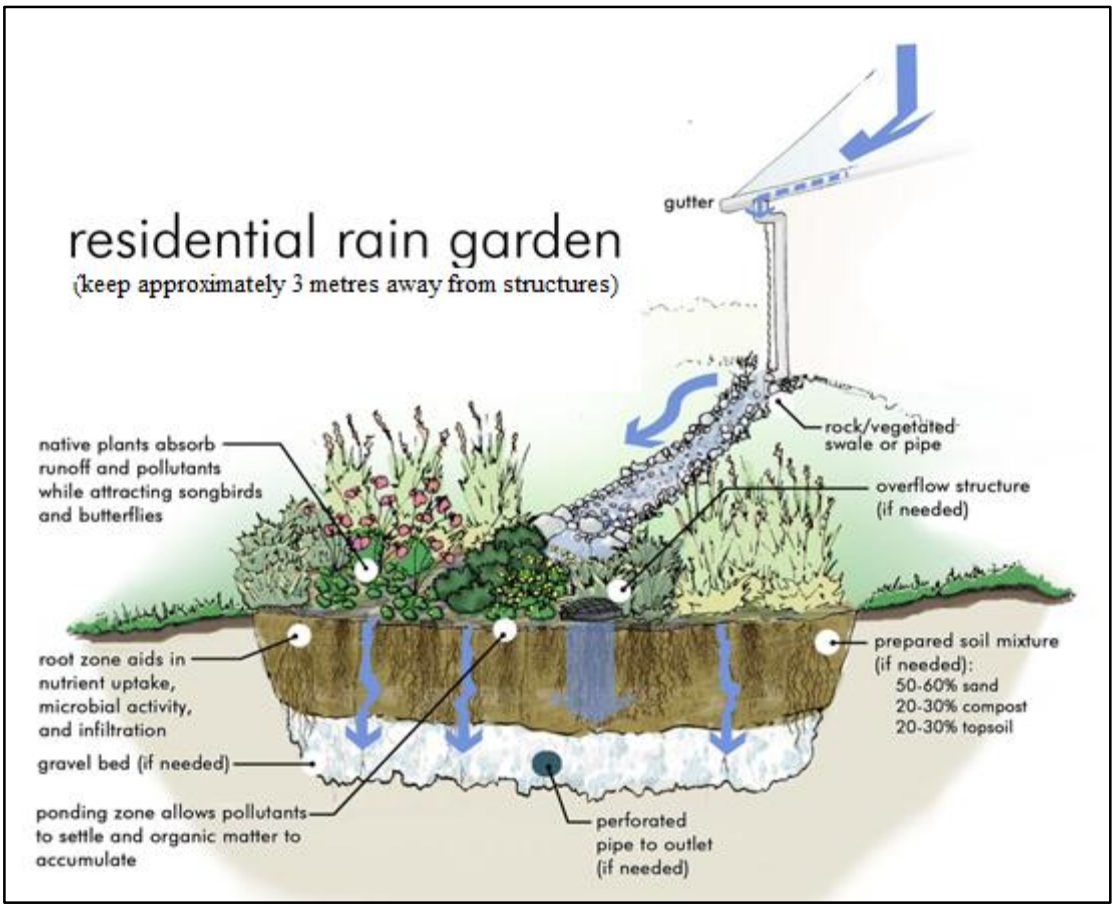

Figure 1.2 Diagram of a Rain Garden. Adapted from TP (2014)

They have been proven to increase groundwater recharge and also retain the contaminants present in urban runoff thus, decreasing potential groundwater and waterway pollution (Dussaillant, et al., 2005).

1.2 Justification

Research into rain gardens is of increasing importance as their use becomes more common. Currently, they are not as prevalent in the UK as in other countries such as the USA where guidelines have been in place since the 1990s to promote their use (Prince George's County, Maryland. Department of Environmental Resources, 1999). However their popularity in the U.K is certain to increase with the introduction of legislation such as 'The Flood and Water Management Act' (2010) which promotes the use of SuDS to protect people and property from flood risk. Recent developments in this area have proven the governments comittment to this ideal by confirming that non-residential or mixed development must ensure that sustainable drainage systems for the management of run-off are put in place, unless demonstrated to be inappropriate. Under these arrangements, in 'considering planning applications, local

planning authorities should consult the relevant lead local flood authority on the management of surface water; satisfy themselves that the proposed minimum standards of operation are appropriate' (Pickles, 2014).

Previous research in this area has focused primarily on the degree to which groundwater is replenished by these systems and computer models have been developed to quantify the extent of that recharge i.e. RECARGA and RECHARGE (Dussaillant 2002; Dussaillant, et al., 2004; Dussaillant, et al., 2005). However, these models do not simulate the generation or treatment of water quality parameters such as pollutant loading and removal. The ability of rain garden to retain pollutants has been well documented through various experiments (Davis, et al., 2001; Farm, 2002; Hsieh & Davis, 2005; Li & Davis, 2008; Blecken, et al., 2009; Jones & Davis, 2013). For example, the rain garden boxes examined by Davis et al. (2003) exibited 99% retention for Cu, Pb and Zn at a flowrate of 4.1cm/h. Despite the detailed research in this area a computer model with the ability to simultaneously predict water budget and retention in a layered soil system such as a rain garden has not previously been developed.

Thus, a design tool which can quantify contaminant retention in rain garden facilities is needed. This can be utilised by both industry and research to examine the long term water balance and pollutant retention capacity of rain gardens and other SuDS.

1.3 Research Aims

The primary aims of this research were as follows:

1. To develop a computer modelling tool which could predict pollution retention in a rain garden
2. To use the model and additional experiments to examine various aspects of rain garden design with respect to pollutant retention. This model should be of non-complex design in order to increase usability and allow for quick simulation times.

In order to achieve these aims, the following research objectives were set.

For Aim 1:

1. Investigate the key factors affecting pollutant retention, specifically heavy metals, including both soil physiological properties and hydraulic parameters and examine which equations best model the effects of these influences on heavy metal retention.
2. Develop and verify a simple dual-permeability model specifically designed to simulate both water flow and contaminant retention in a rain garden using the findings from

Objective 1. Dual-permeability refers to the multiple flow processes that can occur in soil and will be discussed in greater detail in **Section 3.4.1**.

For Aim 2:

3. Design and perform column experiments that both provide a unique contribution to rain garden research and also serve as further validation of the model's algorithms.

4. Perform simulations to examine the effect of rain garden design parameters, including surface area and soil choice, on pollution retention.

5. Investigate the effects of different hydrological processes such as macropore flow on pollutant retention in a rain garden. Macropores are preferential pathways through the soil which have been found to exacerbate the movement of contaminants (Beven & Germann, 2013).

In order to achieve these objectives a detailed methodology was produced (**Chapter 2**).

1.4 Report Outline

The main body of this report has been divided into 9 chapters, the content of which are outlined briefly below:

- **Chapter 1** introduces the study, outlines the research problem and defines the main objectives of this thesis.
- **Chapter 2** details the five step methodology approach used to achieve the objectives and overall aim of this project.
- **Chapter 3** examines the literature and research issues relevant to the development of the model. Previous methods of modelling hydraulic functions and retention are reviewed. This provides the groundwork for development of a specifically tailored model to predict pollutant capture in rain gardens.
- **Chapter 4** provides a comprehensive account of all the components of the model and its development. Preliminary validation of the model based on previous literature results is also shown.
- **Chapter 5** gives a detailed account of the column experimental design, results and statistical analysis.

- **Chapter 6** compares the column experimental results with the predictions of the model providing further validation.
- **Chapter 7** applies the model to the design of a rain garden in Thanet, Kent. This chapter provides recommendations for soil type and also examines the effects of macropore flow on heavy metal retention.
- **Chapter 8** gives a detailed discussion of the project which addresses all aspects pertinent to the proposed model
- **Chapter 9** concludes the main body of the thesis. The main accomplishments of this project are reiterated and the success of this thesis measured against the objectives set. This chapter also makes recommendations for further work.

In addition the report includes four appendices.

- **Appendix A** details popular dual permeability models.
- **Appendix B** outlines the methods used to solve the main equations found in the numerical model.
- **Appendix C** is a collection of information directly related to the column experimental design including equipment diagrams, wiring plans and programming code for the instrumentation.
- **Appendix D** contains detailed column experiment results for soil moisture content, water head, outflow, soil parameters and heavy metal concentrations.
- **Appendix E** contains a list of publications and conferences presented at.

1.5 Conclusion

This chapter has provided a foundation for this thesis, detailing the field of research and emphasizing the research gaps. The research aim has been justified, an outline of the main objectives given and the structure of the report outlined hence allowing the research to continue with a detailed methodology.

2 METHODOLOGY

2.1 Introduction

Based on the objectives outlined in Chapter 1, a five stage methodology was developed in order to achieve the main aim of the project which was to develop and utilise a computer modelling tool which can predict pollution retention in a rain garden. This five stage methodology is illustrated in **Figure 2.1**.

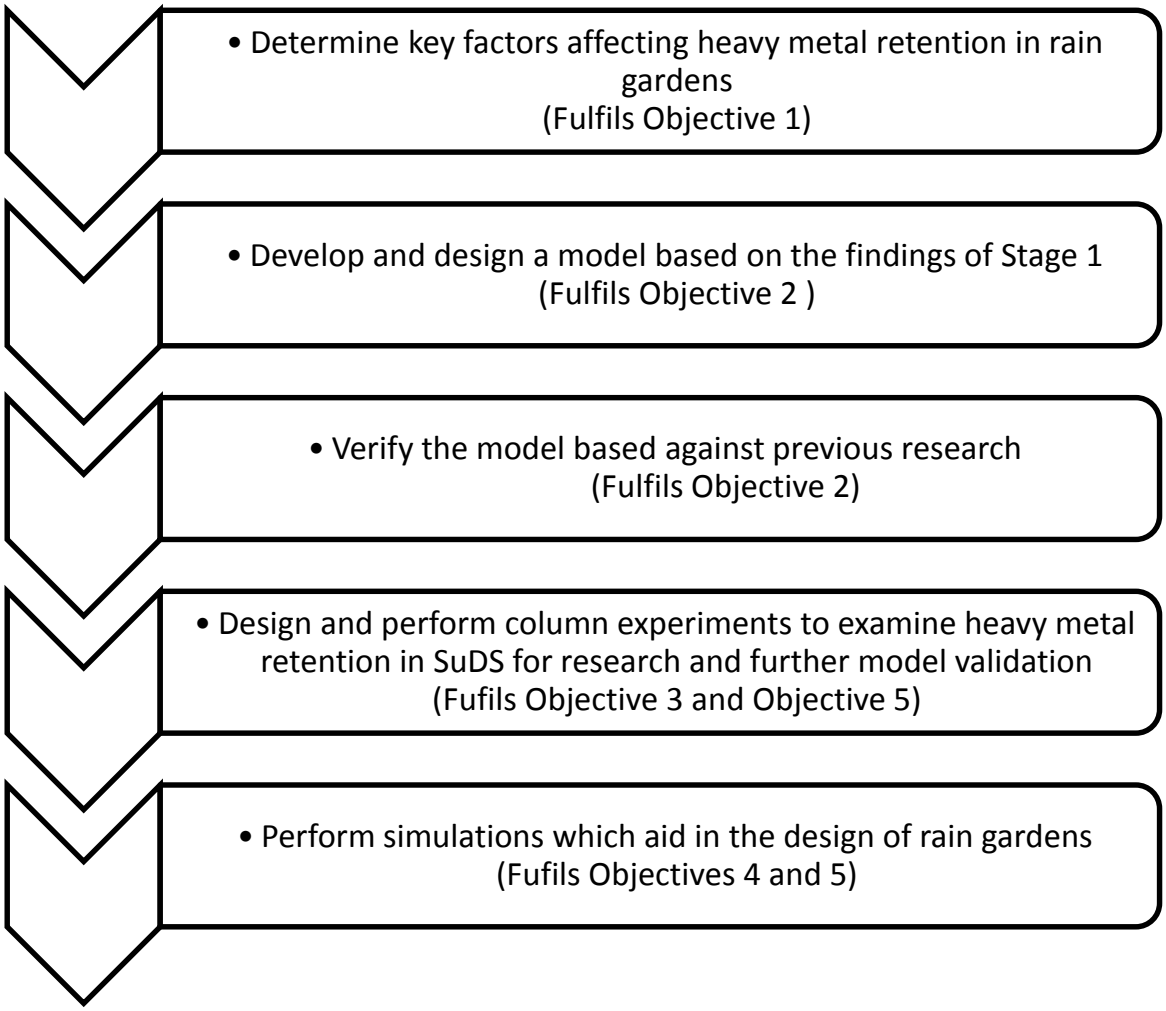

Figure 2.1 Five Stage Methodology

2.2 Stage 1 - Identification of Key Factors

In order to complete Objective 1, an extensive literature review was undertaken, which is detailed in **Chapter 3**. The purpose of this review was to identify the key factors which effect heavy metal retention in a rain garden and from the findings determine the most appropriate equations and methods for the proposed model. This review encompassed a wide range of

topics starting with previous SuDS groundwater modelling tools. Following this, a brief summary of the principle contaminants in storm water runoff (nutrients, hydrocarbons and heavy metals), factors which influence their retention and possible retention modelling equations are given. It was decided in **Section 3.2** to focus solely on one contaminant type (heavy metals). The review is then split into sections which examine modelling flow in variably saturated soil (**Section 3.4**) and predicting heavy metal retention (**Section 3.5**).

Several types of literature were consulted in order to gain understanding of the above topics including journal articles, software manuals and reports. A thorough search of all the available databases along with consultations with professionals and academics was undertaken in order to ensure as much of the appropriate information was accessed as was possible.

This stage provided a solid base for the thesis by determining the most appropriate methods of predicting water transport and pollutant retention, thus successfully fulfilling Objective 1.

2.3 Stage 2 - Development and Design of the Model

A model was developed utilising the knowledge gathered during the literature review (**Chapter 3**). The purpose of the model was to provide a screening tool for both design and research with long term hydrological data. Thus, the aim of this research was to create a non-complex tool which required few parameters and relatively fast simulation run time. Thus all possible equations were evaluated with regards to these needs. The rationale behind all decisions made and a detailed discussion of model development is contained in **Chapter 4**. The model was evaluated against a set of standards for pollutant retention models specified by previous literature. It was deemed to meet these standards, thus partially completing Objective 2.

2.4 Stage 3 - Verification of the Model

The model was verified in three parts; the matrix, macropore and pollutant retention sections (**Section 4.4**). This validation was completed against selected experimental and model results, which reflect situations common to rain gardens. For the matrix section this was layered soil profiles and sharp wetting fronts. For the macropore section, varying infiltration rates were examined. Finally experiments examining heavy metal retention in many types of soil (including specifically in rain garden substrate) were used to validate the pollutant retention component. This validation was important to ensure that the model was functioning correctly before any detailed theoretical simulations were performed. This completed Objective 2.

2.5 Stage 4 - Design and Complete Column Experiments

Column experiments were designed to both give an adequate validation of the model and also a unique contribution to this field of research. This was achieved by analysing past experiments and identifying an area where research is lacking; this was found to be the effect of macropore flow on the retention of heavy metals in a rain garden under typical English climatic conditions. This was examined as macropore flow has been observed to increase the flow of contaminants through soils (Beven & Germann, 2013). The experimental design comprised of five columns (3 columns with normally packed soil (matrix columns) and 2 columns which contained preferential pathways (macropore columns)). This provided results as to the impact of macropore flow on heavy metal retention and hydrological properties, and further served to confirm the results of the proposed model through validation. A detailed examination of the design of the column experiments, their results and further validation of the model is found in **Chapters 5** and **6**. This successfully met Objective 3 and partially fulfilled Objective 5.

2.6 Stage 5 - Perform Simulations

Simulations using the verified computer model were performed to examine the following scenarios

- Effect of rain garden design parameters including surface area and soil choice on pollutant retention (**Section 7.5.1**).
- Investigate the pollutant retention capabilities at different points in the rain gardens life cycle where increased macropore flow and metal accumulation will have an effect on retention (**Section 7.5.1** and **7.5.2**).
- Sensitivity of heavy metal retention to various parameters such as saturated hydraulic conductivity (K_{sat}) and area ratio (**Section 7.5.3**). The area ratio is defined as the ratio of drainage area to rain garden area.

This was achieved using the model to design a proposed rain garden in Thanet, Kent in collaboration with Kent County Council. Further details of this simulation are contained in **Chapter 7**. This successfully completed Objectives 4 and 5.

3 LITERATURE REVIEW

3.1 Introduction

Rain gardens have been used in their current form in the USA for at least the past two decades to improve storm water quality and enhance groundwater recharge (Bitter & Bowens, 1994). In 1993, Biohabitats and Engineering Technologies Associates (ETA) investigated SuDS practices and in association with Prince George's County, Maryland's Department of Environmental Protection developed a set of guidelines for their construction (Bitter & Bowens, 1994). These recommendations formed the first basis for designing these systems and included grading requirements, soil amendments, plant material selection, maintenance requirements and an evaluation procedure to determine pollutant removal effectiveness.

Following this publication, more guidelines were produced by various companies and local authorities (e.g. Design of Stormwater Filtering Systems (Claytor & Schueler, 1996)). These guidelines were not incredibly accurate however and were simply based on findings from selected existing systems. Often the pollution retention capabilities were categorised not as percentages but as low, high, very high etc., in addition no account was taken of rate of infiltration, amount of precipitation or macropore flow, all factors which effect pollution retention (Bitter & Bowens, 1994).

Over the following years, two main areas of research regarding rain gardens and other SuDS became prevalent. These are groundwater recharge and pollution retention.

3.2 Groundwater Recharge

Dussaillant (2002) developed a numerical model called RECHARGE to design and evaluate groundwater recharge capacities of rain gardens. RECHARGE is based on the Richards equation and includes the important pertinent processes of interception and depression storage, run-on from impervious surfaces, ponding, infiltration through a layered system and evapotranspiration (Dussaillant, et al., 2004). The function of this model was to simulate the water balance of a rain garden; it can also be used as a design tool to plan crucial dimensions including surface area, depression depth and thickness of the storage zone layer. A simpler model (RECARGA) was later created based on the Green-Ampt equation and compared with RECHARGE with favourable results (Dussaillant, et al., 2005).

A more complex model was proposed by Aravena and Dussaillant (2009) based on the Richards equation coupled to a surface water balance using a two-dimensional finite-volume code. This model was found to show good performance when compared to other standard models for numerous test cases (less than 0.1% absolute mass balance error).

These models have limitations however as they do not predict macropore flow or pollutant retention.

3.3 Urban Runoff Contaminants

The pollution retention capability of a rain garden has been well documented (Davis, et al., 2001; Farm, 2002; Hsieh & Davis, 2005; Li & Davis, 2008; Blecken, et al., 2009; Jones & Davis, 2013). The contaminants present are usually split into three distinct groups, nutrients, heavy metals and petroleum and aromatic contaminants. A summary of the contaminants, factors which influence their retention, possible retention modelling equations and references is given in **Table 3.1**.

The negative percentage values refer to the rain garden increasing the concentration of pollutant concentration.

Table 3.1 Summary of Urban Runoff Pollutants and their removal

Pollutant	Retention in rain gardens	Factors which effect retention	Transport mechanism	Removal Phenomenon	Possible Modelling methods	Additional Reccommendations	References
Nutrients							
Nitrogen	-201% - 71%	Flowrate Presence of Nitrogen in soil Temperature Water Content pH Vegetation Macropore Flow	Advection - Dispersion	Vegetation uptake Denitrification Sorption Nitrification	Langmuir/Freundlich Isotherm	Use soil with low nitrogen content to prevent leaching	(Hunho et al., 2003; Rahil & Antopoulos, 2007; Bratieres, et al., 2008; Doltra & Munoz, 2010)
Ammonia	0% - 86%						
Nitrate	-630%- 96%				Denitrification function Langmuir/Freundlich Isotherm	Plant with vegetation with high nitrate uptake	
Phosphorus	4%-95%	Presence of Phosphorus in soil		Mineralization Vegetation uptake Sorption	Organic Pool method Langmuir/Freundlich Isotherm Method proposed by Sharpley et al (1984)	Use soil with small grain diameter Use vegetation with high phosphorus uptake (Carex)	(Sharpley, et al., 1984; Mc Gechen & Lewis., 2002; Bratieres, et al., 2008)
Heavy Metals							
Lead	67-99%	Flowrate Soil Type Vegetation Macropore Flow	Advection-Dispersion	Sorption Vegetation uptake	Linear/Langmuir isotherm	Soils with high organic matter content and small grain size preferable Accumulation of heavy metals in soils can cause public health concerns	(Boller, 1997;Davis et al. 2001; Davis et al. 2003; Farm, 2002;Hsieh & Davis, 2005;Jang et al. 2005;; Li & Davis, 2008; Hatt et al. 2008)
Copper	66%-95%						
Zinc	67%-99%						
Cadmium	61%-99%						
Chromium	60%-98%						

Pollutant	**Retention in rain gardens**	**Factors which effect retention**	**Transport mechanism**	**Removal Phenomenon**	**Possible Modelling methods**	**Additional Reccommendations**	**References**
Hydrocarbons							
Napthalene	90% - 97%	Flowrate Total suspended sediment concentration Vegetation Macropore Flow	Advection-dispersion	Sorption Biodegredation Vegetation uptake	Linear/ Langmuir equation	A thin mulch layer should be used as the upper layer of a rain garden. Deeply rooted vegetation should be used	(Chang and Corapcioglu, 1998; Gao et al. 2000; Roncevic et al. 2005; Hong et al. 2006; LeFevre et al. 2012)
Toluene	83%			Sorption Vegetation Uptake			
Motor oil	80%						

As can be seen from **Table 3.1** conflicting advice is given regarding the retention of different pollutants. For example, the thin layer of mulch suggested for the retention of hydrocarbons and heavy metals would almost certainly result in the leaching of nutrients through the system unless suitable vegetation was in place. Therefore, before designing a rain garden all urban storm water contaminants should be examined.

To review, the goal of this thesis was to develop a non-complex model which can be used to design and evaluate the pollutant retention capabilities of a rain garden. As the period of this thesis was finite, it was decided to focus solely on one element of the runoff pollution namely heavy metals. This decision was based on the following factors:

1. Heavy metals have the least amount of differing removal phenomenon thus providing an ideal starting point for developing a simple pollution retention model (Li & Davis, 2008).

2. Nutrients and hydrocarbons are heavily dependent on vegetation uptake, thus simply choosing the appropriate plants at the time of design can result in a significant decrease in their concentration (Bratieres, et al., 2008). Heavy metals do not accumulate in vegetation and are thus more dependent on the rain garden system design parameters such as soil type and depth. It would therefore be more beneficial to create a model which predicts their retention based on design factors (Li & Davis, 2008).

3. Unlike nutrients or hydrocarbons which biodegrade, the accumulation of heavy metals in the upper layers of the system poses a significant health hazard (Li & Davis, 2008). It is thus, of utmost importance to predict the quantity of build-up, so that remedial work can be completed if necessary.

4. The isotherms which have been initially suggested to describe heavy metal sorption also match those recommended for the sorption of nutrients and hydrocarbons meaning they could be easily adapted to predict their retention (**Table 3.1**).

5. All the above contaminants depend on hydraulic factors such as macropore flow. The proposed model will accurately predict these factors independent of heavy metal retention. This allows for the addition of subroutines which predict other phenomena e.g. nutrient uptake by plants and hydrocarbon biodegredation, at a later date (**Table 3.1**).

The next section will examine numerical methods of calculating water flow through a rain garden. This is important as factors such as soil moisture content and macropore flow effect heavy metal retention.

3.4 Water Modelling

Rain garden soil is predominately unsaturated owing to rapid infiltration rates, plant and soil characteristics. In soil mechanics, unsaturated soil is commonly referred to as the vadose zone and contains air in addition to water in the pore space. The most basic measure of water in unsaturated soil is water content (θ (m^3/m^3)) which is defined as the volume of water per bulk volume of the soil. Water is retained in unsaturated soil by forces whose effect is quantified in terms of pressure. Numerous types of pressure exist in unsaturated hydrology, but matric pressure (h (cm)) is of unique importance as it substantially influences the chief transport process. Matric pressure is defined as the pressure in a soil pores relative to the pressure of air. Another important soil characteristic is hydraulic conductivity (K (cm/s)) which is a measure of how easily water moves through the medium for a given driving force. For saturated flow it is generally assumed that the flow rate of water is equal to the hydraulic conductivity times the driving force (typically gravity and pressure differences). This relation is known as Darcy's law. Flow through unsaturated porous media is a highly dynamic phenomenon however and cannot be quantified by such a simple relationship. In addition several flow processes can exist in the vadose zone resulting in non-equilibrium water transport. These flow types can be broadly separated into preferential and matrix flow.

The three basic modes of preferential flow are (1) macropore flow, through larger continuous pores; (2) funnelled flow, caused by flow impeding features such as impermeable rock that concentrate flow in adjacent soil; and (3) unstable flow, which converges flow in wet, conductive fingers. Macropore flow is by far the most common preferential pathway in highly conductive homogenous soils such as those in rain garden. Common macropores in SuDS include wormholes, root holes and fractures. When macropores are filled with water, flow through them can be significantly higher than through the surrounding soil thus macropore flow is typified by a small storage and large flow capacity. In contrast, matrix flow is characterised by a large storage and small flow capacity. It is a relative slow and even movement of water and solutes through the soil while sampling all pore spaces.

3.4.1 Dual Permeability Water Modelling

Most common flow modelling software is referred to as a dual permeability model and include both types of flow. There are four key considerations of all dual permeability models: methods of modelling macropore and matrix flow, initiation of macropore flow and determination of water transfer between the flow types. Each of these considerations requires a separate

Table 3.2 Important Equations for Dual-Permeability Modelling

Method	Theory	Advantages	Disadvantages	Application to Rain Garden Water Modelling	References
Matrix Flow					
Richards	Conservation of mass for soil water flow combined with Darcy's law.	Highly accurate Can be combined with van Genuchten equations to reduce parameters needed.	Very complex equation requires finite difference or finite element models to solve.	Has been previously applied to rain garden devices in both 1D and 2D. Very complex so requires long computational time which is contrast to the requirements for a simple numerical model.	(Dussaillant, 2002; Larsbo et al., 2005; Simunek et al., 2009)
Green-Ampt	Darcys law coupled with an assumption that water infiltrates into dry soil as a sharp wetting front.	Simpler alternative to Richards equation Previously applied to rain garden facilities.	Requires additional redistribution equation.	Has been previously applied to rain garden devices. Does not give important soil characteristic such as soil moisture	(Ahuja et al., 2000; Dussaillant, 2002)
KWE	Assumes that soil moisture/ matric potential waves move through the soil kinematically.	Simple and accurate.	Not as accurate as more complex equations such as Richards equation.	Can also be used to model macropore flow thus potentially simplifying model as opposed to the Richards equation. Has been applied to situations common to rain gardens i.e. layered soil profile, complex boundary conditions.	(Smith, 1983; Singh, 1997)

Method	Theory	Advantages	Disadvantages	Application to Rain Garden Water Modelling	References
Macropore Flow					
Poiseuille	Approximates the macropore as a cylindrical tube.	Relatively simple equation.	Need geometrical properties of macropores which are hard to obtain.	The cylindrical assumption will overestimate macropore flow in a rain garden device.	(Ahuja et al., 2000; Jury & Horton., 2004)
KWE	Assumes water flow move through the macropores as a kinematic wave.	Simpler alternative to Richards equation.	Gravity based model so only applicable to vertically orientated macropores.	Can also be used to model matrix flow to simplify the proposed model.	(Larsbo et al., 2005; Beven & Germann, 2013)
Richards	Similar version to matrix Richards equation however gravity rather than capillarity is the dominant force.	Highly accurate Can also be used for matrix flow Can be used for horizontal and vertical macropores.	Complex equation requires finite difference or finite element models to solve.	Not deemed an accurate method as its founding assumptions are based on capillary (matrix) flow.	(Simunek et al., 2009)
IN3M method	The inflow quantity of each macropore is proportional to its macropore drainage area, which is defined as the area that drains to a macropore.	Simple equation.	Not been benchmarked against other models Based on macropore geometrical properties which are hard to obtain.	Not applicable as macropore drainage area for rain garden soil is not available.	(Weiler, 2005)

Method	Theory	Advantages	Disadvantages	Application to Rain Garden Water Modelling	References
Macropore Initiation					
Predefined Pressure head	Flow through macropores starts upon the soil reaching a certain predefined pressure head.	Simple method. The choice of a pressure head of −10 cm (MACRO) has been proven to be a reasonable devisor point for matrix and macropore flow.	May not be suitable for all conditions.	Can be calibrated to suit rain garden soil however this would require extensive field work.	(Larsbo et al., 2005)
Rainfall surpasses infiltration rate	Once rainfall surpasses the infiltration rate of the soil, flow through macropores begins.	Can be easily calculated using Green-Ampt equation.	Macropore can be underestimated as it can occur before the infiltration rate is reached	Easy implemented into a numerical model, however may underestimate macropore flow.	(Pot et al., 2005)
Matrix saturation	Flow through macropores starts upon the soil reaching saturation.	Easy to calculate	Macropore flow can occur before saturation leading to an under-prediction of preferential flow in drier conditions and a over-prediction in wetter conditions	Easy implemented into a numerical model, however may underestimate macropore flow.	(Ahuja et al., 2000)

Method	Theory	Advantages	Disadvantages	Application to Rain Garden Water Modelling	References
Water Transfer					
Mass driven-effective water content	The water transfer between matrix and macropores and vice-versa is a function of the soil moisture content in both flow regimes.	Simple to use Doesn't require many parameters.	Has only been used in conjunction with a 'cut and join' approach to hydraulic functions and may need adaptation to be used with other techniques.	Accurate in soils similar to SuDS but never previously been applied to rain gardens.	(Larsbo et al., 2005)
Mass driven-pressure head	The water transfer between matrix and macropores and vice-versa is a function of the pressure head in both flow regimes.	Accurate.	Complex and may be fundamentally numerically unstable as the product of two highly non-linear terms needs to be calculated.	Accurate in soils similar to SuDS but never previously been applied to rain gardens.	(Simunek et al., 2009)
Green-Ampt	Water transfer is described using the Green-Ampt equation for cylindrical pores.	Simple to use term.	Requires geometric parameters of the macropores Generally assumes water transfer from macropores to matrix only.	Accurate in soils similar to SuDS but never previously been applied to rain gardens.	(Ahuja et al., 2000)

A summary of all relevant hydrological computer models is given in **Appendix A**.

3.4.2 Evapotranspiration

Evapotranspiration is an important factor of modelling water movement in soils. It refers to the sum of evaporation and transpiration of the plants present in the rain garden. In previous literature, energy-balance approaches have proven to be the most popular method of calculating evapotranspiration, specifically the Penman equation and its revisions (Dingman, 1994; Campbell & Norman, 1998). The Penman-Monteith equation has been shown to be reliable in various situations and climatic conditions; this is due to incorporation of various calibrated parameters such as leaf area index, vegetation height and canopy resistance (Allen, et al., 1989; Ventura et al., 1999).

However, there are continuing problems applying energy-balance equations such as the above as they require a significant amount of data which is difficult to obtain, especially wind and relative humidity. Other simpler methods such as the Priestly-Taylor equation exploit the intrinsic conservative and seasonal predictability of evaporation (Priestly & Taylor, 1972). The Priestly-Taylor equation has been shown to give a good estimation of evapotranspiration for numerous different situations including irrigation and intrinsically dry and wet conditions (Ding, et al., 2013, Ngongondo, et al., 2013). Fowler (2002) compared monthly average approaches as well as daily estimates using the Priestly-Taylor equation and it was seen that, for estimating long-term soil water balance, a monthly average performs as well as a daily value. It has also been used by RECHARGE to model evapotranspiration in rain gardens.

In this method, the total potential evaporation (E_p) (cm) is given by (Priestly & Taylor, 1972):

$$\mathrm{E_p} = \propto \frac{\Delta}{\Delta+\gamma}\frac{R_n}{\lambda} \qquad (3.1)$$

where $\propto$ (Dimensionless) is the ratio of actual to equilibrium evaporation commonly taken as 1.26, Δ (Dimensionless) is the slope of the saturation vapour pressure curve at air temperature, R_n (W/m²) is the net radiation, G (W/m²) is the soil heat density, γ is the psychrometric constant ($6.66\text{x}10^{-4}$ 1/ºC), λ (ºC) is the latent heat of vaporization. In some cases a plant canopy can intercept part of the incoming radiation, in such a situation the total potential evaporation can be split into the potential soil evaporation E_s (cm/s) and the potential plant transpiration T_p (cm/s). Thus, if the transmissivity coefficient of the plant canopy is denoted by τ (Dimensionless), the potential soil evaporation and the potential plant transpiration are given by:

$$E_s = \tau \frac{\Delta}{\Delta+\gamma} \frac{n}{\lambda} \quad (3.2)$$

$$T_p = (\alpha - \tau) \frac{\Delta}{\Delta+\gamma} \frac{R_n}{\lambda} \quad (3.3)$$

The transmissivity coefficient τ can be approximated by (Campbell & Norman, 1998):

$$\tau = \exp(-\beta . \mathrm{LAI}) \quad (3.4)$$

where β (Dimensionless) is the attenuation coefficient and *LAI* (Dimensionless) is the leaf area index.

3.4.3 Conclusions on Water Modelling

As is clear from this section, there are numerous dual-permeability approaches in existence, however they do not currently meet the needs required to model flow in a rain garden with a simple layered profile and coupled upper boundary conditions (for ponded and non-ponded conditions). Thus, a new model must be created, the previous models used for groundwater recharge estimations for rain gardens are not sufficient as they do not include macropore region flow modelling which has been shown to have an impact on heavy metal retention. The information gathered above with regards to current methods for prediction of water flow in both regions, initiation of macropore flow and interaction between the matrix and macropore regions will be used to develop the water modelling section of the pollutant retention model. The steps taken to design such a model will be fully detailed in **Chapter 4**.

The next stage of the literature review is to examine current methods of modelling heavy metal transport and capture in order to facilitate the design of the pollutant retention segment of the computer model.

3.5 Heavy Metal Adsorption

As stated previously (**Table 3.1**) adsorption is the principal mechanism by which pollutants are removed from runoff in a sustainable drainage system such as a rain garden. The adsorption process is a surface phenomenon in which a multi-component fluid (gas or liquid) mixture is drawn towards the surface of a solid adsorbent and forms an attachment through physical or chemical bonds (Foo & Hameed, 2010).

The overall strength with which metals are retained in soils is dependent on several factors (Alloway, 2013)

(i) 'residual' properties determined by the metal source material (in the case of rain gardens this is urban runoff)

(ii) The intrinsic affinity of individual metal ions for soil adsorption surfaces and soluble soil ligands:

(iii) The available adsorption surfaces present in soils (humus, metal oxides, alumina-silicate clays etc.)

(iv) The changeable properties of soil, including pH, redox potential , water content, temperature, biological activity, salt concentration etc.

(v) Soil-metal contact time.

A general depiction of metal behaviour in soil as 'fractionation' in the solid phase and 'speciation' in the solution phase, is shown in **Figure 3.1**.

M_{inert} is inert metal, contained in a dorm which only reacts to changes in long term (over a period of years) solution conditions. $M_{non\text{-}labile}$ represents non-labile metals that are held in kinetically constrained forms and react to changing conditions slowly (days to months). Non-labile metals are known to exist within soil solids linked to ligands such as humic/fulvic acid.

M_{labile} are metals which respond reversibly (Adsorption or desorption) and almost instanteously to changes in solution equilibrium.

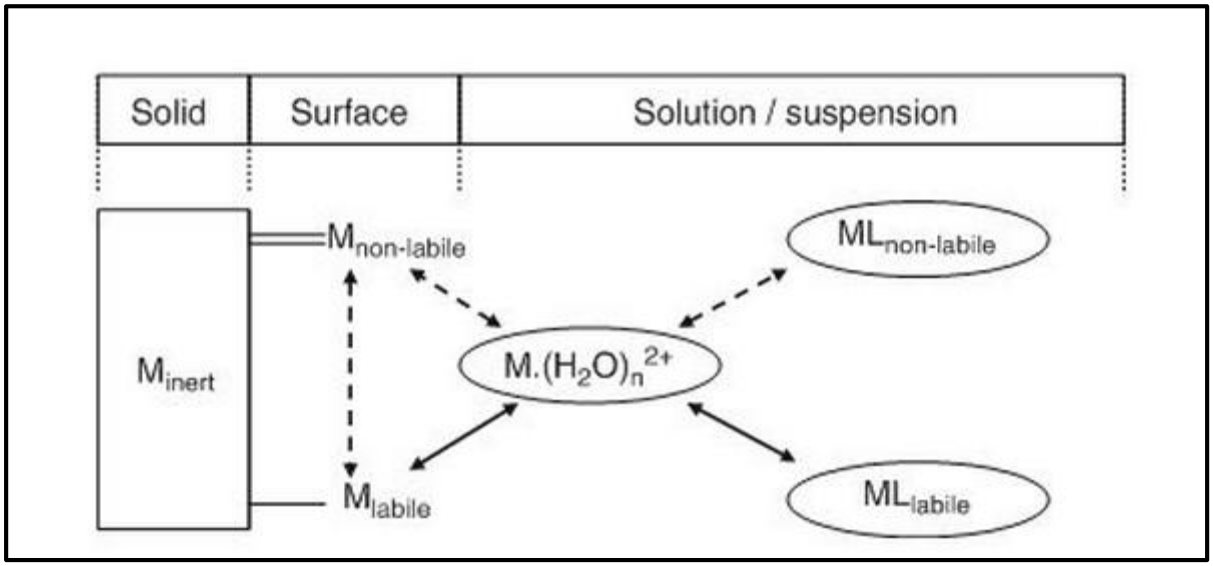

Figure 3.1 Heavy Metal Behaviour in Soil. Adapted from Alloway (2013)

$M.(H_2O)^{2+}$ represents free hydrated metal ions. These are often assumed to be bioavailable but there is evidence to suggest the complexes in the solution (ML_{labile} and $ML_{non\text{-}labile}$) also

contribute to bioavailability. All forms of metal contained in solutions or suspended is subject to transportation in water.

Examples of the above surface and solid metal states with specific reference to rain garden devices is shown in **Table 3.3**.

Table 3.3 Surface and Solid Metal States in a Rain Garden

Metal State	Example
M_{inert}	Secondary (e.g., phosphate, carbonate) metal compounds solubilised by slow oxidation reactions or dissolution over extended periods
$M_{non\text{-}labile}$	Surface adsorbed metals held strongly on mineral or organic surfaces
M_{labile}	Some specifically-adsorbed metal ions on Fe/Mn/Al hydrous oxide surfaces and humus.

By far the most common types of metals contained in urban runoff are Cu, Pb and Zn, these will be examined in greater detail in the subsequent section.

3.5.1 Cu

Traffic is responsible for a large amount of Cu present in urban runoff and thus input into rain garden soil. This is attributed to both rail transport (corrosion of overhead wires) and road transport (brake and tire wear). Additional Cu sources include external building applications such as Cu roofs. This can result in maximum Cu concentrations of 140 μg/L in urban runoff (Gobel et al. 2007).

The most common forms of Cu are cuprous (Cu^{1+}) and cupric (Cu^{2+}). Cuprous Cu is unstable in urban runoff transferred to rain garden soil and soluble Cu^{1+} compounds form Cu^{2+} ions or compounds and/or Cu(s) as a precipitate. When Cu^{2+} is introduced into the soil, the cupric ion binds to inorganic matter. The Cu^{2+} ion forms stable complexes with $–NH_2$, -SH, and, to a lesser extent, -OH groups in these organic acids. It has been found in speciation studies that in excess of 98% of the soluble Cu in soil was bound to organic ligands. Results from long-term studies indicate that Cu moves from easily extracted pools to more strongly bound forms. This results in limited desorption of Cu from soil. The proportion of Cu^{2+} in a solution decreases with increasing pH. In rain gardens and native European soils the pH ranges from pH 3.4-6.8,

resulting in 73% to 99.96% of Cu being complexed. Excess Cu in the soil can result in detrimental impacts to plants, invertebrates and microorganisms. The table below shows the Cu threshold concentrations for plants and invertebrates.

Table 3.4 Cu Threshold Concentrations for Plants and Invertebrates (Alloway, 2013)

	Range (mg Cu Kg^{-1} soil)
Monocotyledon Plants e.g palms, grasses, corn, lillies, tulips, daffodils	18-537
Dicotyledon Plants e.g. roses, oaks, maples and sycamore	36-698
Arthropods e.g. insects, arachnids, crustaceans	31-1460
Annelida and Nematoda e.g worms	150-500

The wide range of toxicity values is attributed to the discrepancies between spiked tests and long term studies. For example it has been found that soils which have been inundated with Cu to test the detrimental effects on plants and invertebrates show larger toxicity than those in field tests which have been exposed to a gradual accumulation of Cu over many years. The latter scenario would be most applicable to rain garden. European risk assessments of Cu recommend a PNEC (Predicted No Effect Concentration) of between 10 and 200 mg kg^{-1}. Clean-up standards for Cu soils are generally higher than this ecological standard and the clean-up limit for Cu in residential soils and industrial soils are 100 mg kg^{-1} and 200 mg kg^{-1} respectively in Sweden (the U.K has no guidelines on Cu concentrations in soils) (Provoost et al., 2006).

3.5.2 Pb

In the past the vast majority of Pb in urban runoff was attributed to leaded petrol since its' elimination, Pb concentration has decreased. It is still present in smaller concentrations however which is attributed to Pb roofs, tyre and brake pad abrasion with a maximum concentration of 575 μg/L in urban runoff (Gobel et al. 2007).

Dissolved Pb exists in several states in a soil solution: organic complexes, inorganic ion pair and free Pb^{2+}. It was found by Sauve et al. (1997) that the free Pb^{2+} activity in soils can be predicted accurately solely as a function of pH and is not dependent on other characteristics such organic matter content. Pb in soils generally exists in the Pb^{+2} oxidation state, but is less soluble with increasing pH in the soil solution due to sorption onto organic matter. Pb has been found to be strongly adsorbed onto humic matter, clay minerals depending on soil composition. It exhibits stronger retention in soil than other heavy metals such as Cu and Zn. This is supported by previous experimental findings relating to rain gardens which will be discussed later. Despite this sorption in longer term studies Pb leaching through soils has been observed. This leaching has been attributed to the release of organic matter from the soil which contained Pb. This will not be the case in rain garden soil as organic matter will not leave the device.

High levels of Pb in urban soils have been identified as a concern as soil is seen as an important pathway of human lead exposure, in particular to children engaged in hand-to-mouth and pica behaviour. As rain gardens may be located in residential and school areas these findings are of concern when designing these devices.

In the U.K the regulatory limit of Pb in soils is 450 and 750 mg Kg^{-1} for residential and industrial landuse respectively. If these levels are exceeded in a rain garden as predicted by Li and Davis, several options are available for remediation including removal and amendment with phosphate.

3.5.3 Zn

The presence of Zn in urban runoff is attributed primarily to tyre debris and Zn coated roofs, this can result in concentrations of up to 2000 μg/L (Gobel et al. 2007).

Similar to Pb and Cu, Zn exists as the Zn^{2+} oxidation state in soils. This concentration is regulated by sorption and mineral dissolution reactions where sorption is the dominant reaction. Zn can experience strong sorption onto numerous soil components such as organic matter and on Fe and Mn oxides. Alternatively weaker reversible reactions can occur by adsorption through ion exchange on clay mineral surfaces. Soil acidity also decreases the solubility of Zn in a similar fashion to Pb with the free ion fraction decreasing with increasing pH.

When Zn is initially input into soil, there is an almost immediate reaction in which Zn adsorbs onto the solid phase. This reaction is rapid, following this slower reactions occur that form

bonds between the Zn and soil from which desorption is slow. This limits the release of Zn from the soil but increases toxicity.

Although Zn is an essential nutrient for plants, excess content in soil may result in plant toxicity. Typically there is a 10% reduction in plant yield at soil concentrations of 100 mg/Kg. This is due to increased plant Zn concentrations causing reduced root growth or stunted shoot growth. In the U.K the regulatory limit of Zn in soils is 500 mg/Kg for industrial land-use, no current limits are in existence for residential areas however in Sweden it is 350 mg/Kg (Suave et al., 1997).

3.5.4 Heavy Metal Fractions

Depending on soil properties and the heavy metals present, adsorption of the metal is associated with different chemical fractions. The chemical fraction of a metal is the determining factor for environmental mobility, bioavailability and the likelihood of desorption. The sequential extraction method developed by Tessier (1979) provides a useful analytical method for partioning of particulate trace metals into five geochemical phases:

Fraction 1. Exchangeable

The metals in this fraction are highly bioavailable and show mobility relative to their environment and are potentially available to plants. Changes in ionic composition could result in desorption of metals in this fraction.

Fraction 2. Bound to Carbonates

Metals in this fraction are also bioavailable and susceptible to changes in pH.

Fraction 3. Bound to Iron and Manganese Oxides

Iron and manganese oxides exist in soils as the adhesive between particles or as a particle coating.

Fraction 4. Bound to Organic Matter

It has been found that metals can bind to numerous forms of organic matter such as living organisms and coatings on mineral particles. However under oxidising conditions in natural waters, organic matter can be degraded resulting in the release of soluble metal.

Fraction 5. Residual

The metals held in this fraction are generally found in the crystal structure of primary and secondary minerals. These metals are not expected to be released into the environment over a reasonable time span under conditions found in nature.

Numerous studies have quantified the metal fractions in both rain garden and road side soils using Tessier's (1979) method. It has been found that metal fractions in F1 are generally low, the bulk of accumulation occurring in environmentally inaccessible fractions (F3 through F5) therefore metals captured in rain garden media are expected to remain largely immobile (Sansalone & Buchberger,1997; Wilcke, et al., 1998; Li, et al., 2001; Li & Davis, 2008).

There has been much criticism of Tessier's and other sequential extraction methods due to the non-selectivity of reagents used in testing which may alter the characteristics of sediments tested. This usually results in metals collected for fractions 1-3 were underestimated and fractions 4-5 overestimated (Zimmerman & Weindorf, 2010). This is turn underestimates the possible release of metals from the soils.

Therefore, traditional chemical testing such as Tessier's (1979) method cannot ensure that all toxic chemicals of importance are identified and measured in the sediment of interest; nor can they be used to estimate synergistic effects among compounds in a solution (Wang, et al., 1998). Biological testing has, therefore, become an important tool in enhancing the traditional environmental monitoring programmes based on chemical tests to characterise complex chemical mixtures in sediments and water. Biological toxicity testing is based on exposing organisms to all the bioavailable chemicals in a test sample and then noting the changes in biological activity.

In conclusion, although recent research into heavy metal fractions in rain gardens and other SuDS have shown that heavy metals are strongly retained in the soil, these findings are limited by the analysis techniques used and should be treated with caution. In future it is recommended that more accurate methods which reflect natural soil conditions be used such as biological testing.

As stated in **Section 1.3**, the main aim of this thesis is to predict the adsorption of heavy metals in rain garden soil. Over the years, many isotherm models (Langmuir, Freundlich, Brunauer-Emmett-Teller, Sips etc.) have been developed to predict adsorption. An adsorption isotherm is a curve representing the process controlling the retention or movement of a substance from the aqueous porous media to a solid-phase at a constant temperature and pH (Ho, et al., 2001).

3.5.5 Sorption Experiments

Several studies have been completed into the suitability of selected isotherms for modelling the adsorption of heavy metals onto various absorbents and in rain garden systems (Davis et al., 2001, Li & Davis, 2008).

The accuracy of a great range of isotherms was examined by Ho et al. (2001). Here the sorption of the metals Cu and Pb onto peat was examined using sorption experiments and the results compared with those calculated using the Langmuir, Freundlich, Redlich-Peterson, Toth, Temkin, Dubinin-Radushkevich and Sips (combined Langmuir-Freundlich) isotherm models. It was found that in all cases the three parameter Sips isotherm equation offered the best fit to the equilibrium data.

Jang et al. (2005) also examined heavy metal removal (Cu, Pb, Zn) from urban storm water by various types of mulch using sorption experiments. The results from these experiments were then compared to the predictions given by the Langmuir and Freundlich isotherms in order to ascertain the better predictor of adsorption. It was found that the Langmuir isotherm was more accurate in all cases with an R^2 (correlation coefficient) value of between 0.997 and 0.999 as opposed to values as low as 0.848 for the Freundlich model.

Li and Davis (2008) modelled the absorption of Cu, Pb and Zn in a rain garden using a linear isotherm. They compared their results to an 85-90cm core sample from a 4.5 year old rain garden system with media consisting of 50% sand, 30% top soil and 20% mulch. Their model not only took into account the absorption of the metals to the media but also to total suspended solids (TSS) in the urban runoff. This was accomplished by incorporating the average input TSS and a filter parameter into the calculation of metal distribution coefficients which were used to determine the quantity of contaminant retained. Their results indicated a successful prediction of heavy metal retention especially in the cases of Pb and Zn with Cu however, the retention was not modelled as accurately, possibly owing to its weaker association with the soil, desorption or incorrect linear assumptions. Li and Davis (2008) concede that if a more accurate numerical model is required, non-steady state and nonlinear isotherms would be needed but this would greatly increase model complexity and input data requirements.

Genc-Fuhrman et al. (2007) examined the potential use of alumina, activated bauxsol-coated sand, bauxsol-coated sand, fly ash, granulated activated carbon (GAC), granulated ferric hydroxide, iron oxide-coated sand (IOCS), natural zeolite, sand and spinel as sorbents for

removing heavy metals from storm water; in this case the relevant metals tested were Cd, Cu and Zn. The results of their experiments were then compared to the predictions of the Freundlich isotherm which was deemed to give a better fit than the Langmuir model. For the adsorbents, fly ash, spinel and bauxsol-coated sand, low values for R^2 were obtained (as low as 0.2), this was blamed on other removal mechanisms which the Freundlich isotherm was unable to predict. Low R^2 values for substances such as sand can also be caused by leaching of some metals from the sorbents and oversaturated conditions which results in precipitation becoming the leading removal mechanism over sorption. The results from other sorption experiments are shown in **Table 3.5**.

Table 3.5 Results of a Variety of Heavy Metal Sorption Experiments

Metals Tested	Adsorbent	Isotherms	Verification Method	Findings	Source
Cadmium	Pine bark	Freundlich	Visual	Good Correlation	(Al-Asheh & Duvnjak., 1997)
Copper Lead	Tea waste GAC	Freundlich Langmuir	Correlation Coefficient	Both Isotherms performed well with R^2> 0.95 for both metals	(Amarasinghe & Williams, 2007)
Cadmium Copper Lead	Red Mud Fly Ash	Langmuir	Correlation Coefficient	Fly Ash exhibited the greater amount of retention. The Langmuir isotherm performed well for both adsorbents and for all metals with R^2>0.95 in every case.	(Apak, et al., 1998)
Cadmium	Juniper Fiber	Langmuir Freundlich	Correlation Coefficient	The Langmuir isotherm exhibited a fractional advantage over the Freundlich isotherm with an R^2 value of 0.997 as opposed to 0.938.	(Min, et al., 2004)
Copper Zinc	Clay	Langmuir	Correlation Coefficient	Langmuir Isotherm performed well with an R^2 value of 0.99 for both metals	(Vengris, et al., 2001)
Copper Lead Zinc	Zeolite	Sips, Redlich-Peterson, Toth, Dubinin-Radushkevich, Linewer-Burk	Correlation Coefficient	All the isotherms showed good accuracy with R^2>0.92 in all cases. However Sips was to some extent the best fitting curve.	(Peric, et al., 2004)
Cadmium Copper	Activated carbon, kaolin, bentonite, diatomite and waste materials such as compost	Langmuir Freundlich	Correlation Coefficient	For copper the Langmuir isotherm was more accurate on all the absorbents save for compost where the Freundlich model proved better with a R^2 value of 0.95 as opposed to 0.94. For cadmium, the Langmuir model suited active carbon, compost and cellulose pulp waste better whereas the Freundlich equation gave better results for kaolin, bentonite and diatomite.	(Ulmanu, et al., 2003)

From the findings of previous experiments, it is clear that four principal isotherms are apparent as the most common methods of heavy metal prediction; the linear, Langmuir, Freundlich and Sips isotherms. These will be examined in the following sections.

3.5.6 Linear Isotherm

The linear isotherm is the simplest in isotherm theory and is essentially an interpretation of Henry's law of gases (Kulprathipanja, 2010). It assumes that the media-sorbed pollutant concentration (C_s) (mg/kg) is directly proportional to the dissolved pollutant concentration (C) (mg/L) (Kulprathipanja, 2010):

$$C_s = K_d C \tag{3.5}$$

where K_d is the linear distribution coefficient (L/kg). The distribution coefficient is one of the determining factors of pollutant retention; it is a measure of the ability of a media such as soil to retain contaminants and also the affinity of the metal to sorb to the specific media. It varies between both media and metals with metals such as Pb and Zn having higher distribution coefficients in soils than Cu (Li & Davis, 2008). If the concentrations are low it has been found that this isotherm can quite accurately describe adsorption (Kulprathipanja, 2010). This supports its use as a method for the prediction of pollutant retention in rain gardens as the levels of heavy metal concentrations are typically low (Davis, et al., 2001). As opposed to other more complex equations, only one parameter is needed, K_d which gives it a decided advantage when information about soil is not readily available.

It has been found from experiments that the capacity for a media to retain heavy metals varies widely (Davis, et al., 2001; Morera, et al., 2001; Li & Davis, 2008). It depends not only on the constituents of the soil such as organic matter content but also on factors such as pH and adsorption preferences which will be discussed later (**Section 3.5.10**). The linear isotherms main advantage is its simplicity and the relative ease by which its parameters can be obtained however this results in a lack of accuracy as experienced by Li and Davis (2008). Increasing accuracy can be obtained by exploiting more complex isotherms.

3.5.7 Langmuir Isotherm model

The Langmuir isotherm has conventionally been used to assess and compare the capacities of various bio-sorbents. At low pollutant input concentrations, it essentially reduces to a linear isotherm as detailed above and obeys Henry's law. At higher input concentrations it assumes monolayer adsorption, meaning the adsorbed layer is one molecule thick and that adsorption is

only present at a fixed number of definite sites that are identical and equivalent, with no lateral interaction and steric hindrance between the adsorbed molecules. This signifies that an equilibrium saturation point can be reached whereby once a molecule occupies a site no further adsorption occurs (Foo & Hameed, 2010). In a device such as a rain garden, this can lead to a complete saturation of the soil media with heavy metals resulting in the input concentration travelling through the system without being adsorbed. This is a situation which requires further examination and design, and will be discussed later. The nonlinear form of the Langmuir isotherm can be represented as follows (Foo & Hameed, 2010):

$$C_s = \frac{K_L S_{max} C}{1 + K_L C} \tag{3.6}$$

where K_L (L/kg) is the Langmuir isotherm coefficient and S_{max} (mg/Kg) is the total concentration of sorption sites available.

Numerous studies have examined the Langmuir coefficients for various absorbents (Ulmanu, et al., 2003; Seelsaen, et al., 2006; Amarasinghe & Williams., 2007; Nwachukwu & Pullford, 2008). It was found that the Langmuir provided an accurate prediction for a wide range of media, pH values and metals with R^2>0.92 in all cases, however a number of disadvtanges were identified.

It does not account for the surface roughness of particles in the adsorbate (Foo & Hameed, 2010). Rough surfaces can have multiple sites for adsorption which disagrees with the Langmuirs monolayer theory. Although in rain garden, soils with low particle roughness are generally used such as mulch or peat, the use of sand to reduce nutrients is becoming increasingly common (Hsieh & Davis, 2005). Thus the Langmuir isotherm may not always be appropriate, the Freundlich isotherm however models multilayer absorption and will be examined next.

3.5.8 Freundlich Isotherm

The Freundlich isotherm is the earliest known sorption isotherm equation. It is an empirical model which can predict non-ideal sorption (this is non-uniform sorption with stronger binding sites being occupied first) as well as multilayer sorption (Ho, et al., 2002). In recent years the Freundlich isotherm has been extensively applied in heterogeneous systems and can be represented as (Ho, et al., 2002):

$$C_s = K_F C^{a_F} \tag{3.7}$$

where K_F (L/kg) is the Freundlich constant and a_F (Dimensionless) is the Freundlich exponent. This equation has been criticised in the past few years because it lacks a fundamental theromodynamic basis as it does not reduce to Henry's law at low concentrations (Ho, et al., 2002). This could cause a problem as typically heavy metal concentrations in storm water are low, however the Freundlich isotherm has shown good results when previously tested at these low levels (Genc-Fuhrman, et al., 2007).

3.5.9 Sips Isotherm

The Sips isotherm model is a three parameter isotherm and is a combined form of the Langmuir and Freundlich expressions derived for modelling hetrogeneous adsorption systems. This combination of isotherms reduces the inaccuracies experienced when applying them individually. At low input concentrations, it reduces to a Freundlich isotherm; while at high concentrations, it predicts the monolayer adsorption typical of the Langmuir isotherm. It can be represented as (Ho, et al., 2001):

$$C_s = \frac{K_{LF} C^{nLF}}{1+(a_{LF} C)^{nLF}} \tag{3.8}$$

where K_{LF} (L/kg) is the Langmuir-Freundlich isotherm constant, n_{LF} (Dimensionless) and a_{LF} (Dimensionless) are Langmuir-Freundlich isotherm exponents. The Sips isotherm however does not obey Henry's law at low concentrations (as it reduces to the Freundlich isotherm) typical of the heavy metals in runoff, thus it has no thermodynamic grounding. It also has three parameters which need estimation and has not commonly been used in the prediction of heavy metal retention when compared to the other isotherms examined so experimental values of these parameters are lacking.

3.5.10 Other Impacting Factors on Heavy Metal Retention

Co-ion effect and Competitive Adsorption

Storm water runoff generally contains a combination of several metals, this results in a co-ion effect which can have a crucial role in sorption. This effect is produced by the existence of different ions in runoff such as Cu^{2+}, Pb^{2+}, Zn^{2+} which compete with one another for sorption sites. Several experiments have examined this phenomenon and it has been found that in mixed metal solutions, the adsorption capabilities of a particular metal ion has been lessened by the presence of other metals which results in a decrease in removal efficiency (Jang, et al., 2005).

For example, the adsorption of Cd is strongly affected by the occurrence of competing cations such as divalent Ca and Zn, which compete with Cd for sorption sites in the soil (Bradl, 2004).

In the case of Jang et al. (2005), the order of adsorption was similar to the results obtained for single component testing of Pb>Cu>Zn. This corresponds to the findings of Bradl (2004) for peat and Gomes et al. (2001) for subsoil. This finding is reflected in the majority of the cases discussed, the main exceptions to this being the linear isotherm cases of Davis et al. (2001) and Li and Davis (2008) who found that for rain garden soil specifically the order of adsorption followed Pb>Zn>Cu. These experiments, however did not reach complete breakthrough. Heavy metal breakthrough is defined as the point at which inflow metal concentration is equal to outflow concentration. Thus, these experiments could have reached the same sorption preference found by the experiments of Gomes et al. (2001), Brandl (2004) and Jang et al. (2005) if a longer experimental period had been observed. In the case of Li and Davis (2008) additional factors could have played a part, such as soil composition and the presence of other metal ions which inhibited the adsorption of Cu.

Effects of pH

Soil pH is a crucial parameter which affects metal-solution and soil-surface chemistry and adsorption. Usually, heavy metal adsorption is small at low pH values as the quantity of negatively charged surface sites is low and increases with increased pH. Adsorption then increases at intermediate pH values from near zero to near complete adsorption over a small pH range; this pH range is known as the pH-adsorption edge. This result has been exhibited well by the findings of Bradl (2004) where the absorption of Cd, Cu and Zn onto sediment increases from near zero at pH 4 to near complete at pH 7. This conclusion is confirmed by the findings of Christensen et al. (1996) who examined the retention of these heavy metals in sandy aquifer material and found that the adsorption capacity of the soil greatly diminished with decreasing pH.

As pH has such an impact on adsorption, studies have attempted to quantify its effects using an extension of the Freundlich isotherm. Van der Zee and van Riemsdijk (1987) suggested the inclusion of soil pH as H^+ and organic carbon in the Freundlich isotherm

Van der Zee and van Riemsdijk (1987) found their approach accurately reflects the molecular impact pH has on heavy metal retention and is a useful as a tool for assessing metal capture across the pH range from extremely acidic to basic soils. However, as well as increasing accuracy, their approach also requires the quantification of a number of complex parameters.

As a rain garden is an artificial creation it is possible to use soils in the optimum pH range, which can then be maintained. Of course this approach is not appropriate in areas which are prone to acid rain but these cases can be assessed separately.

Organic Matter Content and Chemical Composition of Soil.

It has been shown that both organic matter content and the chemical composition of soil can greatly affect its ability to retain metals. Hsieh and Davis (2005) examined the retention of Pb for a variety of different media compositions. It was found that levels of organic matter were seen to increase the retention of Pb. However when mulch (29.8% organic matter) was the main component of the substrate, a drop in retention was seen, this can be explained by the high number of larger coarse particles in this material, that leads to voids and preferential channels which can inhibit metal capture. Cu also has an affinity to organic matter by its preference for binding to organic ligands. The addition of organic carbon to rain garden column experiments performed by Blecken et al. (2009) also resulted in larger removal of Cu further proving the influence of organic matter on the adsorption of Cu. Further sinks for Cu include iron and maganese oxides and sulphides (Fraction 4). Zn is less affected by organic matter but is readily sorbed to minerals present in soils such as clays.

3.5.11 Conclusions

In conclusion, the isotherms which will have proved the most accurate and beneficial in previous research are the linear, Langmuir and Freundlich isotherms. Each isotherm provides certain advantages, the simplicity of the linear isotherm provides a good starting point for the pollutant retention model and proves useful when information regarding the soil type is used and it is also to date the only model which has been applied to existing SuDS. The Langmuir isotherm is a more complex and more accurate equation which has been used effectively on numerous soils however it is not applicable to all soil types such as those with high surface roughness. The Freundlich isotherm is again complex but can be used in situations where the Langmuir isotherm is inappropriate such as for coarse grained soils. The Sips isotherm was also proven to be applicable but it introduces additional complexities in the form of a third unknown variable (Ho, et al., 2001)

Section 3.5.10 showed that caution must be taken when selecting adsorption distribution coefficients so as to account for both the co-ion effect and also the degree to which factors such as chemical composition of the soil and the organic matter content will affect heavy metal

retention. The value of pH is also important as it has a direct impact on the capacity of the soil to adsorb heavy metals.

These isotherms cannot be used solely to model the retention of pollutants in a rain garden as they simply predict the mass of pollutant removal per mass of media. The retention of metals in a SuDS such as a rain garden is far more complex and dependent on other factors such time, depth and the volume of input; this will be examined in the next section.

3.6 Heavy Metal Transport and Retention

3.6.1 Transport and Retention in the Matrix Region

The principle mechanisms which control solute transport in soil have been identified as advection and hydrodynamic dispersion (Freeze & Cherry, 1979). Advection is related to average water flux or velocity. The hydrodynamic dispersion is analogous to a diffusion-like process which is assumed to be the result of Brownian motion of solute particles. Brownian motion is the presumption that particles suspended in a fluid move in a random pattern. The dispersion component also adheres to Fick's law which states that the flux moves from regions of high concentration to regions of low concentration with a magnitude proportional to the concentration gradient. These assumptions lead to the parabolic advection-dispersion equation (ADE):

$$\frac{\partial C}{\partial t} = D\frac{\partial^2 C}{\partial z^2} - v\frac{\partial C}{\partial z} \tag{3.9}$$

where C (mg/L) is the solute concentration, D (cm^2/s) is the dispersion coefficient, v (cm/s) is the average pore water velocity, z (cm) is the vertical distance travelled and t (s) is the time. This is the mass conservation equation for transport of nonreactive solute through homogeneous porous media. In order for the dispersion coefficient to equal diffusion, a solute moving by advection in the direction of the mean transport at a rate different from v must have time to mix with the wetted soil. If this is not the case, as with larger scales (regional) and deeper soils, the ADE cannot describe the transport with a constant D, as increased variability in the constituency of soils enhance solute dispersion (**Section 3.6.1.2**). The ADE is the most popular method of solute modelling and has been used by numerous hydrological models including MACRO and HYDRUS albeit in different forms. For example the equation used by MACRO is shown below (Larsbo & Jarvis, 2003):

$$\frac{\partial(C\theta)}{\partial t} + \frac{\partial(C)}{\partial t} = \frac{\partial}{\partial z}\left(D\theta\frac{\partial C}{\partial z} - qC\right) - U \quad (3.10)$$

where θ (m^3/m^3) is the soil moisture content, q (cm/s) is the water flow rate and U (mg/L) is a sink term for pollutants that represents a variety of diverse processes (i.e. mass exchange between flow domains, kinetic sorption, solute uptake by crops, biodegradation). The reliability of the ADE is dependent on the situation to which it is applied. It is most accurate when used to model movement of bulk solutes over moderate distances (< 3m). At microscopic scales it is erroneous due to insufficient mixing to validate Fickian assumptions.

It has been found that the ADE does not accurately quantify some key aspects of solute transport through porous media. For instance, the dispersion coefficient has been found to increase with soil depth whereas in the ADE is it assumed to be constant. In addition the fundamental assumption of ADE that particles move by Brownian motion has been found to be far too restrictive in many cases. In order to address these problems several other equations have been suggested for modelling solute transport in soil, these are discussed briefly below (van Dam, et al., 2004).

Stochastic-convective model (SCM)

This hypothesis assumes the soil volume is composed of stream tubes with randomly distributed travel times (Jury & Scotter, 1994). The values of these travel times are presented as a probability density function which is assumed to be lognormal. With this transport, mechanism solutes are assumed never to leave their stream tubes, thus the SCM is only able to model longitudinal spreading within the entire soil volume. It is simpler to implement than the ADE, however it is unable to handle non-uniform solute applications. It has been found that the SCM is adept at modelling regional-scale transport of pollutants from subsurface diffuse sources, such as pipeline leakage.

Continuous-time random walk (CTRW)

This mechanism models solute transport in terms of the probability of a random displacement with a random travel time (Berkowitz, et al. 2000). This approach offers numerous benefits including its ability to model movement which is neither stochastic convective nor advective-dispersive but some approximation of these. Unfortunately this model is difficult to implement and requires considerably more parameters than other equations.

Fractional advective-dispersion equation (FADE)

This approach characterizes the intermediate stages between the SCM and the ADE and includes the ADE as a special case. Its creation was prompted by the failure of the ADE to accurately quantify field scale solute leaching (Benson, et al., 2000). This model is physically based on the Lévy process, this is the assumption that a solute particle does not continuously move between stream tubes but undergoes advective episodes during which Brownian dispersive episodes occur intermittently. The main disadvantage of this approach is the difficulty in solving the multidirectional fractional derivatives of which the equation is composed.

The advantages and disadvantages of the above methods are shown in **Table 3.6**.

Table 3.6 Advantages and Disadvantages of Models of Pollutant Transfer Methods

Model	Advantages	Disadvantage
ADE	• Popular method • Data sets and parameters widely available • Well researched • Can be solved analytically and numerically • Simple underlying mathematics	• Not reliable over large travel distances • Fickian assumptions have limited physical basis • Inaccurate at larger field and regional scales • Assumptions relating to the dispersion constant inaccurate at large depths (>3m)
SCM	• Physically based assumptions • Experimental support • Can accurately quantify field scale solute transport	• Travel time probability density function requires calibration • Application to layered soils is difficult • Solute application must be uniform
CTRW	• Generalises solute movement • Can model both Fickian and non Fickian movement	• Limited application to unsaturated transport

		• Requires large number of measurements • Not well researched
FADE	• Well established physical and mathematical basis • More flexible than ADE and SCM	• Complex equation • Not well researched.

3.6.1.1 Advection-Dispersion-Adsorption Equation

Advection-dispersion has been used to succesfully predict the movement of heavy metals through soils (Chang, et al., 2001; Sun & Davis, 2007; Ogata & Banks, 1964). This can be solved both numerically and analytically. The analytical solution of the advection diffusion equation for one-dimensional solute transport in semi-infinite soil columns is described by Ogata and Banks (1964) as:

$$C(z,t) = \left(\frac{C}{2}\right)\left\{erfc\left[\frac{(z-vt)}{2\sqrt{Dt}}\right] + \exp\left(\frac{vz}{D}\right) erfc\left[\frac{(z+vt)}{2\sqrt{Dt}}\right]\right\} \quad (3.11)$$

where *erfc* is the error function.

In order to model retention a retardation factor (R) is incorporated into the ADE (**Eq. 3.9).** This factor governs the retention of the pollutants and is dependent on the isotherm being used. The value of *R* (kg/ m^3) can be calculated as follows (Ho, et al., 2001):

$$R = 1 + \frac{\rho}{\theta}\frac{\partial C_s}{\partial C} \quad (3.12)$$

where ρ (kg/ m^3) is the bulk mass density. The retardation factor was developed by Hashimoto et al. (1964) to enable the prediction of solute dispersive transport through columns.

The combination of the ADE a retardation factor results in the advection-dispersion-adsorption:

$$R\frac{\partial C}{\partial t} + v\frac{\partial C}{\partial z} - D\frac{\partial^2 C}{\partial z} = 0 \quad (3.13)$$

Again as above this equation can be solved numerically or analytically (Ogata & Banks, 1964):

$$C(z,t) = \left(\frac{C}{2}\right)\left\{erfc\left[\frac{(Rz-vt)}{2\sqrt{RDt}}\right] + \exp\left(\frac{vz}{D}\right) erfc\left[\frac{(Rz+vt)}{2\sqrt{RDt}}\right]\right\} \quad (3.14)$$

The use of these retardation coefficients allows for the prediction of retention as a function of both the depth of the system (which facilitates examinations regarding the depth at which polllutants reach in the rain garden) and the time (the pollutant values in the soil can be assessed

in years allowing for life cycle and remedial work evaluations to be made). For example as detailed in **Section 3.5** Pb has found to exceed soil concentration safety limits in the upper layers of rain garden.

3.6.1.2 Dispersion

Dispersion performs an important role in the transport of contaminants through porous media. It takes place as a function of two separate processes: (i) molecular diffusion (e_e) (cm^2/s), which is due to Brownian motion and (ii) mechanical dispersion (D_m) (cm^2/s) which is produced by varying velocities and flow path distribution (Gaganis, et al., 2005). Thus the formula for the dispersion coefficient generally combines both these elements (Matsubayashi, et al., 1997):

$$D = D_m + e_e \tag{3.15}$$

It is commonly assumed that mechanical dispersion is proportional to the average linearized pore water velocity (v) (cm/s) and dispersivity (d) (cm) resulting in the equation (Freeze & Cherry, 1979):

$$D_m = dv \tag{3.16}$$

The values of d vary and are generally smaller in a laboratory column (0.5 to 2cm) than for those measured in the field (5 to 20 cm) (Warrick, 2003). It has also been found that this value is independent of water content and flow rate (Costa & Prunty, 2006). Molecular diffusion can also be further dissected into a function of tortuosity (τ_o (Dimensionless)) and binary diffusion coefficient of the solute in water (D_0) (cm^2/s):

$$e_e = \tau_o D_0 \tag{3.17}$$

e_e generally applies on a microscopic level however when flow rates are small (Jury & Horton, 2004).

It has been noted that for larger water flows the transport process shifts from advection-dispersion (where α is independent of depth) to a possibly stochastic dispersive process with dispersivity increasing at greater depths (Costa & Prunty, 2006). This may not be due solely to higher flow rates but due to the preferential flow caused by them. This was not identified by the authors but the breakthrough curves they supply for the higher flow rate show anomalies which could indicate a preferential flow pattern.

3.6.2 Transport and Retention in the Macropore Region

The advection-dispersion equation can be used to model solute transport in both the matrix and macropore regions, in some dual permeability models such as RZWQM (Ahuja, et al., 2000) and IN3M (Weiler, 2005) sorption in the macropore region is often neglected. This assumption is certainly valid in short periods with high infiltration rates where water transport through macropores is typified by high velocity and minimal soil-water contact which is necessary for sorption. However when macropores are saturated, the period of soil-runoff contact is significantly increased which can lead to sorption in this area (Knechtenhofer, et al., 2003).

3.6.3 Pollutant Transfer

The transfer between matrix and macropore regions is typically represented by a first order advection-dispersion equation (MACRO, HYDRUS), advection equation (SIMULAT) or in the case of the RZWQM instant mixing with a boundary matrix layer (Kohne et al., 2009). Pollutant transport (P) (mg/L) in the direction from macropore (C_{ma}) (mg/L) to matrix (C_{mi}) (mg/L) in MACRO is expressed by (Larsbo & Jarvis, 2003):

$$P = \left(\frac{G_f D_e \theta_{mat}}{d_p^2}\right)(C_{ma} - C_{mi}) + C_{ma} \tag{3.18}$$

where G_f (Dimensionless) is a geometry factor, d_p (cm) is an effective 'diffusion' pathlength, D_e (cm^2/s) is an effective diffusion coefficient, θ_{mat} (m^3/m^3) is the mobile water content in the matrix.

3.6.4 Conclusions

The advection-dispersion equation has proven in the past to be an accurate method of predicting the transport of heavy metals through soil. By combining this equation with various isotherm retardation factors it is possible to both model the adsorption and transport of heavy metals simultaneously in soil which reduces computation time and simplifies any proposed model. Pollutant transport in the macropores is generally modelled using only the advection-dispersion equation and adsorption in this region is largely neglected unless tackled by a more complex model such as HYDRUS. Pollutant transfer is often only deemed to occur from the macropore region (where no sorption occurs) to the matrix region (RZWQM, MACRO). A further point of consideration is the diverse range of processes represented by U in **Eq. 3.10** which may have to be considered such as mass exchange between flow domains (**Section 3.6.3**), solute uptake by crops, biodegradation. The advection-dispersion-retardation equations in the matrix already

encompasses the kinetic sorption component of the term U. The other components of U are dealt with as follows:

Solute absorption by plants: As stated above in previous experiments the proportion of heavy metal uptake by vegetation was found to be minimal in comparison with the percentage which was retained by the soil via adsorption (Li & Davis, 2008; Blecken, et al., 2009). Thus for this reason in the initial version of the proposed model, it is assumed to be negligible.

Biodegradation: This is not an issue with heavy metals as unlike carbon-based (organic) molecules and substances such as pesticides, metals do not degrade. There are two exceptions: to this mercury and selenium but these are not present in significant concentrations in urban runoff (Natural Resources Conservation Service, 2000).

Finally, a critical issue in dealing with heavy metals in a rain garden system is the build-up of heavy metals in the upper layer of soil (Sun & Davis, 2007). This accumulation, especially of Pb, may lead to metal concentrations in the soil which contravene public health standards; this can be avoided by monitoring the levels of contamination in the soil and removing the upper layer when required. The proposed pollutant retention model could help predict approximately when this removal should occur.

3.7 Summary

This literature review was focused on the optimum method of developing a computer model for determining the pollutant retention capability of rain gardens. It provides a summary of the important factors which influence heavy metal capture, the crucial features of dual permeability modelling and the main issues regarding retention prediction. This information provides the basis on which the numerical model can be designed which will be discussed in the next chapter.

4 MODEL DEVELOPMENT

4.1 Introduction

In this chapter, the development of a heavy metal retention modelling tool is described. As discussed in the literature review (**Section 3.4.1**) and **Appendix A**, several popular hydrological models (HYDRUS, MACRO, RZWQM etc.) are available for the prediction of pollutant retention processes in soil. However these models do not meet the specific needs of predicting heavy metal retention in rain gardens: they are typically complicated to use, do not model heavy metals and are predominantly designed for agricultural applications. Therefore a model called HM07 was developed which incorporated all of the important factors relating to the retention of heavy metals in rain garden soils as identified by the literature review (**Chapter 3**) and shown in **Table 4.1**.

Table 4.1 Important Factors in Heavy Metal Retention

Parameter Type	Factor
Hydrological	Water flow in the matrix and macropore regions Initiation of macropore flow Interaction between regions Pore water velocity Dispersion
Soil	Heterogeneity of Soil Organic matter content Isotherm Distribution Coefficient
Other	pH value

The following is a description of the methods used to develop the proposed model, for ease of explanation it has been divided into both a hydrological and pollutant component.

4.2 Hydrological Component

In order to model both the matrix and the macropore regions of flow in soil, a dual-permeability approach was used. This method described the soil as two overlapping pore domains with water flowing relatively quickly in one region (through macropores and fractures) and slower in the other region (matrix).

As stated in the literature review (**Section 3.4.1**) the predominant methods used to calculate water flow in the matrix zone are: the Green-Ampt equation followed redestribution, the kinematic wave equation (KWE) and Richards equation, for macropore flow: Richards equation, KWE, Poeusielles law and the IN^{3}M equation. As the purpose of this thesis was to develop a simple computer model the Richards equation can be immediately ruled out. It was also proposed that the same equation by utilised for both matrix and macropore regions, this left only the KWE as an option. This equation has previously proven successful at modelling water in the matrix region for situations that would be prevalent in a rain garden system such as complex surface flux patterns and layered soil (Smith, 1983). It is also accurate at replicating flow in macropores and has been used by computer models such as MACRO (Larsbo, et al., 2005).

The difference in the form of the KWE between the two regions lies in the parameters and boundary conditions used which are discussed below.

4.2.1 Matrix Region

As a rain garden is a layered system, discontinuities arise in the soil moisture content between layers and it is thus more beneficial to utilise the pressure head (h) (cm) version of the KWE:

$$\frac{\partial h}{\partial t} + \frac{\partial q}{\partial \theta}\frac{\partial h}{\partial z} = 0 \qquad (4.1)$$

where q (cm/s) is the water flux, θ (m^3/m^3) is the soil moisture content and t (s) and z (cm) are the position in time and space respectively.

As discussed in **Section 3.4** there are a number of parameters crucial to soil water flow (θ and unsaturated hydraulic conductivity (K) (cm/s)), these parameters are important both for the quantification of water behavouir in the rain garden and also to solve **Eq 4.1**. These were found using the van-Genuchten-Mualem functions assuming no hysteresis. These equations are as follows (van Genuchten, 1980):

$$K(\Theta) = K_s\,\Theta^{\frac{1}{2}}\left[1-\left(1-\Theta^{\frac{1}{m}}\right)^{m}\right]^2 \quad (4.2)$$

$$\theta = \frac{\theta_{sat}-\theta_{res}}{\left[1+(\alpha_{vg}|h|^{n_{vg}})\right]^{m_{vg}}} + \theta_{res} \quad (4.3)$$

Where Θ (Dimensionless) is the relative water content:

$$\Theta = \left[\frac{1}{1+(\alpha_{vg}h)^{n_{vg}}}\right]^{m_{vg}} \quad (4.4)$$

where α_{vg} (1/cm) and n_{vg} (Dimensionless) are the van Genuchten parameters and m_{vg}=1-1/n_{vg}, K (cm/s) is unsaturated hydraulic conductivity, K_s (cm/s) is the saturated hydraulic conductivity, θ_{sat} (m^3/m^3) and θ_{res} (m^3/m^3) are the saturated and residual soil moisture contents respectively.

The Mualem functions were chosen over the alternative Brooks and Corey functions as although the Brooks and Corey method gives accurate results, a discontinuity is present in the slope of both the soil water retention curve and the unsaturated conductivity curve near bubbling pressure (van Genuchten, 1980). This can prevent rapid convergence in numerical saturated-unsaturated flow problems and consequently could cause difficulties simulating flow in a rain garden which will undergo numerous wetting and drying events.

4.2.1.1 Numerical Solution of the Matrix KWE and Boundary Conditions

The pressure head form of the KWE (**Eq. 4.1**) is discretised using a Crank-Nicholson type finite difference scheme where the weight can be changed from 0.5 (traditional Crank-Nicholson) to 1.0 (fully implicit).

The upper boundary condition is dependent on the water balance in the rain garden surface depression which can be expressed as:

$$A_{rg}\frac{dh_s}{dt} = Q_{rain} + Q_{runon} - Q_{infiltration} - Q_{runoff} - Q_{evaporation} \quad (4.5)$$

where A_{rg} (cm^2) is the rain garden area, h_s (cm) is the surface water ponded depth and the flows Q (cm^3/s) are the inputs and outputs to the rain garden depression where Q_{rain} (cm^3/s) is the input from rain directly on the rain garden surface area and Q_{runon} (cm^3/s) is the flow input from the surrounding catchment area. It is assumed that rain and runoff are uniformly distributed over the rain garden area.

As the KWE is typically used in cases where the water inflow is approximately equal to or less than the soil saturated hydraulic conductivity (Smith, 1983) it must be combined with another

equation in order to calculate $Q_{infiltration}$ (cm^3/s) thus the kinematic model is supplemented with the Green-Ampt equation (Weaver, et al., 1994). This approach has previously proven accurate at modelling contaminants in the vadose zone and is thus deemed a reasonable method of developing this model (Weaver, et al., 1994).

Q_{runoff} occurs once the ponded depth (h_s) surpasses the maximum depression depth h_d and water overflows from the facility. The upper boundaries of the rain garden result in either a head (equal to h_s if the rain garden is ponded) or a flux condition.

The KWE combined with the system of boundary condition equations was solved using the Thomas algorithm. This explanation is further expanded in **Appendix B1**.

4.2.1.2 Evapotranspiration and Transpiration

The Priestly and Taylor (1972) method was chosen to calculate evapotranspiration for this model as it is simpler and requires less parameters than other more complex equations such as the Penman-Monteith approach. In the method developed by Priestly and Taylor (1972), potential soil evaporation (E_s) (cm/s) and plant transpiration (T_p) (cm/s) are given by **Eq. 3.2** and **3.3** respectively.

There are limitations on the two above values. In the case of evaporation (E_{actual}) (cm/s), the maximun is limited by maximum infiltration rate of water into the soil (q_f) (cm/s) (this can be calculated using the Green-Ampt, KWE or Richards equation):

$$E_{actual} = minimum\{E_s, q_f\} \tag{4.6}$$

Evaporation ($Q_{evaporation}$) forms part of the water balance equation (**Eq 4.5**)

It is assumed that rain and runoff are uniformly distributed over the rain garden area.

Transpiration is only active in the root zone and must be incorporated into the KWE (**Eq 4.1**). Plant transpiration (T_{actual}) (cm/s) removes moisture from the soil and thus is subtracted from the water mass balance equation which is the KWE:

$$\frac{\partial h}{\partial t} + \frac{\partial q}{\partial \theta}\frac{\partial h}{\partial z} - T_{actual}t_s = 0 \tag{4.7}$$

where t_s is the time step.

4.2.2 Macropore Region

4.2.2.1 Initiation of Macropore Flow

There are numerous methods to determine the initiation of macropore flow: infiltration, saturation, a cut and join approach, all of which were discussed in **Section 3.4.1**. Typically rain gardens experience significantly more water input than agricultural conditions which are described by prior hydrological models. The sudden increase in infiltration rates caused by runon from impervious surfaces especially after prolonged dryness has been shown to result in macropore flow in unsaturated conditions (Pot, et al., 2005). In addition, during prolonged periods of relatively light rainfall or in cases where the soil is saturated, ponding occurs. In these conditions it may be more apt to utilize the saturated switching point proposed by the RZWQM and IN^{3}M.

However there is still a distinct lack of knowledge into activation of macropore flow due to rainfall induced infiltration (Beven & Germann, 1982), therefore macropore flow will only be initiated when inflow exceeds infiltration and ponding occurs. This assertion is supported by the field experiments undertaken by Weiler and Naef (2003) who found that in grassland soils macropore flow only occured upon ponding of the soil surface. These findings were consistent for various rainfall rates ranging from 11.2 mm/h to 69 mm/h.

4.2.2.2 Numerical Solution of the Macropore KWE and Boundary Conditions

As stated earlier in this chapter, by far the most promising equation for modelling preferential flow is the KWE (Mdaghri-Alaoui & Germann, 1998; Larsbo, et al., 2005). As the KWE is also used for modelling flow in the matrix region it further simplifies the proposed computer model.

Germann (1990) derived the following relation from boundary-layer flow theory in cylindrical pores (q) (cm/s):

$$q = b_m w^{a_m} \tag{4.8}$$

where w (m^3/m^3) is the mobile moisture content in the macropore, b_m (cm/s) is the conductance and a_m (Dimensionless) is the macropore exponent.

Boundary layer theory is an extensive area of fluid mechanics research and involves the investigation of a thin slow moving layer of fluid adjacent to a surface. Further information regarding this derivation is available from Germann (1990).

The following continuity equation is applicable for cylindrical macropores in which the flow is gravity driven:

$$\frac{\partial q}{\partial t} + c_m \frac{\partial q}{\partial z} = 0 \quad (4.9)$$

where the macropore celerity c_m (cm/s), denotes one dimensional water velocity is given by:

$$c_m = \frac{dq}{dw} = a_m b w^{(a_m - 1)} = a_m b^{1/a_m} q^{(a_m - 1)/a_m} \quad (4.10)$$

A summary of the boundary conditions and methods for solving this equation are detailed in **Appendix B2**.

The KWE treats the soil as a block so rather than calculate the flow through each individual macropore as Pouiselle's equation does, it predicts the macropore flow through the soil as a whole. This removes problems associated with determining specific numbers of macropores and their properties.

The exponent a_m determines the dominant flow mechanism (matrix or macropore). Germann et al. (1997) have suggested ranges for a_m; a_m=2 for pure preferential flow along tubes e.g. macropores, a_m=3 for fracture flow e.g. along cracks, $3<a_m<11$ is a transitional flow between the two regimes and $11<a_m<30$ is diffusive flow.

The conductance b_m is dependent on a variety of factors such as macroporosity, deformation of macropores etc.

It has been shown however, that the maximum soil conductance parameter within the profile at a field site is related directly to the surface derived macroporosity as shown in **Figure 4.1** (Buttle & McDonald, 2000).

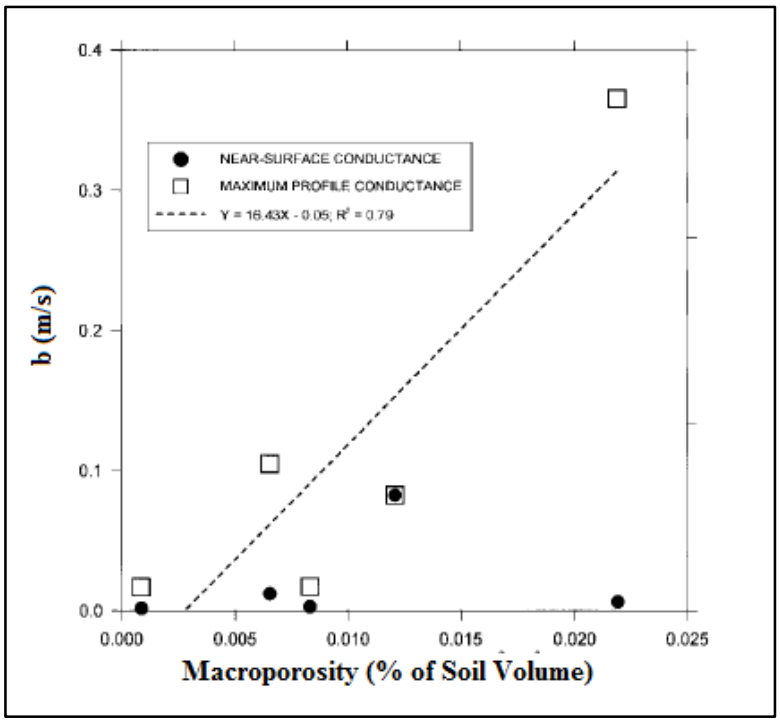

Figure 4.1 Relationship Between Near-Surface and Maximum Soil Profile Conductance Parameters and Conductance (*b*). Adapted from Buttle and McDonald (2000).

This illustrates that b_m is more dependent on the macroporosity of soil than the deformation of the macropores themselves. It also shows that a certain degree of macroporosity is needed before macropore flow is initiated; in this case 0.003%. This is due to the shallow nature of some macropores which exist in soils with low near surface macroporosity. These shallow macropores have a negligible conductance (b_m) value. The macroporosity of rain gardens is difficult to ascertain due to the lack of data. However from existing data relating to both agriculture and forested watershed it is presumed that the macroporosity in a rain garden falls within the range of **Figure 4.1** (0.0-0.02%) (Weiler & Naef, 2003, Buttle & McDonald). This a valid assumption as hydraulic parameters of the soils examined by Weiler & Naef (2003) were similar to those of rain gardens (Dussaillant, 2001).

With regards to the value of the parameter a_m, it may be more realistic to use a value in the transitional range. This is supported by findings of Allaire-Leung et al. (2000) that the parameter a_m of macropores lies between 1.1 and 1.2 indicating transitional flow (a_m value of 1 would correspond to pure preferential flow). In respect to experimental findings, it was also found by Mdaghri-Alaoui and Germann (1998) that soil generally lies in this range and pure preferential flow is rare.

4.2.2.3 Interaction between Matrix and Macropore Regimes

As discussed in **Section 3.4.1**, there are several methods of the modelling interaction between matrix and macropore regimes. The Green-Ampt equation is the simplest, however it requires specific information regarding the dimensions of the macropores e.g. radius, depth etc. and is therefore not appropriate for use in conjunction with the KWE. Therefore a first-order transfer equation similar to that used by HYDRUS was chosen to model flow from macropores to matrix as this is by far the dominant direction (Jury & Horton, 2004). This transfer equation has been shown to be accurate for agricultural and effluent modelling and is applicable to the case of heavy metal movement through rain gardens (Simunek, et al., 2009; Jiang, et al., 2010).

The first order water transfer term assumes water transfer (Γ_w) (cm/s) is proportional to the difference in pressure head between the two pore systems (Gerke & van Genuchten, 1993):

$$\Gamma_w = \alpha_w(h_f - h_m) \tag{4.11}$$

where α_w (1/s) is a first-order mass transfer coefficient for water and h_f (cm)and h_m (cm) are the water heads in the macropore and matrix respectively. It has been found that under free-flowing conditions in well ventilated channels, as is assumed to be the case in rain gardens, $h_f = 0$ (Weiler, 2005).

For the case of HM07, as discussed in **Section 4.2.2.1**, macropore flow is initiated upon ponding of the facility which happens close to soil saturation. When the soil is saturated no transfer between the regions can occur. Thus, transfer is assumed to be negligible. For unsaturated soil in rain gardens all of the water contained in the macropores transfers directly to matrix region instantaneously due to the high hydraulic conductivity of the media. This was also observed during the experiments completed as part of this project (**Section 5.4.2**). Therefore in both cases of unsaturated and saturated soil water transfer is assumed to be negligible.

4.3 Pollutant Retention Component

The pollutant retention component comprises of an equation which will both model the transport of heavy metals and their retention in the soil.

4.3.1 Heavy Metal Transport Modelling

There are several approaches which can be taken when modelling pollutant retention and transport through soil: stochastic-convective model, ADE, fractional advection-dispersion

equation and the continuous-time random walk method, all of which are detailed in **Section 3.6**.

The most common method, the ADE has a proven track record of modelling contaminant behaviours in soils and has been used by HYDRUS and MACRO amongst others for this purpose. Its main disadvantages are rooted in its assumption of Fickian transport which creates difficulties when applying it to field scale movement and it has been found to be most reliable when used to model the transport of solutes over distances of a few meters or less in moderate to small sized soil volumes, this makes it ideal for the modelling of transport through rain gardens and other SuDS. It is also a relatively simple equation and has had much research devoted to it in the past unlike the other methods which are relatively recent developments.

4.3.2 Advection-Dispersion-Adsorption Equation

In order to incorporate retention into the advection-dispersion a retardation factor (R) creating the advection-dispersion-adsorption equation (**Eq. 3.13**):

The retardation factor (R) (kg/m^3) is calculated using isotherms. The linear, Langmuir and Freundlich isotherm were all selected for the pollutant retention model as they all fulfil specific roles. The simplicity of the linear isotherm provides a good starting point for the pollutant retention model; it is also to date the only model which has been applied to existing rain garden devices (Li & Davis, 2008). The Langmuir isotherm is a more complex and more accurate equation which has been used effectively for numerous soils however it is not applicable to all soil types such as those with high surface roughness; for these soils the Freundlich isotherm is used. Care should be taken when selecting adsorption capabilities to account for both the co-ion effect and also the degree to which factors such as chemical composition of the soil and organic matter content affects the heavy metal retention. The value of pH was not be taken into account with regards to the isotherm equation as it is possible to engineer a specific value of pH in a rain garden and the chosen values for the sorption capacity and isotherm coefficients reflected this. The value of *R* was calculated as follows for the selected isotherms as presented in **Table 4.2** where K_d (L/kg) is the linear distribution coefficient, K_L (L/kg) is the Langmuir isotherm constant S_{max} (mg/kg) is the total concentration of sorption sites available, K_f (L/kg)and a_F are the Freundlich isotherm constant and exponent respectively.

Table 4.2 Retardation Coefficients for Isotherms

Isotherm	Retardation Factor (R)
Linear	$R = 1 + \frac{\rho}{\theta} \mathrm{K_d}$ (4.12a)
Langmuir	$R = 1 + \frac{\rho}{\theta} \frac{K_L S_{max}}{(1+K_L C)^2}$ (4.12b)
Freundlich	$R = 1 + \frac{\rho}{\theta} (a_{LF} K_F C^{a_{LF}-1})$ (4.12c)

The 1D advection-dispersion-adsorption equation can be solved in two ways either analytically using the Ogata-Banks approach (**Eq. 3.14**) or discretised employing a Crank-Nicholson type finite difference scheme where the weight can be changed from 0.5 (traditional Crank-Nicholson) to 1.0 (fully implicit). A detailed explanation of the initial and boundary conditions in the multi-layered model is given in **Appendix B3**.

The total metal accumulation M_{Acc} (mg) in the system can be calculated by a mass balance:

$$M_{Acc} = \sum_{t=t_s}^{t} V C_0 t - \sum_{t=t_s}^{t} V C_e t \quad (4.13)$$

Where V is the water volume (L) and C_o (mg/L) and C_e (mg/L) are the influent and effluent metal concentrations. This equation calculated the mass of metal accumulation over time by subtracting the concentration outflow from inflow for a specified depth of soil.

It has also been shown that the above method can be used to calculate heavy metal retention in the macropore region of soil (Simunek, et al., 2009).

4.4 Preliminary Validation

In summary, HM07 predicts water movement and heavy metal retention in rain garden. It adopts a dual-permeability approach and divides the flow into two flow regimes: matrix and macropore. A summary of the key equations used in this model is given by **Table 4.3**.

Table 4.3 Summary of Key Equations used by HM07

Process	Equation/Approach
Model Type	Dual Permeability Model
Water flow, Matrix	KWE
Water flow, Macropore	KWE
Solute Transport	Advection-Dispersion
Sorption	Linear, Langmuir, Freundlich Isotherm

In order to facilitate the identification of any faults with the various components of HM07, it was split into three parts: matrix, macropore and pollutant retention for ease of validation.

4.4.1 Matrix Region

The model models the flow in this region using the KWE. The validation of this region was completed by testing the model against two distinct scenarios. The first was a 24 hour simulation of a sharp wetting front carried out by Celia et al. (1990), where the soil column was 100 cm deep with θ_{sat}=0.268 m^3/m^3, θ_{res}=0.102 m^3/m^3, K_s=33.2 cm/h, α_{vg}=0.0355 cm^{-1}, n_{vg}=2, homogeneous initial head distribution of -1000cm, and the upper boundary condition was fixed at -75cm. The KWE results agree well with those of Celia et al. (1990) as can be seen in **Figure 4.2**.

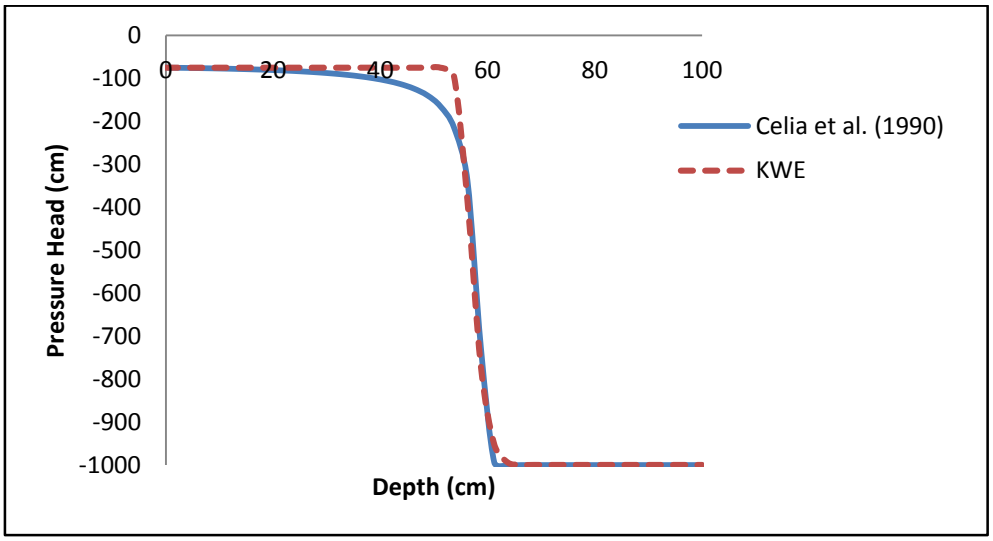

Figure 4.2 Comparison of KWE Results with Celia et al. (1990) Simulation.

Along with a visual agreement, the efficiency indexes also showed good results (**Table 4.4**).

Table 4.4 Efficiency Indexes for the Matrix Regime of HM07 and Celia et al. (1990) Results.

Error Estimator	Result
Coefficient of determination (R^2) (Dimensionless)	0.996
Nash-Sutcliffe Efficiency Index	0.995
Root Square Mean Error (cm)	30.5

As is illustrated by **Figure 4.3** the main source of error occurs at the onset of the sharp wetting front is due to a minor numerical instability, however despite this it is clear that the KWE still exhibits satisfactory results.

The second validation case was chosen to be the layered soil profile case 1.2 of Pan and Wierenga (1995), the soil characteristics are given in **Table 4.5.**

Table 4.5 Mualem-van Genuchten Parameters of Pan and Wierenga (1995) Case 1.2

Soil Characteristic	Top Layer	Middle Layer	Lower Layer
Texture	Loamy fine sand	Clay Loam	Loamy Fine sand
Depth (cm)	10	30	10
α_{vg} (1/cm)	0.028	0.010	0.028
n_{vg} (unitless)	2.24	1.4	2.24
θ_{res} (cm^3/cm^3)	0.0286	0.106	0.0286
θ_{sat} (cm^3/cm^3)	0.366	0.469	0.366
K_{sat} (cm/h)	22.5	0.546	22.5

The initial condition was suction head profile of -1000 cm, the upper boundary condition was a constant rainfall rate of 1.25 cm/h and the lower boundary condition was zero flux. The model yielded similar results for both pressure head and soil volumetric water content predictions as seen in **Figure 4.3(a)** and **Figure 4.3(c)**. A comparison is also shown between KWE and RECHARGE (Dussaillant, et al., 2004) to provide a comparison between the results of a

complex equation such as Richards (which RECHARGE uses) and the simpler KWE (**Figure 4.3(b)**).

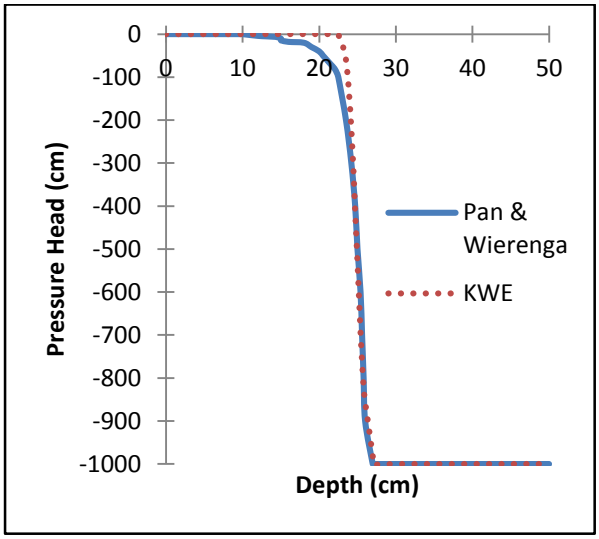

(a) Pressure Head Simulation KWE and Pan & Weirenga (1995)

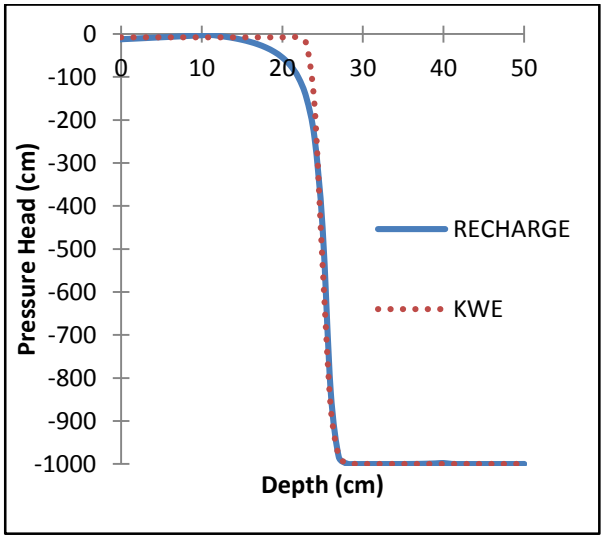

(b) Pressure Head Simulation KWE and RECHARGE

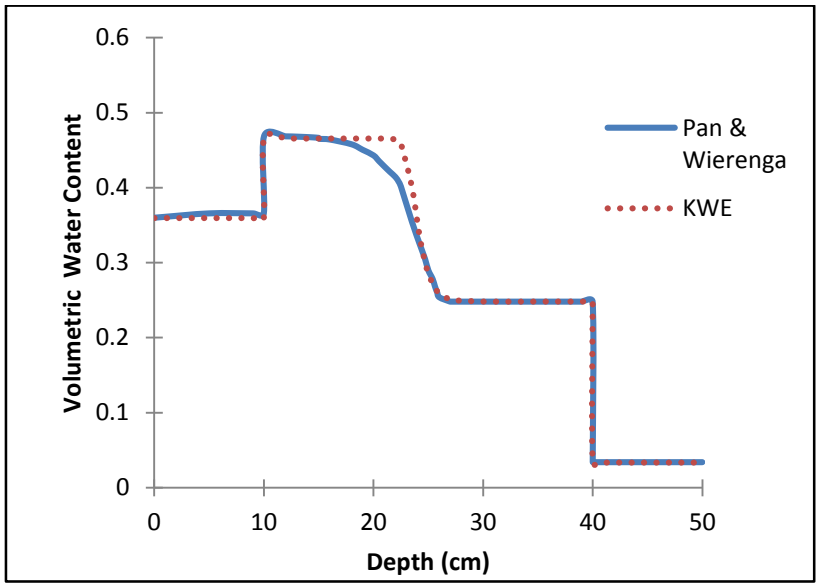

(c) Soil Moisture Content

Figure 4.3 Comparison of the Results from KWE Model with Layered Soil Simulation with case 1.2 Pan & Wierenga (1995).

Table 4.6 Efficiency Indexes for the Model and Case 1.2 of Pan and Wierenga (1995)

Efficiency Index	Pressure head	Volumetric water content
Coefficient of determination (R^2)	0.993	0.931
Nash-Sutcliffe Efficiency Index	0.990	0.921
Root Square Mean Error	43.6 cm	0.0380 m^3/m^3

Efficiency indexes were calculated for the above simulations and are listed in **Table 4.6**. Again as seen in both **Figure 4.2** and **Figure 4.3** respectively the main source of error occurs at the onset of the sharp wetting front, though from **Table 4.6** a good correlation is still seen.

The results of these validation runs illustrate that the KWE and consequently HM07 can successfully handle the situations of sharp wetting fronts, dry initial conditions and layered soil profiles in the matrix region, conditions common to rain gardens. It was therefore decided to continue to validate HM07 for the macropore flow case.

4.4.2 Macropore Region Flow

The movement of flow through macropores is one of the most crucial aspects in relation to pollutant modelling as it quantifies the total volume of water through the pores and also the velocity of this movement. HM07 uses the KWE to model this flow. The following column experiments completed by Mdaghri-Alaoui & Germann (1998) were chosen as suitable validation cases for the macropore segment of this model as the six runs, which were performed on a layered soil, encompass a range of infiltration, conductance and exponent values (a_m, b). Runs 1-2 were classified as non-preferential flow thus only runs 3-6 are examined here and their soil characteristics are shown in **Table 4.7** below.

Table 4.7 Parameters from Mdaghri-Alaoui & Germann (1998)

Parameter	**Run 3**	**Run 4**	**Run 5**	**Run 6**
Total Soil Depth (cm)	43			
Column Diameter (cm)	39			
Upper Boundary Condition (q) (cm/h)	7.92	8.28	9.4	10.1
Duration of Infiltration(s)	4100	4500	4000	3000
a_m	4.77	4.73	4.38	5.60
b_m **(cm/h)**	1.52×10^6	1.63×10^6	0.69×10^6	15.3×10^6

Mdaghri-Alaoui & Germann (1998) undertook these experiments to examine the drainage outflow for several infiltration rates, on soil which originated from calcareous silty-sandy lake sediments. The upper layer 0-0.16 m was well structured with a porosity of 0.52 and a sandy loam texture, the lower layer below 0.16 m had a porosity of 0.5 and was sandy in consistency. The bulk density was found to increase slightly with depth.

A comparison between the KWE prediction and the experimental results for case 3-6 is shown in **Figure 4.4**.

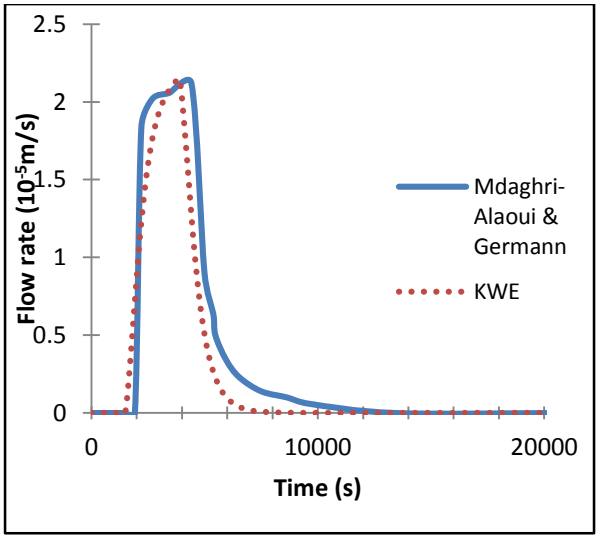

(a) Case 3

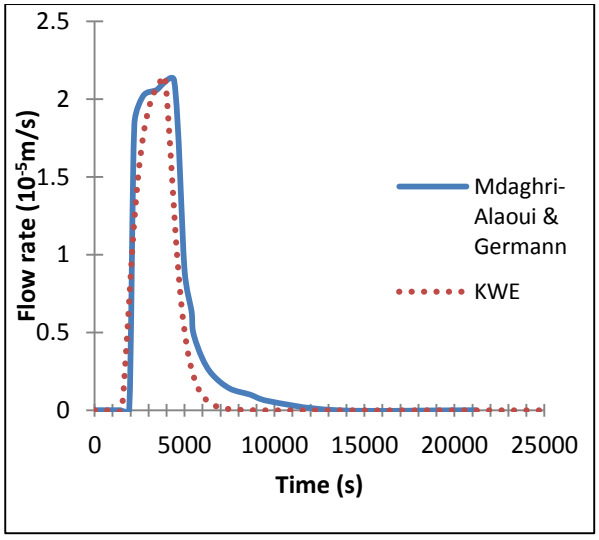

(b) Case 4

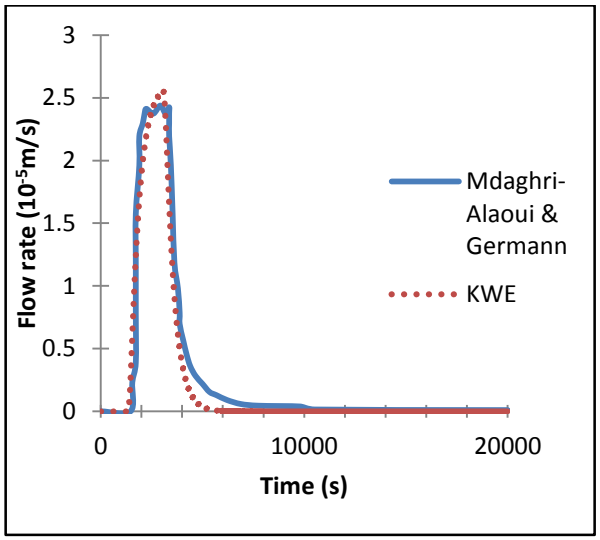

(c) Case 5

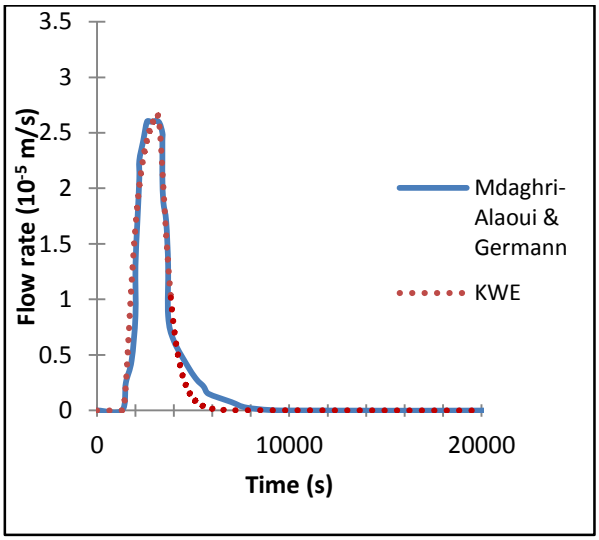

(d) Case 6

Figure 4.4 Comparison of KWE with Cases 3-6 in Mdaghri-Alaoui and Germann (1998)

The KWE accurately captured the peak flow rate (**Figure 4.4**) but failed to fully predict the drainage wave in cases 3 and 4, yet at higher input rates the correlation between the experimental and model drainage wave improved (cases 5 and 6). Despite these slight inaccuracies the R^2 value was still high (**Table 4.8**) with values of over 0.89 in all cases.

Table 4.8 Efficency Indexes for the Macropore section of HM07 (KWE) and Runs 3-6 of Mdaghri-Alaoui and Germann (1998)

Efficiency Index	Run 3	Run 4	Run 5	Run 6
Coefficient of determination	0.93	0.92	0.89	0.96
Nash-Sutcliffe Efficiency Index	0.80	0.90	0.87	0.96
Root Square Mean Error (x 10^{-5} m/s)	0.386	0.253	0.330	0.204

4.4.3 Pollutant Retention (Linear Isotherm)

The linear isotherm method used in HM07 was validated against the experimental results of Davis et al. (2001). This dataset was chosen as the experiments were specifically focused on rain garden performance. They consisted of the heavy metal retention evaluation of several small columns (3.5 cm depth) filled with topsoil (parameters shown in **Table 4.9**). Although this is not fully representative of heavy metal behaviour in rain garden, it provides a valuable preliminary validation, further validation was carried out using larger column experiment results (**Chapter 6**)

Table 4.9 Parameters from Davis et al. (2001)

Parameter	Value
Copper (Cu) Input Concentration (mg /L)	80
Depth of Column (cm)	3.5
Diameter of Column (cm)	1.9
Input Rate (cm/h)	63.6
Duration of Input (Hours)	50
Bed Volume (cm^3)	9.9
Linear Adsorption Coefficient (L/Kg)	550

Figure 4.5 shows the total concentration of Cu absorbed by the soil. It is clear from this figure that an accurate correlation between experimental and model results is seen, with only a small divergence in results after approximately 10 hours. However despite this small inaccuracy the

efficiency indexes for this simulation (shown in **Table 4.10**) display a good agreement between model and experimental data.

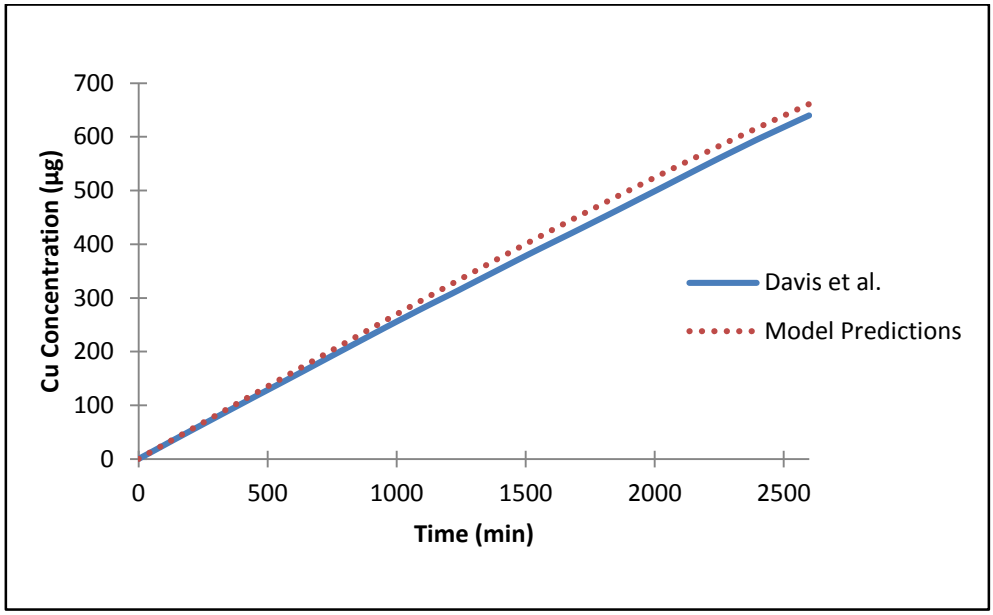

Figure 4.5 Comparison of Linear Isotherm (Model) Results for Cu Retention to Experiments of Davis et al. (2001)

Table 4.10 Efficiency Indexes for Linear isotherm (Model) and Davis et al. (2001) Results for Cu Concentration.

Error Estimator	Result
Coefficient of Determination	0.999
Nash-Sutcliffe Efficiency Index	0.993
Root Square Mean Error (µg)	16.0

4.4.4 Pollutant Retention (Langmuir and Freundlich Isotherms)

In order to validate the Langmuir and Freundlich isotherms, the results of experiments completed by the Highways Agency were used. These experiments investigated and attempted to quantify the behaviour of pollutants present in highway runoff (heavy metals and hydrocarbons) in the unsaturated zone of roadside soils (Highways Agency Research Group, 2010). This research consisted of laboratory based column studies using a synthetic highway runoff to replicate the effects of long term infiltration of pollutants through several soil types. The two principle heavy metals examined by the Highways Agency were Cu and Zn. The soils chosen were oolitic, lower greensand, lower greensand aquifer, chalk aquifer and deposits over chalk as these are the most predominant roadside soils in the U.K. Soil samples were taken

from areas of uncontaminated land and contained very little heavy metal accumulation. Altogether 32 columns were prepared (10 oolitic, 3 lower greensand, 3 lower greensand aquifer, 9 chalk aquifer and 7 deposits over chalk) and exposed to infiltration regimes that simulated 125-300 years of typical climatic conditions. The outflow from these columns was monitored at regular intervals (weekly) for a period of 4 months and measurements taken of contaminant concentrations at the outlets. This resulted in a total of 24 samples per column. Hydrodynamic and soil characteristics such as pore water velocity, bulk density, porosity, pore volume and dispersion coefficients were also measured over the time scale of a day. The computer codes CXTFIT 2.1 and CFITM were used to derive retardation factors through the use of the non-linear least squares data fitting capability of these models.

Batch studies were also completed to quantify the sorption characteristics of the soils including Langmuir and Freundlich parameters. Batch studies involve the addition of a known concentration of metal solution to a volume of soil for a specified period. At the end of this time, the concentration of the solution is measured and the adsorption capacity of the media calculated. It is noted that care should be taken when selecting the Freundlich and Langmuir parameters to use as Pang, et al. (2004) reported that adsorption parameters for heavy metals followed the order of batch>column>field. This is due to different experimental conditions relating to batch tests which do not encompass the wide variety of reactions occurring in either column experiments or the field. In batch experiments, leaching of the metals through the soil is not accounted for and this leads to an increase in the sorption parameters. Therefore it is not appropriate to use batch results to model heavy metal behaviour in the field without some sort of sensitivity analysis or safety factor. Pang et al. (2004) further confirm this by suggesting that retardation factors are inversely related to flow velocities and metal concentrations and this should be taken into account when applying laboratory results to the field. Thus it is proposed that a safety factor be applied to parameters obtained from batch and column experiments.

In addition, Pang et al. (2004) determined that flow velocity was the most influential aspects affecting non-equilibrium transport in aquifer media with increased velocity decreasing retardation factors.

Water was supplied to the column with a highly accurate flow rate ranging from .005 cm/h to 55 cm/h and the inflow concentrations for Cu and Zn were 10000 μg/L and 30000 μg/L respectively. The average hydrodynamic and characteristic parameters of the soil columns are

shown in **Table 4.11**. These soils were chosen for validation as their composition is the most similar to rain garden soil (Dussaillant, 2001)

Table 4.11 Parameters of Soils Columns

Column Description	Pore Water Velocity (cm/d)	Dispersion Coefficient (cm^2/d)	Bulk Density (g/cm^3)	Calculated Porosity (m^3/m^3)	Freundlich Parameters		Langmuir Parameters	
					K_f	a_f	K_L	S_{max}
Ooilitic Soils	7.404	1.105	1.28	.4278	687	0.81	9.29	7347
Lower Greensand Aquifer	7.175	0.507	1.53	.3325	251	0.33	10.11	1634

4.4.4.1 Freundlich Isotherm

To ensure an accurate comparison with the experimental data, a time step of 1 day and a distance step of 1cm were chosen when applying the isotherm. These were found to be the optimum values for computer performance as using smaller resolutions did not change the results of the isotherm.

A comparison of the laboratory results for Cu retention in the oolitic soil column with the predictions of the Freundlich isotherm is shown in **Figure 4.6**. As the majority of soils display excellent retention of Cu, the comparison between the Freundlich isotherm and column results are displayed in terms of % retained.

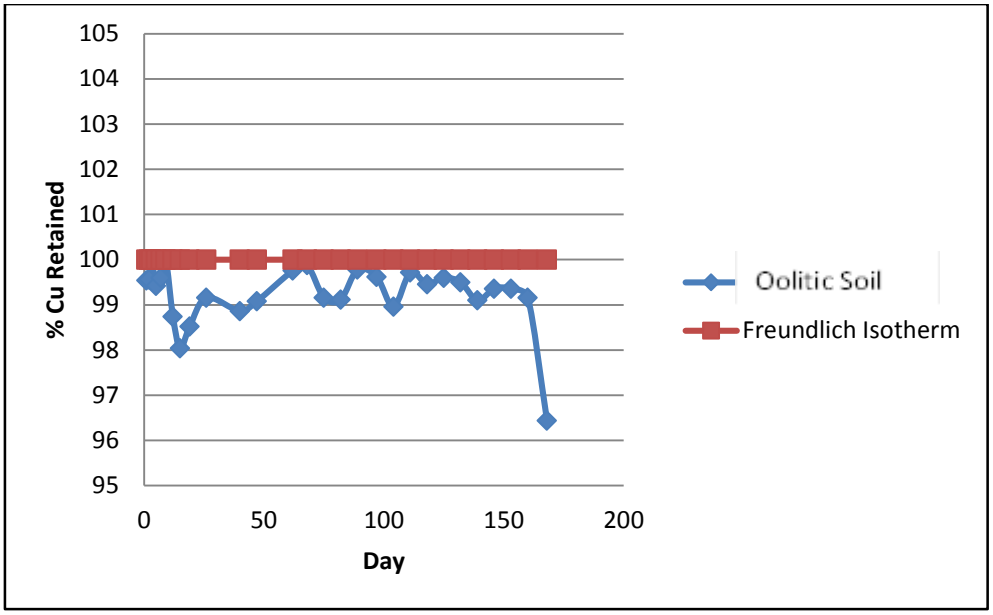

Figure 4.6 Comparison of Freundlich Isotherm with the Outflow of Cu Concentration from Column 1 (Oolitic Soils).

Oolitic soil exhibited a strong retention capacity for Cu; this is reflected well by the predictions of the Freundlich isotherm (**Figure 4.6**).

A comparison of the laboratory results for Zn outflow concentration in the lower greensand aquifer column with the predictions of the Freundlich isotherm is shown in **Figure 4.7**. As breakthrough was achieved, the results are displayed in terms of Zn outflow concentration.

In the case of the lower greensand aquifer the Zn outlet concentration increased from day 7 to breakthrough at day 97. The Freundlich isotherm gives an adequate representation of the overall trend and prediction of breakthrough (Day 75). As can be seen from **Figure 4.7** on several occasions the Zn outflow concentration is greater than the inflow concentration (30000 µg/L). This is unexplained by the report but could be attributed to either desorption of Zn from the medium or subsurface initiation of macropore flow both of which are beyond the scope of the equation used. It is also possible that particulates of Zn existed in the outflow which resulted in high Zn concentration readings, this problem could have been eliminated by repeated sampling

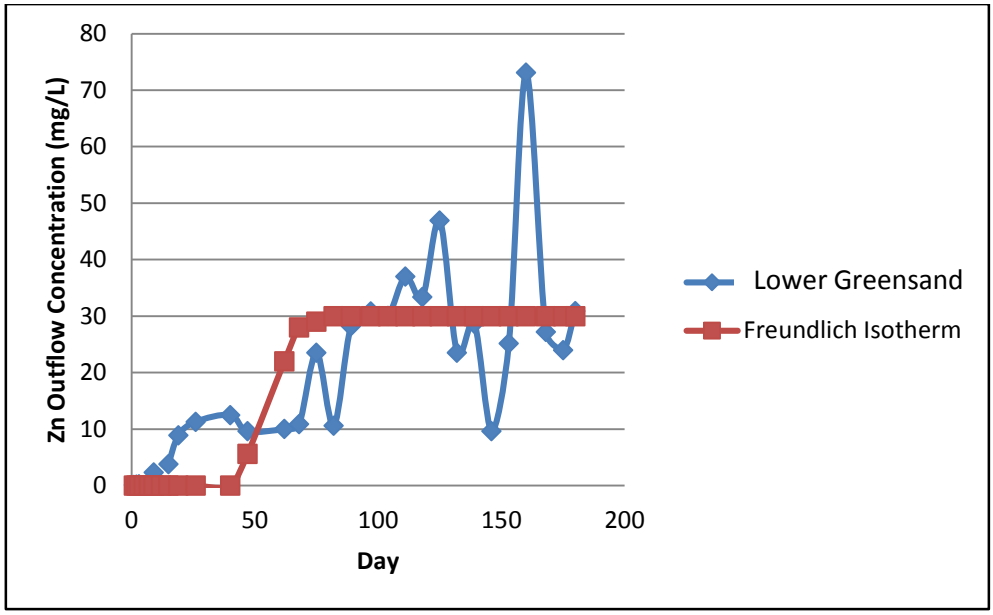

Figure 4.7 Comparison of Freundlich Isotherm with the Outflow Zn Concentration from Lower Greensand Aquifer

It is worth comparing overall column Cu output to that predicted by the Freundlich isotherm which is shown in **Table 4.12**. The total mass input of Cu and Zn is 290 mg and 870 mg respectively.

Table 4.12 Mass Output for Freundlich Isotherm

Soil	Column Output (mg)	Freundlich Isotherm Predicted Output (mg)
Total Cu Outflow Oolitic Soil	1.075	0
Total Zn Outflow in Lower Greensand Aquifer	552	534

Though some discrepancies between model and column results exist, overall when compared to the possible total mass outflow, the Freundlich isotherm gives an accurate estimate of Cu and Zn output from the columns.

4.4.4.2 Langmuir Isotherm

A comparison of the laboratory results for Cu retention in the oolitic soil column with the predictions of the Langmuir isotherm is shown in **Figure 4.9**. Oolitic soil exhibited a strong retention capacity for Cu, this is reflected by the predictions of the Langmuir isotherm.

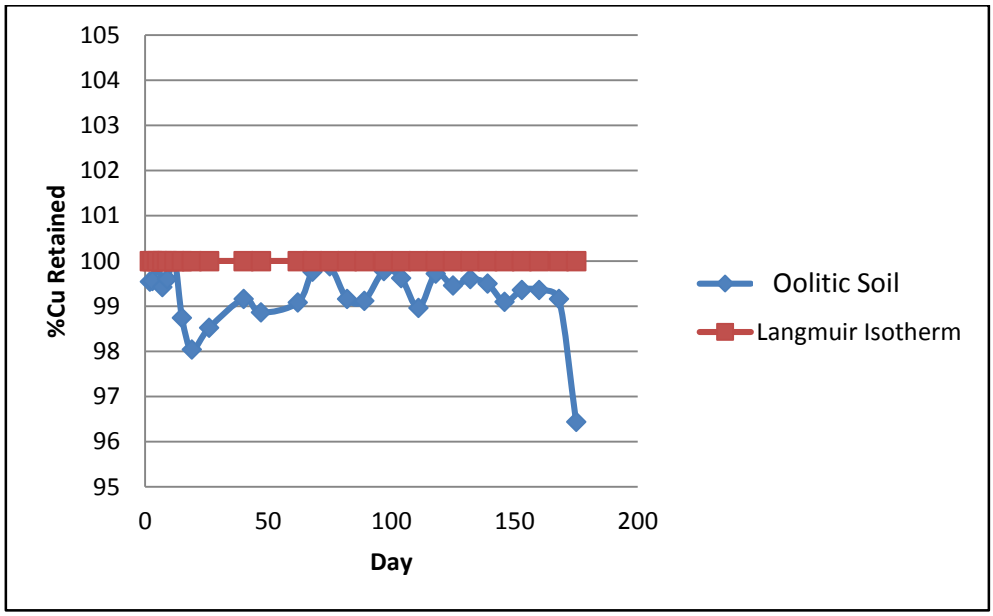

Figure 4.8 Comparison of Langmuir Isotherm with the Outflow Cu Concentration from Oolitic Soils

A comparison of the laboratory results for Zn outflow concentration in the lower greensand aquifer column with the predictions of the Langmuir isotherm is shown in **Figure 4.9**.

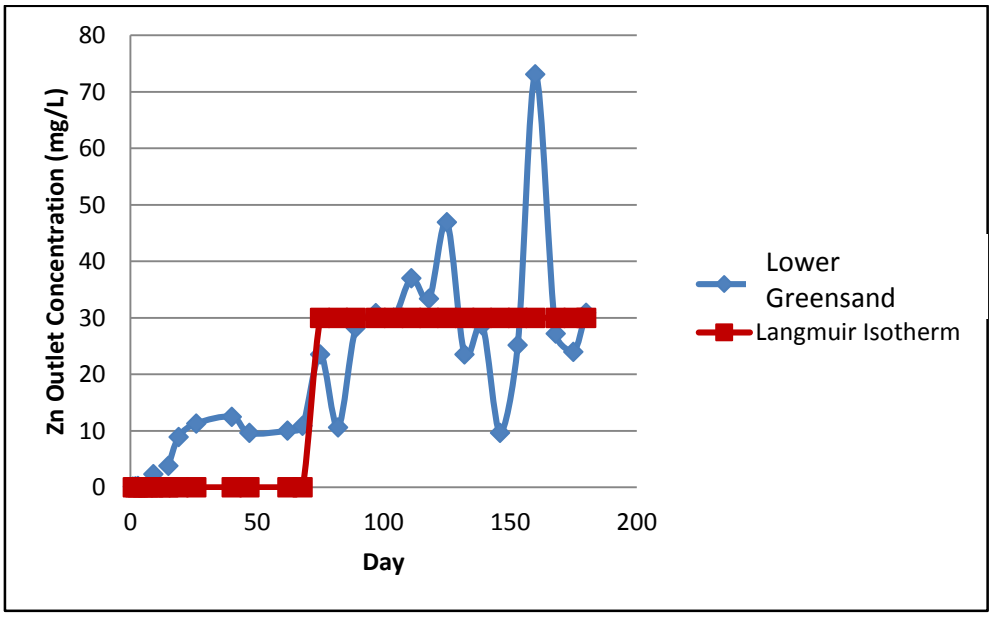

Figure 4.9 Comparison of Langmuir Isotherm with the Outflow Zn Concentration from Lower Greensand Aquifer

Again Cu outlet flow is compared to that predicted by the Langmuir isotherm which is shown in **Table 4.13**. The possible mass output of Cu and Zn is 290 mg and 870 mg respectively.

Table 4.13 Mass Output for Langmuir Isotherm

Soil	Column Output (mg)	Langmuir Isotherm Predicted Output (mg)
Total Cu Outflow Oolitic Soil	1.075	0
Total Zn Outflow in Lower Greensand Aquifer	552	480

As can be seen from **Table 4.13**, there a notable difference between the total outflow from the column and that predicted by Langmuir Isotherm for the case of Zn retention in the Greensand Aquifer (13%), this is attributed to its inability to accurately predict retention in coarse soil.

4.4.4.3 Comments on the Langmuir and Freundlich Isotherms

For both heavy metals it was found that the Freundlich isotherm marginally outperformed the Langmuir Isotherm. This was attributed to the Langmuir isotherms problems predicting retention in coarse and granular soils such as the Greensand Aquifer.

It should be noted that retardation factors were also derived from the column studies themselves in addition to the batch experiments. It was observed that the retardation factors calculated from the batch experiments were higher than those derived from the columns. This could be a factor in the inaccuracies seen when modelling the retention of Zn. This discrepancy has been reported by numerous researchers (Pang, et al., 2004; Markiewicz-Patkowska, et al., 2005; Antonisdis, et al., 2007) and has been attributed to numerous causes. The main factor has been identified as the reduction in sorption caused by a multi-element sorption system (column experiments) vs. a single-element sorption system (batch studies). The reduction in retention in multi element systems is attributed to competitive adsorption between the different metals in solution which has been discussed in **Section 3.5.10**.

4.4.4.4 Sensitivity Analysis

A sensitivity analysis was performed on a selection of columns using the Freundlich equation. Only the Freundlich equation was examined as it was proven to be the most effective at predicting heavy metal retention in soils. Two column results were chosen for examination, Cu

retention in Column 1 (oolitic soil) which was high and Zn retention in column 11 which was low. The parameters examined were pore water velocity, dispersion coefficient, bulk density and porosity.

Pore Water Velocity

The impact of varying pore water velocity on the retention of Cu is shown in **Figure 4.10**. As can be seen from **Figure 4.10** only an addition of 700% to the calculated pore water velocity resulted in a decrease in Cu retention in the column and a further 100% addition was needed to reach breakthrough. This corresponds to a velocity of 59 cm/day (+700%) and 66 cm/day (+800%) respectively. Breakthrough is defined as the time taken for outflow concentration to equal inflow concentration.

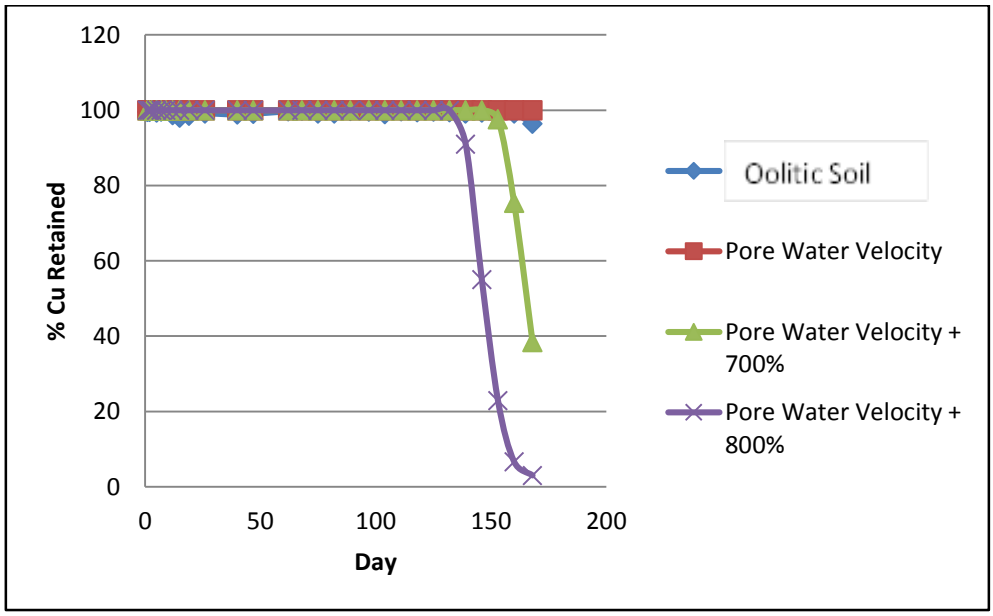

Figure 4.10 Sensitivity Analysis of Pore Water Velocity on Freundlich Isotherm Results for Cu Column 1 (Oolitic soils)

The impact of varying pore water velocity on the retention of Zn is shown in **Figure 4.11**. For the case of Zn retention, an addition of 50% to pore water velocity (resulting in v = 14.35 cm/day) can decreased time to breakthrough from day 82 to day 40. However, if the velocity is decreased by 50% (to 3.6 cm/day) the breakthrough does not occur until day 180.

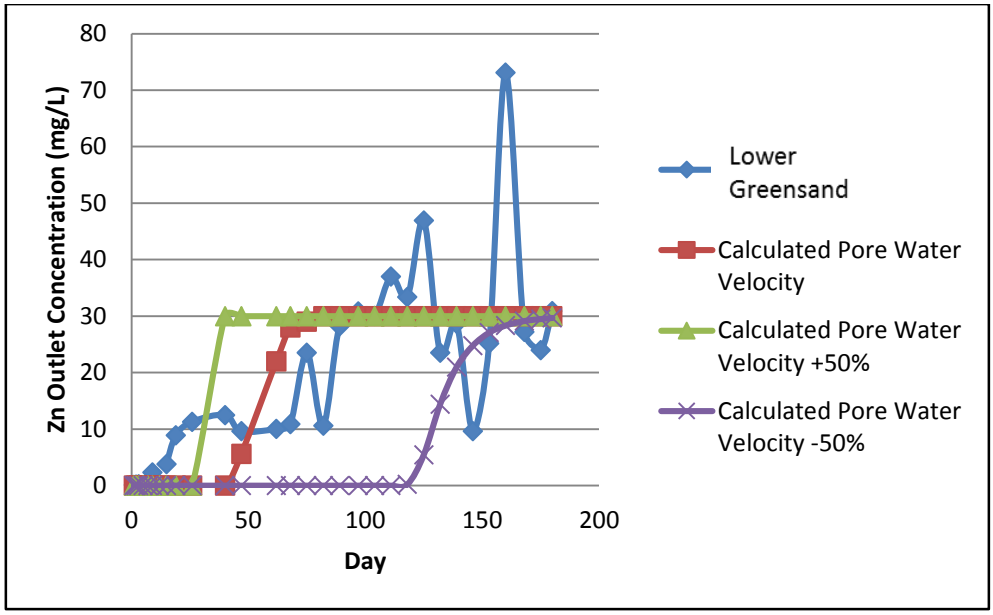

Figure 4.11 Sensitivity Analysis of Pore Water Velocity on Freundlich Isotherm Results for Zn Column 11 (Lower Greensand Aquifer)

Dispersion Coefficient

For both cases examined, the dispersion coefficient only had a minimal effect <10% increase on retention when it was increased by a factor of 1000%, thus it will not be examined further here.

Bulk Density

The impact of varying bulk density on the retention of Cu is shown in **Figure 4.12**. It was found that a reduction of 90% was required to reduce retention to near breakthrough. If the bulk density is reduced by 99% retention is almost negligible.

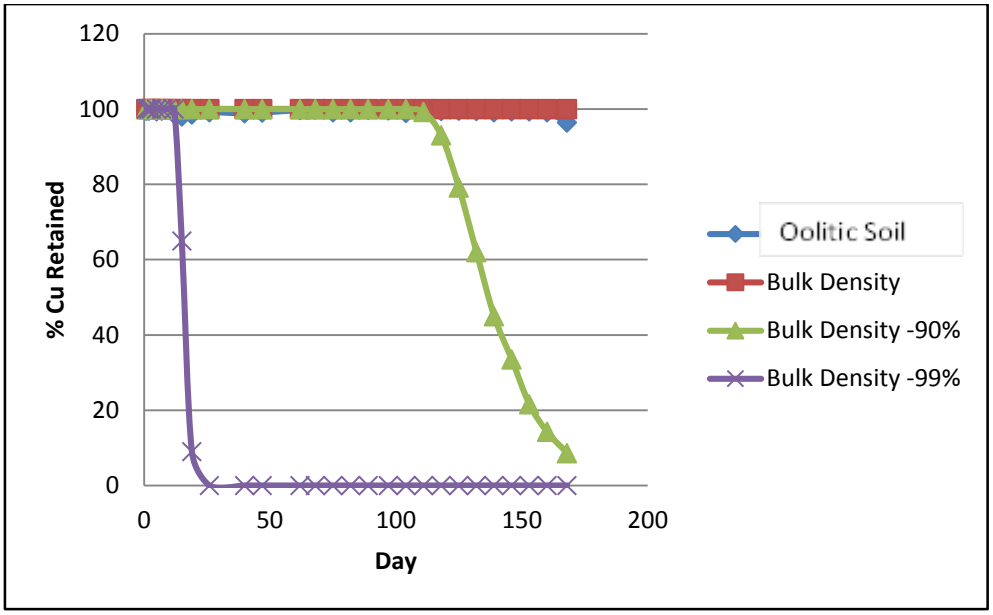

Figure 4.12 Sensitivity Analysis of Bulk Density on Freundlich Isotherm Results for Cu Column 1 (Oolitic Soil)

The impact of varying bulk density on the retention of Zn is shown in **Figure 4.13**. A reduction of 50% in bulk density resulted in a decrease in breakthrough time from day 82 to day 47. An increase in bulk density by 100% increased time to breakthrough dramatically to day 106.

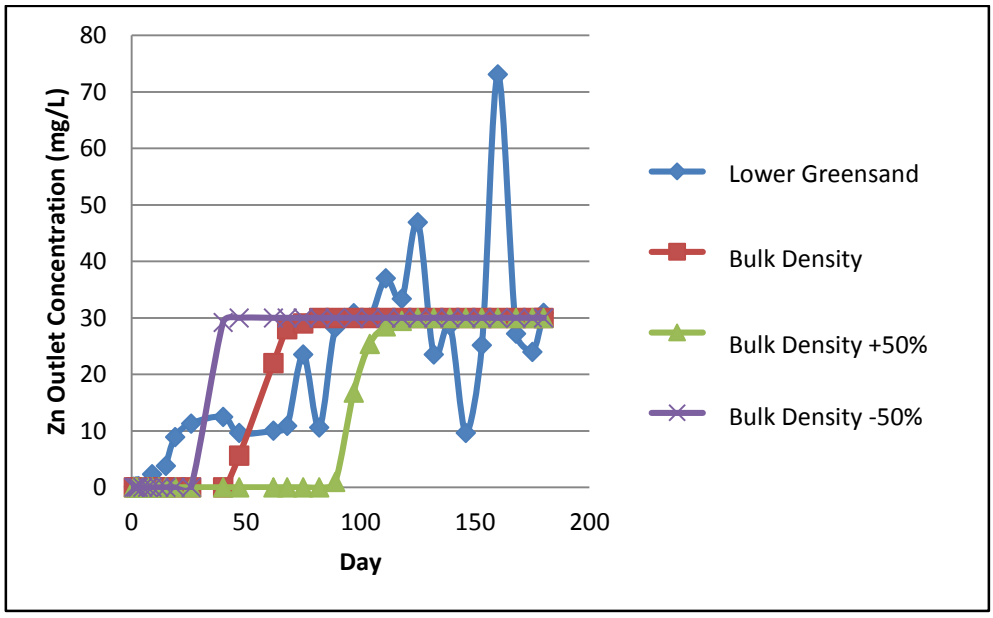

Figure 4.13 Sensitivity Analysis of Bulk Density on Freundlich Isotherm for Zn Column 11 (Lower Greensand Aquifer)

Porosity

For Cu retention, the porosity was increased and decreased by 99% however it did not have an impact on results.

The impact of varying porosity on the retention of Zn is shown in **Figure 4.14**. **Figure 4.14** shows an increase in porosity resulted in a decrease in breakthrough time from day 82 to day 62. A decrease in porosity by 50% results in a breakthrough at day 150.

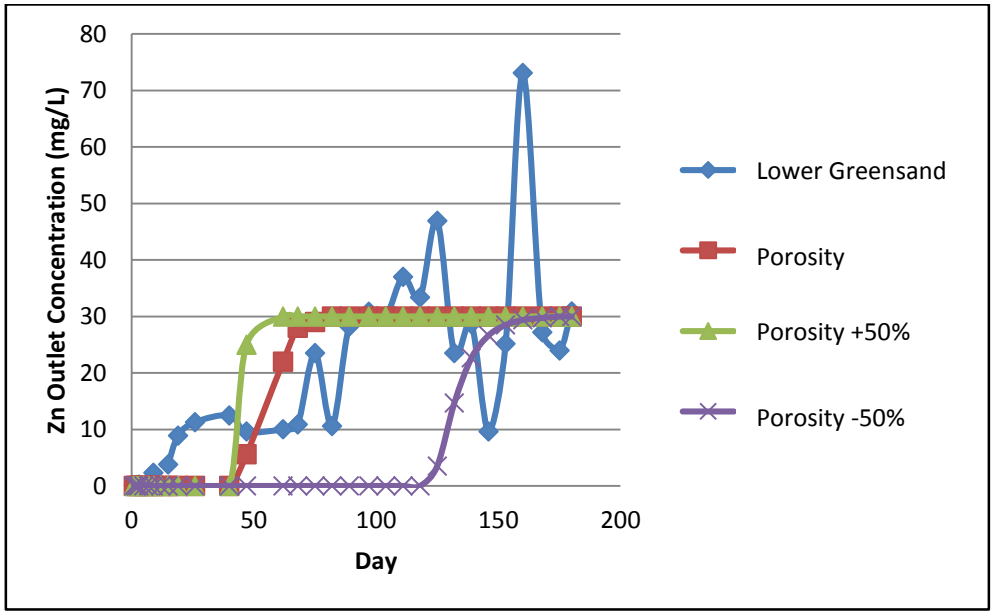

Figure 4.14 Sensitivity Analysis of Porosity on Freundlich Isotherm for Column 11 (Lower Greensand Aquifer)

Conclusions on Sensitivity Analysis

It is evident that for the case of high retention, only dramatic increases (velocity) or decreases (bulk density) had an effect on the % of Cu retained. The other factors of dispersion coefficient and porosity had no significant impact.

For Zn retention a lesser increase or decrease in values is needed to affect retention. In line with the Freundlich equation the effect of an increase or decrease in bulk density was found to be relative to the effect on retention. For velocity and porosity a reduction was seen to have a greater effect than an increase.

As stated previous the KWE is not as accurate as the Richards Equation however this inaccuracy was deemed to be unimportant as the above finding indicates that minor deviations in hydrological parameters do not greatly influence heavy metal retention. Thus the choice of the KWE has proven sensible.

4.5 Conclusion

In the above section a computer model was developed to accurately quantify heavy metal capture in a rain garden facility. This was achieved by evaluating current hydrological and pollutant retention models and selecting or adapting the method used to best suit a rain garden application for example incorporating a switchable boundary condition in the KWE. A flow chart of the proposed model is shown below (**Figure 4.15**).

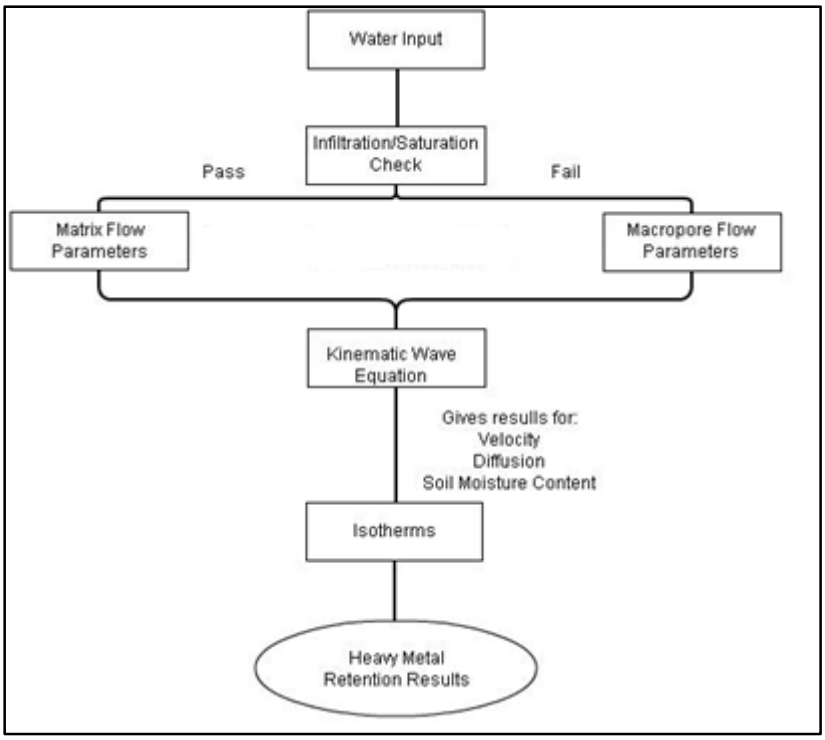

Figure 4.15 Flow Chart of Model

A summary of all the important equations and processes included in the model is shown in **Table 4.14.**

Table 4.14 Model Summary

Process	**Equation/Approach**
Model Type	Dual Permeability Model
Water flow, Matrix	Kinematic Wave Equation
Water flow, Macropore	Kinematic Wave Equation
Potential Evapotranspiration	Priestly-Taylor Equation
Initiation of Macropore Flow	Upon Ponding of the System
Solute Transport,Matrix	Advection-Dispersion
Solute Transport, Macropores	Advection-Dispersion.
Water Transfer/Solute Transfer	None as macropores only initiated upon soil saturation and transfer cannot occur when matrix is saturated.
Sorption, matrix	Linear, Langmuir, Freundlich Isotherm
Sorption, macropore	If the subsoil has low permeability and macropore flow rate restricted - Linear, Langmuir, Freundlich Isotherm Else-No Sorption

At the beginning of this chapter a number of requirements for this model were mentioned. These factors are listed in **Table 4.15** along with the aspects of the proposed composite model which fulfil them.

Table 4.15 Requirements for the Model

Model Requirements	**Proposed Model factors**
Physically based descriptions of phenomenon in porous media with readily measurable parameters	The model uses physically based descriptions of both the matrix and macropore regions. The parameters used (for matrix, K_{sat}, θ_{sat}, etc. and for macropores: *a*, *b* etc.) are measurable from experimental data and also are readily available from previous studies.
Ability to consider soil heterogeneity: at a minimum soil layering	Soil layering is considered by the model
Changeable upper boundary conditions which capture the different conditions of the soil surface i.e. ponding and different rainfall rates. Other processes should be included such as surface runoff and evaporation.	A switchable upper boundary condition is used whereby a head type is used for cases of ponding and flux is used for non-ponding events. Runoff from the device and evaporation are also considered.
Changeable lower boundary conditions which represent different situations such as groundwater table and gravity flow	A switchable lower boundary condition is used whereby a head type is used for cases of groundwater table and flux is used for cases of gravity flow.
Ability to initiate macropore flow at both surface and subsurface layers	The complete macropore network of the soil is taken into account by the value of conductance.
Inverse and/or uncertainty estimation procedures	A sensitivity analysis similar to that preformed for the Langmuir and Freundlich isotherm will be completed for all simulations which will examine the relevant uncertain parameters.

As is evident from **Table 4.15**, the model fulfilled all of the specified requirements, therefore it was used for the modelling of heavy metal transport in rain gardens. In this chapter a detailed validation of the subroutines of the model was carried out with satisfactory results. In **Chapter 6** this model was further validated using column experiments.

5 COLUMN EXPERIMENTS: DESIGN AND RESULTS

5.1 Introduction

In order to examine the retention of heavy metals in SuDS and further validate the model a series of experiments were performed. In this chapter the aim of the experiments is briefly discussed, the methodology used is detailed and finally the results shown and analysed. In a subsequent chapter (**Chapter 6**) a validation of the model with the experimental results is completed.

5.2 Aim of Column Experiments

As stated in **Section 1.3** a component of the second aim of this research was to use experiments to examine aspects of a rain garden device with respect to pollutant retention. Numerous laboratory and field experiments have previously examined heavy metal retention in a rain garden device (Davis, et al., 2001; Hsieh & Davis, 2005; Blecken, et al., 2009). However, none examined the influence of macropores on heavy metal retention; this was established as a key factor in pollutant capture in the literature review (**Table 3.1**).

Therefore, the aim of these experiments was to investigate the effect of a single artificial macropore on heavy metal retention in a layered soil column (with similar soil layout to a rain garden) under typical English climatic conditions.

Soil column experiments in both the saturated and unsaturated regimes are widely used for applied and theoretical studies in such diverse fields as transport model evaluation, fate and transport of pesticides, explosives, microbes, heavy metals and non-aqueous phase liquids. (Lewis & Sjostrom, 2010). Their popularity is due to their apparent simplicity and reproducibility (Lewis & Sjostrom, 2010). In terms of heavy metal sorption studies, column experiments have inherent advantages over other approaches such as batch studies as mentioned in **Section 4.4.4.3**. A further advantage is that column experiments work at a high solid to solution ratio close to the one encountered in a natural rain garden device (Burgisser et al., 1993). Due to these reasons, column experiments were chosen as a suitable method for examining heavy metal retention in rain garden soil.

A number of experiments have examined the effect of the presence of macropores on the transport and retention of tracers in soil. It was found that in the majority of cases the macropore acted as an active preferential pathway exclusively under saturated conditions (Lamy, et al., 2009). However numerous studies have suggested that macropore flow occurs under both unsaturated and saturated conditions (Nimmo, 2012).

To the author's knowledge only one column experiment has examined the influence of macropores on the movement of heavy metals. Camobreco et al. (1996) applied an artificial heavy metal solution to both undisturbed (containing macropores) and homogenised soil columns of length 35 cm. A rainfall of approximately 3 cm/day (unsaturated conditions) was simulated for 31.5 days. It was found that the homogenised columns fully capture the metals however the macropore columns did not. Their outflow concentrations were relatively low however at less than 30% of the input concentration. This experiment did not fully quantify the macropore flow in the undisturbed columns so it is unclear the extent to which bypass of the matrix region occurs.

This experimental study will indicate whether macropore flow typically occurs in rain gardens under both average and high intensity rainfall.

5.3 Column Experimental Design

5.3.1 Composition & Macropore Presence

The experiment consisted of five columns with length 1.2 m and diameter 0.15 m. Each with an identical substrate composition consisting of a 30 cm lower layer of coarse sand with a 60 cm upper layer of 50% compost/50% coarse sand mix by volume, an additional 30 cm was left clear at the top of the column to allow for ponding. The constituents of both the sand and the compost are given in **Table 5.1**. This composition was chosen as it reflects a typical design of rain gardens currently in use, the top layer mix of soil was also an optimum choice for heavy metal retention and water infiltration (Morgan, 2011). The sand used in the experiments of Morgan (2011) had a grain size of 220μm-2000μm which corresponds well with the coarse sand used in these experiments which had a diameter of 600μm-2180μm. This type of soil has a very high hydraulic conductivity and has been found to have high retentive capacity for heavy metals. As macropores have a 'natural speed limit', this high hydraulic conductivity may reduce the impact of macropore flow. However, this is representative of the hydrological processes in real garden device. This will be discussed in the conclusion in **Section 5.9**.

Table 5.1 Constituents of Experimental Material

Material	Description	Reference
Coarse Sand	100% Natural, uncrushed Silica Sand (Quartz) Free from silt, clay or organic matter. Geological classification: Lower Greensand, Leighton Buzzard, Beds, UK. Diameter: 1.18mm – 600μm A sieve test was performed, 96.6% of sand was passed the 1mm sieve and was retained by the 500μm sieve and 3.4% passed the 500μm sieve and was retained by the 250μm sieve. Eurocode standard sieves were used.	(DavidBall Specialist Sand, 2013)
Compost	A mix of peat moss, peat and pinebark at a ratio of 1:1:1 Chemical Composition Humic Matter: 0.7% Base Saturation: 78% Phosphorus: 199 mg/L Potassium: 100 mg/L Cu < 50 mg/kg Pb < 50 mg/kg Zn <150 mg/kg	(North Carolina Department of Agriculture, 1995; Waste & Resources Action Programme, 2011)
Note: The compost consisted of peat moss, peat and pinebark. The pinebark had a maximum length of approximately 5cm. Any large clumps of peat were broken up when filling the columns.		

A common problem for column experiments is sidewall flow. Sidewall flow is the preferential movement of water along the column wall-soil interface bypassing the material contents of the column. In order to mitigate this effect several approaches were used:

1. The column walls were roughened using coarse sand paper to optimize soil-column wall adhesion as recommended by Smajstrla (1985).
2. Silicone rings were installed at 30cm intervals on the interior surface of the column prior to the addition of soil as recommended by Corwin (2000). This redirects sidewall flow away from the column walls if it occurs.
3. The columns were filled by the method of slurry packing, this both minimizes sidewall flow as it eliminates the air pockets at the soil column-interface and also ensures homogeneity of the column material. This method was deemed best practice by Oliveira et al. (1996) and Lewis & Sjostrom (2010).

Two of the columns contained artificially created macropores which extended through both upper and lower layers of soil. These were of 1 cm in diameter in accordance with previous solute transport experiments (Allaire-Leung, et al., 2000). These macropores were created by inserting a metal rod through the length of the column from top to bottom following the procedure of Kay et al. (2005). In order to prevent collapse, this insertion process was completed before each experimental run. It was observed that the rod was easily inserted into the substrate each time indicating that collapse did not occur

In summary, two sets of columns were created, three with normally packed homogeneous soil (Matrix Columns) and two with preferential pathways (Macropore Columns).

5.3.2 Input Metals

The metal contaminants in the input solution for all columns were identical as Cu, Pb and Zn as these are the most common metals present in urban storm water and also have the greatest detrimental effects on the environment as discussed in **Section 3.5** (Brown, et al. 2000; Davis, et al. 2001).

With regards to metal concentration, high values (compared with stormwater heavy metal concentrations) were chosen, 10000 µg/L Cu, 10000 µg/L Pb and 30000 µg/L Zn. These values are identical to those used by the Highways Research Group (2010) and were chosen as it allowed the examination of a large quantity of heavy metal inflow in a short amount of time.

For example the Highways Research group examined approximately a heavy metal input amount equating to a 100 year duration in a six month period.

5.3.3 Conditions

In these experiments it was decided to replicate two common scenarios present in rain gardens i) average and ii) first flush rainfall. Therefore, two separate experimental simulations were carried out which are discussed below.

Average Flow

The average flow replicates a relatively low water input rate for a relatively long period of time (5 hours). This input water rate was determined using data from a weather monitoring station located at Heathrow. **Figure 5.1** below shows the total annual rainfall as a function of intensity.

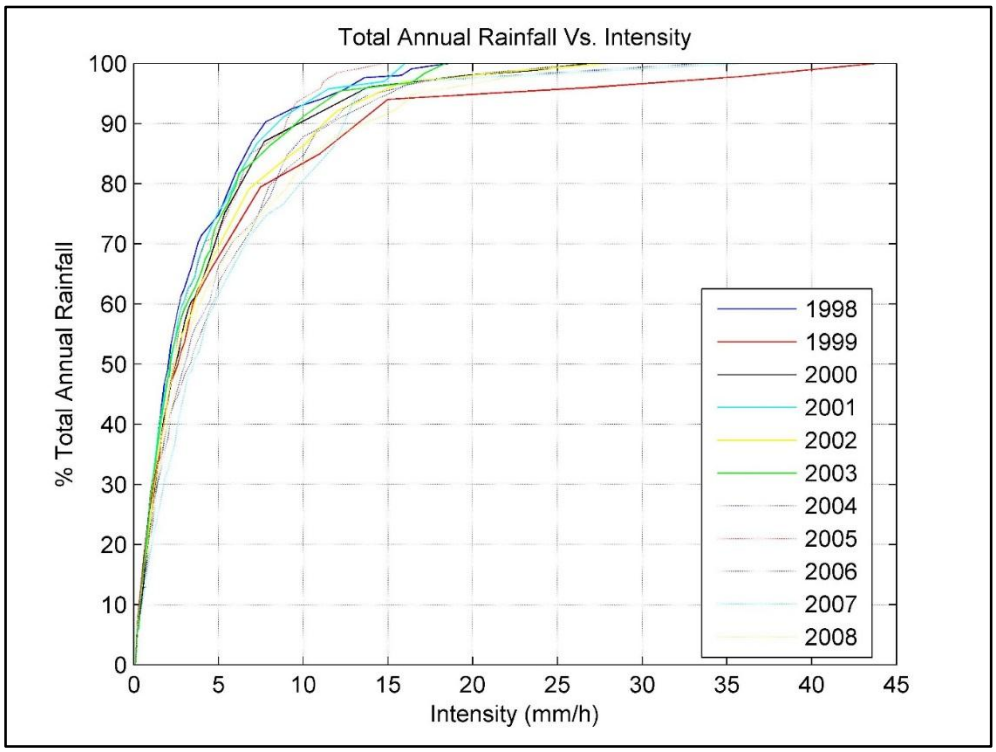

Figure 5.1 Hourly Rainfall at Heathrow Weather Station from 1998-2008

From **Figure 5.1** the average rainfall amount was decided at 10.9 mm/h (circa 90% of total annual rainfall). This was determined to be an adequate reflection of a high average rainfall in the London area. The average input into a rain garden is much higher however as it receives runoff from the impervious surfaces around it. The area ratio of rain garden to impervious surface (see **Section 2.6)** was chosen as 10% as this was found to yield the most beneficial

results in a climate such as that of the U.K (Dussaillant, et al., 2005). This results in a total water input of 120 mm/h.

First Flush

The first flush experiment simulated conditions where there was an extremely high intensity rainfall following a long period of dryness. In this case the columns were allowed to drain for a period of days prior to the start of the experimental run. The value of this high intensity rainfall was again determined using data obtained from a weather monitoring station at Heathrow as shown in the **Figure 5.2** below.

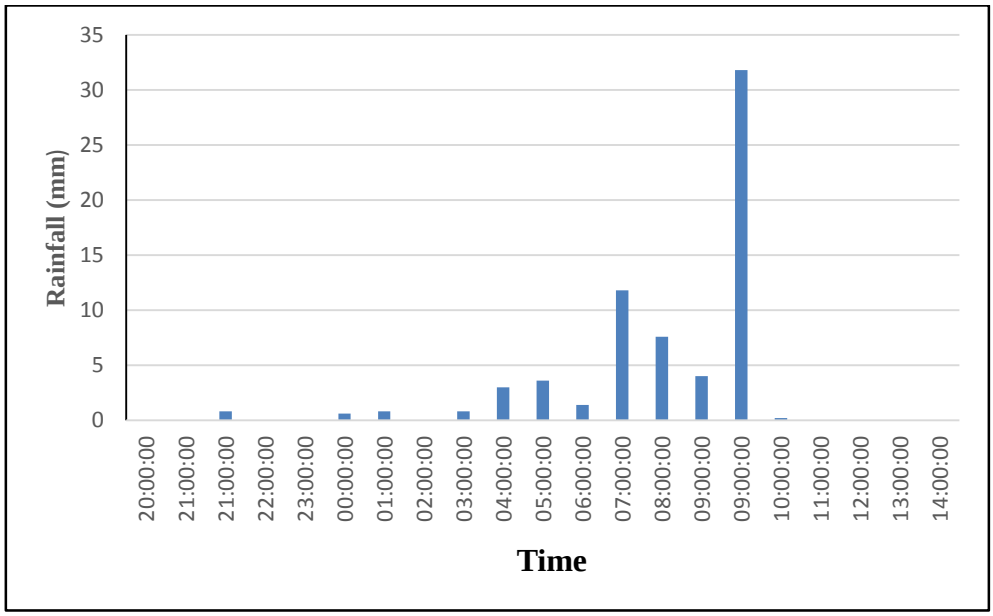

Figure 5.2 Hourly rainfall (mm) at Heathrow from 13/10/04 to 14/10/04

The highest observed rainfall rate was 31.8 mm/h thus a column input rate of between 0 and 31.8 mm/h for 1.5 hours was chosen. As stated previously an area ratio of 10% was chosen so this equates to a column inflow of 350 mm/h. This inflow provided a close to soil saturation scenario for examination of macropore flow activity.

5.3.4 Instrumentation

A number of sensors were installed throughout the columns. In order to measure soil water content eight CS645-L 3-Rod 7.5cm time domain reflectometry (TDR) probes were installed through three of the columns (Column 1 (Macropore Column), Column 2 (Matrix Column) and Column 5 (Macropore Column)). The probes function as a wave guide with reflections of the applied signal along the wave guide happen when the impedance changes. The impedance is directly related to the soil moisture content thus changes in this value result in changes in the

shape of the reflection (Campbell Scientific, Inc., 2010). The shape of the reflection therefore contains the information required for calculation of the water content.

The probes were inserted vertically through specially designed openings in the columns' walls following the procedure detailed by Campbell Scientific, Inc. (2013). Care was taken to minimize soil compaction around the rods as this can lead to errors in the measurements.

To measure water head, eight 229-L water matric potential (WMP) sensors were installed throughout three of the columns (Column 1 (Macropore Column), Column 2 (Matrix Column) and Column 5 (Macropore Column)), as close as possible to the TDR probes so that the values obtained were at consistent locations. A diagram of the columns and sensor positions is given in **Figure 5.3**. These sensors used a heat dissipation method to indirectly measure water head and so required a constant current source. A CE8 current excitation module was used in these experiments.

The sensors were coated in silica flour before insertion into the columns to ensure good contact between soil and sensor. They were installed following the procedure of Campbell Scientific, Inc. (2009).

The water outflow rate from the base of each column was measured using a tipping bucket rain gauge (Two Environmental Measurement Ltd. Golden River 2 mm tip rain gauges, one Texas Instrumentation TR-525M rain gauge, one ADCON RG1 rain gauge and one ONSET 2 mm tip rain gauge). Tipping bucket rain gauges consist of a funnel that collects and channels the precipitation into a small seesaw-like container. After a pre-set amount of precipitation falls, the lever tips, dumping the collected water and sending an electrical signal which is recorded by the datalogger.

The TDR probes, WMP sensors and rain gauges were connected to a datalogger where their measurements were stored.

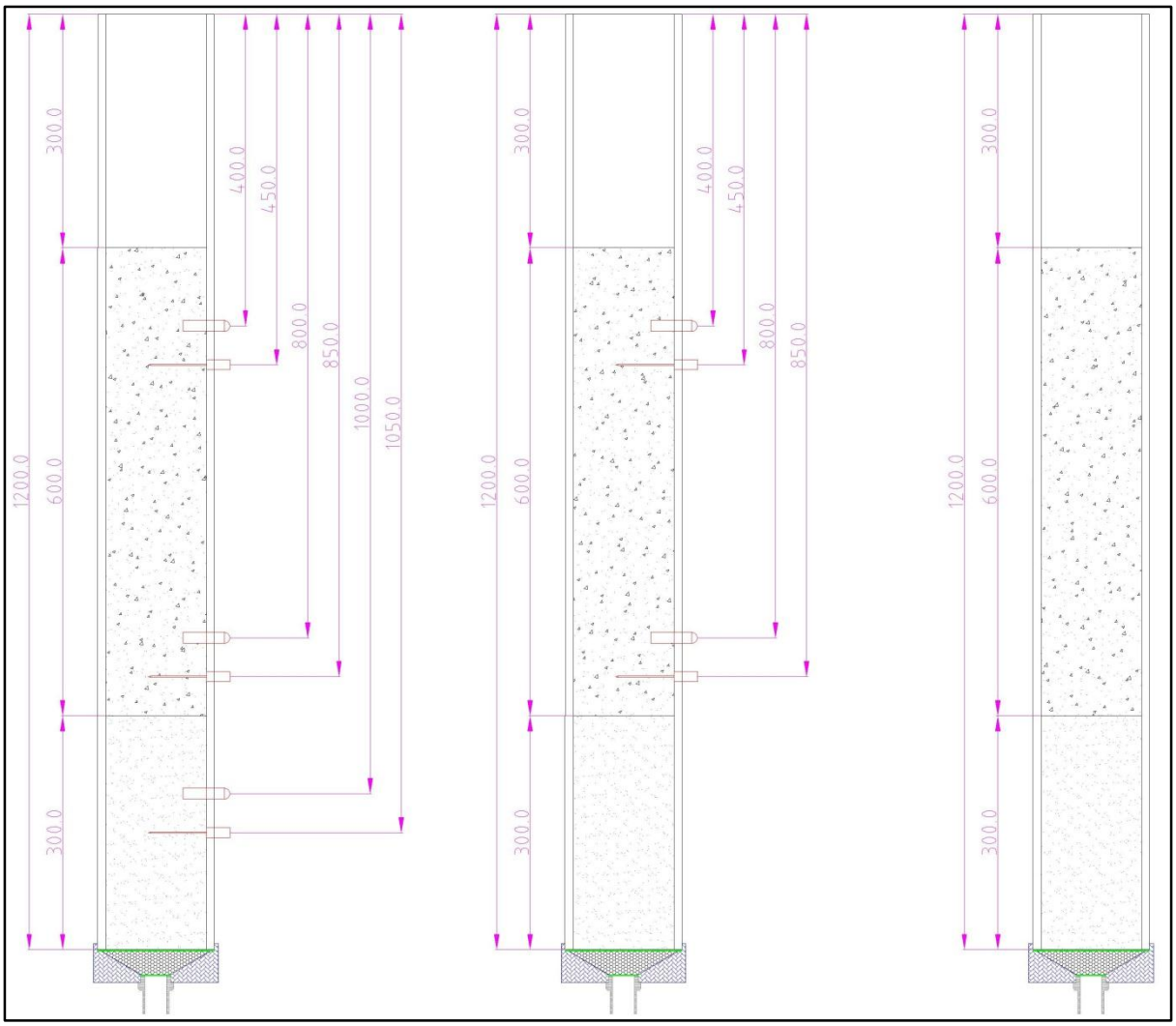

Column 2 (Matrix) Column 5 (Macropore) (Instrumented Columns)

Column 1 (Macropore) (Instrumented Column)

Column 3 (Matrix) Column 4 (Macropore) (Not Instrumented Columns)

Figure 5.3 Diagram of Column Experiments. All units in mm.

5.3.5 Calibration of Instrumentation

Both types of sensors required calibration before use.

The TDR probes were calibrated using the Campbell Scientific software programme PCTDR. For each probe the waveform length is adjusted until an accurate and clear reading is obtained. The waveform lengths vary slightly between probes so this calibration is necessary. Further

information regarding this method is available from Campbell Scientific, Inc. (2010). An example of the calibration procedure is contained in **Appendix C1**.

The WMP sensors were calibrated by inserting them in a column with the soil/sand mix or sand (depending of their respective location). An ELE International jet fill 300mm long tensiometer which gave water head measurements was inserted at a similar depth to the sensors. The column was then saturated and allowed to dry. Readings were taken of the tensiometer and WMP and compared thus calibrating the sensors. Further information regarding the calibration of WMP sensors is available from Campbell Scientific, Inc. (2009). An example of the calibration procedure is contained in **Appendix C2**.

5.3.6 Programming

The TDR probes and WMP sensors both require signals for the datalogger. These signals are made possible by programming the datalogger. The rain gauges were also programmed but this was separate from the probes. The pseudocode for the programming code used is given in **Appendix C4**.

5.3.7 Tracer

To determine whether preferential flow has occurred a tracer (Bromide) was applied to the column. Its outflow was monitored using a Cole-Parmer Bromide Ion Combination Epoxy Electrode and from the breakthrough curves the degree of macropore flow was ascertained (Cole-Parmer, 2008).

5.3.8 Summary

A summary of the experimental conditions and sensor locations is given in **Table 5.2** and illustrated in **Figure 5.3**.

Table 5.2 Summary of Designed Column Experiments

Column No.	Column Title	Diameter of Column		Upper Boundary Flow Condition	Lower Boundary Flow Condition	Upper Boundary Metal Concentration Condition	TDR Positions	WMP Sensors Positions
		Internal	External					
1	Macropore	0.14 m	0.15 m	Average Flow: 10 cm/h First Flush: 35 cm/h	Free Flow Measured with Rain Gauge	10000 µg/L Cu 10000 µg/L Pb 30000 µg/L Zn	At 15cm, 55 cm, depth	At 10 cm, 50 cm depth
2	Matrix						At 15 cm, 55 cm, 75cm depth	At 10cm, 50 cm, 70 cm depth
3	Matrix						N/A	N/A
4	Matrix						N/A	N/A
5	Macropore						At 15 cm, 55 cm, 75 cm depth	At 10 cm, 50 cm, 70 cm depth

5.4 Methodology

The experimental set up is shown in **Figure 5.4** with the inflow being delivered via sprinklers with adjustable flow rates.

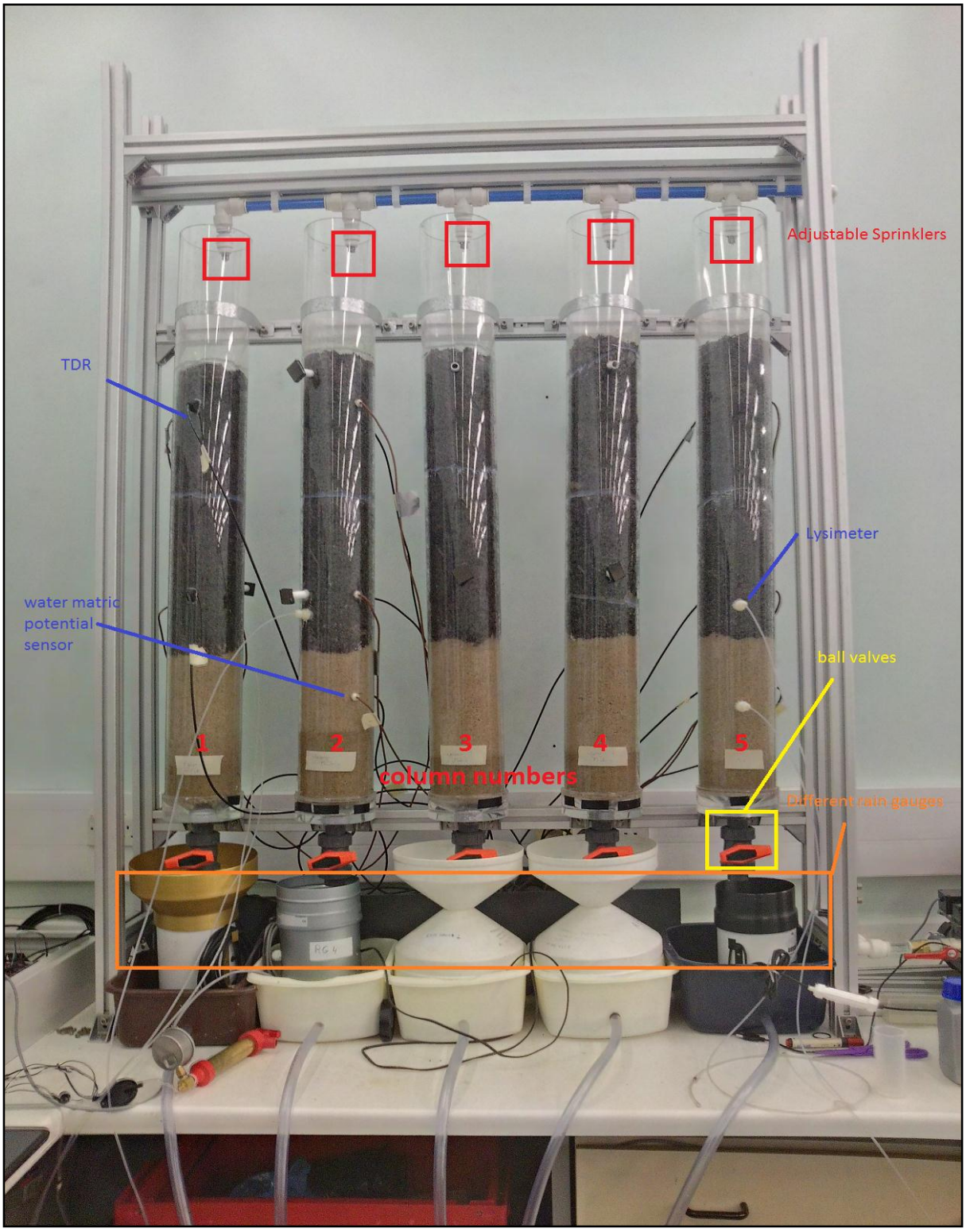

Figure 5.4 Experimental Layout

5.4.1 Average Flow Experiment

1. Solutions were prepared of 1000000 μg/L Cu, Pb and Zn using copper sulphate ($CuSO_4$), lead chloride ($PbCl_2$) and zinc chloride ($ZnCl_2$). These were then added to deionised water to create a solution of 10000 μg/L of Cu and Pb and 30000 μg/L of Zn. In addition, the tracer potassium bromide (KBr) (**Section 5.3.7**) was added at a concentration of 1000000 μg/L. This became the inflow solution. The inflow solution was added to the storage tank.
2. Before the start of the experiment initial readings were taken of temperature in the upper soil of the column using a thermometer.
3. Upon commencement of the experiment the pump was switched on and the adjustable sprinklers set to a rate of 120 mm/h. This was constantly checked throughout the course of the experiment.
4. Measurements of soil water content and water head were taken automatically at 15 minute intervals. Soil temperature readings were taken every hour.
5. One 20 ml sample of water outflow was taken on breakthrough from the base of each column and every hour subsequently. The concentration of Br in the sample was tested using a Combination Ion Selective Electrode. Nitric acid was then added to the outflow samples to preserve them and they were delivered to the laboratory for heavy metal analysis.
6. After 5 hours the inflow ceased and the final outflow samples taken. The columns were then allowed to completely drain out.
7. This was repeated on four separate days.

5.4.2 First Flush Experiment

Steps 1-6 were followed as above however the inflow rate was set to 350mm/h and the inflow was ceased after 1.5 hours. This was not repeated.

The above run of experiments were repeated two more times with the soil replaced each time. This resulted in two more experimental sets comprising of four average flow runs and one first flush run. The first set focused on examining the hydrological parameters and heavy metal outflow concentrations. The second and third experimental sets principally examined the heavy metal outflow concentrations. There were minor differences in the procedure of each of the sets, this is discussed in **Section 5.7**.

5.4.3 Heavy Metal Testing

All samples were sent to the Consultancy Laboratory at the University of Greenwich for analysis. Determinations were by ICP-MS (Thermo X series II). Calibration was via synthetic standards. The magnitude of error was 5% for this equipment and the level of detection was 0.03 µg/L for Cu, 0.01 µg/L for Pb and 0.1 µg/L for Zn (Prof D. Wray, Personal Communication, 18/06/14). This allowed for highly accurate results and the analysis of minute difference between matrix and macropore columns.

5.5 Results

5.5.1 Hydrological Results for Experimental Set 1

The aim of the experiments was to investigate the effect of a single artificial macropore on heavy metal retention in a layered soil column (with similar soil layout to a rain garden) under typical English climatic conditions. Thus it is important to ascertain whether macropore flow had an impact on the hydrological results of soil moisture content, tracer concentration and breakthrough time. General hydrological parameters are given in **Table 5.3** for comparison with results.

Table 5.3 Hydrological Parameters of the Columns

Parameter	Sand/ Soil Mix			Sand	
	Column 1 (Macropore Column)	Column 2 (Matrix Column)	Column 5 (Macropore Column)	Column 2 (Matrix Column)	Column 5 (Macropore Column)
θ_{sat} (m^3/m^3) (Saturated Soil Moisture Content)	0.466	0.491	0.467	0.306	0.343
K_{sat} (cm/h) (Saturated Hydraulic Conductivity)	77	77	77	110	110

5.5.1.1 Average Flow

The labels and positions of the TDR sensors used are listed in **Table 5.4**.

Table 5.4 Labels and Position of TDR Sensors in Columns

TDR Sensors	Column	Position
1	5 (Macropore)	15 cm Depth Soil/Sand Upper Layer
2	5 (Macropore)	55 cm Depth Soil/Sand Upper Layer
3	2 (Matrix)	15 cm Depth Soil/Sand Upper Layer
4	2 (Matrix)	55 cm Depth Soil/Sand Upper Layer
5	1 (Macropore)	15 cm Depth Soil/Sand Upper Layer
6	1 (Macropore)	55 cm Depth Soil/Sand Upper Layer
7	5 (Macropore)	75 cm Depth Sand Lower Layer
8	2 (Matrix)	75 cm Depth Sand Lower Layer

Soil Moisture Content

In order to determine whether macropore flow occurred, soil moisture results of macropore and matrix columns were examined (**Figure 5.5**).

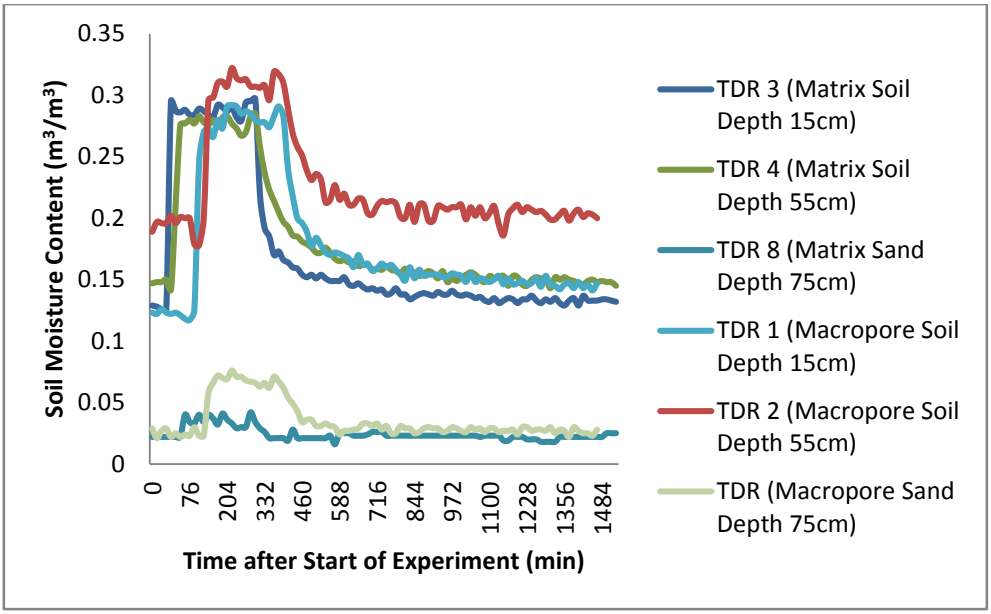

Figure 5.5 Comparison of Soil Moisture Content in Column 2 (Matrix) and Column 5 (Macropore). Run 3.

If the results are compared to the θ_{sat} values contained in **Table 5.3**, it can be seen that the soil moisture content is not near to saturation, thus macropore flow should not be expected to occur in line with other column experiments (Lamy, et al., 2009).

As can be seen from **Figure 5.5** at a depth of 15 cm and 75 cm the soil moisture contents in the columns are comparable. It is noted however that at 55 cm there is a distinct difference in the residual water content values with Column 5 (Macropore) having a considerably larger value than Column 2 (Matrix) at all times. This could be due to macropore flow or heterogeneity of the soil. In order to determine the cause of this discrepancy, the results of Column 2 were compared with the other macropore column (Column 1); the results are shown in

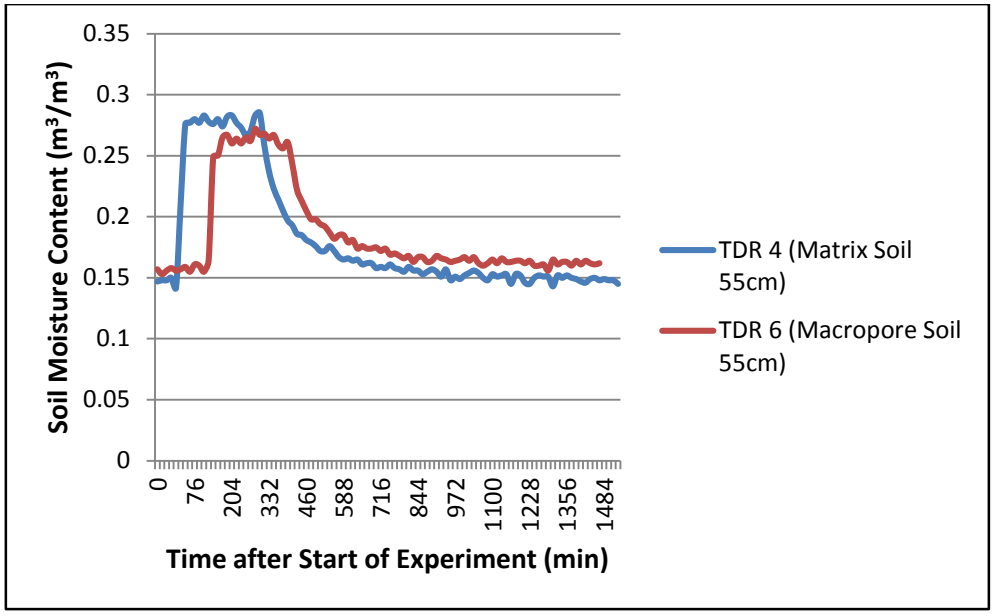

Figure 5.6 Comparison of Soil Moisture Content in Column 2 (Matrix) and Column 1 (Macropore). Run 3.

It is clear that there is no significant difference between the soil moisture contents in the macropore and matrix columns. This indicates that the previous anomalous value might be due to soil packing issues. This is supported by comparison between the TDR values at 75 cm, the soil moisture in Column 5 displays a larger result but not later in time, this indicate that there could be voids in the sand around TDR 8 resulting in the lower value. Without further instrumentation it is impossible to correctly determine the cause of this deviation, thus if any further experiments examining hydraulic properties were carried out using this equipment additional sensors would be installed in Columns 1 and 2.

As there was no significant difference between the values of soil moisture content between the columns, and saturation did not happen, this indicated that macropore flow did not occur and thus did not affect the values of soil moisture content.

Tracer Results

It was found that upon breakthrough tracer inflow concentration was equal to the tracer outflow concentration. This indicated matrix flow and no macropore or other preferential flow activity.

Water Breakthrough Times

Water breakthrough time refers to the point at which water begins to flow from the column. If there is a preferential channel through the soil, the water should typically travel quickly through it and thus will have a shorter breakthrough time than a matrix column (Jury & Horton, 2004). **Table 5.5** shows the breakthrough times for each of the columns for the four runs.

Table 5.5 Breakthrough Times for Columns for Average Flow Experiment

Average Flow Run	Column 1 (Macropore) Breakthrough Time (min)	Column 2 (Matrix) Breakthrough Time (min)	Column 3 (Matrix) Breakthrough Time (min)	Column 4 (Matrix) Breakthrough Time (min)	Column 5 (Macropore) Breakthrough Time (min)
1	35	37	39	37	43
2	37	43	47	37	44
3	47	45	49	48	47
4	41	41	47	48	48

As can be seen from **Table 5.5** there is no considerable difference in breakthrough times between the columns. On average they fall within 10% difference of one another.

5.5.1.2 First Flush

Soil Moisture Content

Figure 5.7 shows a comparison of the soil moisture content between a matrix and macropore column for the first flush experimental run. As can be seen, the values vary by a much greater degree than in the average flow experiment. This is because at higher flow rates the differences in hydraulic parameters such as saturated soil moisture content (**Table 5.3**) have a greater impact. It was thus difficult to ascertain whether macropore flow had occurred so breakthrough times and tracer results were examined.

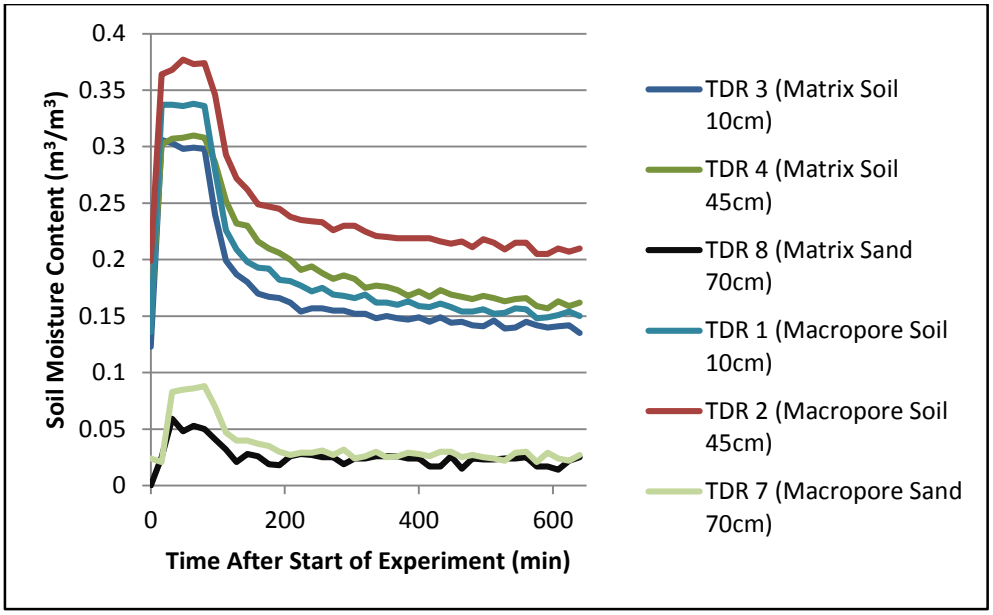

Figure 5.7 Comparison of Soil Moisture Content in Column 2 (Matrix) and Column 5 (Macropore). First Flush.

Tracer Results

It was found that similar to the average flow experiments upon breakthrough tracer inflow concentration was equal to trace outflow concentration. This indicated matrix flow and no macropore or other preferential flow activity.

Breakthrough Times

Table 5.6 shows the breakthrough times for each of the columns for the first flush experiment.

Table 5.6 Breakthrough Times for Columns for First Flush Experiment

Column 1 (Macropore) Breakthrough Time (min)	**Column 2 (Matrix) Breakthrough Time (min)**	**Column 3 (Matrix) Breakthrough Time (min)**	**Column 4 (Matrix) Breakthrough Time (min)**	**Column 5 (Macropore) Breakthrough Time (min)**
18	19	22	22	24

As can be seen from the table above, there is little difference between the breakthrough times of the columns.

5.5.1.3 Discussion

With regards to the average flow columns, water breakthrough times, tracer and soil moisture content findings indicate that if macropore flow was present it did not affect water flow in the columns. This is consistent with previous findings as the columns had not achieved saturation (Lamy, et al., 2009). This supports the possibility of complete water transfer from macropore to matrix region as discussed in **Section 4.2.2.3**.

For the first flush run, soil moisture content differed between the macropore and matrix column indicating that different flow phenomena were happening in each. This finding was not supported by the tracer and breakthrough results, however this may be related to soil compaction or characteristics (see **Section 5.5.1.2**).

It should be noted that the hydraulic conductivities of both the upper (soil/sand mix) and lower (sand) layer are very high with a saturated hydraulic conductivity value of 77 cm/h and 110 cm/h respectively. These values are properties of the soil and was calculated by examining the velocity of the wetting wave using the TDR results. It has been proposed by Nimmo (2007) that macropores in soils have a 'natural speed limit'. This limit varies depending on soil type but has been found to range from 4.16 cm/h to 250 cm/h. The minimum breakthrough times for the columns (Average Flow Run 3: 49 minutes Column 3, First Flush Run: 24 minutes Column 5) indicate that the water velocity through the columns was 110 cm/h for average flow and 225 cm/h for first flush. This is within these speed limits. Thus water could be active in the macropores, yet have the same speed as flow in the matrix region, thus would explain the similar breakthrough and tracer results yet the deviation in soil moisture content.

5.5.2 Heavy Metal Results for Experimental Set 1

The results of the average flow experiments are examined here as these were repeated four times thus allowing for statistical analysis. The results of the first flush run are shown in **Appendix D6**. Before the experiments were started, blank samples (containing no heavy metals) of outflow needed to be obtained for the heavy metal chemical analysis. This was achieved by inundating the columns with a high flow (500 mm/h) of deionised water for 1 hour. A high flow was used as this would produce a washout of heavy metals present in the substrate. Blank samples were collected from each of the columns, their ranges and averages are shown in **Table 5.7**.

Table 5.7 Blank Sample Range and Average for Experimental Set 1

Heavy Metal	Range (µg/L)	Average (µg/L)
Cu	2.06-5.56	3.07
Pb	0.76-1.04	0.85
Zn	22.30-93.45	38.88

In the following figures the results of the four experimental runs are shown and heavy metal outflow concentration is displayed as a function of experimental time (along the four runs). A summary of the initial conditions is given in **Table 5.8**. Each run lasted 5 hours, there was a period of 48 hours between Run 1 and Run 2, 96 hours between Run 2 and Run 3 and 48 hours between Run 3 and Run 4. However soil initial conditions remained similar with a small decrease in soil moisture content for Run 3 owing to the additional drying time (see **Table 5.8**).

Table 5.8 Initial Conditions for Each of the Average Flow Experimental Runs

Column	Position	Initial Soil Moisture Content (m^3/m^3)			
		Run 1	Run 2	Run 3	Run 4
Column 1 (Macropore)	Sand/Soil 15 cm	0.155	0.113	0.089	0.102
	Sand/Soil 55 cm	0.165	0.163	0.157	0.156
Column 2 (Matrix)	Sand/Soil 15 cm	0.121	0.129	0.117	0.12
	Sand/Soil 55 cm	0.146	0.147	0.138	0.145
	Sand 75 cm	0.02	0.022	0.017	0.016
Column 5 (Macropore)	Sand/Soil 15 cm	0.135	0.141	0.123	.136
	Sand/Soil 55 cm	0.193	0.2	0.197	.205
	Sand 75 cm	0.026	0.023	0.021	.024

Cu

Figure 5.8 shows the Cu outflow results for the five columns over the accumulated experimental time.

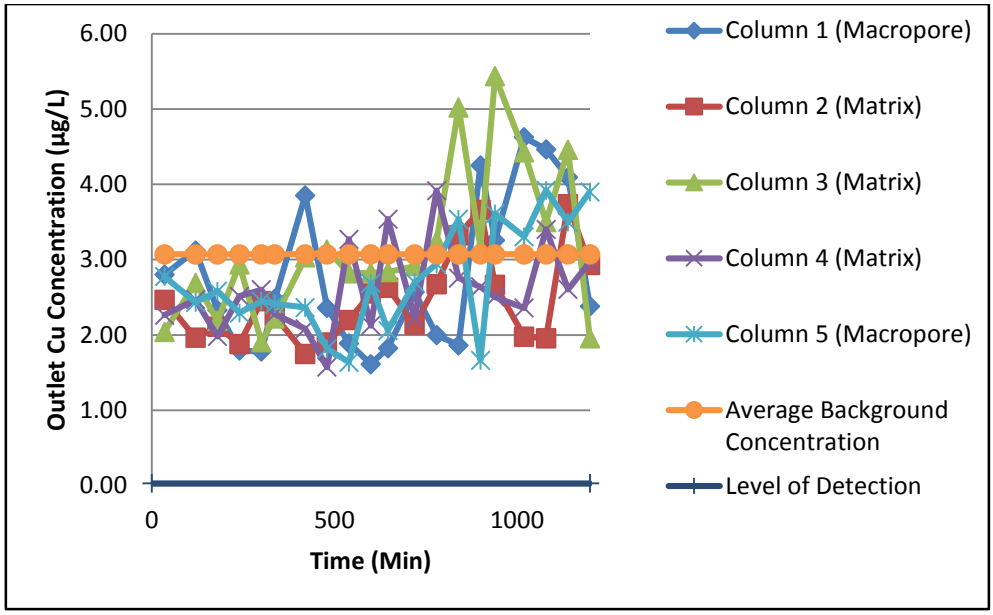

Figure 5.8 Cu Outflow Results

It is clear from **Figure 5.8** that the Cu outflow is incredibly small compared to the inflow (2-5.5 µg/L vs. 10000 µg/L). It is also evident that there is a trend of increasing outflow concentration over time.

Pb

Figure 5.9 shows the Pb outflow results for the five columns over the accumulated experimental time.

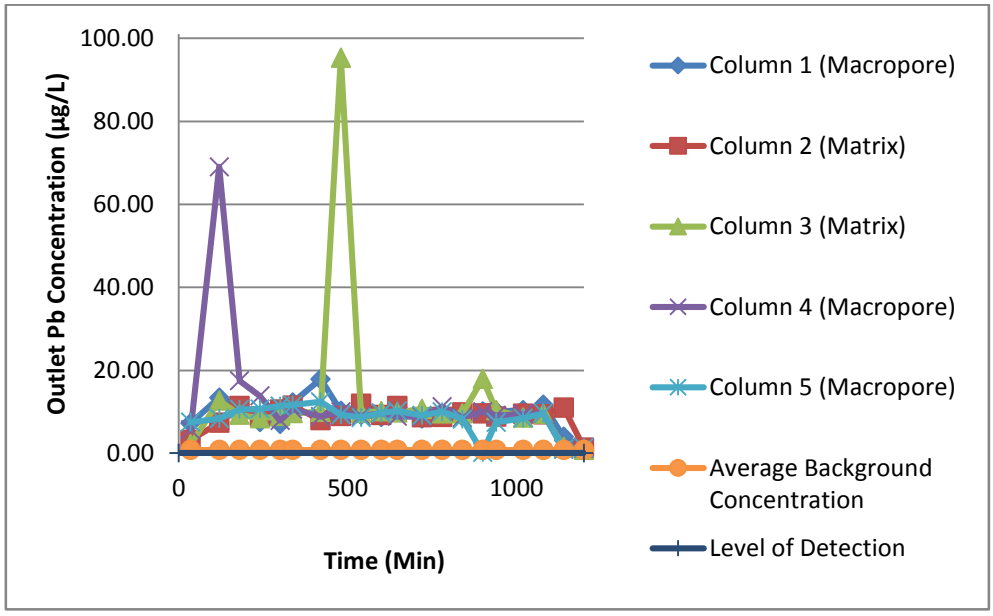

Figure 5.9 Pb Outflow Results

It is clear from **Figure 5.9** that the Pb outflow is incredibly small compared to the inflow (0.23-95 µg/L vs. 10000µg/L). There is a rapid rise in outflow concentration at the start of the experimental time following this, the results become almost constant with a slight increase. There is an unexplained decrease in Pb outflow concentration for the final sample this is attributed to human error or additional sediment present in the sample collected. The high initial values from Column 4 are attributed to early flush out of Pb from the soil. This is supported by the values of the original blank sample from this column which was 1.04 µg/L compared to an average of 0.70 µg/L for the other columns. Inconsistent results were also observed in Column 3; it was difficult to ascertain the cause of these anomalies as this column was not instrumented. However it was observed that there were numerous voids in the columns allowing for sidewall flow (a form of preferential flow).

Zn

Figure 5.10 shows the Zn outflow results for the five columns over the accumulated experimental time.

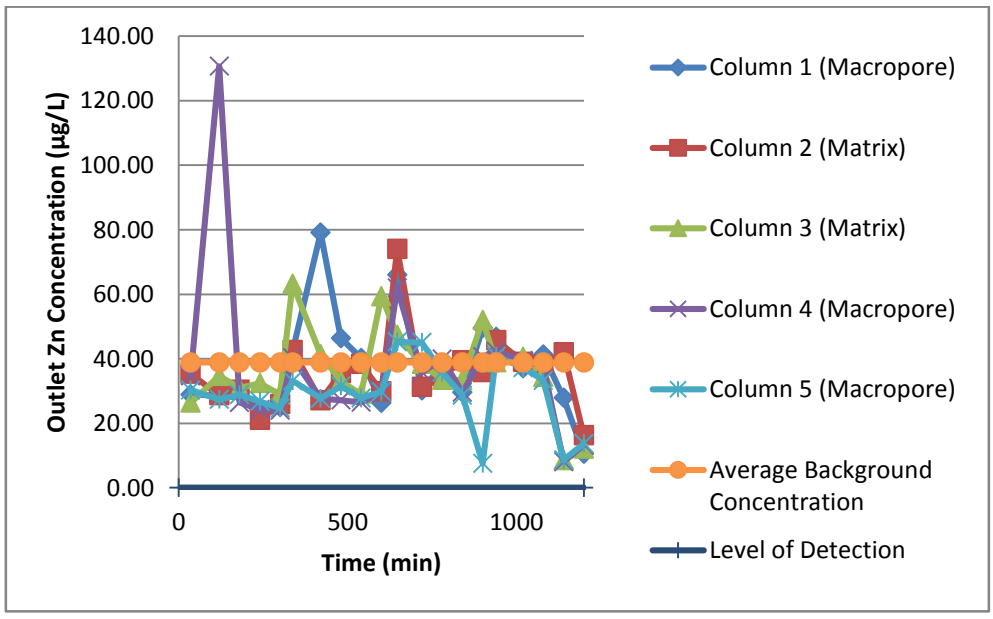

Figure 5.10 Zn Outflow Results

It is evident from **Figure 5.10** that the Zn outflow is incredibly small compared to the inflow (7-130 µg/L vs. 30000 µg/L). There is a very slight increase in concentration over time however similar to Pb, there is a decrease in outflow concentration towards the end of the experiment.

Although it is clear from the results that the columns showed excellent retention of heavy metals, it is less apparent as to whether there is a dramatic difference in outflow between the

different runs and also the different columns. This was the primary reason that statistical analysis was completed.

5.6 Statistical Analysis of Heavy Metal Results

In the following section daily average outflow concentration graphs are displayed. The error bars represent the maximum and minimum concentration values of samples in their respective runs.

Cu

Figure 5.11 shows the plot of mean outflow of the runs for the five columns.

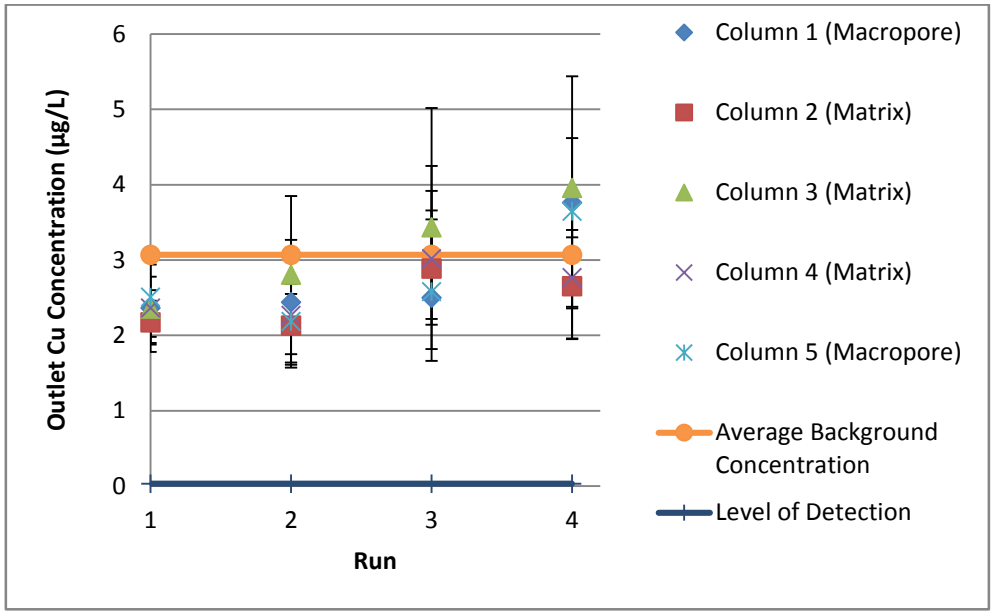

Figure 5.11 Plot of Cu Outflow Mean for the Different Columns.

The above plot clearly shows that similar behaviour can be seen in macropore columns (1 and 5) and in two of the matrix columns (2 and 4). This demonstrates that although preliminary results for soil moisture content and water outflow indicated that macopore flow did not have an impact on hydraulic parameters (**Section 5.5.1**), it did influence Cu transport.

Pb

Figure 5.12 shows the plot of mean outflow of the runs for the five columns.

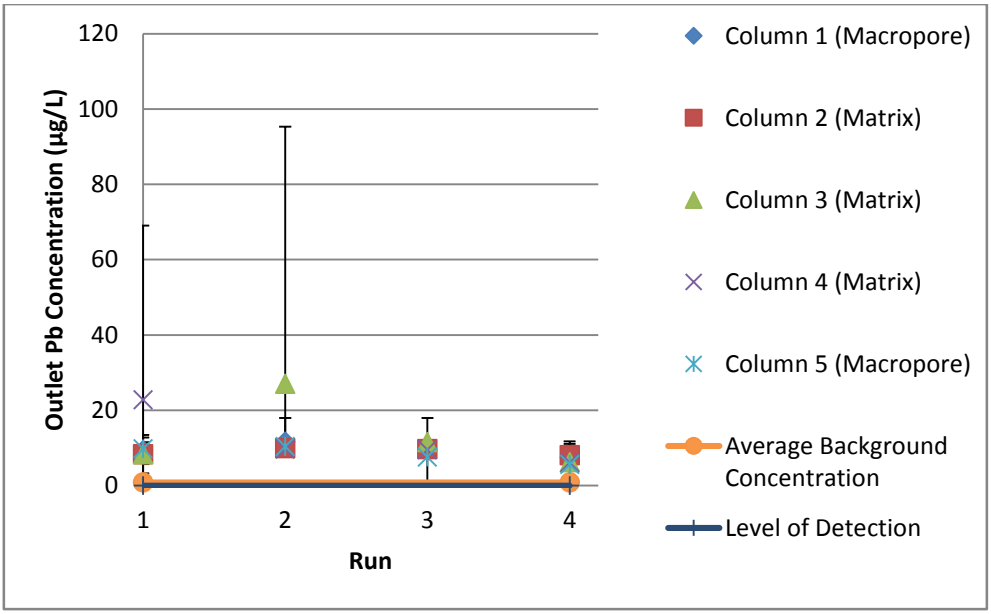

Figure 5.12 Plot of Pb Outflow Mean for the Different Columns.

For the case of Pb high similarity is observed between all columns, except for two exceptionally high concentrations for Column 4 (Run 1) and Column 3 (Run 2). This is attributed to the same reasons as discussed above for Cu. Again Column 4 had a high blank concentration of 30 µg/L compared to an average of 22 µg/L for the other columns.

Zn

Figure 5.13 shows the plot of mean outflow of the runs for the five columns.

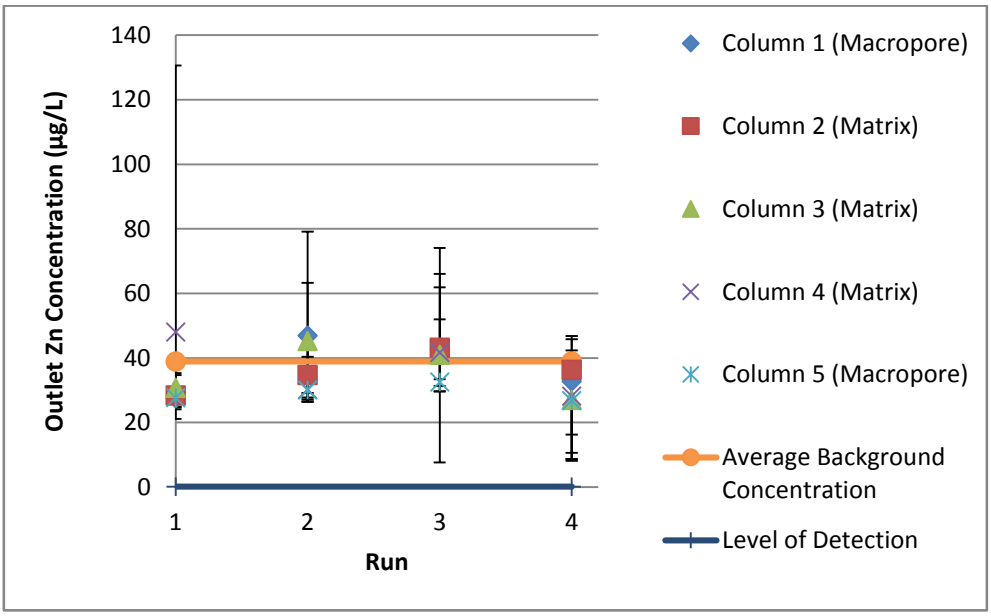

Figure 5.13 Plot of Zn Outflow Mean for the Different Columns.

With Zn there is no discernible pattern between the different types of columns.

5.6.1 T-test (P-value)

The basic t-test (or p-value testing) is the comparison of a t-distribution plot in which the null or alternative hypothesis is proven to be true. In simple terms, the t-test compares the actual difference between two means in relation to the variation in the data (expressed as the standard deviation of the difference between the means).

Two different t-tests were completed; the results are found below.

T-test comparison of columns over different days

Purpose: To compare the runs for the individual columns to investigate whether the outflow concentration increases with time.

1: State hypotheses

Null Hypotheses: Outflow concentration does not change over the runs.

Alternative Hypothesis: Outflow concentration does change over the runs

2: Formulate an analysis plan

Significance level: In accordance with generally accepted values

$P < 0.01$	Very strong presumption against null hypotheses (Highly statistically significant)
$0.01 < P < 0.05$	Strong presumption against null hypotheses (Statistically significant)
$0.05 < P < 0.1$	Low presumption against null hypotheses (Low statistical significance)
$P > 0.1$	No presumption against null hypotheses (Not statically significant)

Test method: Paired t-test – data is not independent

3: Analyse Sample Data

Cu

Table 5.9 shows the p-values for the different columns over the experimental runs for Cu. These values are derived from the t-distributions of all the outflow concentrations obtained on each of the individual runs. It is clear that although the preliminary results (**Section 5.4.2**) indicated that there is no evidence of macropore flow in any of the columns, the p-values indicate that there is a strong presumption against the null hypothesis for Columns 1 and 5

(Macropore) and Column 3 (Matrix) across the runs (comparison of Run 1-4). For Column 1 and 5 this can be due to the macropores present; it is attributed to sidewall flow in Column 3. These results further reinforce the trend indicated in **Figure 5.11**. This may be due to Cu moving through the macropore channels; Cu is the most water-mobile of the heavy metals so even if just a small concentration were present in the macropores it would not be retained to the same extent as in the matrix region as macropores have a lower retentive capacity.

Table 5.9 P-values for Experimental Runs for Cu.

Column	Run 1-2	Run 1-3	Run 1-4	Run 2-3	Run 2-4	Run 3-4
Column 1 (Macropore)	0.7020	0.8339	**0.0211 Significant**	0.9314	**0.0172 Significant**	0.1903
Column 2 (Matrix)	0.7186	**0.0534 Low Significance**	0.2542	**0.0099 High Significance**	0.1175	0.1903
Column 3 (Matrix)	**0.0965 Low Significance**	**0.0238 Significant**	**0.0319 Significant**	0.2012	0.1660	0.4908
Column 4 (Matrix)	0.6889	0.1891	0.2063	0.2008	0.2895	0.3640
Column 5 (Macropore)	0.1514	0.8549	**0.0088 High Significance**	0.4845	**0.0026 High Significance**	**0.0527 Low Significance**

Pb

Table 5.10 shows the p-values for the different columns over the experimental runs for Pb. In general Pb is considered to be a very immobile heavy metal in the soil columns (Li & Davis, 2008). This is supported by the findings of the p-values which predominately support the null hypothesis for each column. There was a problem however with the values obtained for Run 4 which were abnormally low compared to previous results. This explains the low p-values for the comparison of Runs 1, 2 and 3 to Run 4. There are however two p-values which reject the null hypothesis, these are predominately limited to the macropore columns (Column 1 and Column 5).

Table 5.10 P-values for Experimental Runs for Pb.

Column	Run 1-2	Run 1-3	Run 1-4	Run 2-3	Run 2-4	Run 3-4
Column 1 (Macropore)	0.953	0.9669	0.3023	0.2916	**0.0715 Low Significance**	0.4331
Column 2 (Matrix)	0.4287	0.488	0.9321	0.6065	0.3106	0.4165
Column 3 (Matrix)	0.3317	0.210	0.5097	0.4299	0.2718	0.1813
Column 4 (Matrix)	0.3336	0.3272	0.2409	0.8275	0.1404	0.1601
Column 5 (Macropore)	0.6862	0.4221	0.1527	0.2004	**0.0378 Significant**	0.2457

Zn

Table 5.11 shows the p-values for the different columns over the experimental runs for Zn. The results for the p-values in the majority of cases agree with the null hypothesis. This is attributed to the immobility of Zn in the soil column. It is observed that the outflow of Zn was very low on Run 4, which could indicate some problems having occurred such as an incorrect amount of nitric acid being added thus allowing the heavy metals to sorb to the sample bottle walls decreasing the concentration.

Table 5.11 P-values for Experimental Runs for Zn.

Column	Run 1-2	Run 1-3	Run 1-4	Run 2-3	Run 2-4	Run 3-4
Column 1 (Macropore)	**0.0777 Low Significance**	**0.0853 Low Significance**	0.3914	0.7715	0.1432	0.3044
Column 2 (Matrix)	0.1061	**0.0889 Low Significance**	0.1853	0.2291	0.7368	0.3931
Column 3 (Matrix)	0.1442	0.1010	0.6208	0.2851	0.1083	0.1578
Column 4 (Matrix)	0.4504	0.7879	0.3453	**0.0201 Significant**	0.7650	0.0872
Column 5 (Macropore)	**0.0438 Significant**	0.4740	0.8885	0.7369	0.6147	0.2476

Conclusion

It is clear from the results of the p-values that only Cu increases with time. This is to be expected; as stated the experimental duration was short and Cu was the most mobile heavy metal (Davis, et al., 2001), therefore the most likely to increase in outflow concentration over the limited time of these experiments.

T-test comparison of columns with Each Other on Same Day

Purpose: To examine whether columns with the same and different characteristics (matrix/macropore) have similar outflow concentrations i.e. are the results consistent and does macropore flow impact pollutant retention compared with matrix columns.

Step 1: State hypotheses

Null Hypotheses: Outflow concentration does not change between columns

Alternative Hypothesis: Outflow concentration does change between columns

Step 2: Formulate an analysis plan

Significance level: In accordance with generally accepted values

P< 0.01 very strong presumption against null hypotheses

0.01<P<0.05 strong presumption against null hypotheses

0.05<P<0.1 low presumption against null hypotheses

P>0.1 no presumption against null hypotheses

Test method: Unpaired t-test – data is independent

Step 3: Analyse Sample Data

Cu

Comparing Columns with Similar Characteristics

Table 5.12 shows the p-values for a comparison between columns with the same characteristics over the four runs for Cu.

Table 5.12 P-values for Columns with Similar Characteristics for Cu

	Macropore Columns	**Matrix Columns**		
	Column 1-5	**Column 2-3**	**Column 2-4**	**Column 3-4**
Run 1	0.6259	0.4613	0.2766	0.9592
Run 2	0.5704	**0.0126 Significant**	0.6785	0.1288
Run 3	0.8900	0.2904	0.7567	0.436
Run 4	0.7962	**0.0886 Low Significance**	0.7727	**0.0900 Low Significance**

It was found for the case of similar columns i.e. when matrix columns (2-4) were compared to matrix columns and when macropore columns (1 and 5) were compared to macropore columns there was no presumption against the null hypothesis. This indicated that the results of the matrix and macropore columns were consistent within their type. There was one exception however, of Column 2 compared with Column 3 for Run 2, as stated previously there were some problems with Column 3 which were attributed to sidewall flow.

Comparing Columns with Different Characteristics

Table 5.13 shows the p-values for a comparison between columns with different characteristics over the four runs for Cu.

Table 5.13 P-values for Columns with Different Characteristics for Cu

	Column 1-2	**Column 1-3**	**Column 1- 4**	**Column 5-2**	**Column 5-3**	**Column 5-4**
Run 1	0.5319	0.9722	1	**0.0523 Low Significance**	0.4941	0.3345
Run 2	0.4752	0.4038	0.720	0.8337	**0.0375 Significant**	0.8152
Run 3	0.4904	0.1645	0.3783	0.4963	0.1404	0.3646
Run 4	**0.0712 Low Significance**	0.7929	**0.0615 Low Significance**	**0.0225 Significant**	0.6161	**0.0042 Highly Significant**

It is clear that the difference in outflow concentration between macrocpore columns (1 and 5) and matrix columns (2-4) becomes significant in run 4. This is also clearly illustrated by **Figure 5.11**.

Pb

Table 5.14 and **Table 5.15** show the p-values for a comparison between the columns with similar and different characteristics over the four runs for Pb respectively.

Table 5.14 P-values for Columns with Similar Characteristics for Pb

	Macropore Columns	**Matrix Columns**		
	Column 1-5	**Column 2-3**	**Column 2-4**	**Column 3-4**
Run 1	0.7804	0.9827	0.2551	0.2579
Run 2	0.4897	0.3478	0.7257	0.3394
Run 3	0.3725	0.2968	0.3410	0.2260
Run 4	0.5098	0.5063	0.4807	0.9755

Table 5.15 P-values for Columns with Different Characteristics for Pb

	Column 1-2	**Column 1-3**	**Column 1- 4**	**Column 5-2**	**Column 5-3**	**Column 5-4**
Run 1	0.6109	0.6616	0.2867	0.3976	0.4750	0.2994
Run 2	0.3779	0.3974	0.2700	0.7163	0.3584	0.4048
Run 3	0.6712	0.2216	0.7883	0.3095	0.1464	0.3410
Run 4	0.8384	0.6651	0.6398	0.3556	0.8387	0.8622

For Pb in all cases, there is no presumption against the null hypothesis. This is attributed to the immobility of Pb in soils (Li & Davis 2008)

Zn

Table 5.16 and **Table 5.17** show the p-values for a comparison between the columns with similar and different characteristics over the four runs for Zn respectively.

Table 5.16 P-values for Columns with Similar Characteristics for Zn

	Macropore Columns	**Matrix Columns**		
	Column 1-5	**Column 2-3**	**Column 2-4**	**Column 3-4**
Run 1	0.8987	0.4133	0.3729	0.4289
Run 2	**0.0918 Low Significance**	0.1965	0.2700	0.4755
Run 3	0.3253	0.8108	0.8795	0.9232
Run 4	0.5308	0.3106	0.3895	0.9232

Table 5.17 P-values for Columns with Different Characteristics for Zn

	Column 1-2	**Column 1-3**	**Column 1- 4**	**Column 5-2**	**Column 5-3**	**Column 5-4**
Run 1	0.7406	0.1012	0.3506	0.7905	0.1102	0.3546
Run 2	0.2225	0.8865	0.1045	0.1468	**0.0609 Low Significance**	0.9494
Run 3	0.9724	0.8254	0.9010	0.3430	0.3162	0.3329
Run 4	0.6768	0.5540	0.6488	0.2869	0.9851	0.8884

For the majority of Zn case, there is no significant presumption against the null hypothesis. This is attributed to the immobility of Zn in soils (Li & Davis, 2008).

Conclusion

For the case of Pb and Zn the null hypothesis was proven. However for the case of Cu the most mobile heavy metal, it was shown that although the null hypothesis was proven for Runs 1-3, the alternative hypothesis was true for Run 4. This indicates that with increasing time and inflow the outlet concentration of macropore columns is greater than matrix columns. More research is needed into this phenomenon and longer duration experiments should be carried out in the future in order to conclusively prove that the Cu outflow increases in macropore columns over time.

5.6.2 ANOVA concept

ANOVA (ANalyis Of VAriants) is a method of comparing the means of several groups. It is used when there are more than two existing groups, for which a t-test would not give appropriate results. The groups in this case consist of the all the samples (5 samples per column per run) taken from a column on an individual run.

ANOVA comparison of results Two-Way ANOVA

Due to similarities between the one-way ANOVA test and the p-test completed earlier it was decided only to discuss the results of two-way ANOVA analysis.

The two explanatory variables for examination in this experiment were the different columns and the different experimental runs. The two way test not only indicates whether there is significant difference between the individual explanatory variables but also whether they have an influence on one another. The ANOVA results for the different heavy metals are shown in the following tables, **Table 5.18** (Cu), **Table 5.19** (Pb), **Table 5.20** (Zn).

Table 5.18 Two Way ANOVA Analysis Results for Cu Outflow

ANOVA	
Source of Variation	*P-value (Significance)*
Runs	5.58E-07 (High Significance)
Columns	0.027964 (Significant)
Interaction	0.261018

Table 5.19 Two Way ANOVA Analysis Results for Pb Outflow

ANOVA	
Source of Variation	*P-value (Significance)*
Runs	0.128651
Columns	0.544997
Interaction	0.34227

Table 5.20 Two Way ANOVA Analysis Results for Zn Outflow

ANOVA	
Source of Variation	*P-value (Significance)*
Runs	0.105281
Columns	0.467761
Interaction	0.535288

As can be seen only Cu has significant p-values for both the run and column explanatory variables. This supports the findings of both the t-test (**Section 5.6.1**) and the plot of means (**Figure 5.11**) which show that not only does Cu outflow increase over the runs but also that there is a significant difference in outflow between the macropore and matrix columns. There is no substantial interaction between the columns. It is interesting to note however that it is clear from **Figure 5.11** that the difference between the outflow for macropore and matrix columns increases with the increasing runs.

Zn and Pb do not have significant p-values for columns or interaction meaning that there is no difference between the columns and macropore flow did not increase the outflow concentration. The values for the runs however almost reach a low presumption against the null hypothesis. This contradicts what was found by the t-test (**Section 5.6.1**) and may be due to the extremely high and low outflow concentrations observable in **Figure 5.9** and **Figure 5.10** and not due to an underlying increase in outflow. In order to ascertain whether this is the case the two-way ANOVA test has been repeated for Pb (**Table 5.21**) and Zn (**Table 5.22**) for the first three runs ignoring the very low values of Run 4.

Table 5.21 Two Way ANOVA Analysis for Pb Outflow for Three Runs

ANOVA	
Source of Variation	*P-value (Significance)*
Runs	0.4844
Columns	0.480098
Interaction	0.327424

Table 5.22 Two Way ANOVA Analysis for Zn Outflow for Three Runs

ANOVA	
Source of Variation	*P-value (Significance)*
Runs	0.235367
Columns	0.433453
Interaction	0.386567

It is shown from both the above tables that the p-values have increased significantly once Run 4 was removed from the comparison. This proves that the results of the t-test are valid and Pb and Zn are retained by the columns agreeing with previous research (Davis, et al., 2003).

5.7 Results of Further Experiments

It was observed from the results of the above experiments that the outflow heavy metal concentrations were very low and did not significantly exceed background concentrations. Although it was found that the outflow concentration of Cu increased with time in the macropore columns; this outflow concentration was very close to both level of detection and background concentration. This results in a higher degree of error in analysis which may have resulted in the unexplained spikes in outflow concentration (**Figure 5.9** and **Figure 5.10**).

Therefore, the above experiments were repeated two more times with the soil replaced each time. This resulted in two more experimental sets comprising of four average flow runs and one first flush run. In order to gain a better understanding of the results obtained several changes were made to the experimental design:

1. Ph. values were taken for each of the experimental runs.
2. Blank samples were taken over a longer period of time see **Section 5.7.1.2**.
3. At every sample time, 3 samples were taken instead of one.

5.7.1 Experimental Set 2

5.7.1.1 pH Results

The pH was tested using Fisherbrand pH indicator paper litmus 2 to 12 pH. It was found that the pH ranged from 4-5 in the tank before input into the columns and 6-7 for the column outflow. This was consistent for all runs.

5.7.1.2 Blank Samples

A preliminary run was completed in order to obtain a sizeable number of blank samples and obtain a meaningful representation of background heavy metal concentration. This run was identical in duration and sampling times as the average flow runs detailed in **Section 5.4.1** except the input was pure distilled water without additional heavy metals. The blank sample range and average is shown in **Table 5.23**, the complete blank results are given in **Appendix D5**.

Table 5.23 Blank Sample Range and Average for Experimental Set 2

Heavy Metal	Range	Average
Cu	0.727-8.633	2.682
Pb	0.03-3.416	0.896
Zn	2.093-33.400	14.840

5.7.1.3 Results

Below are the results for experimental set 2 for the average flow runs. The results of the first flush run are shown in **Appendix D6**. The initial conditions for the columns were identical to those for experiment set 1 (**Table 5.8**).

Cu

Figure 5.14 shows the Cu outflow for the five columns over the experimental time.

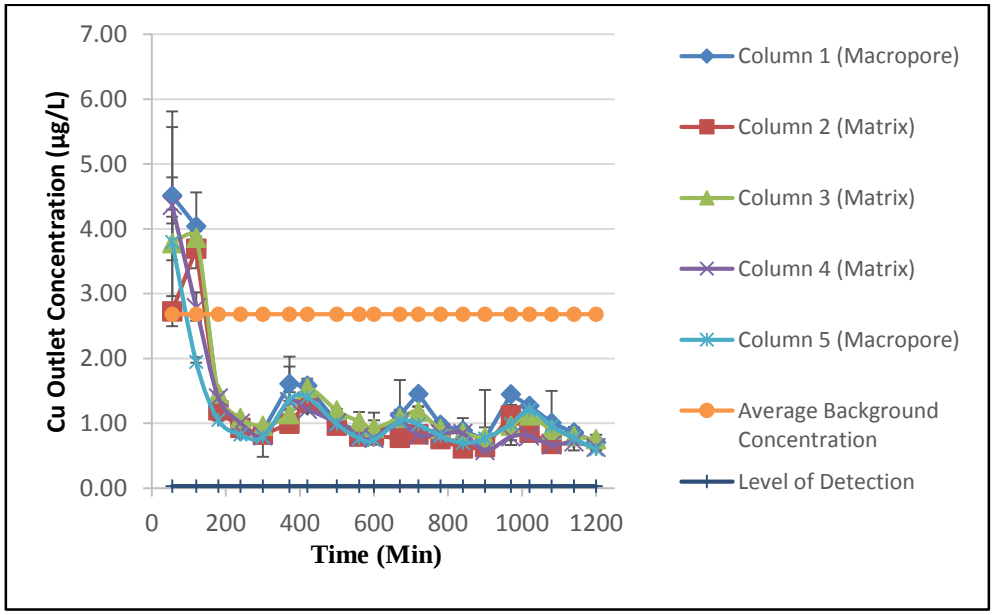

Figure 5.14 Cu Outflow Results for Experimental Set 2

It is clear from **Figure 5.14** that the Cu outflow is small compared to the inflow (0.536-5,.8 µg/L vs. 10000 µg/L). The outflow concentration remains consistent between the columns and is approximately equal to background concentration. This indicates that the inflow heavy metal concentrations are being retained in the columns.

Pb

Figure 5.15 shows the Pb outflow for the five columns over the experimental time.

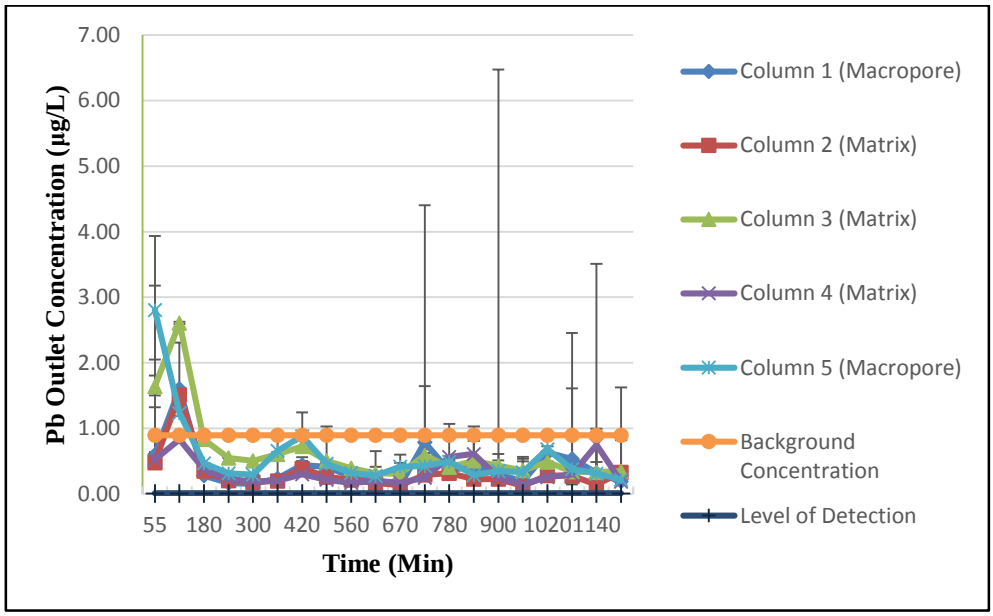

Figure 5.15 Pb Outflow Results for Experimental Set 2

Again, the outflow concentration is small compared to inflow (0.03-6.5 µg/L vs. 10000 µg/L) and the outflow concentration remains approximately to the background concentration.

Zn

Figure 5.16 shows the Zn outflow for the five columns over the experimental time.

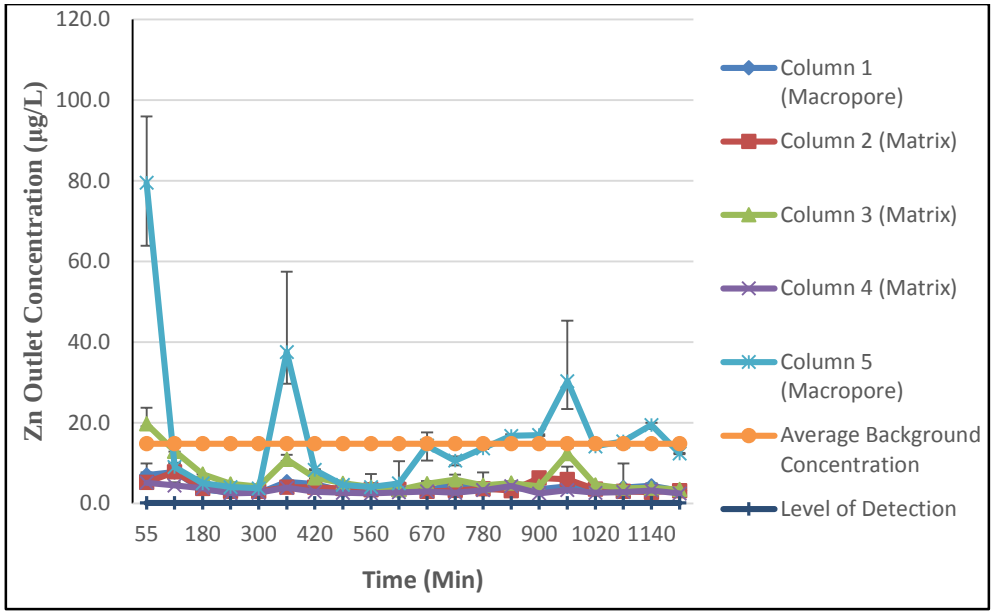

Figure 5.16 Zn Outflow Results for Experimental Set 2

Again, the outflow concentration is small compared to inflow (0.03-95 µg/L vs. 30000 µg/L) and the outflow concentration remains approximately to the background concentration.

Plot of the Means

The plot of the means for each of the heavy metal outflow concentrations, Cu (**Figure 5.17**), Pb (**Figure 5.18**) and Zn (**Figure 5.19**) supports the findings of the above.

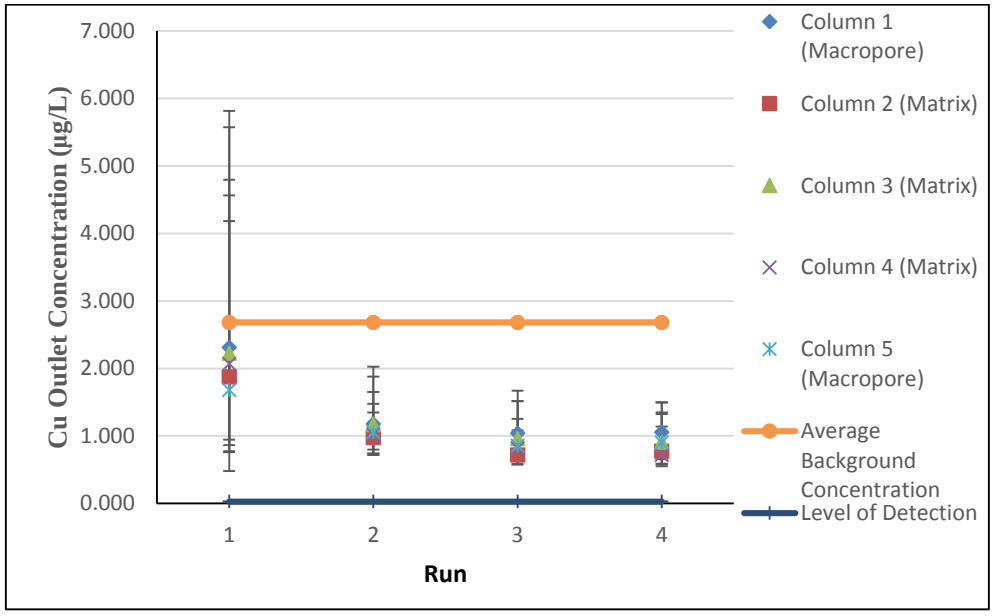

Figure 5.17 Plot of Cu Outflow Mean for the Different Columns for Experimental Set 2

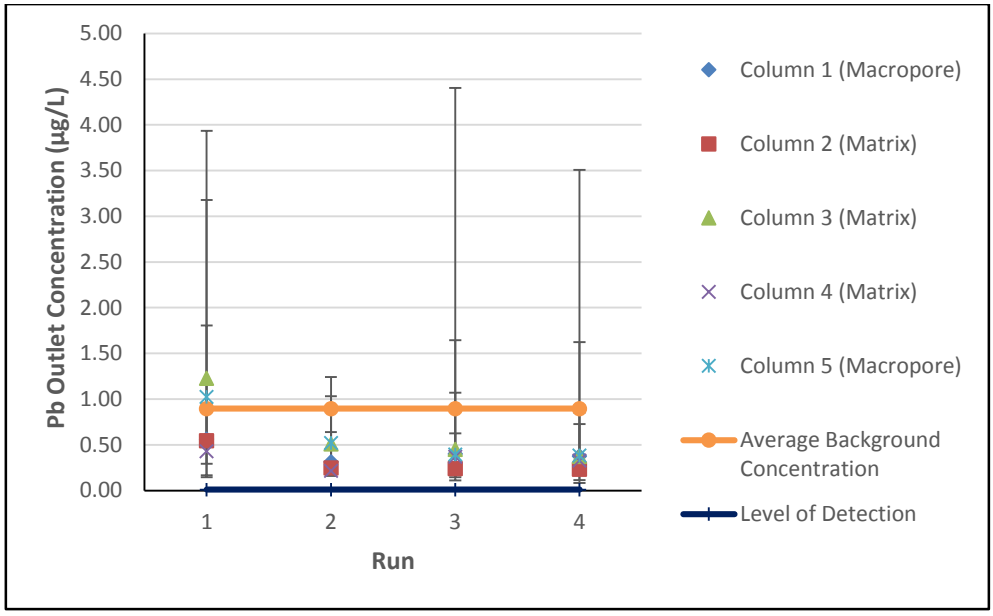

Figure 5.18 Plot of Pb Outflow Mean for the Different Columns for Experimental Set 2

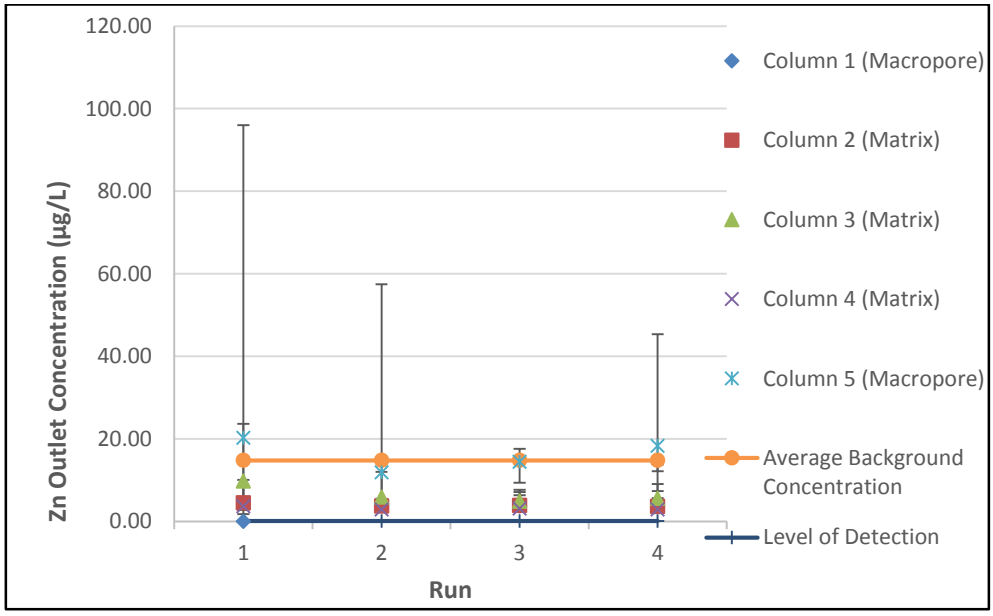

Figure 5.19 Plot of Zn Outflow Mean for the Different Columns for Experimental Set 2

Unlike the increased Cu outflow observed in Experimental Set 1, no pattern is seen from any of the heavy metal outflows in Experimental Set 2. Therefore, it is concluded that all columns retained the inflow concentration which supports previous experimental findings (Davis et al. 2001, Li & Davis, 2008). Therefore no statistical analysis was completed.

5.7.2 Experimental Set 3

5.7.2.1 pH Results

The pH was tested using Fisherbrand pH indicator paper litmus 2 to 12 pH. It was found that the pH ranged from 4-5 in the tank before input into the columns and 6-7 for the column outflow. This was consistent for all runs.

5.7.2.2 Blank Samples

A preliminary run to collect blank samples was completed in an identical fashion to that described by Section 5.7.1.2. The blank sample range and average is shown in **Table 5.23**, the complete blank results are given in **Appendix D5**.

Table 5.24 Blank Sample Range and Average for Experimental Set 3

Heavy Metal	Range (µg/L)	Average (µg/L)
Cu	1.228-7.444	3.223
Pb	0.215-2.097	0.592
Zn	3.639-132.207	22.435

5.7.2.3 Results

Below are the results for experimental set 2 for the average flow runs. The results of the first flush run are shown in **Appendix D6**. The initial conditions for the columns were identical to those for experiment set 1 and 2 (**Table 5.8**).

The outlet concentrations of Cu, Pb and Zn for the average flow runs are shown in **Figure 5.20** (Cu), **Figure 5.21**(Pb with outliers), **Figure 5.22** (Pb without outliers) and **Figure 5.23** (Zn). It is clear that in all cases excellent retention of heavy metals is observed with the outlet concentration staying approximately equal to the average blank concentration. There is also no significant difference between the matrix and macropore columns, indicating the macropores did not diminish retention.

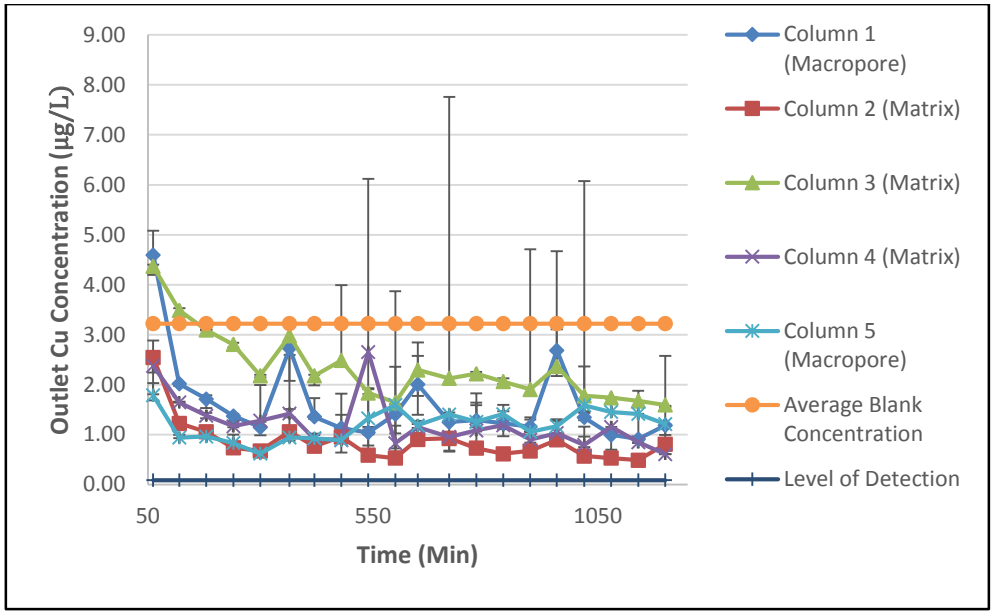

Figure 5.20 Cu Outflow Concentration for Experimental Set 3

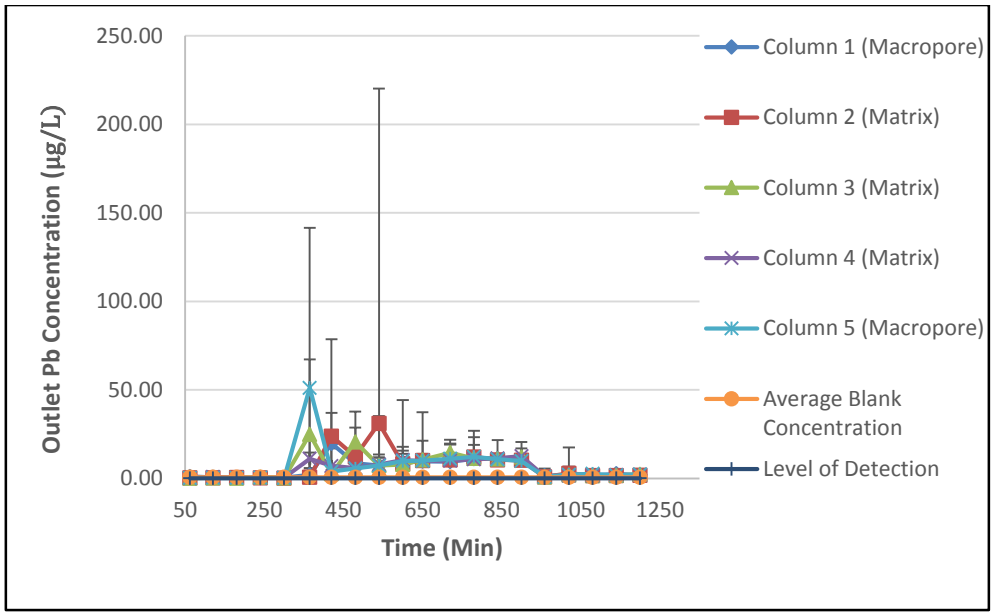

Figure 5.21 Pb Outflow Concentration for Experimental Set 3 with Outliers

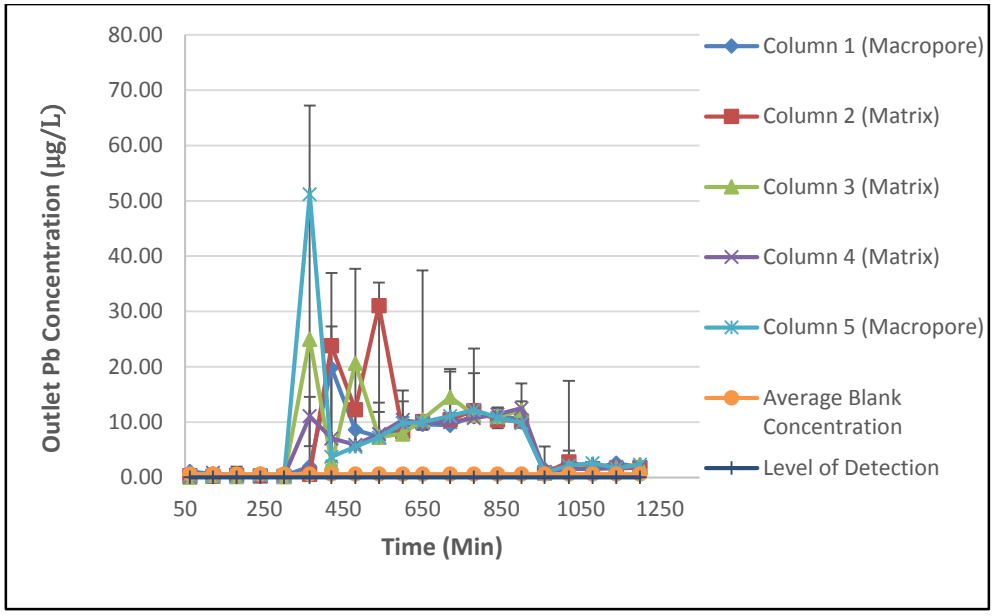

Figure 5.22 Pb Outflow Concentration for Experimental Set 3 without Outliers

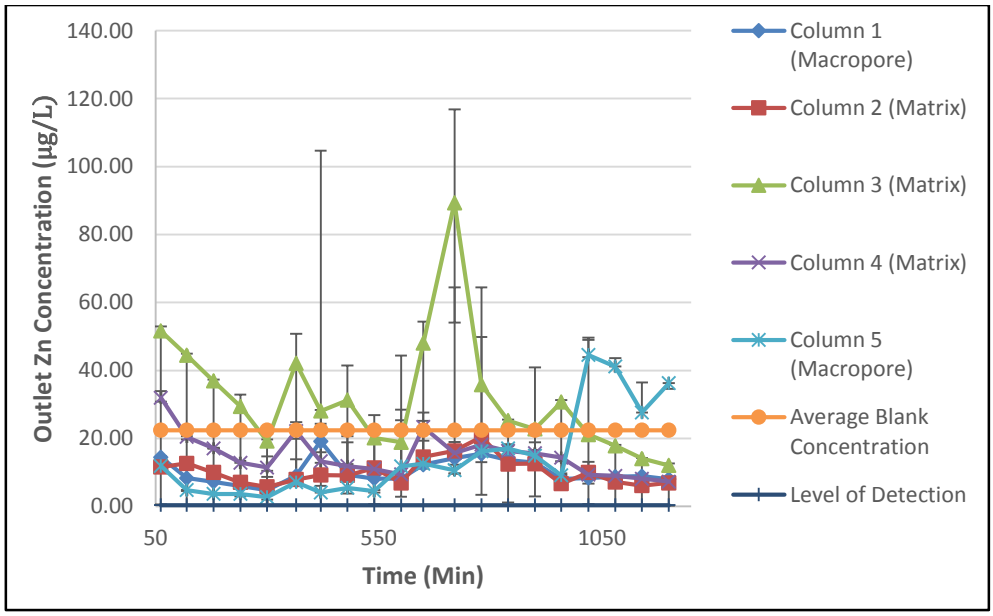

Figure 5.23 Zn Outflow Concentration for Experimental Set 3

Plot of the Means

The plot of the means for each of the heavy metal outflow concentrations, Cu (**Figure 5.17**), Pb (**Figure 5.18**) and Zn (**Figure 5.19**) supports the findings of the above.

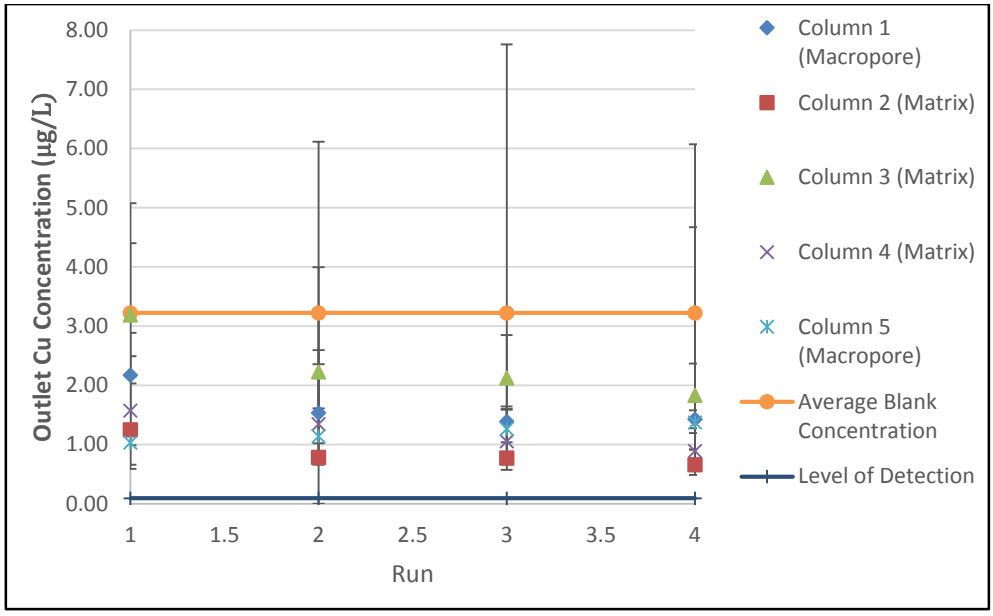

Figure 5.24 Plot of Cu Outflow Mean for the Different Columns for Experimental Set 3

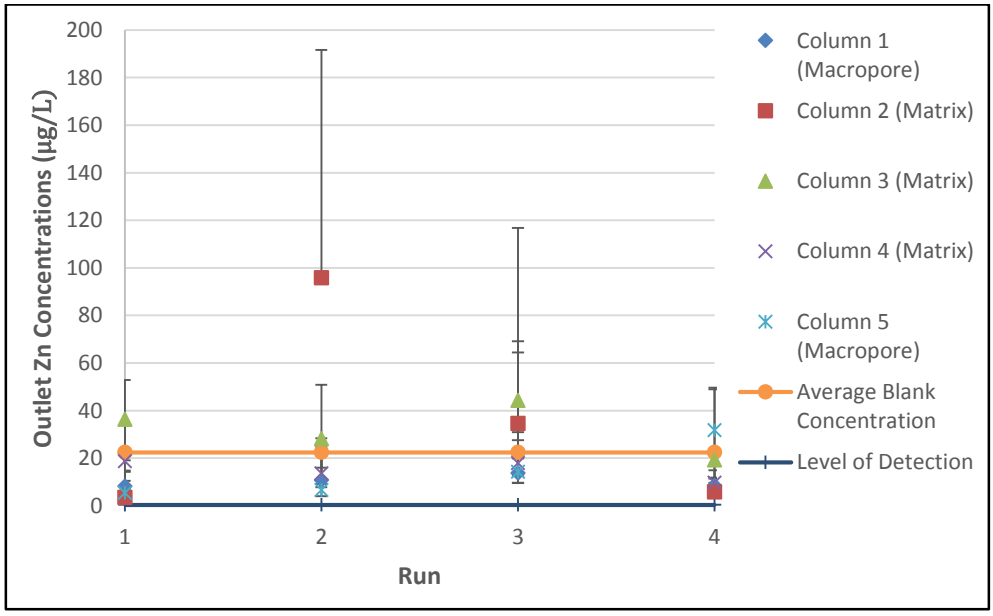

Figure 5.25 Plot of Zn Outflow Mean for the Different Columns for Experimental Set 3

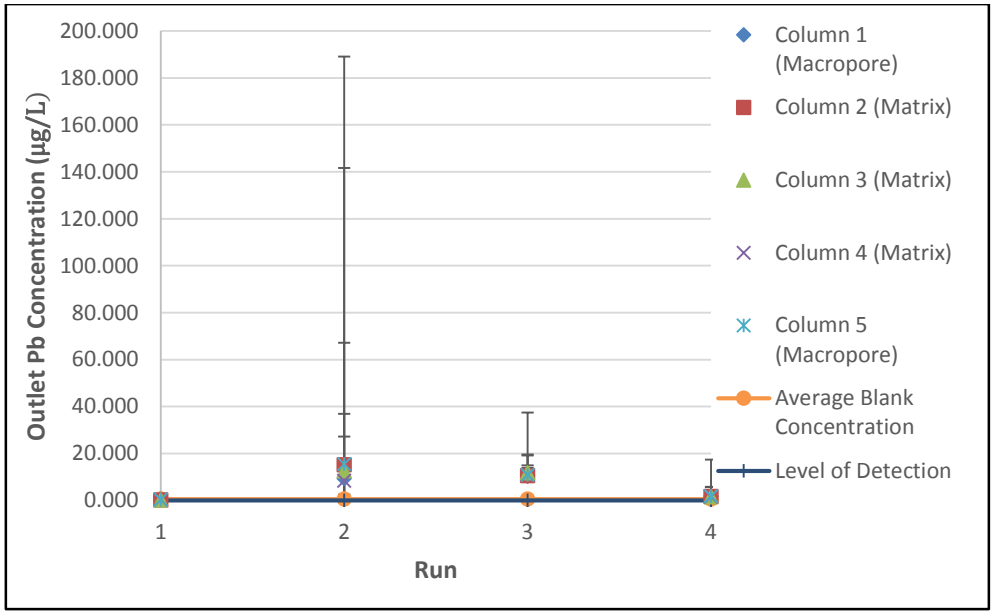

Figure 5.26 Plot of Pb Outflow Mean for the Different Columns for Experimental Set 3 with Outliers

5.8 Comparisons Between Experimental Sets

In this section, the experimental sets are compared to one another in order to determine the variability between sets.

5.8.1 Average Flow Runs

An example of comparison between sets for individual columns is given for each of the heavy metals **Figure 5.27** (Cu) **Figure 5.28** (Pb) and **Figure 5.29** (Zn). The remainder of the comparisons is given in **Appendix D7**.

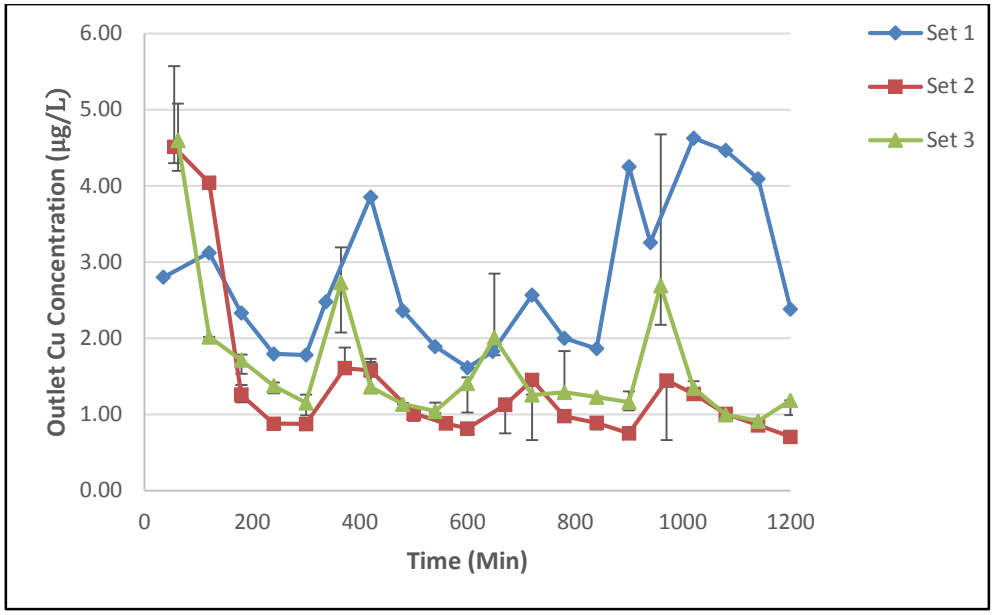

Figure 5.27 Comparison of Outflow Cu Concentration in Column 1 for Different Experimental Sets for Average Flow Runs.

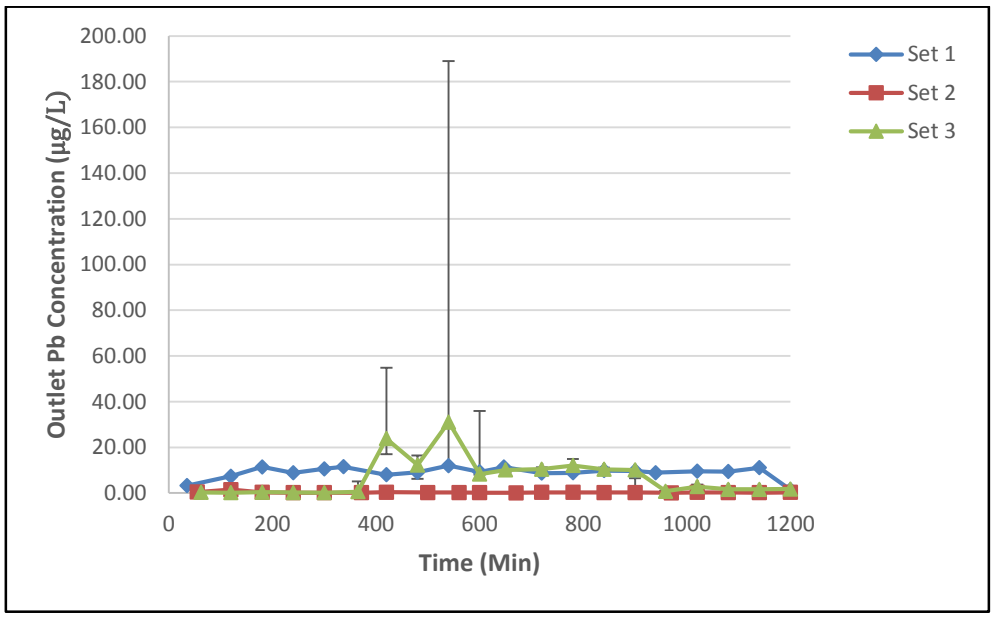

Figure 5.28 Comparison of Outflow Pb Concentration in Column 2 for Different Experimental Sets for Average Flow Runs.

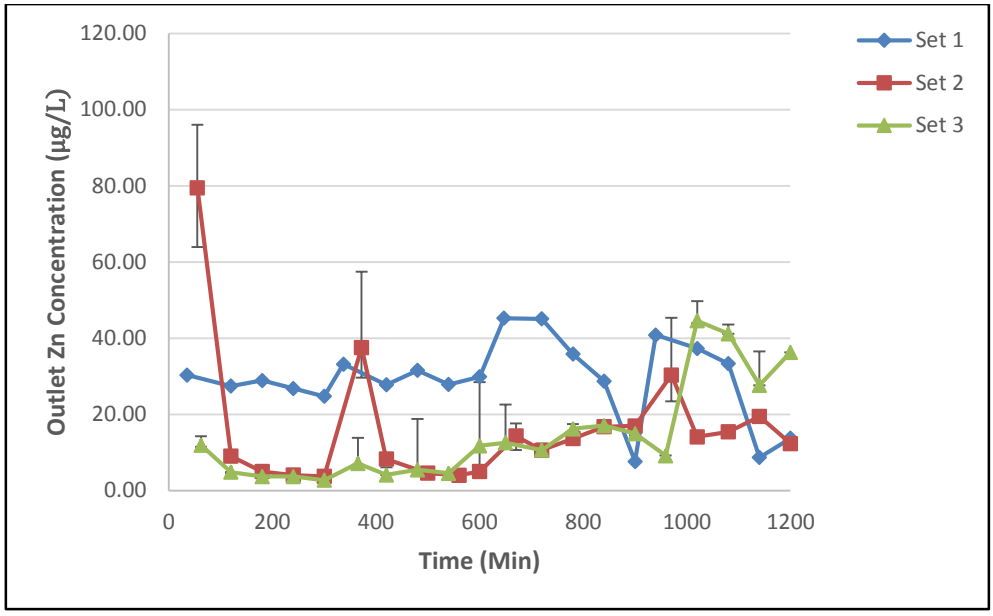

Figure 5.29 Comparison of Outflow Zn Concentration in Column 5 for Different Experimental Sets for Average Flow Runs.

It is clear that for all cases the results of the different sets for the average flow runs are comparable. The small variation between the sets is attributed to differences in background concentration (**Table 5.7** (Set 1) **Table 5.23** (Set 2) **Table 5.24** (Set 3)). This indicates the repeatability of the experiments.

5.8.2 First Flush Runs

An example of comparison between sets for individual columns is given for each of the heavy metals **Figure 5.30** (Cu), **Figure 5.31** (Pb) and **Figure 5.32** (Zn). The remainder of the comparisons is given in **Appendix D8**.

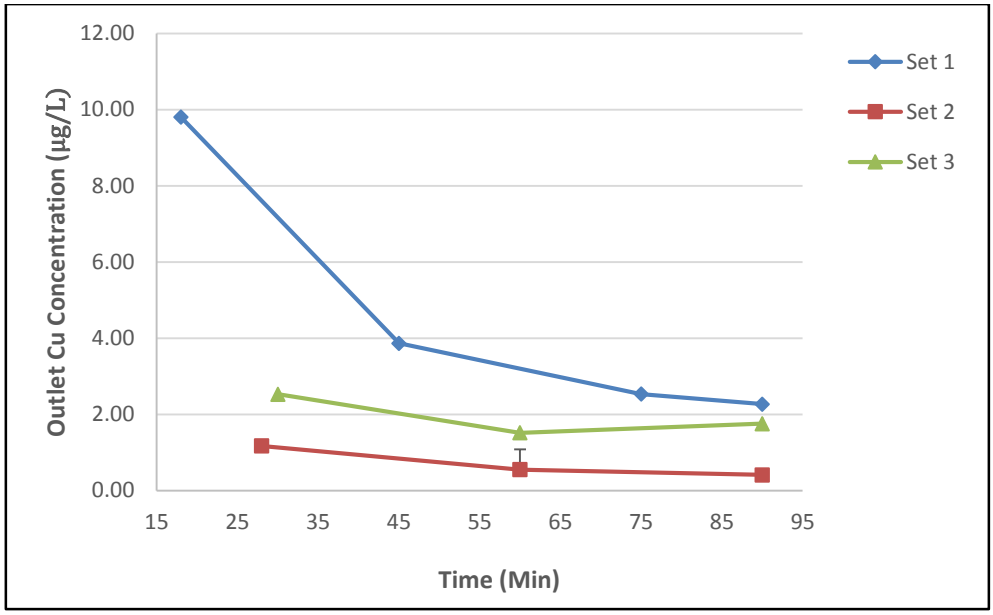

Figure 5.30 Comparison of Outflow Cu Concentration in Column 3 for Different Experimental Sets for First Flush Flow Runs.

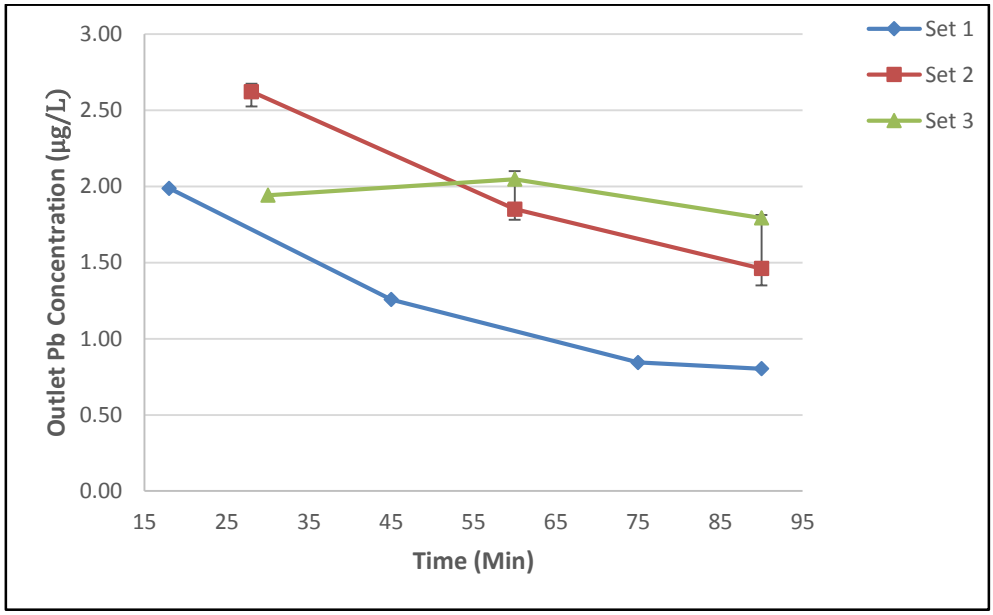

Figure 5.31 Comparison of Outflow Pb Concentration in Column 3 for Different Experimental Sets for First Flush Flow Runs.

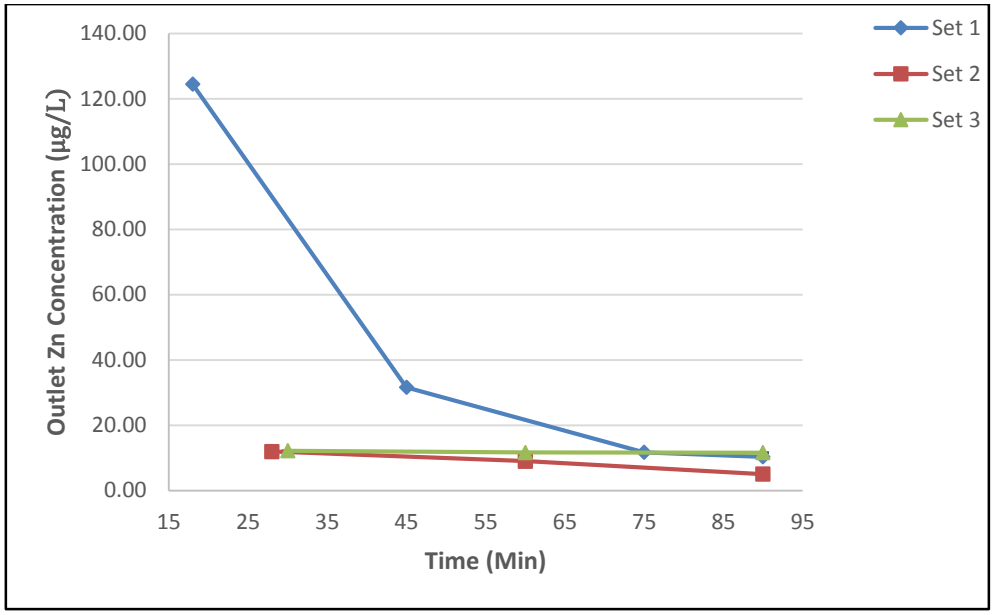

Figure 5.32 Comparison of Outflow Zn Concentration in Column 3 for Different Experimental Sets for First Flush Flow Runs.

It is clear that for all cases the results of the different sets for the first flow flow runs are comparable. The small variation between the sets is attributed to differences in background concentration (**Table 5.7** (Set 1) **Table 5.23** (Set 2) **Table 5.24** (Set 3)). However this variability is small compared to the overall inflow heavy metal concentration of 10,000 µg/L for Cu and Pb and 30,000 µg/L for Zn. This proves that the experiments are consistent and reproducible.

5.9 Conclusion and Discussion

In this project column experiments were performed to investigate the heavy metal capacity of rain garden soil with and without macropores under English climatic conditions. It was found for the average flow experiment a preliminary analysis of the soil moisture content, breakthrough times and tracer results indicated that there was no significant hydrological difference between the two types of columns. This is attributed to previous findings indicating this may have either been due to the 'natural speed limit' in macropores being equal to the matrix flow velocity or water transfer. This finding is supported by previous experimental results which have suggested that macropore flow impacts solute transport only upon saturation (Lamy, et al., 2009).

For the case of a heavier flow (First Flush) the soil moisture contents in the columns deviated from one another significantly indicating macropore flow, although this was not supported by the breakthrough or tracer results. It is clear that further research is required into macropore

flow in rain gardens to truly quantify whether this type of flow is occurring; suggestions for additional experiments are detailed in **Section 9.3**.

The next stage of research was to examine the heavy metal outflow concentrations. From the raw data for all experimental sets, it was clear that for all heavy metals (Cu, Pb, Zn) excellent retention was seen (>99%). This result corresponds to previous findings (Davis, et al., 2001, Sun & Davis, 2007, Li & Davis, 2008, Blecken et al. 2009).

For Set 1, the mean plots indicated a difference in outflow between macropore and matrix columns for Cu, this was supported by the p-values obtained. Both the p-values and ANOVA test also indicated that not only was there a difference between macropore and matrix columns but Cu outflow also increased with time in line with other experimental findings (Davis, et al., 2001). The results for Pb and Zn did not show a similar pattern, here there was no significant difference between the outflows over the runs or between macropore and matrix columns. This corresponds with the findings of other experiments which stated that Cu is the most mobile heavy metal (Li & Davis 2008).

The most interesting result is that despite the fact that hydraulically macropore flow did not have an impact on outflow rate or soil moisture content it exacerbated Cu concentration outflow even over the short run duration of the experimental set 1. This could be explained by a combination of factors; water transfer was the dominant aspect and transferred the majority of macropore flow to the matrix region. This is supported by the findings of Pb and Zn which were unaffected by macropore flow. Cu is the most mobile of heavy metal so even if just a small concentration were present in the macropores it would not be retained to the same extent as in the matrix region as macropores have a lower retentive capacity. The macropore flow travelled at the same speed as the matrix flow and thus did not influence the breakthrough or tracer results but did cause a deviation in soil moisture content as seen in **Section 5.5.1**. This indicates that it is very important to take macropore flow into account when designing rain garden systems something which has not been examined in the past. It has been found by previous field studies that macropores can adsorb heavy metals but that there adsorption sites decrease over time as they reach retention capacity (Knechtenhofer, et al., 2003). This could explain the increase in Cu outflow overtime. It is reiterated that although in general the outflow is of a very low concentration a definite pattern is observed.

For Sets 2 and 3 this pattern was not observed and it was found that there was no significant difference in outflow heavy metal concentration between the macropore and matrix columns. The results of experimental sets were compared and their repeatability proven.

In conclusion under English climatic conditions macropores are not a dominant factor in either the movement of water or pollutant through a rain garden thus the presumptions previously made regarding macropore initiation are proved valid. This is the discovery by Lamy et al. (2009) that macropores are not initiated in unsaturated conditions. It should be noted however that the values for saturated hydraulic conductivity (K_{sat}) in the columns were very high compared to those used in rain gardens thus it is suggested that in the future different soils with different ranges of K_{sat} should be tested (Dussaillant, 2001).

Further suggestions for future work are discussed in **Section 9.3**.

6 COLUMN EXPERIMENT: VALIDATION

6.1 Introduction

In this chapter the results from the column experiments were used to further validate the model. This was completed in a number of steps:

1. The van Genuchten-Mualem parameters for soil were derived for each of the columns using water retentive curves.
2. The unsaturated hydraulic conductivity were derived for each of the experimental runs for each column.
3. For the water flow component of the model the above parameters were input into the model, in addition to the experimental conditions. A simulation was run and this was compared to the experimental results. Its accuracy was determined using the statistical methods such as the coefficient of determination.
4. Step 3 was repeated for the pollutant retention module of the model.

This process completely validated the model and confirmed its accuracy.

6.2 Van Genuchten Parameters

In order to successfully predict movement of water through the rain garden, soil moisture content (θ) (m^3/m^3) and hydraulic conductivity (K) (cm/s) must be derived (see **Section 3.4**).

As discussed in **Section 4.2.1** van Genuchten equations can be used to determine soil θ, K and diffusion (D_e) (cm^2/s) from the value of water head calculated by the KWE. However the van Genuchten parameters (n_{vg} (Dimensionless) and α_{vg} (1/cm)) must be derived for each individual soil type. This is achieved by obtaining the soil retentive curve with the programme SWRC fit which fits estimates the van Genuchten parameters by utilising the experimental data regarding the soil retentive curve to that predicted by the van Genuchten equations and derives its parameters. SWRC fit is a well-respected tool in the hydrological community and has been used by numerous researchers to evaluate soil parameters (Moret Fernandez, et al., 2008, Saito, et al., 2009).

The water retention curve is the relationship between θ and water head (h) (cm). In the case of the experiments both these values were measured by TDR probes and WMP sensors respectively.

Figure 6.1 shows the water retention curve for the upper soil/sand layer in Column 1 fitted with the van Genuchten equation.

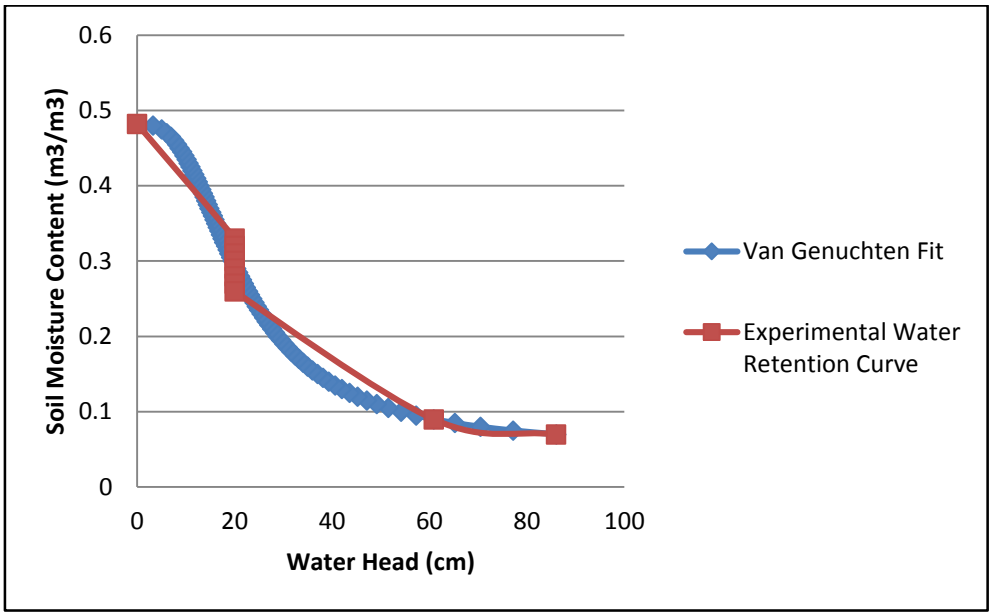

Figure 6.1 Comparison of Water Retention Curve for Soil/Sand Mix with the Van Genuchten Fit.

The van Genuchten parameters for the above figure are given in **Table 6.1**. A coefficient of determination of 0.971 was calculated for the fit.

Table 6.1 Van Genuchten Parameters for Column 1 Sand/Soil Mix

Van Genuchten Parameters	
θ_{sat} Saturated Soil moisture Content (m^3/m^3)	0.482
θ_{res} Saturated Soil moisture Content (m^3/m^3)	0.047819
α_{vg} (1/cm)	0.055673
n_{vg} (Dimensionless)	2.8943

Figure 6.2 shows the water retention curve for the lower coarse sand layer in Column 1 fitted with the van Genuchten parameters.

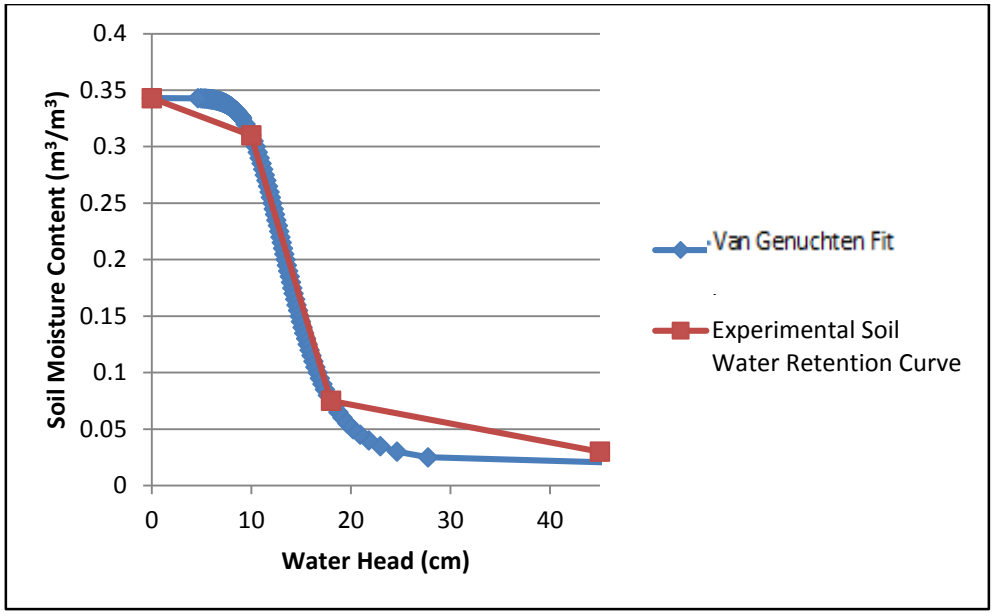

Figure 6.2 Comparison of Water Retention Curve for Sand with the Van Genuchten Fit.

The van Genuchten parameters for the above figure are given in **Table 6.2.** A coefficient of determination of 0.95 was calculated for this fit.

Table 6.2 Van Genuchten Parameters for Column 1 Sand

Van Genuchten Parameters	
θ_{sat} (m^3/m^3)	0.34312
θ_{res} (m^3/m^3)	0.019755
α_{vg} (1/cm)	0.074234
n_{vg} (Dimensionless)	6.691

The soil retentive curves for the other columns and their van Genuchten parameters are given in **Appendix D5**.

6.3 Derivation of Unsaturated Hydraulic Conductivity

In order to examine the movement speed of water through the columns the hydraulic conductivity must be derived. Hydraulic conductivity of a soil is an important parameter for the calculation of both groundwater recharge and solute transport in a rain garden. It is a function of not only fluid and media properties but also the soil-water content and can be described by the following equation (Perkins, 2011):

$$K = K_s k_r \tag{6.1}$$

where K is the unsaturated hydraulic conductivity, K_s (cm/s) is the saturated hydraulic conductivity, and k_r (Dimensionless) is the relative hydraulic conductivity.

Relative hydraulic conductivity k_r is a dimensionless number that has a value between 0 and 1. When this equals unity it denotes a saturated soil medium. Unsaturated hydraulic conductivity is always lower than saturated hydraulic conductivity. It is not constant and can be calculated from pressure head values. The KWE used by HM07 models the movement of the pressure head wave through the soil. Thus using the KWE the hydraulic conductivity and thus the pore water velocity can be obtained.

Instantaneous Profile Method (IPM)

The IPM is a transient approach whereby the sorption (wetting) and/or desorption (drying) curve can be approximated in a single test (Smith, 2000). It is commonly used to calculate the unsaturated hydraulic conductivity using the following equation:

$$K = \frac{V_s}{CAt_s}\left(\frac{1}{dh/dz}\right) \tag{6.2}$$

where V_s (cm^3) is the volume which moves past a specified point, CA (cm^2) is the cross sectional area, t_s (s) is the time taken, and dh/dz is the gradient of hydraulic head.

In order to utilise IPM the following steps were followed:

1. Profiles of soil properties (h and θ) are measured across the distance being examined at various time intervals.
2. Hydraulic gradients at points Z(cm) and L(cm) which are depths of soil at times t and t' were determined from the h versus z graph plotted previously.
3. V_s in t_s was calculated by integrating the differences in θ profile:

$$V_s = CA\int_z^L |\theta' - \theta|\, dz \tag{6.3}$$

$$V_s = \left\{\frac{\theta(L)' + \theta(z)'}{2} - \frac{\theta(L) + \theta(z)}{2}\right\}(L - z)A \tag{6.4}$$

4. The above formulae were used to calculate K. The pressure head assigned to this K value is the arithmetic mean of the pressure heads measured at times t and t' [i.e. $h = (h_t - h_{t'})/2$]

Application of method to Columns

In the instrumented columns TDR and WMP are placed at 10cm depth and 45cm depth. So in order to calculate K from the above equations L=45cm and z=10cm, thus dz=35cm. For the wetting and drying of the columns, it was observed that **Eq. 6.4** combined with **6.2** gave an accurate result for K of between 0 and the input rate of 12 cm/h. However once the flow through the column became steady state i.e. $\frac{1}{dh/dz} \rightarrow 1$, $K \rightarrow q$. This is equivalent to a case where gravity, not diffusion is the dominant influence on flow (Singh, 1997). This would commonly be expected in column experiments where the effects of capillary potential gradients are small.

Figure 6.3 shows the unsaturated hydraulic conductivity of the upper soil/sand layer (between z=10cm and L=45cm) of Column 1 for Run 1(Average Flow Conditions). It is observed that the drying front is not consistent and shows some anomalous results. This is attributed to the fact that this is a layer system and drainage will thus not be at a constant rate.

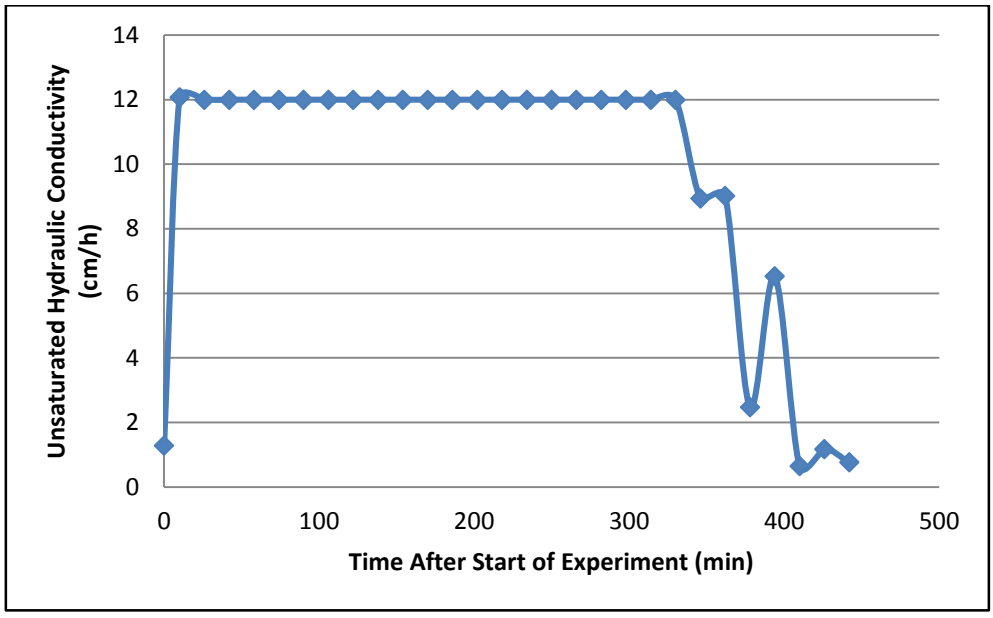

Figure 6.3 Derived Unsaturated Hydraulic Conductivity for Column 1. Average Flow Run.

Figure 6.4 shows the unsaturated hydraulic conductivity in Column 1 for Run 5 (First Flush Flow Conditions). It is observed that the drying front is more consistent than for the average flow conditions. This is attributed to a faster more uniform drainage rate due to the high inflow rate.

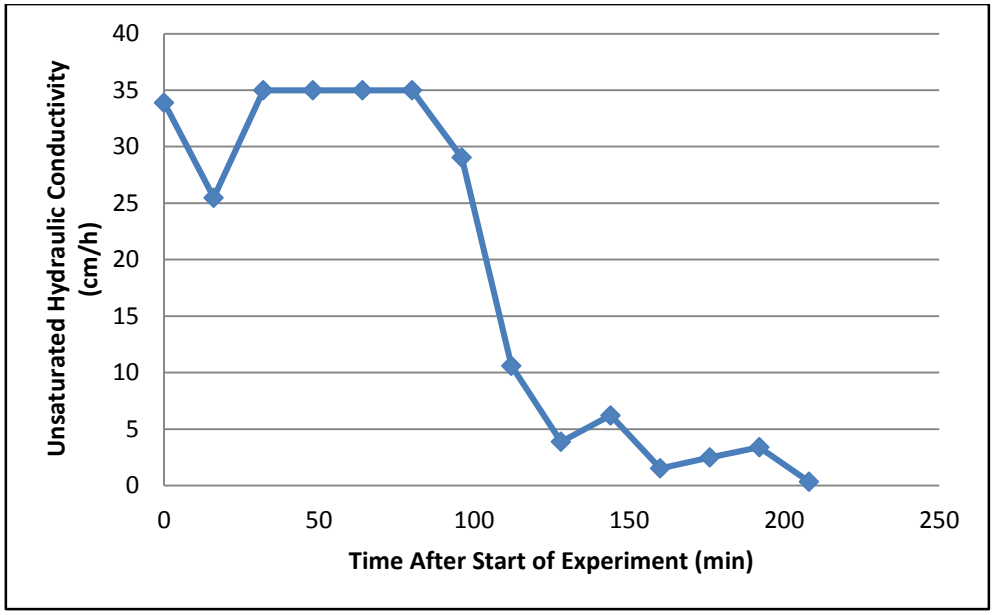

Figure 6.4 Derived Unsaturated Hydraulic Conductivity for Column 1. First Flush Run.

6.4 Validation of Water Component of Model

In the following section the results of the model is validated using column experimental data.

Matrix Region

In order to apply the KWE, the velocity of the water must be obtained. As indicated from **Section 6.3** detailing the unsaturated hydraulic conductivity calculations, the experiments fall under the case of $q=K$ whereby the hydraulic conductivity is equal to the flux. Singh found that for such a case the following equation can be used to calculate the velocity of the pressure wave in the KWE:

$$v = \frac{q}{\theta} \tag{6.5}$$

Average Flow Experiments

The initial and boundary conditions of this run are shown in **Table 6.3**.

Table 6.3 Initial and Boundary Conditions For Average Flow Experiment

Parameter	**Value**	
Upper Boundary Condition	12 cm/h (0.2 cm/min)	
Lower Boundary Condition	Free Flow	
Duration of Experiment	300 min	
Initial Conditions	Soil Moisture Content (m^3/m^3)	Water Head (cm)
15 cm (Soil/Sand Upper Layer)	0.135	-45.1
55 cm (Soil/Sand Upper Layer)	0.193	-31.0
75 cm (Sand Lower Layer)	0.026	-26.0

Below a comparison of the results of the experiment and KWE for soil moisture content at z=15 cm (soil) (**Figure 6.5**), 55 cm (soil) (**Figure 6.6**) and 75 cm (sand) (**Figure 6.7**) is shown. Soil moisture is illustrated instead of water head as this parameter has been shown to have an effect on heavy metal retention (**Section 4.4.4.4**). The van Genuchten parameters used are detailed in **Table 6.1** (soil/sand mix) and **Table 6.2** (sand). The saturated hydraulic conductivity (K_s) was taken as 77 cm/h for the upper soil/sand mix and 110 cm/h for the lower sand layer (see **Table 5.3**).

The KWE was solved using the Thomas algorithm described in **Appendix B1** and implemented in Matlab.

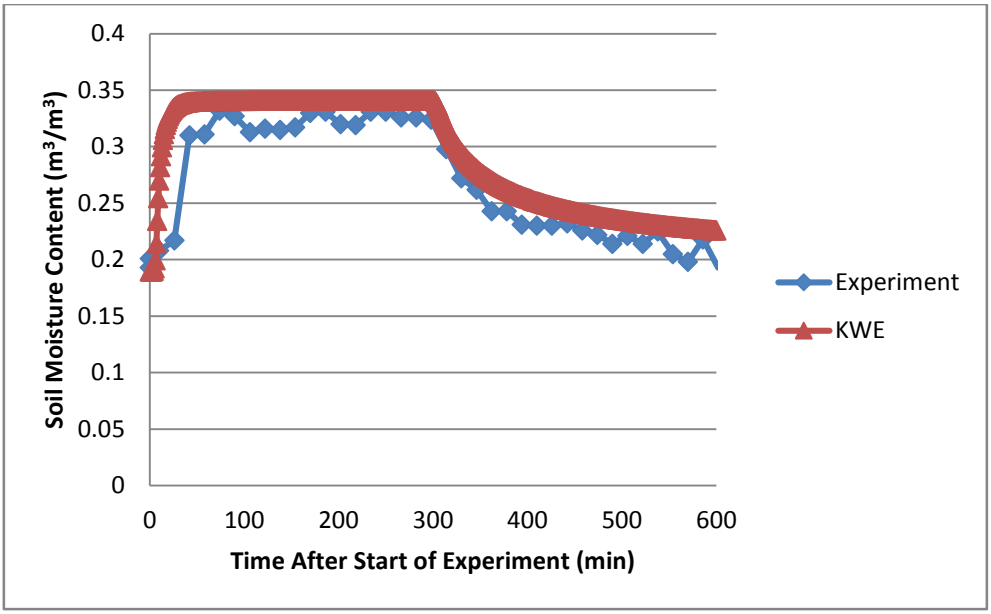

Figure 6.5 Comparison of Experimental Soil Moisture Content at z=15cm with Kinematic Wave Equation for Average Flow Condition

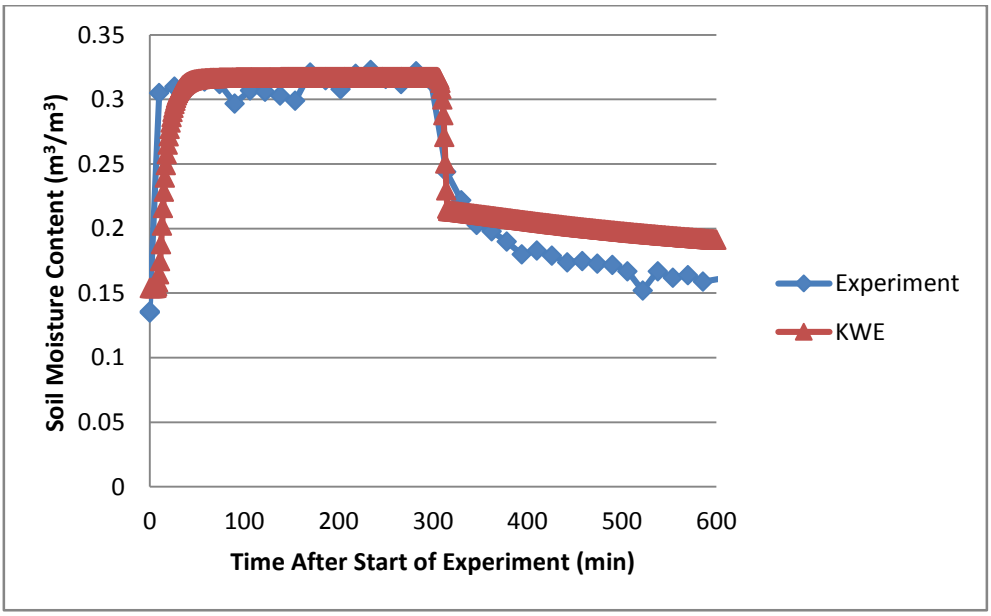

Figure 6.6 Comparison of Experimental Soil Moisture Content at z=55cm with Kinematic Wave Equation for Average Flow Condition

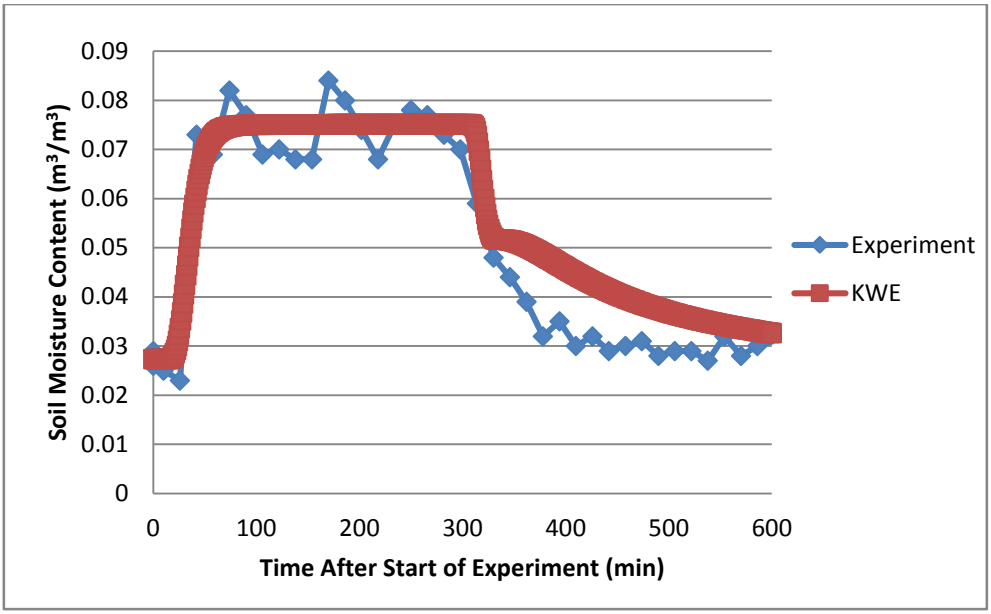

Figure 6.7 Comparison of Experimental Soil Moisture Content at z=75cm with Kinematic Wave Equation for Average Flow Condition

As can be seen from **Figure 6.5** and **Figure 6.6** the KWE captures the overall movement of soil moisture through the column well with R^2=0.92 and a Nash-Sutcliffe coefficient = 0.91 for z=15 cm and R^2=0.86 and a Nash-Sutcliffe coefficient = 0.86 for z=55 cm. However there are some minor inaccuracies in the drainage wave, this is due the steep drainage front characteristic of kinematic wave approximations (Singh, 1997). This minor inaccuracy should not significantly affect heavy metal retention as it only has a slight influence on relevant variables (soil moisture content and pore water velocity) as illustrated in **Section 4.4.4.4** .

For z=75cm the accuracy is given by R^2=0.92 and a Nash-Sutcliffe coefficient = 0.87, the small error is attached to the inaccuracy in the drainage wave which is overestimated by KWE. This is attributed to the very high hydraulic conductivity in the sand layer (110 cm/h) compared with the slower upper layer of compost/sand (77 cm/h) which, causes the discrepancy in velocity between layers. In addition, the KWE diverges more during the drying phase as capillary action is the dominant process, whereas with the KWE, gravity is the dominant mechanism of water movement.

As is illustrated in **Appendix D2**, the hydrological results did not vary between the average runs therefore a validation comparison for only one run is illustrated.

First Flush Experiments

The initial and boundary conditions of this run are shown in **Table 6.4**.

Table 6.4 Initial and Boundary Conditions for First Flush Experiment

Experimental Setup		
Upper Boundary Condition	35 cm/h (.583cm/min)	
Lower Boundary Condition	Free Flow	
Duration of Experiment	90 min	
Initial Conditions	Soil Moisture Content (m^3/m^3)	Water Head (cm)
15cm (Soil/Sand Upper Layer)	0.136	-44.75
55cm (Soil/Sand Upper Layer)	0.201	-31.3
75cm (Sand Lower Layer)	0.025	-26

Below a comparison of the results of the experiment and KWE for soil moisture content at z=15 cm (soil) (**Figure 6.8**), 55 cm (soil) (**Figure 6.9**) and 75 cm (sand) (**Figure 6.10**) is shown.

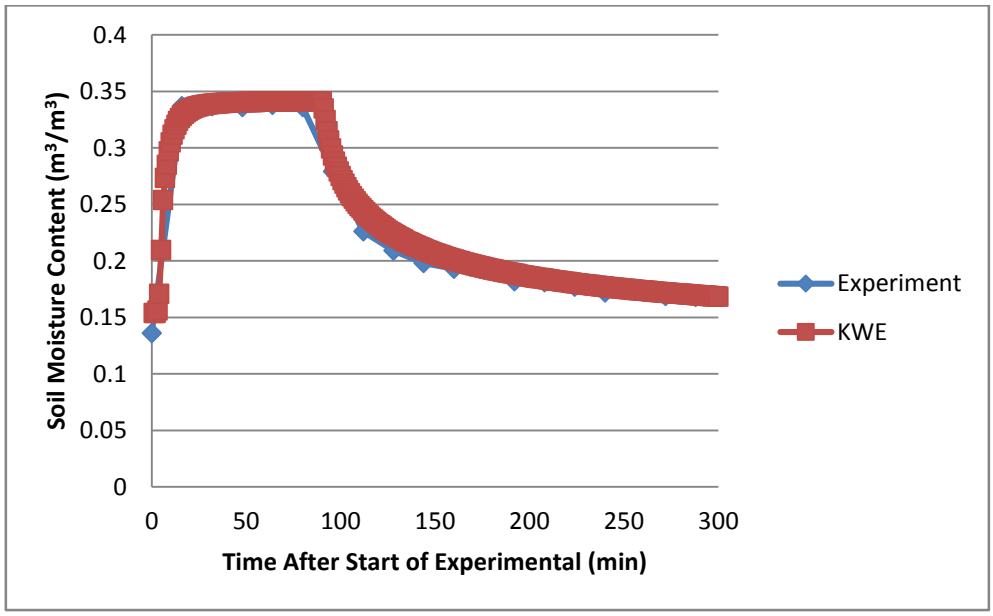

Figure 6.8 Comparison of Experimental Soil Moisture Content at z=10cm with Kinematic Wave Equation for First Flush Flow Condition

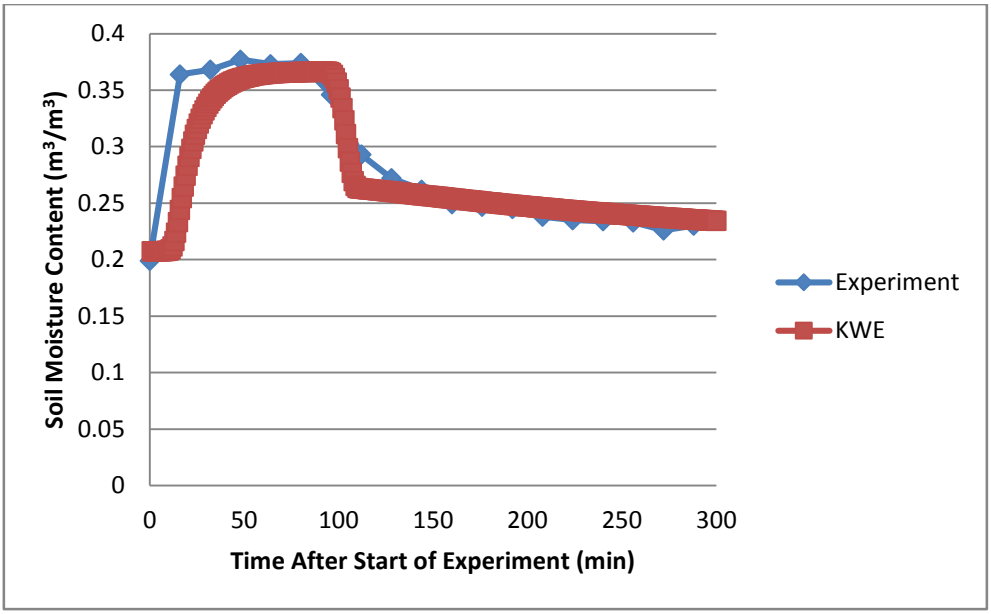

Figure 6.9 Comparison of Experimental Soil Moisture Content at z=55cm with Kinematic Wave Equation for First Flush Flow Condition

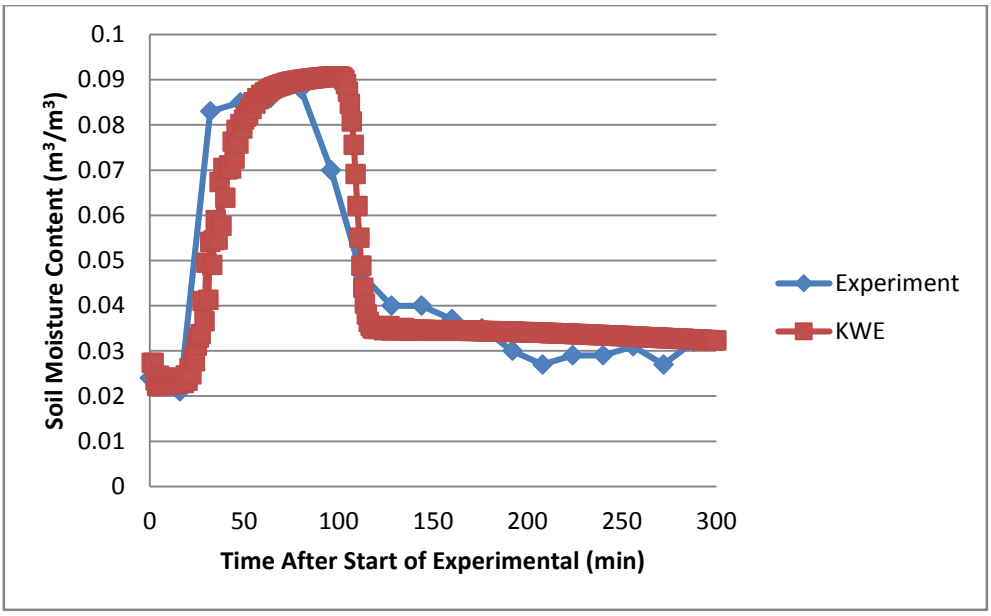

Figure 6.10 Comparison of Experimental Soil Moisture Content at z=75cm with Kinematic Wave Equation for First Flow Condition

Overall the KWE captures the overall movement of soil moisture through the column well with R^2=0.99 and a Nash-Sutcliffe coefficient = 0.98 for *z*=15 cm, R^2=0.96 and a Nash-Sutcliffe coefficient = 0.96 for *z*=55 cm and R^2=0.86 and a Nash-Sutcliffe coefficient = 0.85 for *z*=75 cm. It is clear that the KWE accurately models soil moisture movement at the top of the column but the accuracy decreases with depth. This is evident from the case of *z*=75 cm where the KWE accurately models the wetting, however the prediction for the drainage wave has a very

sharp wetting front compared to the experimental results. This may indicate that diffusion is not being properly quantified, this is an area for future work. This problem could potentially be solved by incorporating an additional diffusion term into the KWE however it has been shown that the KWE is accurate without this addition and it is deemed unnecessary at this time.

Macropore Region

As detailed in the previous chapter (**Section 5.4.2**), no macropore flow was observed with the results of the tracer, breakthrough times and soil moisture content. Thus, one of the major drawbacks of these experiments were their inability to validate the macropore section of this model with experimental results. However, a detailed validation was completed in **Section 4.4.2**, this was deemed appropriate as the KWE displayed accuracy at predicting macropore flow (R^2>0.89) for four cases with different inflow rates and parameters proving its applicability under a wide range of conditions.

6.5 Heavy Metal Retention Validation

As is clear from the previous chapter, breakthrough of the columns was not achieved therefore the results for the linear distribution coefficient were obtained from very similar soils in the literature (**Table 6.5**).

Table 6.5 Linear Distribution Coefficients for Experimental Substrates

Material	**Linear Distribution Coefficient (K_d) (L/kg)**			**Reference**
	Cu	Pb	Zn	
Soil/Sand Upper Layer	4799	171214	11615	(Li & Davis 2008)
Sand Lower Layer	1060	1295	1500	(Christensen et al. 1996,

The figures below show a comparison between the experimental and linear isotherm results for Cu (**Figure 6.11**), Pb (**Figure 6.12**) and Zn (**Figure 6.13**).

The results are shown for Column 3 as this was the column with the lowest retention.

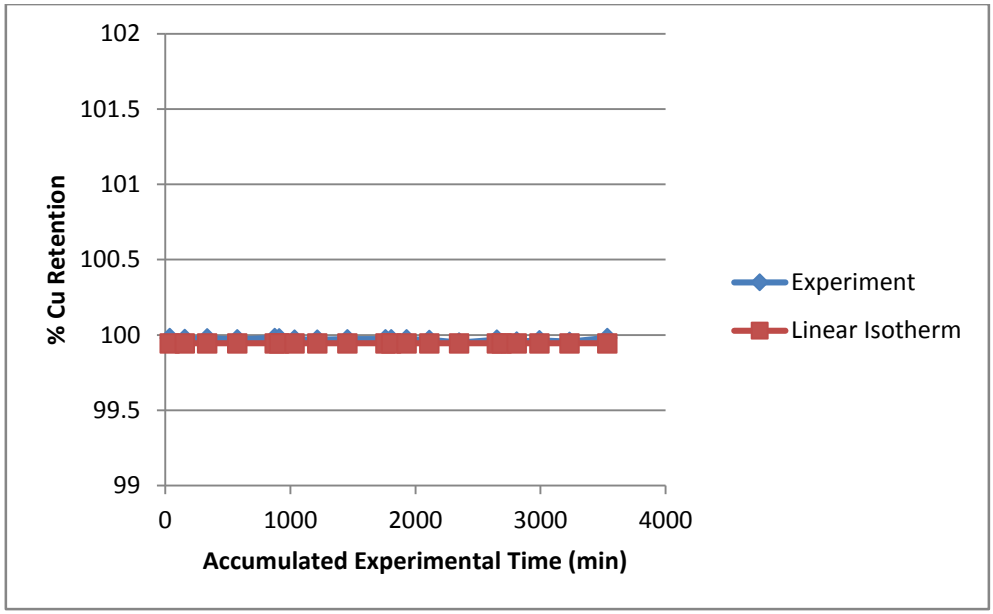

Figure 6.11 Comparison of Linear Isotherm with Experimental Results for Cu.

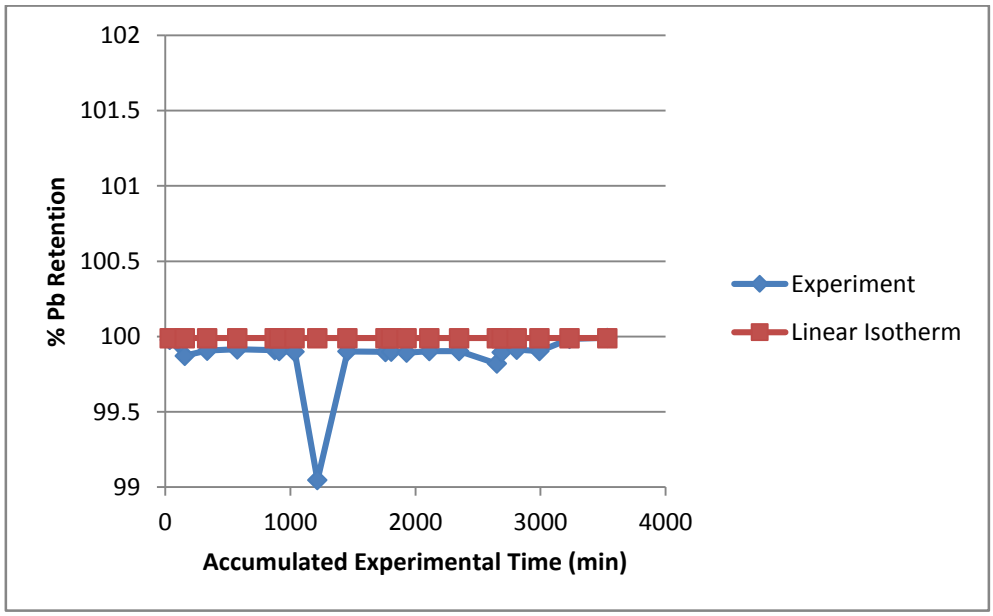

Figure 6.12 Comparison of Linear Isotherm with Experimental Results for Pb.

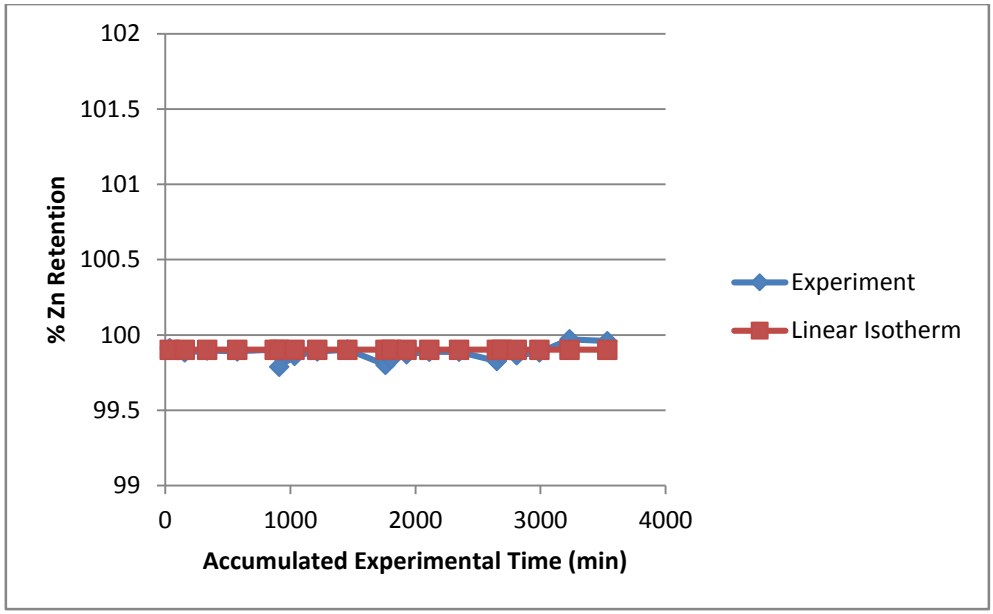

Figure 6.13 Comparison of Linear Isotherm with Experimental Results for Zn.

Overall the linear isotherm replicates the results of the experiment extremely well. In one case there is a drop in the retention of Pb not replicated by the isotherm but still there is only a 1% difference in results.

6.6 Conclusions

The purpose of this chapter was to provide suitable validation for the model.

Although there were some inaccuracies in the prediction of the drainage wave, the KWE is still considered an accurate method of modelling water movement in the matrix section of HM07. Some inaccuracy was expected as it is not as complex as the Richards equation however, it gave a reasonably accurate reflection of the movement of water through the soil. The deviations in the drainage wave approximations did not affect the results of heavy metal retention. This is proven by the results of the sensitivity analysis which showed a very large increase or decrease in pore water velocity and soil moisture content was needed to influence the capture of heavy metals in soil (**Section 4.4.4.4**). Further research is needed to model the drainage wave using the KWE, but currently it still provides a reasonable estimation of hydraulic parameters (as illustrated by the results of R^2). This makes the KWE a reasonable choice for the modelling of flow in a rain garden system.

For the heavy metal retention component the model gave excellent results. This chapter combined with research undertaken in **Section 4.4** successfully validated the model.

7 MODEL APPLICATION

7.1 Introduction

In this chapter, HM07 was applied to the design of a rain garden facility located on a roundabout in Thanet, Kent as shown in **Figure 7.1**. The existing and the proposed site layout are shown in **Figure 7.2** and **Figure 7.3** respectively. The objective of this modelling exercise was to not only examine the impact of different parameters on heavy metal retention in the facility but also demonstrate the utility of the model for the design of such systems. The heavy metals examined in this chapter are Cu^{2+} and Pb^{2+} as stated in **Section 3.5** these are the most common ionic composition of metals in storm water runoff.

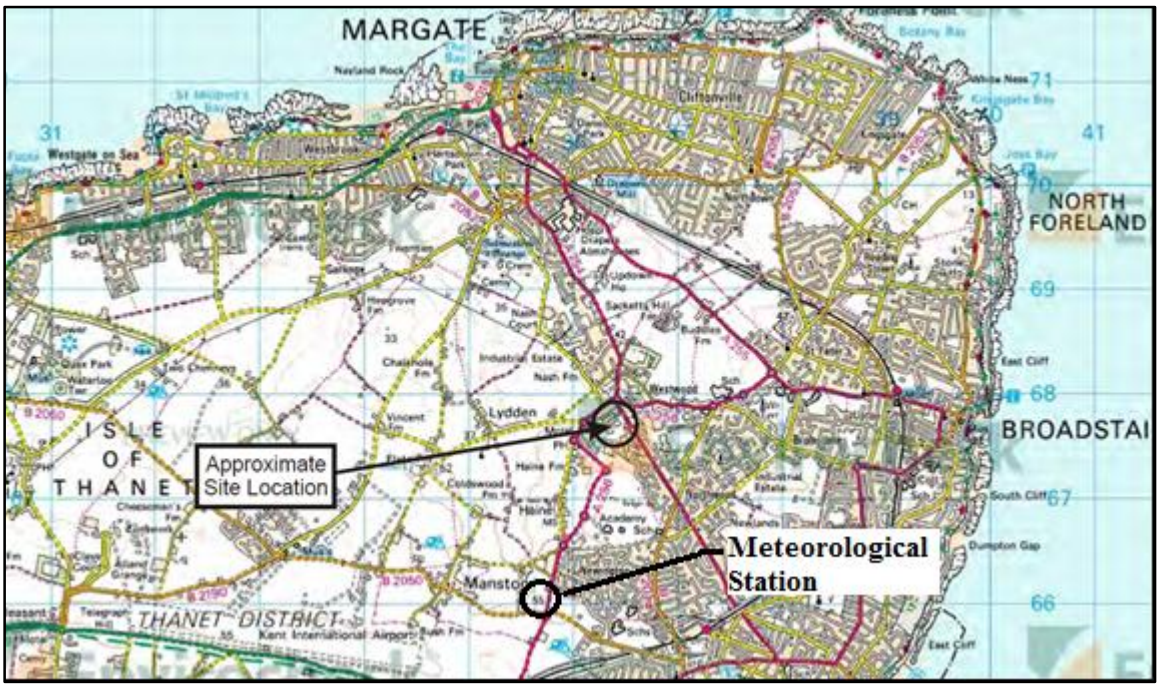

Figure 7.1 Site Location Plan of Rain Garden

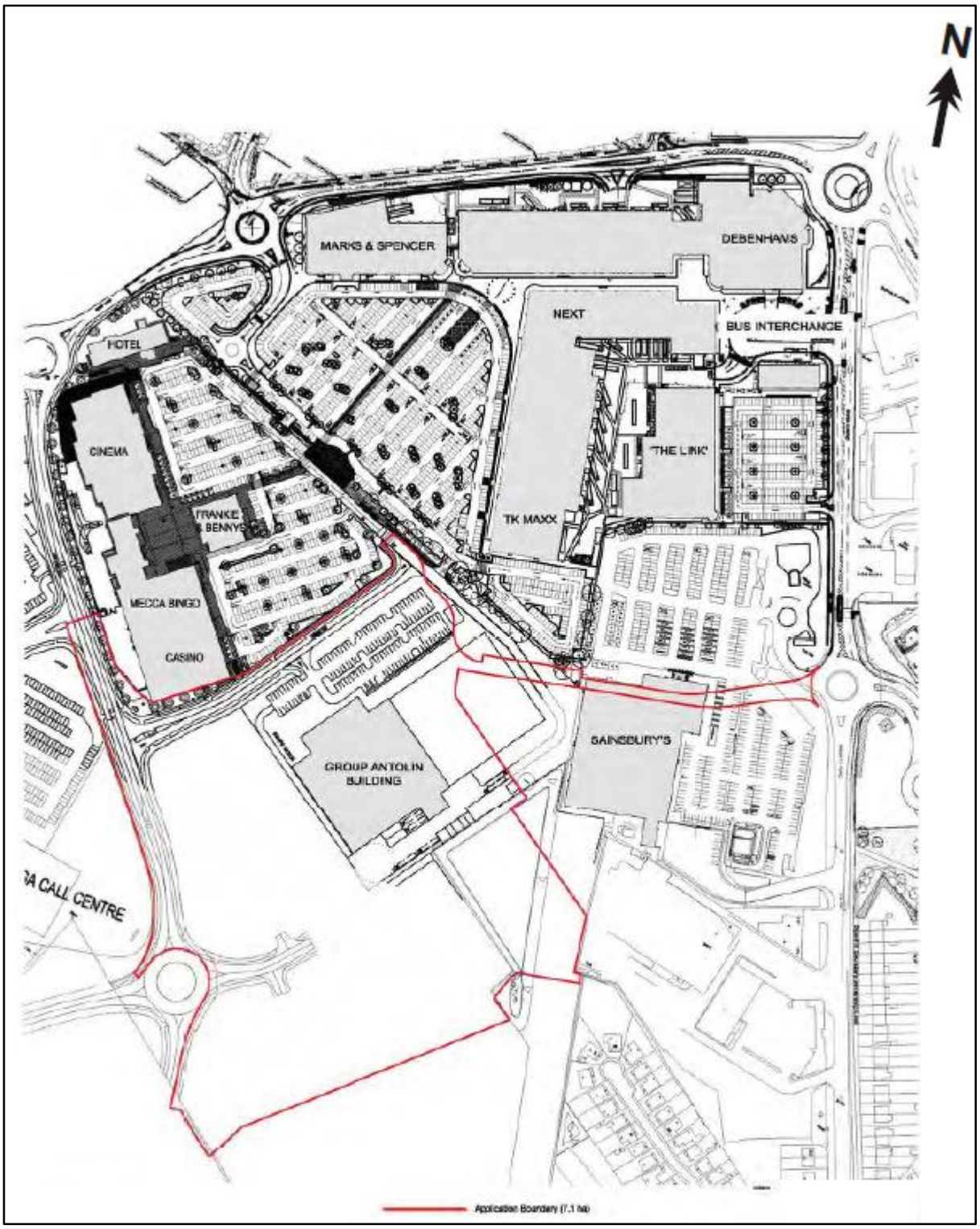

Figure 7.2 Existing Site Layout

Figure 7.3 Proposed Site Layout

7.2 Site Description

The rain garden was to be constructed on a roundabout in Thanet, Kent in the U.K. and receive drainage from the road surrounding it. It was necessary to evaluate the potential pollutant retention of the rain garden at this site as shallow groundwater was present. A preliminary estimation of heavy metal retention in the rain garden using HM07 was viewed as the best method of achieving this and as an efficient and simple tool for informing discussion between Kent Council and the Environment Agency.

Several boreholes and detailed studies were completed by Pam Brown Associates. This allowed for a relatively good characterisation of the subsoil which is a required model parameter. The boreholes indicated an upper layer of made ground consisting of silty clay to 0.4 m and sandy gravel underlying to 1.8 m (Pam Brown Associates, 2012). Groundwater was not encountered directly at the site however it was found that in the vicinity (100 m away) saturated chalk lay

just 1.5 m deep (Pam Brown Associates, 2012). The upper layer was heterogeneous as it consisted of several layers of made ground, however the lower layers of chalk were homogeneous. It was noted that there was a possibility of soluble rocks at the site as indicated by the British Geographical Society (http://www.bgs.ac.uk/products/geosure/soluble.html). It would thus be prudent to complete further site investigation to ensure the rain garden did not contribute to dissolution or degradation of the bedrock.

Table 7.1 Hydraulic Parameters of the Rain Garden

Soil Characteristic	**Root Zone**	**Storage Zone Layer**
Texture	Loam	Sand
Depth (cm)	30	30
Saturated Soil Moisture Content (θ_{sat}) (cm^3/cm^3)	0.41	0.41
Residual Soil Moisture Content (θ_{res}) (cm^3/cm^3)	0.02	0.041
Saturated Hydraulic Conductivity (K_{sat}) (cm/h)	10.16	15

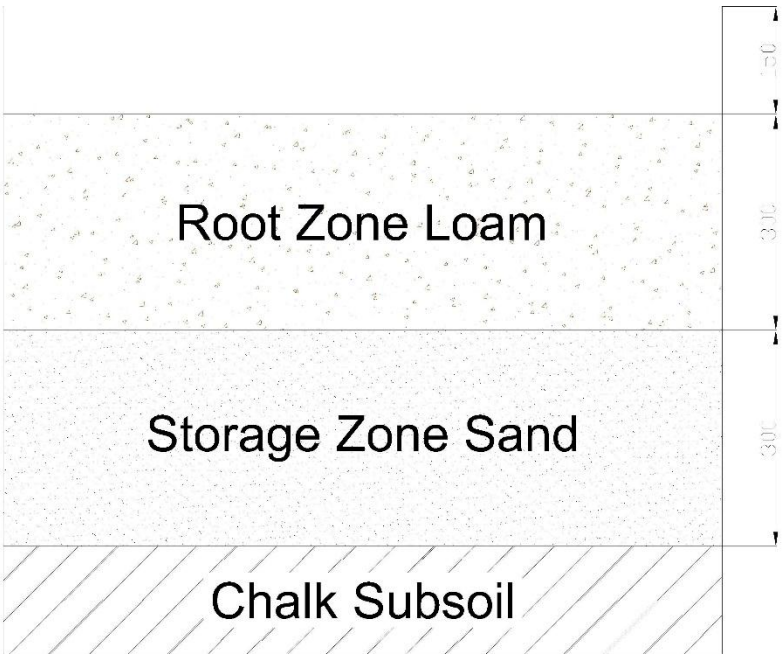

Figure 7.4 Diagram of Rain Garden Device

Hydraulic parameters common to rain garden soils were obtained from Dussaillant (2002) and are provided in **Table 7.1**. a diagram of the device is shown by **Figure 7.4**. The depression depth was set at 15 cm in agreement with previous rain garden design (Dussaillant, 2002)

The K_{sat} of the subsoil was 2 cm/h and was given by a soakaway test; further details are available in the site report (Pam Brown Associates, 2012). Two distinct scenarios were modelled, firstly the transfer and accumulation of heavy metals without macropore flow and secondly, possible groundwater pollution caused by macropores.

A simulation period of ten years was chosen as it was deemed to give an appropriate measure of time at which comprehensive maintenance may be expected. The rainfall data was given by a local weather station at Manston (as shown **Figure 7.1**) approximately three miles from the proposed site (http://badc.nerc.ac.uk/cgibin/midas_stations/station_details.cgi.py?id=775&db=midas_stations) and obtained from the British Atmospheric Data Centre (http://badc.nerc.ac.uk/view/badc.nerc.ac.uk__ATOM__dataent_ukmo-midas). The interval of 2003-2012 was chosen as it gave a sufficiently long period and included dry (2005) and wet (2009) years. The Pb^{2+} input concentration was specified as 0.08 mg/L and corresponds to the suggested level of synthetic runoff for rain garden design provided in Davis et al. (2001), it also matches Pb^{2+} values found in runoff from a busy highway (M25 London orbital road approximately 120000 vehicles per day) measured by Hares and Ward (1999). The Cu^{2+} input concentration of 0.08 mg/L was also consistent with synthetic runoff values; this was double the observed value experienced at roadside sites (Legret & Pagotto, 1999). Only Cu^{2+} and Pb^{2+} were examined in this study as they are most likely to pose a contamination risk, Pb^{2+} due to accumulation and Cu^{2+} due to transfer through the system. Zn^{2+} was not examined as it does not pose a significant risk of groundwater contamination or health risk (Li & Davis, 2008).

7.3 Accumulation and Transfer without Macropores

In this section, the accumulation of Pb^{2+} in the proposed rain garden was evaluated for two upper layer soil substrates; an organically enriched soil (high retentive capacity) commonly used in rain gardens and standard topsoil (low retentive capacity) (Davis et al. 2001, Li & Davis 2008). This was reflected in the linear distribution coefficient (K_d) values shown in **Table 7.2**.

Table 7.2 Heavy Metal Retention Parameters of the Soil

Soil	**Linear Distribution Coefficient (K_d) (L/kg)**				**Reference**
	Pb^{2+}		Cu^{2+}		
	High Retention (Organically-enriched)	Low Retention (Standard topsoil)	High Retention (Organically-enriched)	Low Retention (Standard topsoil)	
Loam	171214	500	4799	550	(Davis et al. 2001, Li & Davis 2008)
Sand	1295		1060		(Christensen et al. 1996)

Area ratios (see **Section 2.6**) were also considered in order to optimally design the device and decrease the frequency of upper layer removal. Pb^{2+} was chosen as the focus as it was the only metal known to exceed safety levels in rain garden soil (Li & Davis, 2008). Cu^{2+} behaviour was also examined as it is the most likely heavy metal to cause groundwater pollution given its high mobility in soil, even with no macropores present, and the fact that it was found not to sorb as easily to soil as Pb^{2+} or Zn^{2+} (Li & Davis, 2008). The K_d values for Pb^{2+} and Cu^{2+} of standard topsoil were similar (500 L/kg and 550 L/kg respectively), however for organically enriched soil, the K_d value for Pb^{2+} is significantly greater than Cu^{2+} (171214 L/kg in comparison with 4799 L/kg). This indicates that Pb^{2+} will sorb to the organic soil at a much higher level than Cu^{2+}.

The accumulation of Cu^{2+} in soil does occur but does not pose a health hazard and thus is not examined for this device (Li & Davis, 2008).

7.4 Macropore flow

Typically macropores only occur in the root zone as this layer has the highest biological activity. The storage zone is designed to be coarse sand or gravel, without organic matter, to encourage flow and storage which makes it relatively inert and discourages growth of roots,

earthworm movement and other activities which increase macropore flow. However as groundwater contamination was the key concern, the worst case scenario of a macropore reaching 1.5m (depth of the groundwater) was examined. In previous studies, macropores have been found to extend to this depth in soils similar to rain garden (Mallants et al., 1997). This formation may take several years of development thus it is assumed that the macropore is active for only a 7 year period compared to the total period of 10 years examined. The macropore also received the maximum inflow possible. The model used the KWE to calculate macropore flow rate, however the maximum flow rate in this case was limited to 2 cm/h owing to the maximum infiltration rate of the lower layer of chalk. This infiltration rate was measured using a soakaway test during the initial site investigation (Pam Brown Associates 2012).

7.5 Results

7.5.1 Matrix Flow

Using HM07 and the parameters discussed above, results for Pb^{2+} concentration in the upper 5 cm of the rain garden after a period of 10 years with an area ratio (*AR*) of 5 and 10% respectively and highly retentive soil are shown in **Figure 7.5**. The maximum concentration in the rain garden with AR=10% was 568 mg/kg. However if the area ratio was decreased to 5% to minimise construction costs, the level of Pb^{2+} accumulation increased significantly to 1209 mg/kg, higher than the allowable Pb^{2+} concentration in soil of 750 mg/kg (Pam Brown Associates, 2012) . This limit was set for industrial land use by the Environment Agency (Pam Brown Associates, 2012).

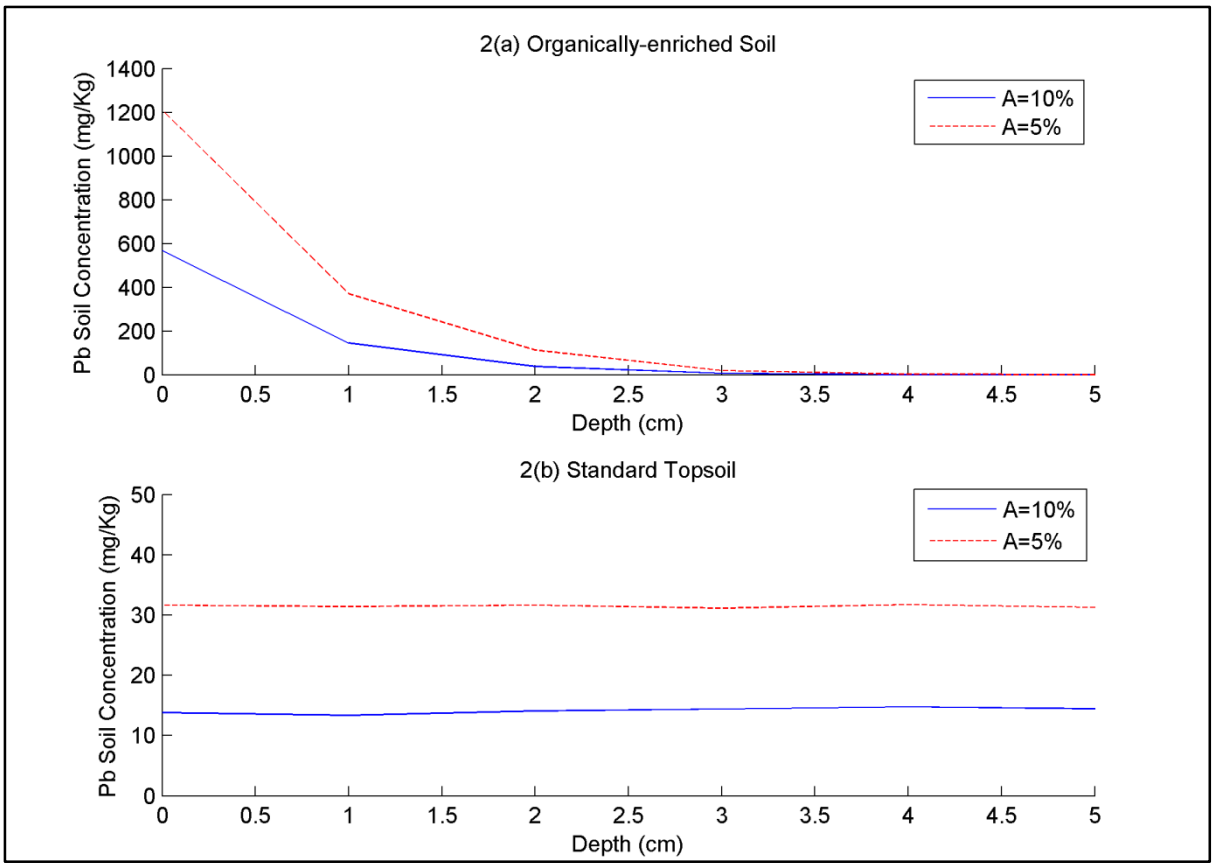

Figure 7.5 Pb^{2+} Concentration in Rain Garden Soil with Highly Retentive (Organically-Enriched) Soil (K_d=171214 L/kg) and Lower Retentive (Standard) Topsoil (K_d=500 L/kg) and Two Area Ratios.

For soil with a lower K_d value, the accumulation in the upper layer of the systems for both area ratios is reduced as illustrated in **Figure 7.5b**.

In addition to accumulation in the system, it is important also to consider the possibility of groundwater pollution caused by this lower retention. **Figure 7.6** shows the simulation results for Pb^{2+} concentration in soil-water for a lower Pb^{2+} retention rate in the upper layer after a period of 10 years. It indicates that in the case of an area ratio of 5%, Pb^{2+} does not reach a depth of lower than 43 cm much lower than the total depth of 60 cm, thus Pb^{2+} was retained in the device.

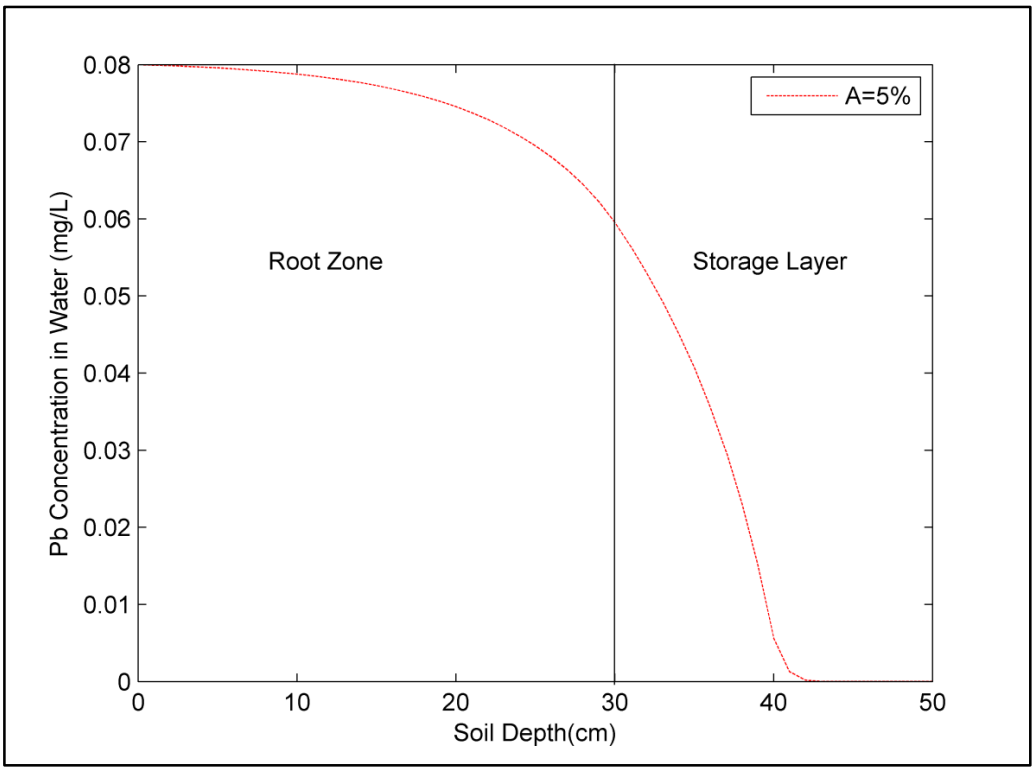

Figure 7.6 Pb^{2+} Concentration in Water for Lower Retentive Topsoil with a 5% Area Ratio after 10 years.

For the case of Cu^{2+}, **Figure 7.7** illustrates results for concentration in soil-water through the soil profile for highly retentive soil with an area ratio of 5 and 10% after 10 years. It shows that Cu^{2+} soil-water concentration is negligible at 30 cm which indicates that all retention is taking place in the upper layer. It also shows that area ratio has little effect on this concentration.

If however, the soil has a lower retention capacity such as normal topsoil (**Table 7.2**) it is observed that the majority of retention after a 10 year period takes place in the lower storage layer (**Figure 7.8**).

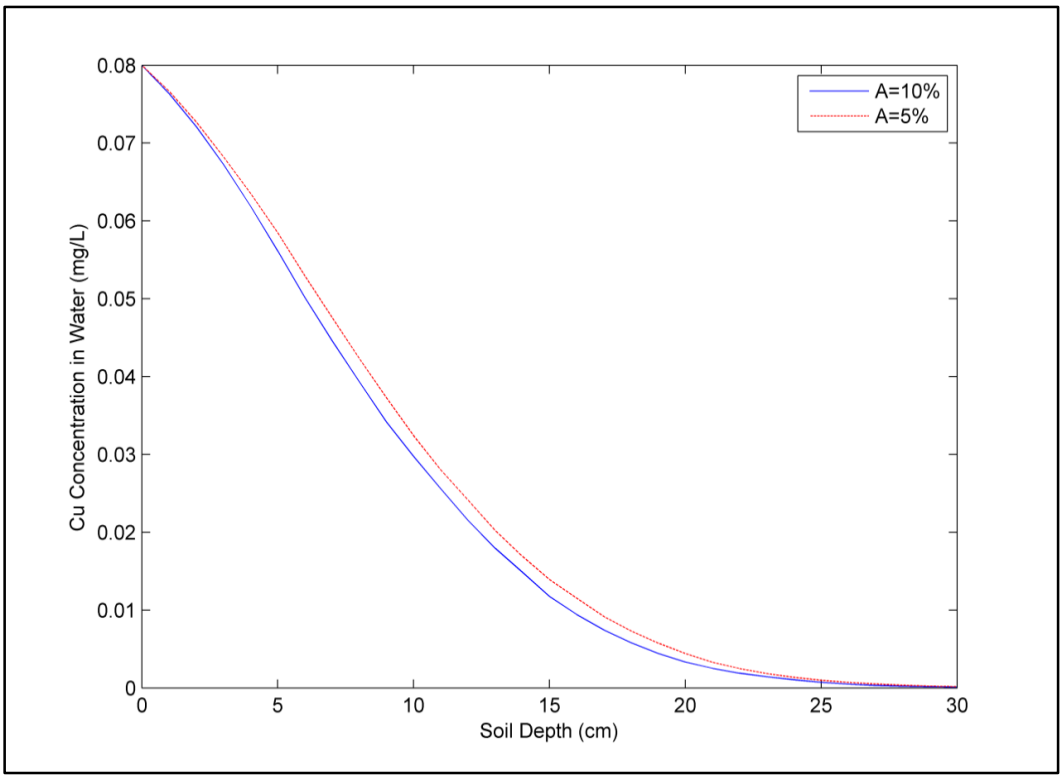

Figure 7.7 Cu^{2+} Concentration in Soil-Water for Highly Retentive (Organically Enriched) Soil and Two Area Ratios after 10 Years.

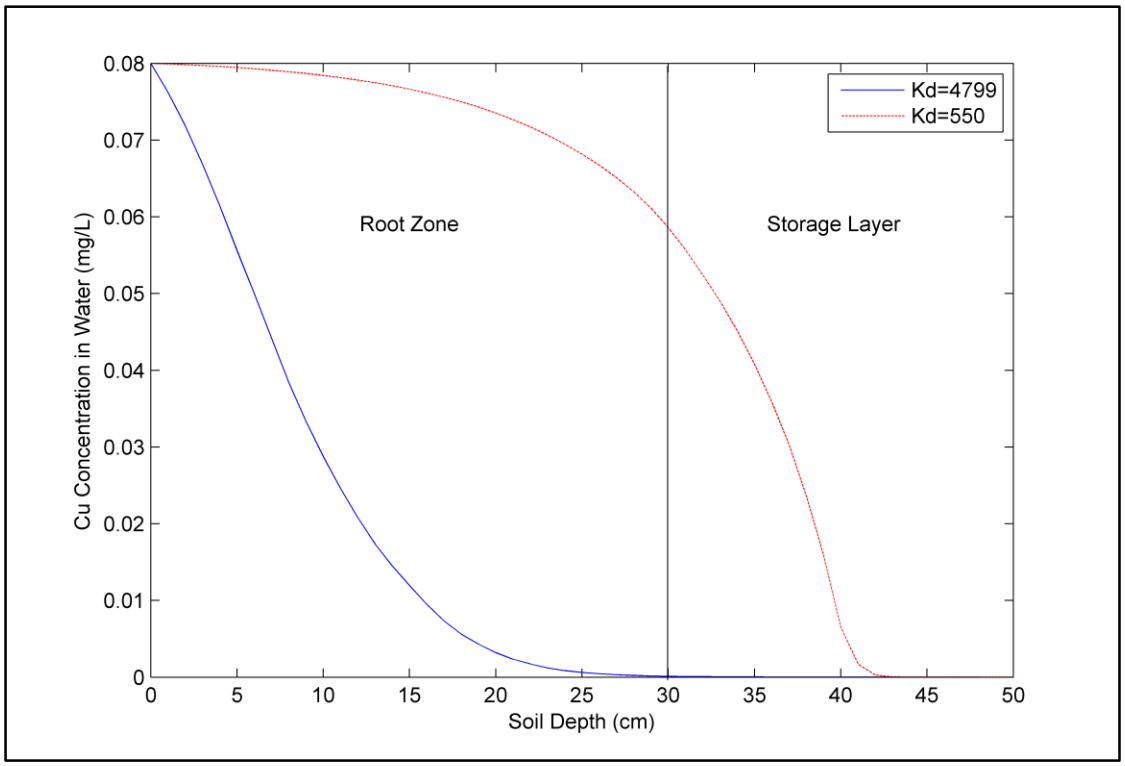

Figure 7.8 Cu^{2+} Concentration in Water for High (K_d=4799 L/kg) and Lower Retentive (K_d=550 L/kg) Soil with a 5% Area Ratio after 10 Years.

7.5.2 Macropore Flow

In this section, the effect of macropore flow on groundwater pollution is examined. **Figure 7.9** shows the Cu^{2+} water concentration in a single macropore for soil with the higher retention value after a period of ten years that has received the maximum water input based on the limiting factors stated in **Section 7.4**. This figure illustrates that Cu^{2+} is removed from the runoff in the root zone and that no groundwater pollution occurs due to macropore flow for organically enriched soil.

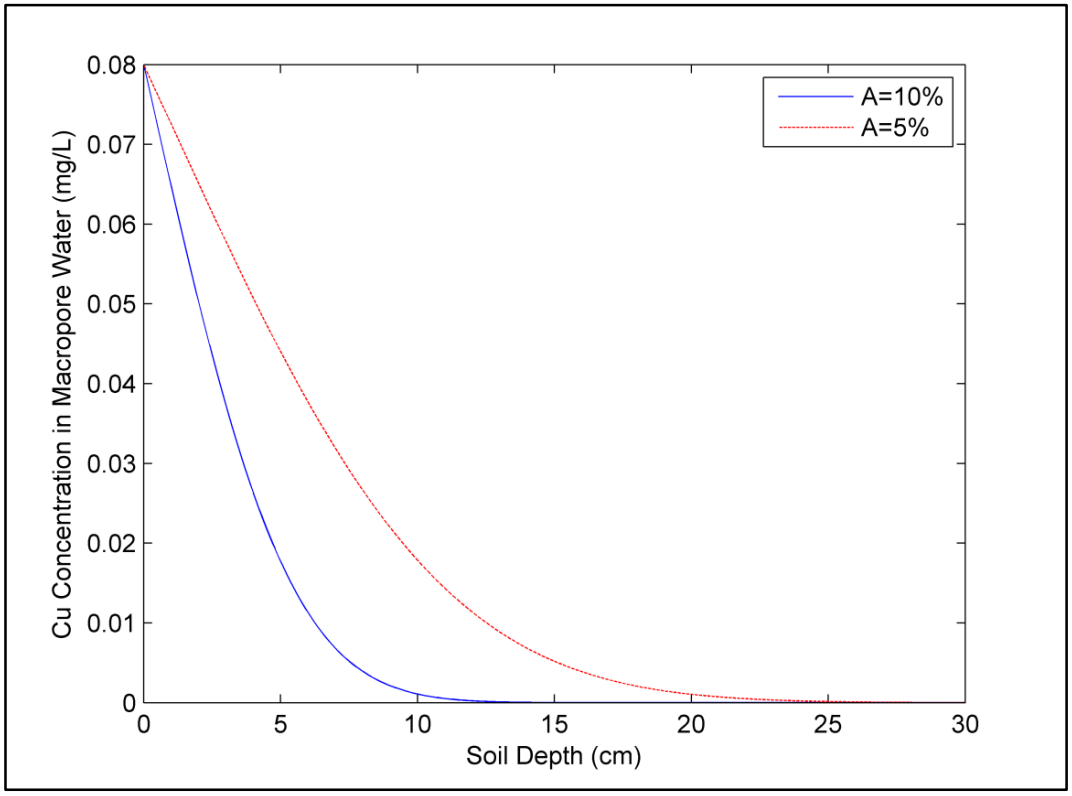

Figure 7.9 Cu^{2+} Concentration in Macropore Water for Highly Retentive (Organically Enriched) Soil and Two Area Ratios after 10 Years.

While **Figure 7.10** shows the Cu^{2+} water concentration in macropore flow for topsoil, Cu^{2+} is removed from the runoff by 55 cm depth for the worst case scenario (low retentive soil and an area ratio of 5%).

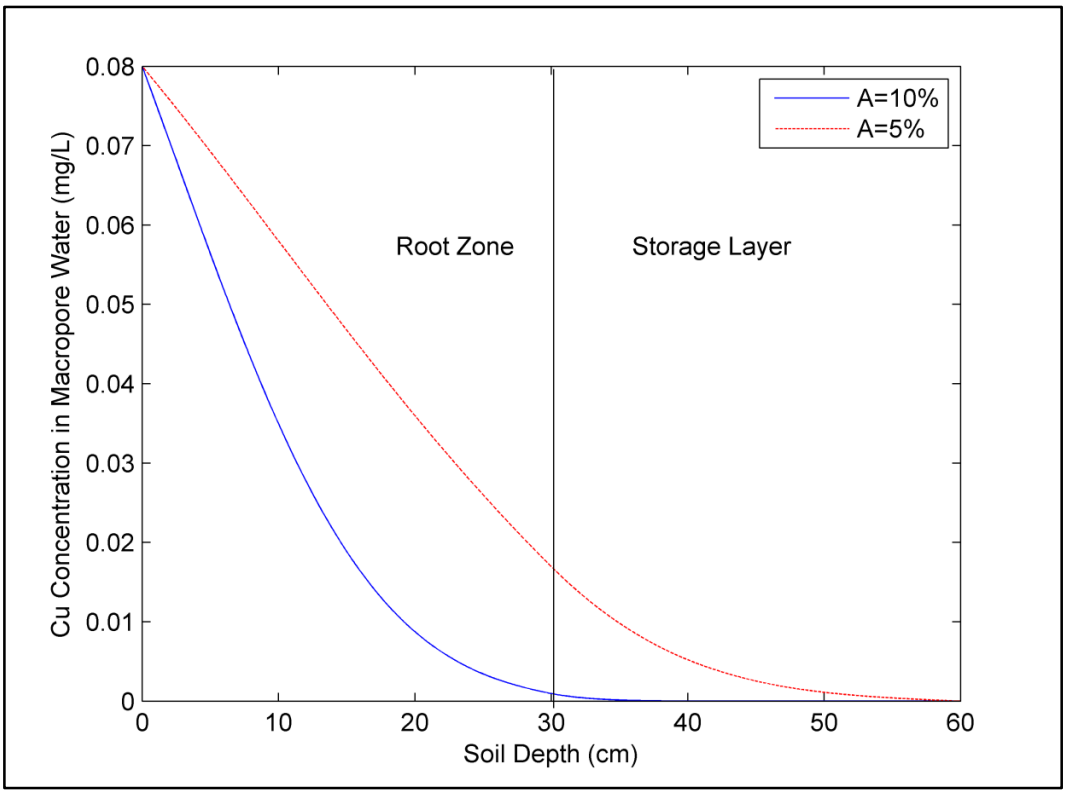

Figure 7.10 Cu^{2+} Water Concentration in Macropore Water for Lower Retentive Topsoil and Two Area Ratios.

7.5.3 Sensitivity Analysis

In order to quantify the effects of uncertainties in important parameter values, a sensitivity analysis was performed. The focuses of this examination were the variables K_d, K_{sat} and A as these have been shown to be the determining factor for retention. The reference values chosen for this analysis are those used earlier which are listed in **Table 7.1** and **Table 7.2**. As the main concern of this examination was to prevent groundwater contamination at the site, the effects of these variables on the Cu^{2+} outlet concentration in water from the upper layer of the system were examined (**Figure 7.11**).

From the sensitivity analysis (**Figure 7.11**), a linear relationship between the outlet water concentration and the value of K_d exists: this is to be expected as the linear isotherm is used. Minor deviances from the reference value do not influence the results substantially, only when the value of K_d is altered by above ±50% are major effects (±10%) on the Cu^{2+} outlet concentration seen. The outlet concentration is most sensitive to the value of saturated hydraulic conductivity K_{sat}. For low values of K_{sat}, outlet concentration is low, which may be due to increased overflow from the system and/or decreased pore water velocity through the

soil. The analysis shows that varying the other parameters did not have a significant impact on results.

A sensitivity analysis was not performed on macropore flow as the potential factors (number, velocity and capacity of macropores) would not significantly affect the results for outlet concentration given the maximum flow rate through the macropores of 2 cm/h determined by the lower layer of chalk.

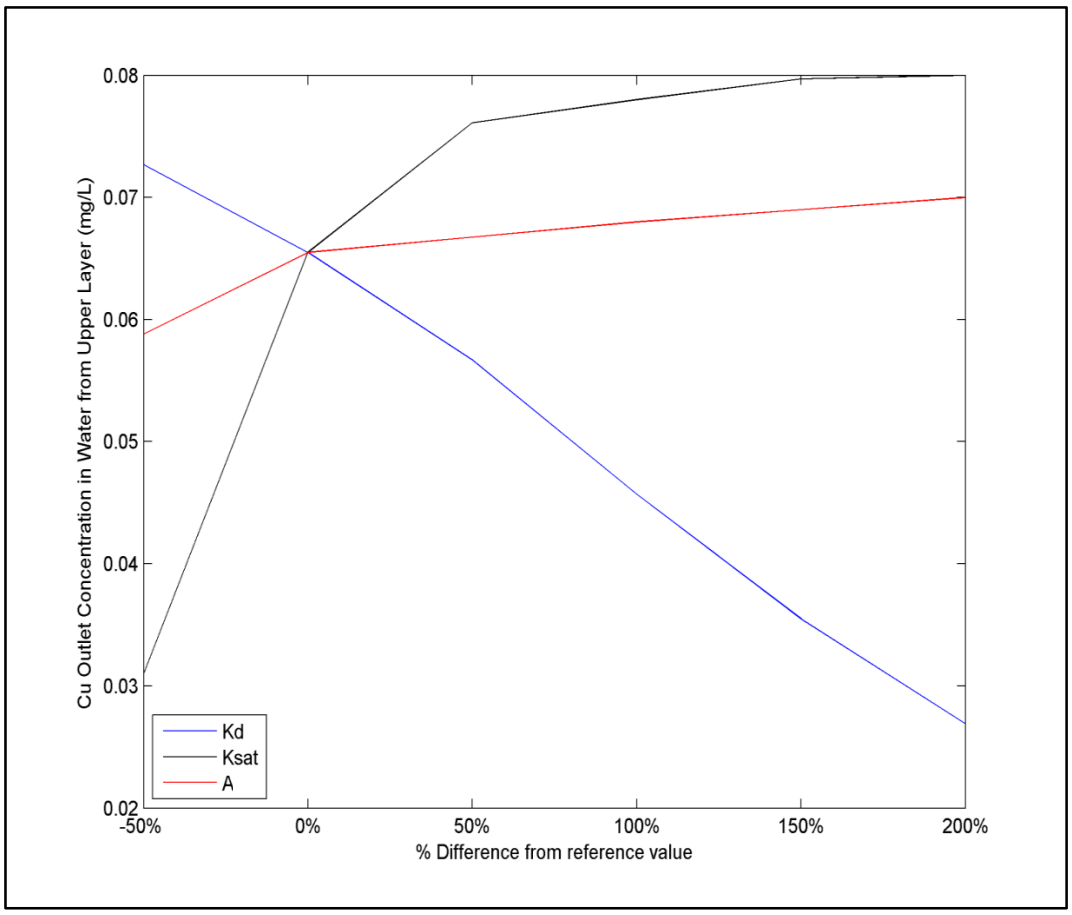

Figure 7.11 Sensitivity Analysis

7.6 Discussion

For highly retentive soils, the results for Pb^{2+} corresponded well to experimental findings by Li and Davis (2008) in that the majority of Pb^{2+} retention was limited to the upper 10 cm of soil (**Figure 7.5a**). The levels of accumulation were diminished when the value of K_d was reduced (**Figure 7.5b**) and a more even distribution of lower Pb^{2+} accumulation through the upper layer of the system was observed. Despite this, in all cases the rain garden demonstrated excellent performance in Pb^{2+} removal and no groundwater contamination was predicted in the 10 year period examined (**Figure 7.6**). However, the risks posed by the accumulation of this

metal required additional investigation. As the roundabout was not accessible to the public, the soil pollutant guidelines for industrial and commercial sites provided by the Environmental Agency were appropriate; the regulatory level for Pb^{2+} in these guidelines is 750 mg/kg (Pam Brown Associates 2012). This indicated that in the case of the lower area ratio (5%), the first 1 cm of soil needs to be replaced within the 10 year period examined after approximately 6 years. This would cause a large degree of inconvenience as it requires vegetation be removed. The reason the contamination is limited to 1cm is due to the high adsorption capacity of the soil for Pb^{2+} however this would not be the case in all circumstances. For example, if the K_d was lower but still large enough to facilitate high rates of retention, a dangerous level of accumulation would be distributed to a greater depth. For A=10% the level of accumulation did not exceed regulatory guidelines provided by the Environmental Agency therefore no action needed to be taken.

If this rain garden was situated in a residential area, the maximum allowable concentration decreases to 350 mg/kg due to the possibility of human contact and thus would require remedial action at more regular intervals even with an area ratio of 10% .This highlights the need to design rain gardens on an individual basis and further underlines the utility of this model.

With regards to Cu^{2+}, again substantial retention was predicted, also in line with experimental evidence (Davis et al. 2001). Results shown in **Figure 7.7** indicate that the water concentration values were minimally affected by a decreased area ratio. A possible reason for this is that a large increase in pore water velocity is required to have an effect on retention, an aspect which needs to be further investigated. The majority of rainfall events at the site are of lower precipitation values (<10mm) thus a significant rise in velocity is only seen during exceptional events minimally affecting retention.

When the K_d value of the upper layer is reduced, the majority of Cu^{2+} capture shifts to the storage zone, but no metal flux is predicted from the rain garden to the subsoil and groundwater (**Figure 7.8**). It is thus, beneficial for the lower storage layer to also have high K_d values to ensure that despite metal flux from the upper layer no pollution reaches the subsoil.

In the case of macropore flow, no Cu^{2+} flux is predicted to enter groundwater (**Figure 7.9** and **Figure 7.10**). This is caused by the limiting infiltration rate of the chalk of 2 cm/h (see **Section 7.4**) which decreases the maximum velocity in the macropore and thus increases sorption, sorption does not typically occur in the macropores as their water velocity can be in excess of 134 cm/h (Jury & Horton, 2004). It is therefore important to consider each situation

individually. Overall, these observations emphasize the relevance of this recently developed model, particularly given that macropores are not considered in the proposed standards for SuDS design (DEFRA, 2011).

In summary, the model results imply that a higher distribution coefficient coupled with a low area ratio results in large levels of Pb^{2+} accumulation. Thus, in order to evenly distribute Pb^{2+} throughout the upper layer of the rain garden, soils with lower Pb^{2+} distribution coefficient may be more efficient. This would reduce the need for frequent costly removal of contaminated soil. Macropore flow did not affect groundwater quality given the limiting infiltration effect of the lower layer of chalk. Therefore, in this particular case, an area ratio of 5% is recommended to decrease construction and maintenance costs. A soil with a lower K_d value can be used for the upper layer to prevent hazardous metal accumulation, but care should be taken to ensure the storage layer has enough retention capacity itself to offset the decreased heavy metal retention this would cause.

It is clear from the findings of this examination that it is of vital importance to monitor the fate of heavy metals in SuDS during the design process, to ensure the creation of an optimum device. The advantages of the developed model over conventional design techniques such as standards (DEFRA, 2011) are also illustrated as it allows for rain gardens to be individually assessed based on their specific situations including climate change, soil conditions and design parameter sets. This can be achieved by running simulations and varying the soil type, layer depth, area ratio and rainfall levels enabling a detailed examination of these different situations and their impact on groundwater recharge and heavy metal retention.

Finally, the model allows for the examination of possible consequences of choosing a design with decreased construction costs such as a low area ratio which could lead to increased overflow and need for increased maintenance. It can also be used to develop maintenance schedules. This can be achieved by running simulations before construction whereby an indication of when Pb^{2+} accumulations reach regulatory limits can be found. These findings can be updated whenever further information is gathered, such as heavy metal runoff concentrations.

In its current state however the model does not simulate the behaviour of other pollutants such as nutrients and hydrocarbons which are also of concern, but the isotherms for these pollutants can be added to this model in the future.

8 DISCUSSION

8.1 Introduction

In this chapter a discussion is given which addresses all aspects pertinent to the proposed model. Firstly, the issue of applicability and purpose will be examined, starting with the models use as a research and design tool for rain gardens and how it compliments current research. Its applicability to other infiltration based SuDS (green roofs) is then examined, along with any adaption which will need to be made.

Secondly, the advantages and limitations of the model are discussed in the context of other options available for the prediction of heavy metal retention in rain garden systems.

Finally, the main contributions of knowledge that this thesis provides are detailed and discussed.

8.2 Application of the Model

8.2.1 Rain Gardens

As discussed in **Chapter 7**, this model can be used to provide an accurate method of predicting heavy metal retention and accumulation in rain gardens over long periods of time.

Currently, there are few studies completed into the long term heavy metal removal capacity of these systems. Paus et al. (2014) examined the saturated hydraulic conductivity (K_{sat}) and heavy metal accumulation of three rain gardens over a period of four years. They found that the K_{sat} increased by between 300 and 600%. This, coupled with a decrease in bulk density of between 10-22%, indicates macropore flow, although this is never identified in the paper. Unfortunately, the metal accumulation is only measured at the end of the four year period so a direct correlation cannot be established between macropore flow and a decrease in retention. However, it was found that the Cd and Zn concentrations were lower than the estimated sorption capacities for the media which could be due to bypass of the matrix regions by preferential flow. It was stated by the authors that there is a need to investigate a wider range of rain gardens to establish the key factors effecting long term infiltration and retention performance. This need could partially met by utilising the fully validated model to examine scenarios including changes of K_{sat} with time and possible macropore flow.

Current research is focussing predominantly on the examination of possible media and their effects on hydraulic conductivity and retention removal (Paus et al. 2014, Jones & Davis,

2013). In the future, the model in this thesis could complement this research by utilising the findings and running simulations which examine the effect of parameter variation. Thus this model provides an excellent addition to research in the field of pollutant retention in SuDS.

8.2.2 Green Roofs

Green roofs are another type of infiltration based SuDS. The general construction of a green roof consists of four layers: vegetation layer, soil layer, filter and drainage material (Czemial Berndtsson, 2010). They are generally separated into two main classes: intensive, typified by deep layers of soil which can support larger flora and extensive, which are characterised by very thin soil layers and large coverage areas. Obviously the main aim of a green roof is different to a rain garden in that it does not increase groundwater recharge but seeks to diminish the peak storm flow (through soil retention) which can cause flash flooding and disruption in cities. It is still important to ensure heavy metals are retained by these systems so that when the delayed runoff reaches either sustainable or conventional drainage systems environmental contamination does not occur. An example of maximum and minimum heavy metal concentrations in urban runoff is given in **Table 8.1** (Gobel et al., 2007).

Table 8.1 Heavy Metal Concentrations in Rainfall

Heavy Metal Concentration (µg/L)	**Rainfall**	
	Min	Max
Cu	1	355
Pb	2	76
Zn	5	235

Green roofs share many similar characteristics to rain gardens such as layered soil profiles and vegetation however there are some unique differences most notably slope and drainage method (as green roofs do not drain into subsoil, their runoff is directed to outflow pipes). It has been found that slope does not influence the shape of the direct runoff hydrograph however it does impact water retention within the green roof: the lower the slope the higher the retention this is due to the decreased infiltration capacity of slopes (Getter, et al., 2007). The kinematic wave equation is commonly used to model unsaturated subsurface flow on hillslopes (Beven, 1982; Singh, 1997; Norbiato & Borga, 2008); therefore it should be easy to adapt the model to suit a

green roof. In addition a simple reservoir routing equation similar to that used by She and Pang (2010) can be incorporated to model the drainage from the device.

There are several computer models which have been used to examine the hydrological performance of green roofs, some have been developed specifically for this purpose (She & Pang, 2010) and others such as HYDRUS (Hilten, et al., 2008) and SWAP (Metselaar, 2012) have been adapted with mixed results. However to the author's knowledge a model has never been used to examine heavy metal retention or pollutant transfer through macropores in these systems.

With regards to metal retention, it has been observed that green roof runoff typically reduces the loads of heavy metals in rainfall and runoff. However some metals appear in green roof runoff in concentrations that would correspond to moderately polluted water (Czemial Berndtsson, 2010). For example, a monitored extensive green roof in Sweden Cu outflow was increased fourfold and only 8% of Zn retained. This supports the work of Gnecco et al. (2013) who found that the use of certain substrates can lead green roofs to become a source of heavy metal contamination. This again has been observed in aging green roof such as the 43 year old intensive green roof at the University of Manchester which has become a source of Pb pollution (Speak, et al., 2014). Other green roofs display excellent retention of heavy metals such as the semi extensive (99% retention of Pb, Zn and Cu) and extensive (99% Pb, 97% Cu, 96% Zn) systems examined by Steusloff (1998).

Macropore flow has never been examined in the context of green roofs but it is of vital importance to consider due to the shallow nature of these systems and could possible explain the large variance in retention between green roofs. It has also been observed by Getter et al. (2007) that over a period of five years, the pore space in an intensive roof increased from 41.41% to 81.84%, this increased water holding capacity but would surely have an impact on metal retention; unfortunately this was not examined.

Another less common aspect of green roof research is their use for vegetable production owing to predicted food shortages in the future (Whittinghill, et al. 2013). If the roofs become contaminated with heavy metals this avenue will not be possible so it is important to take this into account.

The findings above indicate that the behaviour of heavy metals in green roofs is a complex subject dependent on a number of factors. Therefore the application of the discussed model to this area would be a significant contribution to this field of research.

8.2.3 Permeable Pavements

Permeable pavements are an alternative to traditional impermeable asphalt and concrete surfaces. Permeable pavements enable stormwater to either infiltrate into an underground storage basin or soil resulting in groundwater recharge while also potentially removing pollutants (Bean et al., 2007). Permeable pavement designs vary greatly although generally they comprise of a series of layers as shown in **Figure 8.1**.

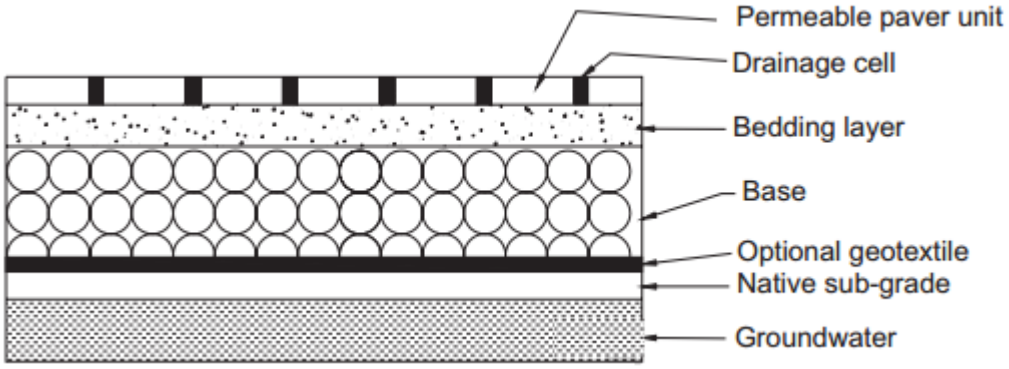

Figure 8.1 Diagram of a Permeable Pavement (Scholz & Grabowiecki, 2007)

This type of permeable pavement comprises of four distinct components:

- paving slabs or bricks;
- unsaturated zone of the base material;
- saturated zone of the base material; and
- sub-grade.

One of the key differences between permeable pavements and other SuDS such as rain gardens and green roofs is the presence of a geotextile. Geotextiles are needed to prevent sand from migrating through the layers, reduce rutting depth and retain and degrade oil and nutrients. In terms of heavy metal retention, Legret et al. (1996) showed that suspended solids and lead can be reduced by PPS up to 64% and 79%, respectively. Generally, PPS are efficient in trapping dissolved heavy metals in surface runoff. However, not all pavers and joint fillings have the ability to trap dissolved heavy metals. Pavements with large joints for infiltration must have a suitable joint filling. Otherwise, metals will pass through them, and may subsequently enter groundwater resources. Particles usually accumulate in geotextiles and on pavement surfaces.

Geotextiles usually separate micropollutants such as cadmium, zinc and copper from the underlying soil, therefore preventing groundwater from becoming contaminated (Legret et al., 1996)

HM07 can be used to predict both the movement of water and the retention of heavy metals in a permeable pavement systems. The unsaturated and saturated zone and subgrade are all types of material with known parameters and can be modelled as layers of soil HM07. The geotextile material is more problematic. There are many types of geotextile material available however their properties are well researched (Aydilek & Edil, 2004). The key parameters required for modelling water transport are porosity and permittivity as detailed in **Section 3.4** both of which have been calculated for a variety of geotextiles (Aydilek & Edil, 2004).

For heavy metal retention, linear, Freundlich and Langmuir retention coefficient for the geotextiles are required. These will need to be obtained via an experiment similar to that completed by Davis et al. (2001).

8.3 Advantages of the Model

When developing this thesis, the aim was to find a balance between a competent, highly accurate model that can be used for research, and an appropriate tool for design purposes (simulating long input rainfall datasets).

Prior to this thesis, no specifically- designed model existed which could be used to predict the extent to which heavy metals were captured in rain garden systems. As discussed in **Appendix A**, HYDRUS is a software package for simulating water, heat, and solute movement in variably saturated media. HYDRUS is generally used to model the water flow and solute transport and then combined with a more complex geochemical speciation model (Jacques, et al., 2008) or uniquely scaled sorption isotherm (Xiao, et al., 2013) to predict metal retention. In both cases, the movement of heavy metals was accurately quantified, however HYDRUS was primarily aimed as a research tool and is difficult to modify, is site specific and requires extensive calibration.

In addition, HYDRUS has been found to require a long CPU time. It was found by Noranbuena-Contreras at al. (2012) that a period of approximately 8 days was required to simulate rainfall infiltration into an embankment with a fine mesh of 3848 nodes and 7457 triangular elements in Hydrus 2-D. Typically HYDRUS 2-D takes three times as long as HYDRUS 1-D but this

still equates to computational time of almost 3 days which would be unacceptable to engineers designing these facilities (PC-PROGRESS, 2012).

The combination of complexity and long computational times make the above option inappropriate as a design tool. These issues are addressed by the model proposed by this thesis, which currently uses a Matlab interface which simply requires the parameters of the rain garden and precipitation values. For the case study in **Chapter 7** it took approximately 4 hours to run for each 10 year case, using hourly data. The model still retains accuracy as illustrated in **Section 4.4.1** whereby it successfully replicated the results of the Richards' equation with an R^2=0.993.

8.4 Limitations

The current study only focused on one of the major pollutant groups present in urban storm water, heavy metals (in particular Cu and Pb); thus the other pollutant groups, hydrocarbons and nutrients are not taken into account. The model however includes hydraulic characteristics which impact all the contaminant groups so in the future it is possible to add further subroutines which include the other contaminants (see **Section 9.3**).

Another factor that became apparent in testing is the kinematic wave equations' inability to fully quantify diffusion occurring during drainage as shown in **Section 6.4**. However the minor influence this inaccuracy has on soil moisture content and pore water velocity does not significantly affect heavy metal retention prediction as illustrated in **Section 4.4.4.4**. More importantly, KWE diverges more from Richards equation when soil gets drier (suction>gravity), but in a rain garden context the soil is encouraged to be perpetually inundated with water from the surrounding area so aridness is rare.

8.5 Contribution to Knowledge

Throughout this project there have been several key contributions to knowledge. These are split into three key sections Model, Experimental and Simulation

8.5.1 Model

As stated numerous times in this thesis, HM07 was created to predict heavy metal retention in a rain garden facility. This model can be used for research (to examine the key factors which make a high performance rain garden system) and also to design these devices (Quinn & Dussaillant, 2014). No other model similar to this existed previously and this is deemed to be a unique contribution to research.

8.5.2 Experimental

The experiment detailed in this thesis was the first to examine the effect of macropores on heavy metal retention in a sustainable drainage system. As discussed in **Section 3.2** macropore flow is a key factor in the capture of pollutants so these experiments are a crucial next step in the research area of pollutant retention in rain gardens. The outflow of these systems was analysed with a very low level of detection: 0.03 µg/L for Cu, 0.01 µg/L for Pb and 0.1 µg/L for Zn with only 5% error, this allows for highly accurate results and the analysis of minute difference between matrix and macropore columns. As discussed in **Section 5.5.1**, it was found that hydraulically there was no difference between matrix and macropore columns possibly owing to speed restrictions in macropores or the assertion in **Section 4.2.2.3** that water transfer between macropore and matrix soils is instantaneous in rain garden soil. The column soil was also of a much higher permeability than that recommended for a rain garden. Despite this finding, macropore flow still has a minor influence on Cu retention, decreasing in macropore columns, this indicates that macropores still have an influence on heavy metal retention and this requires further research. This is a significant finding as it indicates that even for highly permeable soils, macropore flow still facilitates heavy metal transport through the system.

8.5.3 Simulations

It was found during the simulations discussed in **Chapter 7** that soils with high retention capacity are not necessarily suited for rain gardens as they can lead to dangerous levels of accumulation of Pb. This can be prevented by using a less retentive substrate while still maintaining groundwater quality.

It was observed when undertaking the sensitivity analysis that area ratio and saturated hydraulic conductivity did not significantly affect the retention of Cu. This had never previously been simulated to the author's knowledge.

9 CONCLUSION AND FURTHER WORK

9.1 Introduction

This chapter examines the objectives provided in **Section 1.3** and evaluates their progress. Having completed this conclusion, future work is identified.

9.2 Conclusions

In order to provide a comprehensive set of conclusions for this thesis, this chapter has been divided into sections which evaluate the findings of the research in terms of the contributions they have made to the main objectives of this thesis.

With respect to Objective One (Investigate the key factors affecting pollutant retention including both soil type and hydraulic functions and examine which equations best model the effects of these influences on heavy metal retention):

An in-depth literature review (**Chapter 3**) was carried out which provided the necessary background knowledge for this project in terms of understanding theory and the implementation of equations (runoff pollutants, variably saturated flow through porous media, dual-permeability models, solute transport and retention).

As part of this review heavy metals were chosen as the sole focus of the pollutant retention model as they posed the greatest health hazard. In addition, the key factors which affected their retention in rain gardens were identified. These were found to be split into two distinct groups; hydrological and soil related (vegetation also affected retention but to a much lesser extent). The hydrological factors largely revolved around the pore water velocity with increased velocity resulting in decreased retention, soil water content and the presence of macropore flow which can prevent a large amount of retention by transferring the runoff directly through the rain garden. The soil characteristics were dependent on properties such as bulk density and distribution coefficients for various isotherms; it was also found that the organic matter content of the soil had a beneficial impact on heavy metal capture providing that the soil is also well graded.

With regards to water modelling, dual permeability models were examined and methods of modelling flow in both the matrix and macropore regions. Determining the initiation of macropore flow and transfer between the regions were discussed.

In terms of heavy metal retention, the accuracy and applicability of different isotherms were assessed along with methods of solute transport prediction.

This objective was deemed to be complete as the relevant literature was consulted and this provided a solid base from which a computer model could be designed.

With respect to Objective Two (Develop and verify a simple dual-permeability model specifically designed to model both water flow and contaminant retention in a rain garden using the findings from the above objectives and results from literature.):

It was decided to develop a dual-permeability approach to the water modelling section so that both flows in the matrix and macropore regions could be accounted for. The kinematic wave equation was chosen to model water movement in both regions as this provides a simpler alternative to more complex methods such as the Richards equation while still maintaining good accuracy. With regards to the heavy metal modelling three isotherms were chosen: the linear, Langmuir and Freundlich equations, as these showed the most promising results from literature data. All three were examined as they each added beneficial attributes to the model; linear for initial estimations, Langmuir for particles with little surface roughness and Freundlich for coarse particles. These isotherms were incorporated into the one dimensional advection-dispersion-adsorption equation so that both transport and retention could be modelled together. The equations chosen and the reasoning behind these decision were discussed in **Chapter 4**.

A number of requirements were listed in **Table 4.15** which needed to be met in order to develop a useful pollutant retention model. It was found that the created model met all of these requirements (**Table 4.15**).

This model was verified in three parts, the matrix, macropore and pollutant retention sections (**Section 4.4**). The matrix portion was tested against cases which illustrated situations common in rain garden systems, specifically sharp wetting fronts (Celia, et al., 1990) and layered soil profiles (Pan & Wierenga, 1995) and showed excellent results (**Section 4.2.1**). The macropore section was validated against experiments completed by Mdaghri-Alaoui & Germann (1998). These cases were chosen as suitable

validation for the macropore segment of this model as the four runs examined were performed on a layered soil and encompassed a large range of infiltration, conductance and exponent values. The macropore section showed good agreement with the experimental results (**Section 4.4.2**). The linear isotherm model was tested against the experimental results of Davis et al. (2001) as these were performed with rain gardens specifically in mind and again the results were good (**Section 4.4.3**)

The Langmuir and Freundlich isotherms were validated using data from the Highways Research Group (2010) and were found to give accurate results. A sensitivity analysis was also performed and it was found that only dramatic increases (velocity i.e. inflow or saturated hydraulic conductivity (K_s)) or decreases (bulk density) had an effect on the % of heavy metal retained. The other factors of dispersion coefficient and porosity had no significant impact. This indicated that for the case of increases in velocity caused by high inflow rates or high K_s and decreases in bulk density caused by heterogeneity of the soil retention was not decreased dramatically (**Section 4.4.4**).

From the detailed model developed and the preliminary validation discussed in **Chapter 4**, this objective was deemed to be complete.

With respect to Objective Three (Design and perform column experiments that both provide a unique contribution to rain garden research but also serve to provide further validation of the model routines):

This objective was achieved by analysing past experiments and identifying an area where research is lacking; this area was the effect of a single artificial macropore on heavy metal retention in a layered soil column (with similar soil layout to a rain garden) under typical English climatic conditions. The findings of these experiments indicated that although macropore flow did not impact the hydraulic performance of the columns, retention of the most mobile heavy metal, Cu, decreased slightly by the presence of macropores. This was attributed to macropore flow moving at the same speed as flow in the matrix region due to its natural speed limit and the high permeability of the soil. However retention in the macropores was less than the matrix region resulting in increased outflow Cu concentration from those columns.

The overall heavy metal retention of the columns was high (>99%) proving that under English climatic conditions macropores are not a dominant factor in either the

movement of water or pollutant through a rain garden. This finding supports the presumptions previously made regarding macropore initiation and transfer.

Finally the results of the column experiments were compared to the prediction of the model. Unfortunately, it was not possible to validate the macropore section due to inconclusive results and the high hydraulic conductivity of the soil. The predictions of the kinematic wave equation agreed well with the results from the matrix region (R^2>0.86). It was found that similar to the preliminary validation there were problems quantifying the drainage wave although this would not significantly affect pollution retention results (**Section 6.4**). Finally it was shown that there was good agreement between the predicted heavy metal outflow by the linear isotherm and the column results (**Section 6.5**).

From the experimental results (**Chapter 5**) and validation (**Chapter 6**) this objective was deemed to have been met.

With respect to Objective Four (Perform simulations to examine effect on pollutant retention of rain garden design parameters including surface area and soil choice):

In **Chapter 7**, the model was applied to the design of a rain garden system for a planned roundabout in Kent, U.K. The preliminary design considered an upper root zone layer with organic soil and a sandy storage sublayer each 30 cm thick, for a rain garden with area ratio of 5 and 10%. One of the principle scenarios examined was the accumulation and movement of metals without macropores. It was shown that levels of lead can build up in the upper layers of the system and constitutes a health hazard (surpass Environment Agency U.K. standard of 750 mg/Kg) after 10 years. Simulations showed that Cu was successfully retained (no significant concentrations below 50 cm of rain garden soil depth). Therefore in this case it was recommended that soil with a lower retention capacity be used for the upper layer to prevent hazardous Pb accumulation, but care should be taken to ensure the storage layer had enough retention capacity itself to offset the decreased heavy metal retention this would cause. This finding is in contrast to intuitive knowledge which suggests the use of specialist soil with a high capacity for metal retention be used in these devices. Care should be taken however when selecting soil with distribution coefficients based on batch and column studies. As discussed in **Section 4.4.4.3** the adsorption parameters for heavy metals followed the order of batch>column>field. Thus it is proposed that a safety factor be applied to

parameters obtained from batch and column experiments in the future, or that sensitivity analysis be completed to ensure that sufficient retention occurs even if the distribution coefficient is significantly decreased.

With respect to Objective Six (Investigate the effects of different hydrological processes such as macropore flow):

Rain garden soils have different characteristics from the agricultural clay soils which are typically examined with regards to macropore flow; they have a high saturated hydraulic conductivity and are not as prone to cracking at the soil surface. They therefore require different approaches and equations to model preferential flow. Rain garden soils typically have higher infiltration rates and a finer consistency which results in a very high hydraulic conductivity, this facilitates easy transfer from the macropore to matrix region (**Section 4.2.2.3**). Therefore a water transfer term is often not needed as the worst case scenario (no transfer of water) only occurs when the rain garden is saturated when no transfer is possible. This is often not the case in agricultural soils (modelled by HYDRUS, MACRO and RZWQM) whose consistency often causes ponding before saturation.

The column experiments further supported this argument: they indicated that macropore flow travelled at the same velocity as matrix flow or possibly was transferred into the matrix region. The outflow concentration of Pb and Zn was unaffected by the macropores present. Cu showed an increase in outflow concentration from the macropore columns indicating that macropore flow does affect the retention of the most mobile of heavy metals. A detailed discussion of these issues is available in **Chapter 5**.

Finally with regards to the simulations completed in **Chapter 7** macropore flow was examined by the model for a case where groundwater contamination was a possibility due to preferential flow bypassing the retention capabilities of a rain garden. Results indicated that, due to site conditions macropore flow was not a threat to groundwater at this location for the time frame considered. In addition, a sensitivity analysis was completed to examine the effects of other parameter: saturated hydraulic conductivity (K_{sat}), area ratio and distribution coefficient. The outlet concentration is most sensitive to the value of saturated hydraulic conductivity K_{sat}. For low values of K_{sat}, outlet concentration was low, which may be due to increased overflow from the system and/or

decreased pore water velocity through the soil. The analysis showed that varying the other parameters did not have a significant impact on results. The results are detailed in **Chapter 7** and this objective was deemed to be met.

Further sensitivity analysis was carried out to examine the hydrological parameters related to retention predicted by the Freundlich isotherm (**Section 4.4.4.4**). It was found that pore water velocity had a minimal effect on retention whereas porosity (soil moisture content) and diffusion were negligible. This supported the use of less complex equations such as the kinematic wave equation which gave accurate results but was less precise than the more complex Richards equation which required more computational power.

9.3 Further Work and Recommendations

It is suggested that further work on this project address the limitations discussed in **Section 8.4**. This would begin by expanding the model to include hydrocarbons and nutrients possibly using the methods outlined in **Table 3.1**. The priority would be hydrocarbons as these have been identified by the Highways Agency as significantly damaging to the natural environment (Highways Research Group, 2010). The movement of hydrocarbons through soil is often comprised of a three-fluid phase system with air, water, and a nonaqueous phase liquid. This is generally the case for high contamination levels however with regard to urban runoff where concentrations are lower, a simplified approach would be appropriate. This method would take the form of a special advection-dispersion-adsorption equation adapted to include biodegradation, isotherms for sorption, and a term for volatilisation. The final contaminant, nutrients would be harder to model as they are composed of a number of different constituents, nitrogen, ammonia, nitrate and phosphorus, all with different removal phenomena. Again an adapted advection-dispersion-adsorption equation could be utilized (similar to HYDRUS and MACRO) but it would need to include a denitrification function and an additional method to calculate plant uptake such as the Feddes model (Simunek, et al., 2003; Larsbo, et al., 2005). Phosphorus would be the easiest and most important nutrient to examine initially as it is the limiting nutrient in most inland waters. These additions to the model would create a more design tool allowing for the examination of multiple pollutant retention in addition to groundwater recharge, further increasing knowledge in this research area.

Following this, the model could be adapted to apply to other SuDS such as green roofs (**Section 8.2.2**). This would require a more elaborate evapotranspiration scheme (for example Penman-

Monteith) as due to the shallow nature of these systems this process is more critical than in the deeper soils of a rain garden. In addition, evapotranspiration is closely tied to the other benefits of green roofs such as heat insulation. No current model exists to predict the pollution retention in these systems so this addition would prove valuable.

In addition, it would be possible to expand this model to two dimensions. This would allow the examination of water flow and pollutants movement in lateral directions. This would expand the applicability of the model to more complex scenarios and systems such as permeable pavements.

With regards to experiments, it was suggested by experimental and analytical knowledge that water transfer is a dominant process in a rain garden system. It is recommended that further experiments be completed in this area to investigate this phenomenon. These could take a form similar to studies completed by Arora & McGuire (2011) where tensiometers were used to directly measure the moisture content of macropores. This would provide evidence as to whether water transfer was occurring or that macropore flow was at the same speed as matrix flow owing to the high hydraulic conductivity of rain garden soil.

Finally, it would be advisable to complete the experiments detailed in this thesis with longer simulation times and a lower saturated hydraulic conductivity (K_s). As mentioned previously (**Section** Error! Reference source not found.) the K_s values for the column soil were higher than that recommended for rain gardens thus in future they should be decreased. This can be achieved by using a different texture soil or possibly carefully compacting the soil to eliminate the voids that cause high hydraulic conductivity. This combined with a longer run time will facilitate a greater understanding of the influence of macropore flow on heavy metal transport in a rain garden system.

The most critical research in the future should be the examination of the effect of macropore flow on heavy metal retention in sustainable drainage systems (initially rain gardens but can be expanded to green roofs in the future). These experiments can form the basis to refine the existing model to truly give an accurate representation of water flow and contaminant transport in these devices and create a platform for expanding this model to other systems such as green roofs.

REFERENCES

Ahuja, L., Hanson, J.D., Rojas, K.W. & Shaffe, M.J., 2000. *Root Zone Water Quality Model - Modeling Management Effects on Water Quality and Crop Production.* Colorado: Water Resources Publications, LLC.

Al-Asheh, S. & Duvnjak, Z., 1997. Sorption of cadmium and other heavy metals by pine bark. *Journal of Hazardous Materials,* 56(1-2), pp. 35-51.

Allaire-Leung, S., Gupta, S. & Moncrief, J., 2000. Water and solute movement in soil as influenced by macropore characteristics 2. Macropore tortuosity. *Journal of Contaminant Hydrology,* 41(3-4), pp. 303-315.

Allen, R. G., Jensen, M. E., Wright, J. L. & Burman, R. D., 1989. Operational estimates of reference evapotranspiration. *Agronomy Journal,* 81(4), pp. 650-662.

Allison, G., Gee, G. W. & Tyler, S. W., 1994. Vadose-zone techniques for estimating groundwater recharge in arid and semiarid regions. *Soil Science Society of America Journal,* 58(1), pp. 6-14.

Alloway, B., 2013. *Heavy metals in soils: trace metals and metalloids in soils and their bioavailability*. Dordrecht: Springer.

Amarasinghe, B. & Williams, R., 2007. Tea Waste as a low cost adsorbent for the removal of Cu and Pb from wastewater. *Chemical Engineering Journal,* 132(1-3), pp. 299-309.

Antoniadis, V., McKinley, J. D., & Zuhairi, W. Y., 2007. Single-Element and Competitive Metal Mobility Measured with Column Infiltration and Batch Tests. *Journal of Environmental Quality*, 36(1), 53-60.

Apak, R., Tutem, E., Hugel, M. & Hizal, J., 1998. Heavy metal cation retentions by unconventional sorbents (Red Muds and Fly Ash). *Water Research,* 32(2), pp. 430-440.

Aravena, J. E. & Dussaillant, A., 2009. Storm-water infiltration and focused recharge modeling with finite-volume two-dimensional Richards equation: Application to experimental rain garden. *Journal of Hydraulic Engineering,* 135(12), pp. 1073-1080.

Arora, B. M. B. P. & McGuire, J. T., 2011. Inverse estimation of parameters for multidomain flow models in soil columns with different macropore densities. *Water Resources Research,* Volume 47, p. W04512.

Aydilek, A. H., & Edil, T. B., 2004. Evaluation of Woven Geotextile Pore Structure Parameters Using Image Analysis. *Geotechnical Testing Journal*, 27(1), 1-12.

Bean, E. Z., Hunt, W. F., & Bidelspach, D. A., 2007. Field Survey of Permeable Pavement Surface Infiltration Rates. *Irrigation and Drainage Engineering* , 133(3), 244-255.

Benson, D., Wheatcraft, S. & Meerschaert, M., 2000. Application of a fractional advective-dispersion equation. *Water Resources Research,* 36(6), pp. 1403-1412.

Berkowitz, B., Scher, H. & Silliman, S., 2000. Anomalous transport in laboratory-scale, heterogeneous porous media. *Water Resources Research,* 36(1), pp. 19-158.

Beven, K., 1982. Kinematic subsurface stormflow. *Water Resources Research,* 17(5), pp. 1419-1424.

Beven, K. & Germann, P., 1982. Macropores and water flow in soils. *Water Resources Research,* 18(5), pp. 1311-1325.

Beven, K. & Germann, P., 2013. Macropores and water flows in soils revisited. *Water Resources Research,* 49(6), pp. 3071-3092.

Bitter, S. D. & Bowens, J., 1994. Bioretention as a water quality best management pratice. *Watershed Protection Techniques,* 1(3), pp. 114-116.

Blecken, G. T., Zinger, Y., Deletic, A. & Fletcher, T., 2009. Influence of intermittent wetting and drying conditions on heavy metal removal by stormwater biofilters. *Water Research,* 43(18), pp. 4590-4598.

Boller, M., 1997. Tracking heavy metals reveals sustainable deficits of urban drainage systems. *Water Science Technology,* 35(9), pp. 77-87.

Bradl, H. B., 2004. Adsorption of heavy metal ions on soils and soils constituents. *Journal of Colloid and Interface Science,* 227(1), pp. 1-18.

Bratieres, K., Fletcher, T., Deletic, A. & Zinger, Y., 2008. Nutrient and sediment removal by stormwater biofilters: A large scale design optimisation study. *Water Research,* 42(14), pp. 3930-3940.

British Geological Survey, 2012. *Groundwater and climate change.* [Online] Available at: http://www.bgs.ac.uk/discoveringGeology/climateChange/general/groundwater.html [Accessed 1 April 2012].

Brown, P., Gill, S. & Allen, S., 2000. Metal removal from wastewater using peat. *Water Research,* 34(16), pp. 3907-3916.

Burgisser, C. S., Cernik, M., Borkovec, M. & Sticher, H., 1993. Determination of nonlinear adsorption isotherms from column experiments: An alternative to batch studies. *Environmental Science & Technology,* 27(5), pp. 943-948

Buttle, J. M. & McDonald, D. J., 2000. Soil macroporosity and infiltration characteristics of a forest podzol. *Hydrological Processes,* 14(5), pp. 831-848.

Camobreco, V., Richards, B., Steenhuis, T. & Peverly, J. M. M., 1996. Movement of heavy metals through undisturbed and homogenized soil columns. *Soil Science,* 161(11), pp. 740-750.

Campbell Scientific, Inc., 2010. *TDR100 instruction manual,* Logan: Campbell Scientific.

Campbell Scientific, Inc., 2013. *TDR probes CS605, CS610, CS630, CS635, CS640, CS645,* Logan: Campbell Scientific, Inc..

Campbell Scientific, I., 2009. *229 heat dissipation matric water potential sensor instruction manual,* Logan: Campbell Scientific, Inc..

Campbell, G. & Norman, J., 1998. *An Introduction to Environmental Biophysics.* New York: Springer Verlag.

Celia, M. A., Boulatas, E. T. & Zarba, R. L., 1990. A general mass conservative numerical solution for the unsaturated flow equation. *Water Resources Research,* 26(7), pp. 1483-1496.

Chang, C. M., Wang, M. K, Chang, T. W., Lin, C. & Chen, Y. R., 2001. Transport modeling of copper and cadmium with linear and nonlinear retardation factors. *Chemosphere,* 43(8), pp. 1133-1139.

Chang, Y. & Corapcioglu, M. Y., 1998. Plant-enhanced subsurface bioremediation of nonvolatile hydrocarbons. *Journal of Environmental Engineering,* 124(2), pp. 162-169.

Christensen, T. H., Lehmann, N., Jackson, T. & Holm, P. E., 1996. Cadmium and nickel distribution coefficients for sandy aquifer material.. *Journal of Contaminant Hydrology,* 24(1), pp. 75-84.

Claytor, R. A. & Schueler, T. R., 1996. *Design of Stormwater Filtering Systems,* Chesapeake: Center of Watershed Protection.

Cole-Parmer, 2008. *Cole-Parmer Laboratory Bromide Ion Electrode instruction manual,* Vernon Hills: Cole Palmer Instrument Company.

Corwin, D.L., 2000. Evaluation of a simple lysimeter-design modification to minimize sidewall flow. *Journal of Contaminant Hydrology,* 42 (1), pp. 35–49

Costa, J. L. & Prunty, L., 2006. Solute transport in fine sandy loam soil under different flow rates. *Agricultural Water Management,* 83(1-2), pp. 111-118.

Czemial Berndtsson, J., 2010. Green roof performance towards management of runoff water quantity and quality: A review. *Ecological Engineering,* 36(4), pp. 351-360.

DavidBall Specialist Sand, 2013. *Standard Reference Materials BS 1881-131:1998.* [Online] Available at: http://www.davidballspecialistsands.co.uk/wp-content/uploads/2013/05/BS1881-131-Fractions-A-E.pdf [Accessed 30 June 2015].

Davis, A. P., Shokouhian, M., Sharma, H. & Minami, C., 2003. Water quality improvement through bioretention: lead, copper, and zinc removal. *Water Environment Research,* 75(1), pp. 73-82.

Davis, A., Shokouhian, M., Sharma, H. & Minami, C., 2001. Laboratory study of biological retention for urban stormwater management. *Water Environment Research,* Volume 73, pp. 5-14.

DEFRA SuDS Team, 2011. *National Standards for Sustainable Drainage Systems,* London: DEFRA.

Dietz, M. E., & Clausen, J. C., 2005. A field evaluation of rain garden flow and pollutant treatment. *Water, Air and Soil Pollution, 167*, 123-138.

Dingman, S., 1994. *Physical Hydrology.* New York: Prentice Hall.

Ding, R., Kang, S., Li, F., Zhang, Y. & Tong, L., 2013. Evapotranspiration measurement and estimation using modified Priestly-Taylor model in an irrigated maize field with mulching. *Agriculture and Forest Meterology,* 168(1), pp. 140-143.

Doltra, J., & Munoz, P., 2010. Simulation of nitrogen leaching from a fertigated crop rotation in a Mediterranean climate using EU-Rotate_N and Hydrus-2D models. *Agricultural Water Management,* 97, 227-285.

Dussaillant, A. R., 2002. *Focused groundwater recharge in a rain garden: Numerical modeling and field experiment,* Madison: University of Wisconsin.

Dussaillant, A. R., Cuevas, A. & Potter, K. W., 2005. Raingardens for stormwater infiltration and focused groundwater recharge: simulations for different world climates. *Water Science and Technology: Water Supply,* 5(3-4), pp. 173-179.

Dussaillant, A. R., Wu, C. H. & Potter, K. W., 2004. Richards equation model of a rain garden. *Journal of Hydrologic Engineering,* 9(3), pp. 219-225.

Ellis, J. & Mitchell, G., 2006. Urban diffuse pollution: key data information approaches for the Water Framework Directive. *Water Environment Research,* 20(1), pp. 19-26.

Farm, C., 2002. Metal sorption to natural filter substrates for storm water treatment-column studies.. *The Science of the Total Environment,* 298(1-3), pp. 17-24.

Foo, K. & Hameed, B., 2010. Insights into modeling of adsorption isotherm systems. *Chemical Engineering Journal,* 156(1), pp. 2-10.

Fowler, A., 2002. Assessment of the validity of using mean potential evaporation in computations of the long-term soil water balance. *Journal of Hydrology,* 256(3-4), pp. 248-263.

Freeze, R. & Cherry, J., 1979. *Groundwater.* Prentice Hall: Englewood Cliffs, NJ.

Gaganis, P., Skouras, E. D., Theodoropoulou, M. A., Tsakiroglou, C. D. & Burganos, V. N., 2005. On the evaluation of dispersion coefficients from visualisation experiments in artificial porous media. *Journal of Hydrology*, 307(1-4), pp. 79-91.

Gao, B., Yang, L., Wang, X., Zhao, J. & Shang, G., 2000. Influence of modified soils on the removal of diesel fuel oil from water and the growth of oil degradation micro organisms. *Chemosphere*, 41(3), pp. 419-426.

Genc-Fuhrman, H., Mikkelsen, P. S. & Ledin, A., 2007. Simultaneous removal of As, Cd, Cr, Cu, Ni and Zn from stormwater: Experimental comparison of 11 different sorbents. *Water Research*, 41(3), pp. 591-602.

Gerke, H. & van Genuchten, M., 1993. Evaluation of a first-order water transfer term for variably saturated dual-porosity flow models. *Water Resources Research*, 29(4), pp. 1225-1238.

Germann, P., 1990. Preferential flow and the generation of runoff: 1 Boundary layer flow theory. Water Resources Research, 26 (12), pp. 3055-3063.

Germann, P., Dipietro, L. & Singh, V., 1997. Momentum of flow in soils assessed with TDR-moisture readings. *Geoderma*, 80(1-2), pp. 153-168.

Getter, K. L., Bradley Rowe, D. & Andresen, J. A., 2007. Quantifying the effect of slope on extensive green roof stormwater retention. *Ecological Engineering*, 31(4), pp. 225-231.

Gnecco, I., Palla, A., Lanza, L. & La Barbera, P., 2013. The role of green roofs as a source/sink of pollutants in storm water outflows. *Water Resource Management*, 27(14), pp. 4715-4730.

Gobel, P., Dierkes, C., & Coldewey, W., 2007. Storm water runoff concentration matrix for urban areas. *Journal of Contaminant Hydrology*, 91(1-2), 26-42.

Gomes, P. C., Fontes, M., da Silva, A., Mendonca, E. & Netto, A., 2001. Selectivity sequence and competitive adsorption of heavy metals by Brazilian soils. *Soil Science of America Journal*, 65(4), pp. 1115-1121.

Great Britain, 2010. *Flood and Water Management Act, c.27*, London: The stationary office.

Hares, R., & Ward, N. , 1999. Comparison of the heavy metal content of motorway stormwater following discharge into wet biofiltration and dry detention ponds along the London Orbital (M25) motorway. *Science of the Total Environment*, 235(1-3), 169-178.

Hatt, B., Fletcher, T. & Deletic, A., 2008. Hydraulic and pollutant removal performance of stormwater filters under variable wetting and drying regimes. *Environmental Science and Technology,* 42(12), pp. 2535-2541.

Highways Research Group, 2010. *Fate of highway contaminants in the unsaturated zone.,* Nottingham: Highways Agency.

Hilten, R. N., Lawrence, T. M. & Tollner, E. W., 2008. Modeling stormwater runoff from green roofs with HYDRUS-1D. *Journal of Hydrology,* 358(3-4), pp. 288-293.

Hong, E., Seagran, E. A. & Davis, A. P., 2006. Sustainable oil and grease removal from synthetic stormwater runoff using bench-scale bioretention studies. *Water Environmental Resource,* 78(2), pp. 141-155.

Ho, Y., Porter, J. & McKay, G., 2002. Equilibrium isotherm studies for the sorption of divalent metal ions onto peat: copper, nickel and lead single component systems. *Water, Air and Soil Pollution,* 141(1-4), pp. 1-33.

Hsieh, C. & Davis, A., 2005. Multiple event study of bioretention for treatment of urban stormwater runoff. *Water Science and Technology,* 51(3-4), pp. 177-181.

Hunho, K., Seagran, E. A., & Davis, A. P. 2003. Engineered bioretention for removal of nitrate from storm water runoff. *Water Environmental Research*, 75(13), 355-367.

Jacques, D., Simunek, J., Mallants, D. & van Genuchten, M., 2008. Modelling coupled water flow, solute transport and geochemical reactions affecting heavy metal migration in a podzol soil. *Geoderma,* 145(3-4), pp. 449-461.

Jang, A., Seo, Y. & Bishop, P. L., 2005. The removal of heavy metals in urban runoff by sorption on mulch. *Environmental Pollution,* 133(1), pp. 117-127.

Jiang, S., Pang, L., Buchan, G. D., Simunek, J., Noonan, M. J. & Close, M. E., 2010. Modeling water flow and bacterial transport in undisturbed lysimeters under irrigations of dairy shed effluent and water using HYDRUS 1D. *Water Research,* 44(4), pp. 1050-1061.

Jones, P. S. & Davis, A. P., 2013. Spatial accumulation and strength of affiliation of heavy metals in bioretention media. *Environmental Science and Technology,* 139(4), pp. 479-487.

Jury, W. A. & Horton, R., 2004. *Soil Physics.* New Jersey: John Wiley & Sons, Inc..

Jury, W. & Roth, K., 1994. A unified approach to stochastic-convective transport problems. *Soil Science of America Journal,* 58(5), pp. 1327-1336.

Jury, W. A., & Scotter, D. R. 1994. A unified approach to stochastic-convective transport problems. *Soil Science Society of America Journal*, 58(5), 1327-1336.

Kay, P., Blackwell, P. A. & Boxall, A. B., 2005. Column studies to investigate the fate of veterinary antibiotics in clay soils following slurry application to agricultural land. *Chemosphere,* 60(4), pp. 497-507.

Klein, R., 1979. Urbanization and stream quality impairment. *Journal of the American Water Resources Association,* 15(4), pp. 948-963.

Knechtenhofer, L. A., Xifra, I., Scheinost, A., Fluher, H. & Kretzschmar, R., 2003. Fate of heavy metals in a strongly acidic shooting-range soil: small-scale metal distribution and its relation to preferential water flow. *Journal of Plant Nutrition and Soil Science,* 166(1), pp. 84-92.

Kohne, J. M., Kohne, S. & Simunek, J., 2009. A review of model applications for structured soils: a) Water flow and tracer transport. *Journal of Contaminant Hydrology,* 104(1-4), pp. 4-35.

Kulprathipanja, S., 2010. *Zeolites in Industrial Seperation and Catalysis.* New Jersey: John Wiley & Sons.

Larsbo, M., & Jarvis, N. 2003. *MACRO 5.0 A model of water flow and solute transport in macroporous soil*. Technical description. Swedish University of Agricultural Sciences.

Lamy, E., Lassabatere, L., Bechet, B. & Andrieu, H., 2009. Modeling the influence of an artificial macropore in sandy columns on flow and solute transfer. *Journal of Hydrology,* 379(3-4), pp. 392-402.

Larsbo, M., Roulier, S., Stenemo, F., Kasteel, R., & Jarvis, N., 2005. An improved dual-permeability model of water flow and solute transport in the vadose zone. *Vadose Zone Journal,* 4(2), pp. 398-406.

Larsson, M., Jarvis, N., Torstensson, G. & Kasteel, R., 1999. Quantifying the impact of preferential flow on solute transport to tile drains in a sandy field soil. *Journal of Hydrology,* 215(1-4), pp. 116-134.

LeFevre, G. H., Hozalski, R. M. & Novak, P. J., 2012. The role of biodegradation in limiting the accumulation of petroleum hydrocarbons in raingarden soils. *Water Research,* 46(20), pp. 6753-6762.

Legret, M., & Pagotto, C. 1999. Evaluation of pollutant loadings in the runoff waters from rural highway. *Science of the Total Environment,* 235(1-3), 143-150.

Legret, M., Colandini, V., & LeMarc, C. 1996. Effects of a porous pavement with reservoir structure on the quality of runoff water and soil. *Science of the Total Environment*, 190, 335-40.

Leij, F. J., Dane, J. H. & van Genuchten, M. T., 1991. Mathematical analysis of one-dimensional solute transport in a layered soil profile. *Soil Society of Americal Journal,* 55(1), pp. 944-953.

Leopold, L., 1968. *Hydrology for urban land planning: a guidebook on the hydrologic effect on land use,* Reston: U.S. Geological Survey.

Lewis, J. & Sjostrom, J., 2010. Optimizing the experimental design of soil columns in saturated and unsaturated transport experiments. *Journal of Contaminant Hydrology,* 115(1-4), pp. 1-13.

Li, H. & Davis, A. P., 2008. Heavy metal capture and accumulation in bioretention media. *Environmental Science and Technology,* 42(14), pp. 5247-5253.

Liu, J., Zhang, J. & Feng, J., 2008. Green-Ampt model for layered soils with nonuniform initial water content under unsteady infiltration. *Soil Science Society of America Journal,* 72(4), pp. 1041-1047.

Li, X., Poon, C.-s. & Liu, P. S., 2001. Heavy metal contamination of urban soils and street dusts in Hong Kong. *Applied Geochemistry,* 16(11-12), pp. 1361-1368.

Mallants, D., Mohanty, B. P., Vervoort, A., & J, F. 1997. Spatial analysis of saturated hydraulic conductivity in a soil with macropores. *Soil Technology*, 10(2), 115-131.

Markiewicz-Patkowska, J., Hursthouse, A., & Przbyla-Kij. 2005. The interaction of heavy metals with urban soils: sorption behaviour of Cd, Cu, Cr, Pb and Zn with a typical mixed brownfield deposit. *Environment International*, 31(4), 513-521.

Matsubayashi, U., Devkota, L. & Takagi, F., 1997. Characteristics of the dispersion coefficient in miscible displacement through a glass beads medium. *Journal of Hydrology,* 192(1-4), pp. 51-64.

McGechan, M. & Lewis, D. R., 2002. Sorption of phosphorus by soil, part 1: Principles, equations and models. *Biosystems Engineering,* 82(1), pp. 1-24.

McGrath, G., Hinz, C. & Sivapalan, M., 2008. Modelling the impact of within-storm variability of rainfall on the loading of solutes to preferential flow pathways. *European Journal of Soil Science,* 59(1), pp. 24-33.

Mdaghri-Alaoui, A. & Germann, P. F., 1998. Kinematic wave approach to drainage flow and moisture distribution in a structured soil. *Hydrological Sciences Journal,* 43(4), pp. 561-578.

Metselaar, K., 2012. Water retention and evapotranspiration of green roofs and possible natural vegetation types. *Resources, Conservation and Recycling,* 64(1), pp. 49-55.

Min, S., Han, J., Shin, E. & Park, J., 2004. Improvement of cadmium ion removal by based treatment of Juniper fiber. *Water Research,* 38(5), pp. 1289-1295.

Morera, M., Echeverria, J., Mazkiaran, J. & Garido, J., 2001. Isotherms and sequential extraction procedures for evaluating sorption and distribution of heavy metals in soils. *Environmental Pollution,* 113(2), pp. 135-144.

Moret-Fernandez, D., Arrue, J., Perez, V. & Lopez, M., 2008. A TDR-pressure cell design for measuring the soil-water retention curve. *Soil and Tillage Research,* 100(1-2), pp. 114-119.

Morgan, J. G., 2011. *Sorption and Release of Dissolved Pollutants Via Biortention Media. MSc Thesis,* Minnesota: University of Minnesota.

Mualem, Y., 1978. Hydraulic conductivity of unsaturated porous media: Generalized macroscopic approach. Water Resources Research, 14 (2), pp. 325-334.

Natural Resources Conservation Service, 2000. *Heavy Metal Soil Contamination,* Auburn: United States Department of Agriculture,.

Ngongondo, C., Xu, C., Tallaksen, L. & Alemaw, B., 2013. Evaluation of the FAO Penman-Monteith, Priestley-Tayor and Hargreaves models for estimating reference evapotranspiration in southern Malawi. *Hydrology Research,* 44(4), pp. 706-723.

Nimmo, J. R., 2007. Simple predictions of maximum transport rate in unsaturated soil and rock. *Water Resources Research,* 43(5), p. W05426.

Nimmo, J. R., 2012. Preferential flow occurs in unsaturated conditions. *Hydrological Processes,* 26(5), pp. 786-789.

Norambuena-Contreras, J., Arbat, G., Garcia Nieto, P. & Castro-Fresno, D., 2012. Nonlinear numerical simulation of rainwater infiltration through road embankment by FEM. *Applied Mathematics and Computation,* 219(4), pp. 1843-1852.

Norbiato, D. & Borga, M., 2008. Analysis of hysteretic behaviour of a hillslope-storage kinematic wave model for subsurface flow. *Water Resources,* 31(1), pp. 118-131.

North Carolina Department of Agriculture, 1995. *Topsoil.*, North Carolina Department of Agriculture: Raleigh.

Nwachukwu, I. O. & Pulford, I. D., 2008. Comparative effectiveness of selected adsorbent materials as potential amendments for the remediations of lead, copper and zinc contaminated soil. *Soil Use and Management,* 24(2), pp. 199-207.

Ogata, A. & Banks, R., 1964. A solution of the differential equation of longitudinal dispersion in porous media. *United States Geological Survey,* Volume 441-A.

Oliveira, I.B., Demond, A.H., Salehzadeh, A., 1996. Packing of sands for the production of homogeneous porous media. *Soil Science Society of America Journal,* 60 (1), pp. 49–53.

Pam Brown Associates. 2012. *Phase 1 desk study and phase 2 geoenvironmental investigation: town centre consolidation,* Westwood Cross, Thanet. Burton on Trent: Pam Brown Associates.

Pan, L. & Wierenga, P., 1995. A transformed pressure head-based approach to solve Richards' equation for variably saturated soils. *Water Resource Research,* 31(4), pp. 925-931.

Pan, Y., Gong, H., Zhou, D., Li, X. & Nakagoshi, N., 2011. Impact of land use change on groundwater recharge in Guishui River Basin, China. *Chinese Geographical Society*, 21(6), pp. 734-743.

Pang, L., Close, M., & Flintoft, M., 2004. Attenuation and transport characteristics of cadmium, zinc and lead in selected New Zealand aquifer systems. *Journal of Hydrology* (NZ), 2, 95-110.

Paus, K. H., Morgan, J., Guilliver, J. S., Leiknes, T. & Hozalski, R., 2014. Assessment of the hydraulic and toxic metal removal capacities of bioretention cells after 2 to 8 years of service. *Water Air Soil Pollution,* 225(1), p. 1801.

PC-PROGRESS, 2012. *HYDRUS-2D:FAQ 21-30.* [Online] Available at: http://www.pc-progress.com/en/Default.aspx?hydrus-faq-21-30 [Accessed 14 July 2014].

Peric, J., Trgo, M. & Vukojevic Medvidovic, N., 2004. Removal of zinc, copper and lead by natural zeolite-a comparison of adsorption isotherms. *Water Research,* 38(7), pp. 1893-1899.

Perkins, K. S., 2011. Measurement and Modeling of Unsaturated Hydraulic Conductivity. In: *Hydraulic Conductivity-Issues, Determination and Applications.* s.l.:InTech, pp. 419-434.

Pot, V., Simunek, J., Benoit, P., Coquet, Y., Yra, A. & Martinez-Cordon M. J., 2005. Impact of rainfall intensity on the transport of two herbicides in undisturbed grassed filter strip soil cores. *Journal of Contaminant Hydrology,* 81(1-4), pp. 63-88.

Pickles, E., 2014. *Effective provision of advice to local planning authorities in relation to water drainage management - new consultation announced,* London: UK Government

Priestly, C. & Taylor, R., 1972. On the assessment of surface heat flux and evaporation using large-scale parameters. *Monthly Weather Review,* 100(2), pp. 81-92.

Prince George's County, Maryland. Department of Environmental Resources, 1999. *Low-Impact Development Hydrologic Analysis,* Maryland: U.S Environmental Protection Agency.

Provoost, J., Cornelis, C. & Swartjes, F., 2006. Comparison of soil clean-up standards for trace elements between countries: Why do they differ? *Journal of Soils and Sediments,* 6(3), pp. 173-181.

Quinn, R. & Dussaillant, A., 2014. Modeling heavy metal behavior in Sustainable Drainage Systems: A case study. *Clean,* 42(2), pp. 160-168.

Rahil, M. & Antonopoulos, V., 2007. Simulating soil water flow and nitrogen dynamics in a sunflower field irrigated with reclaimed waste water. *Agricultural Water Management,* 92(3), pp. 142-150.

Roncevic, S., Dalmacja, B., Ivancev-Tumbas, I., Trickovic, J., Petrovic, O., Klasnja, M. & Agbata, J., 2005. Kinetics of degradation of hydrocarbons in the contaminated soil layer. *Archives of Environmental Contamination and Toxicology,* 49(1), pp. 27-36.

Saito, H., Seki, K. & Simunek, J., 2009. An alternative deterministic method for the spatial interpolation of water retention parameters. *Hydrology and Earth System Sciences,* 13(4), pp. 453-465.

Sansalone, J. J. & Buchberger, S. G., 1997. Partitioning and first flush of metals in urban roadway storm water. *Journal of Environmental Engineering,* 123(2), pp. 134-143.

Sauve, S., McBride, M. & Hendershot, W., 1997. Speciation of lead in contaminated soils. *Environmental Pollutions,* 98 (2), pp. 149-155.

Seelsaen, N., McLaughlan, R., Moore, J. & Stuetz, R., 2006. Pollutant removal efficiency of alternative filtration media in stormwater treatment. *Water Science and Technology,* 54(6-7), pp. 299-305.

Serrano, S., 2001. Explicit solution to Green and Ampt infiltration. *Journal of Hydrologic Engineering,* 6(4), pp. 336-340.

Sharpley, A., Jones, C., Gray, C. & Cole, C., 1984. A simplified soil and plant phosphorus model: II. Prediction of Labile, Organic, and Sorbed Phosphorus. *Soil Science Society of America Journal,* 48(4), pp. 805-809.

She, N. & Pang, J., 2010. Physically based green roof model. *Journal of Hydrologic Engineering,* 15(Special Issue), pp. 458-464.

Simunek, J., Jarvis, N. & van Genuchten, M. T., 2003. Review and comparison of models for describing non-equilibrium and preferential flow and transport in the vadose zone. *Journal of Hydrology,* 272(1), pp. 14-35.

Simunek, J., Senja, M., Saito, H., Sakai, M., & van Genuchten, M. Th., 2009. *The HYDRUS-1D software package for simulating the one dimensional movement of water, heat and multiple solutes in variably saturated media,* Riverside, California: Department of Environmental Sciences, University of California Riverside.

Singh, V. P., 1997. *Kinematic Wave Modeling in Water Resources*. New York: John Wiley & Sons, INC.

Smajstrla, A., 1985. A field lysimeter system for crop water use and water stress studies in humid regions. *Soil & Crop Science Society of Florida —Proceedings*, pp. 28.

Smith, K. A., 2000. *Soil and Environmental Analysis.* New York: Marcel Dekker Inc.

Smith, R. E., 1983. Approximate soil water movement by kinematic characteristics. *Soil Science of America Journal,* Volume 47, pp. 3-8.

Speak, A., Rothwell, J., Lindley, S. & Smith, C., 2014. Metal and nutrient dynamics on an aged intensive green roof. *Environmental Pollution,* Volume 184, pp. 33-43.

Steusloff, S., 1998. Input and output of airborne agressive substances on green roofs in Karslruhe. In: J. Breuste, J. Feldmann & O. Uhlmann, eds. *Urban Ecology.* Heidelberg: Springer-Verlag.

Sun, X., & Davis, A. P. 2007. Heavy metal fates in laboratory bioretention systems. *Chemosphere*, 66(9), pp. 1601-1609.

Tessier, A., Campbell, P. & Bisson, M., 1979. Sequential extraction procedure for the speciation of particulate trace metals. *Analytical Chemistry*, 51(7), pp. 844-851.

The Guardian, 2009. *Percentage of global population living in cities, by continent.* [Online] Available at: http://www.guardian.co.uk/news/datablog/2009/aug/18/percentage-population-living-cities
[Accessed 1 April 2012].

TP, 2014. *Rain Garden Design.* [Online] Available at: http://www.trickpod.net/rain-garden-designs/11/rain-garden-design-what-are-the-benefits-applying-rain-garden/#
[Accessed 2 June 2014].

Ulmanu, M., Maranon, E., Fernandez, Y., Castrrillon, L., Anger, I., & Dumitriu, D., 2003. Removal of copper and cadmium ions from diluted aqueous solutions by low cost and waste material adsorbents. *Water, Air and Soil Pollution,* 142(1-4), pp. 357-373.

van Dam, J., de Rooij, G., Heinan, M. & Stagnitti, F., 2004. *Concepts and dimensionality in modeling unsaturated water flow and solute transport.* Wageningen, Kluwer Academic.

van der Zee, S. & van Riemsdijk, W., 1987. Transport of reactive solute in spatially variable soil systems. *Water Resources Research,* 23(11), pp. 2059-2069.

van Genuchten, M. T., 1980. A closed-form equation for predicting the hydraulic conductivity of unsaturated soils. *Soil Science Society of America Journal,* Volume 44, pp. 892-898.

Vengris, T., Binkiene, R. & Sveikauskaite, A., 2001. Nickel, copper and zinc removal from waste water by a modified clay sorbent. *Applied Clay Science,* 18(3-4), pp. 183-190.

Ventura, F., Spano, D., Duce, P. & Synder, R. L., 1999. An evaluation of common evapotranspiration equations. *Irrigation Science,* 18(4), pp. 163-170.

Warrick, A., 2003. *Soil Water Dynamics.* New York: Oxford University Press Inc..

Waste & Resources Action Programme (WRAP), 2011. Guidelines for the specification of quality compost for use in growing media. Banbury: WRAP.

Weaver, J., Charbeneau, R. & Lien, B., 1994. A screening model for nonaqueous phase liquid transport in the vadose zone using Green-Ampt and kinematic wave theory. *Water Resources Research,* 30(1), pp. 93-105.

Weiler, M., 2005. An infiltration model based on flow variability in macropores development sensitivity analysis and applications. *Journal of Hydrology,* 310(1-4), pp. 294-315.

Weiler, M. & Naef, F., 2003. An experimental tracer study of the role of macropores in infiltration in grassland soils. *Hydrologic Process,* 17(2), pp. 477-493.

Whittinghill, L. J., Bradley Rowe, D. & Cregg, B. M., 2013. Evaluation of Vegetable Production on Extensive Green Roofs. *Agroecology and Sustaianble Food Systems,* 37(4), pp. 465-484.

Wilcke, W., Muller, S., Kanchanakool, N. & Zech, W., 1998. Urban soil contamination in Bangkok: heavy metal and aluminium partitioning in topsoils. *Geoderma,* 86(3-4), pp. 211-228.

Xiao, H., Bottcher, J. & Simunek, J., 2013. Simulation of the Heavy Metal Transport in Unsaturated Soils: Use of Scale Factors to Quantify Variable Sorption Isotherms. In: J. Simunek, M. T. van Genuchten & R. Kodesova, eds. *Proceedings of the 4th International Conference "HYDRUS Software Applications to Subsurface Flow and Contaminant Transport Problems".* Prague: March 21-22, pp. 385-394.

Zimmerman, A.J. & Weindorf, D.C., 2010. Heavy metal and trace metal analysis in soil by sequential extraction: A review of procedures. *International Journal of Analytical Chemistry*, 2010, pp. 1-7.

A. DUAL-PERMEABILITY MODELS

A1. RECHARGE and RECARGA

Previously, research regarding the water balance in rain gardens has only modelled matrix flow which is acceptable only for groundwater recharge calculations e.g RECHARGE and RECARGA (Dussaillant, 2002). This flow has been modeled using the Richards' equation for soil water flow in unsaturated conditions (Dussaillant, et al., 2004):

$$\frac{\partial\theta(h,z)}{\partial t} = \frac{\partial\theta}{\partial h}\frac{\partial h}{\partial t} = \frac{\partial}{\partial z}\left[K(h,z)\left\{\frac{\partial h}{\partial z}+1\right\}\right] - S(h,z) \quad \text{(A.1)}$$

where θ (m^3/m^3) is the soil volumetric moisture content, h (cm) is the suction head, z (cm) is the vertical position, t (s) is time, K (cm/s) is the unsaturated hydraulic conductivity and S (cm/hour) is the plant transpiration rate. This method was employed by the computer model RECHARGE where no hysteresis was assumed and thus the van Genuchten-Mualem functions (see **Section 4.2.1**) can be used to calculate the important soil properties θ and K. This has given accurate results when compared with previous research into water balances and field experiments. The simpler Green-Ampt equation can also be used to model flow in a rain garden as is seen in the computer model RECARGA (Dussaillant, et al., 2005). This equation divides infiltration into two distinct intervals, the time before ponding and the time after ponding where t_p (hour) is time of ponding:

$$\frac{dF}{dt} = i \qquad 0 \le t \le t_p \quad \text{(A.2)}$$

$$\frac{dF}{dt} = K_s\left(1+\frac{B}{F}\right) \qquad t_p \le t \quad \text{(A.3)}$$

with:

$$B = \left(h_{wf}+h_s\right)(\theta_{sat}-\theta_{ini}) \quad \text{(A.4)}$$

where F is the infiltration (cm), i (cm/s) is the water supply intensity, K_s (cm/s) is the saturated hydraulic conductivity, h_{wf} (cm) is the average capillary suction head at the wetting front, h_s (cm) is the ponded depth at the soil surface at time t, θ_{sat} (m^3/m^3) is the saturated volumetric water content and θ_{ini} (m^3/m^3) is the (uniform) initial soil moisture at t=0.

The Green-Ampt equation is a popular method used to model the development of the cumulative infiltration depth and the infiltration rate in homogeneous and layered soils under ponding conditions that develop during intense rainfall events (Serrano, 2001; Liu, et al., 2008).

Its popularity is attributed to its ease of implementation and simplicity as it is derived from several basic assumptions about the wetting process during water infiltration. During an actual wetting event where the soil surface has a constant matric potential head *h* with associated water infiltration θ, water enters the media behind a wetting front that moves downwards with time. This process is changed by the Green-Ampt equation to one that has a discontinuous change in water content at the wetting front. Additionally, the following assumptions are made:

- The soil in the wetted region has constant properties.
- The matric potential head at the moving front is constant.

This results in the Green-Ampt prediction having a sharper wetting front than the actual solution. This can decrease accuracy especially in soils prone to diffusion such as sands and loamy clay.

The drainage rate (d_r (cm/hour)) between layers is modelled using the following equation

$$d_r = K = K_s \Theta^{\frac{1}{2}} \left[1 - \left(1 - \Theta^{\frac{1}{m_{vg}}} \right)^{m_{vg}} \right]^2 \quad \text{(A.5)}$$

where Θ (m^3/m^3) is the soil dimensionless water content and m_{vg} (dimensionless) is a van Genuchten parameter. This has compared accurately with RECARGE and thus is found to be a suitably accurate way of predicting water flow in an unsaturated soil.

As stated previously both these models are suitable for determining groundwater recharge by only examining flow in the matrix region however this is not always appropriate. For example, when pollution retention is also being examined it is no longer acceptable to solely model matrix flow as high flow rates in the macropore region may lead to the rapid transfer of contaminants through the soil with limited adsorption as is seen in the experiments completed by Farm (2002).

As mentioned in **Table 3.1**, macropore flow influences the retention of all runoff contaminants. Macropores are large continuous openings in soil which can result in the rapid downward movement of solutes and pollutants through the soil system (Beven & Germann, 2013). In a rain garden environment they could be caused by numerous factors such as the voids left behind by plant root decay, earthworm movement and cracks in soil formed by the natural wetting and drying process.

It is thus of crucial importance to model matrix and macropore regimes of water flow through soil thus only dual permeability models will be examined.

A2. Dual Permeability models

HYDRUS

HYDRUS is one of the most well-known and utilised dual-permeability models in existence. It has been applied to a wide variety of circumstances including modelling water flow in agricultural fields, constructed wetlands and more recently in green roofs with varied results (Hilten, et al., 2008). HYDRUS is a capillary preferential flow model meaning the whole flow is controlled by both capillary and gravity forces (Kohne, et al., 2009). It describes water, heat and solute movement in the vadose zone, later updates HYDRUS (2D/3D) have additional boundary condition specifications and means for determining spatially distributed model parameters (Kohne, et al., 2009).

HYDRUS models water flow in both the matrix and macropore regions using the Richards equation which it solves using a finite element method. The rate of water exchange between the flow domains is presumed to be proportional to the difference in pressure heads between the two flow regions.

MACRO

MACRO is another widely used dual-permeability model athough primarily in the agricultural sector. It is a gravity driven preferential flow model meaning that macropore flow is controlled by gravity only and thus always moves in a downward direction (Kohne, et al., 2009).

MACRO uses two different methods to calculate water movement in the different regions, it combines a kinematic wave description of water flow for the macropore region with Richards equation for matrix flow. The kinematic wave model assumes that the wetting front proceeds by convective film flow in the mobile region and does not exchange water with the immobile region (Kohne, et al., 2009). The following representation of the kinematic wave equation is used by MACRO (Larsbo et al., 2005):

$$\frac{\partial \theta}{\partial t} = \frac{\partial K}{\partial z} - U_w \qquad \text{(A.6)}$$

where U_w (1/s) is a sink term for water which represents a wide range of parameters such as soil water content, water exchange and plant transpiration. The advantage of using this method is that no water retention properties of the macropore region are needed which reduces complexity. However the assumption that flow is gravity driven limits the applicability of this model to situations where the macropores are solely vertically oriented.

For water transfer MACRO uses a term that is based on a first-order approximation of the water diffusion equation (Larsbo, et al., 2005). It is also noted that MACRO only calculates flow from macropores to matrix and not in the reverse direction.

With regards to the initiation of macropore flow, in MACRO a predefined pressure head of -10 cm is used to divide the flow regimes. This value is based on experimental results along with complex pedotransfer functions (Larsbo, et al., 2005).

Root Zone Water Quality Model (RZWQM)

The RZWQM predates both HYDRUS and MACRO and employs a combination of dual-permeability modelling with mobile and immobile soil water zones. Therefore along with the standard macropore and mobile soil matrix, a third transport region is present in the form of the immobile soil matrix (Kohne, et al., 2009).

In the mobile soil matrix, vertical water infiltration is calculated using the Green-Ampt equation followed by the Richards equation for redistribution. The Green-Ampt equation is also used to determine vertical infiltration in the soil and radial infiltration in macropores. When the rainfall rate surpasses the infiltration rate (determined by the Green-Ampt equation), overland flow is intiated (Ahuja, et al., 2000). This flow is directed into the macropores until the flow rate capacity limit set by Poiseuille's law is reached. For every time step, the flow is successively routed downwards through the macropore channels. For each depth increase the flow in the macropores can laterally infiltrate into the surrounding soil matrix if saturation has not occured. This water exchange is determined by the lateral Green–Ampt equation, occurs in only one direction from the macropore to matrix region and can be restricted by a sorptivity (impedance factor) (Ahuja, et al., 2000). The RZWQM has some limitations commonly associated with dual-permeability models, such as difficulty in determining input parameters and some which require calibration, but overall it has been shown to adequately simulate the important processes involved with water movement (Kohne, et al., 2009).

The Infiltration-Initiation-Interaction Model (IN^3M)

IN^3M is based on analytical solutions of the Green-Ampt equation combined with a simple accounting scheme. The advantage of this method is that the use of analytical solutions eliminate the numerical instability present in other dual permeability models (Weiler, 2005). Vertical matrix infiltration is calculated in a similar manner to RECARGA using the Green-Ampt method to determine infiltration rate followed by the Buckingham-Darcy law of vertical water flow for soil water distribution between rainfall events. When the soil matrix becomes

saturated, macropore input is determined to have begun, this inflow q_{in} (cm/s) is given by (Weiler, 2005):

$$q_{in} = (i(t) - i_{mat}(t)MDAn_{mac}) \quad \text{(A.7)}$$

where i (cm/s) is the water supply intensity, i_{mat} (cm/s) is the infiltration rate into the soil matrix, *MDA* (cm^2) is macropore drainage area and n_{mac} ($1/cm^2$) is the macropore density. In this model only water transfer from the macropores to the matrix is considered (q_{int} (cm/s)) and for a soil layer with a given height of z_s for one vertically oriented macropore is given as (Weiler, 2005):

$$q_{int}(t) = \pi[y(t)^2 - y(t - t_s)^2]\frac{z_s\theta_s}{\Delta t} \quad \text{(A.8)}$$

where t_s (s) is the time step, *y(t)* (cm) is the radial distance of the wetting front at time *t,* and $y(t - t_s)$ is the radial distance of the wetting front at the previous time and θ_s (cm^3/cm^3) is the change in soil moisture content over the timestep t_s. This is a relatively easy approach compared with the complex parameters required by models such as HYDRUS however it has been found to overestimate water transfer between regions (Kohne, et al., 2009).

A3. Initiation of Macropore Flow

Initiation of macropore flow is a complex process often not accurately quantified by current dual permeability models (Nimmo, 2012). These models such as MACRO, RZWQM and IN^3M often use predefined values or saturation in the matrix region to determine the point at which macropore flow begins. However this assumption is in contrast to previous experimental findings, field results and observations. It has been shown that macropore flow can take place in a variety of different scenarios not specified by previous models such as in soil much drier than saturation, in partly filled pores or prior to the onset of ponding, an additional signifigant finding is that higher moisture contents can actually reduce macropore flow (Nimmo, 2012).

It is clear that the processes involved with modelling unsaturated flow through soil are extremely complex which has lead to the simplified assumptions of the above models. However the assertation that macropore flow only occurs upon saturation can result in incorrect predictions of preferential flow which can cause damage to water supplys and ecosystem assessments. This may occur as macropore flow can be prominant in drier soils, a trend not accurately quantified by the above models (Nimmo, 2012).

In order to prevent these errors several methods of determining the initiation of preferential flow are examined.

Infiltration: Although this method has not been used in previous hydrological models, high rates of infiltration have been shown to initiate macropore flow in several experiments (Pot, et al., 2005; McGrath, et al., 2008; Lamy, et al., 2009). Field observations were completed by Pot et al. (2005) into the impact of rainfall intensity on the transport of two herbicides in undisturbed grassed filter strip soil cores. It was found that for the highest rainfall intensities (0.308 and 0.326 cm/h) macropore flow was apparent however at lesser intensities it did not occur. This indicates that there is a direct correlation between infiltration intensity and macropore flow. If using this method a problem arises however as to how best to determine the rainfall rate which initiates macropore flow.

Saturation: The initiation of macropore flow is commonly assumed to occur when the soils saturated moisture content is reached. Alternatively macropore flow is presumed to initiate when ponding occurs.

Cut and join: In the model MACRO a predefined pressure head of -10cm is used to divide the regions. This value may be inappropriate for rain gardens as it is based on pedotransfer functions and detailed experimental detail relating to agricultural situations. This method has been observed to underestimate the degree to which preferential flow occurs (Larsson, et al., 1999).

A4. Interaction between Matrix and Macropore Regions

The final phenomenom that needs to be considered with regards to a dual-permeability approach is interaction. As can be seen from the models which have been described above there are several methods which can be used

Mass transfer driven by effective water content

This is the method utilised by MACRO and also in some versions of HYDRUS depending on the conditions being tested (though mass transfer driven by pressure head is favourable).

In HYDRUS it can be represented by the following equation (Simunek, et al., 2003):

$$\Gamma_w = \frac{\partial \theta_m}{\partial x} = \omega\left[S_e^f - S_e^m\right] \quad \text{(A.9)}$$

where Γ_w (cm/s) is water transfer, θ_m (m^3/m^3) is the soil moisture content of the matrix, x (cm) is the horizontal distance, ω (cm/s) is a first order rate coefficient, and S_e^f (m^3/m^3) and S_e^m (m^3/m^3) are effective fluid saturation of the macropore and matrix regions respectively. This equation is relatively simple and easy to use as it does not require many parameters only residual and saturated water contents and not the retention function for the matrix region

explicitly (Simunek, et al., 2003). As mentioned above the dual permeability model MACRO uses an adaptation of the mass transfer term that is based on a first-order approximation of the water diffusion equation. This equation has only been used in conjunction with a 'cut and join' approach to hydraulic functions and may need adaptation to be combined with other techniques. It is also noted that the above equation only refers to flow from macropores to matrix and not in the reverse direction.

Mass transfer driven by pressure heads

This method is seen as more complex as water retention curves for both regions need to be calculated. Also it may be numerically unstable as the product of two highly non-linear terms needs to be calculated (Simunek, et al., 2003). The rate of water transfer between the macropore and matrix regions based on the variance in pressure heads between the two pore regions as shown above.

Other Methods

Simunek et al. (2003) determined from examining these interaction models only very minute variances were observed when comparing water mass transfer and water content profile in the matrix. From this Weiler (2005) surmised that an appropriate depiction of interaction may not be contingent on the chosen model but more on the parameterization of the approach.

Thus Weiler (2005) suggests the following equation to represent horizontal infiltration with radial symmetry based on the Green-Ampt assumption. This is the method used by IN^3M which also assumes that there is only mass transfer from the macropore to matrix regions and not the reverse.

B. DISCRETIZATION OF KEY EQUATIONS

B1. Matrix Kinematic Wave Equation

Kinematic waves are simple partial differential equations (PDE) with a sole unknown field variable (e.g. flow or water head (h)) in terms of two independent variables, namely time (t) and space with a number of parameters containing information about the movement of the wave. Usually, the wave can be advecting and diffusing, in simple situations however the wave is mostly advecting creating the equation shown by **Eq. 4.1**. In the case of subsurface flow the diffusion element however during validation (**Section 4.4.1**), it was shown to decrease numerical inconsistencies and so is included here. The equation can be expressed as:

$$\frac{\partial h}{\partial t} + c\frac{\partial h}{\partial z} = D\frac{\partial^2 h}{\partial z^2} - S \tag{B.1}$$

Where h (cm) is water head, t (s) is time, z (cm) is vertical distance, c (cm/s) is the kinematic waves' celerity, $c=\partial q/\partial\theta$, q (cm/s) is the water flow rate, θ (m^3/m^3) is the soil moisture content, D_o (cm^2/s) is diffusion coefficient and the sink term, S (cm/s) represents the depth averaged evapotranspiration if a uniform root distribution is assumed. There are numerous difficulties involving using $\partial\theta$ due to its tendency towards zero. Thus the moisture capacity function (M (1/s)) where $M=\partial h/\partial q$ is utilised:

$$\frac{\partial q}{\partial \theta} = \frac{\partial q}{\partial h}\frac{\partial h}{\partial \theta} = \frac{1}{M}\frac{\partial q}{\partial h} \sim \frac{1}{M}\frac{dq}{dh} \tag{B.2}$$

So

$$\frac{\partial h}{\partial t} + \frac{1}{M}\frac{dq}{dh}\frac{\partial h}{\partial z} = -S \tag{B.3}$$

$$q = -K\frac{1}{M}\left(M\frac{\partial h}{\partial x}\right) + K = K\left(1 - \frac{\partial h}{\partial x}\right) \sim K\left(1 - \frac{dh}{dx}\right) \tag{B.4}$$

The time discretization uses a time step Δt where the time iteration progresses $0,1....n,n+1,...N$ with n being the past time and $n+1$ being the present time.

The spatial discretization follows a constant Δz with m nodes numbered $1,....m$. Node 1 is located at the soil surface, at the interface with the atmosphere and node m is at the bottom of the soil profile.

In order to solve this equation the Crank-Nicolson method (where i represents position and n time) is utilised to transform the components of the PDE into the following:

$$\frac{\partial h}{\partial t} = \frac{h_i^{n+1} - h_i^n}{\Delta t} \tag{B.5}$$

$$\frac{\partial h}{\partial x} = \frac{w_{CN}}{2\Delta z}\left((h_{i+1}^{n+1} - h_{i-1}^{n+1}) + (h_{i+1}^n - h_{i-1}^n)\right) \tag{B.6}$$

$$\frac{\partial^2 h}{\partial x^2} = \frac{w_{CN}}{\Delta z^2}\left((h_{i+1}^{n+1} - 2h_i^{n+1} + h_{i-1}^{n+1}) + (h_{i+1}^n - 2h_i^n + h_{i-1}^n)\right) \tag{B.7}$$

Substituting these back into **Eq. B.1** results in:

$$\frac{h_i^{n+1} - h_i^n}{\Delta t} + \left(\frac{q_i^n - q_{i-1}^n}{\theta_i^n - \theta_{i-1}^n}\right)\frac{w_{CN}}{2\Delta z}\left((h_{i+1}^{n+1} - h_{i-1}^{n+1}) + (h_{i+1}^n - h_{i-1}^n)\right) = \frac{D_e w_{CN}}{\Delta z^2}\left((h_{i+1}^{n+1} - 2h_i^{n+1} + h_{i-1}^{n+1}) + (h_{i+1}^n - 2h_i^n + h_{i-1}^n)\right) - S_i^n \tag{B.8}$$

and simplifying.

$$(h_i^{n+1} - h_i^n) + \left(\frac{q_i^n - q_{i-1}^n}{\theta_i^n - \theta_{i-1}^n}\right)\frac{w_{CN}\sigma}{2}\left((h_{i+1}^{n+1} - h_{i-1}^{n+1}) + (h_{i+1}^n - h_{i-1}^n)\right) = \frac{w_{CN}\lambda}{2}\left((h_{i+1}^{n+1} - 2h_i^{n+1} + h_{i-1}^{n+1}) + (h_{i+1}^n - 2h_i^n + h_{i-1}^n)\right) - S_i^n \tag{B.9}$$

Where

$$\sigma = \frac{\Delta t}{\Delta z} \tag{B.10}$$

$$\lambda = \frac{2D_e\Delta t}{\Delta z^2} \tag{B.11}$$

Where w_{CN} (Dimensionless) is the Crank-Nicolson coefficient, when w_{CN}=0 the method is fully explicit and fully implicit when w_{CN}=1, w_{CN}=0.5 is the classic Crank-Nicolson method. The tridiagonal matrix scheme can now be used to solve equation A.1. The tridiagonal matrix algorithm (TDMA), also known as the Thomas algorithm is a basic form of the Gaussian elimination that can be employed to solve tridiagonal system of equations:

$$a_i h_{i-1} + b_i h_i + c_i h_{i+1} = d_i \tag{B.12}$$

Which represents a set of m simultaneous equations for m unknowns $h_{1,\ldots\ldots}h_{i-1},h_i,h_{i+1,\ldots}m$ that can be shown in a matrix form as {P}[h]=[d]

$$\begin{bmatrix} b_1 & c_1 & 0 & 0 & \cdots & 0 \\ a_2 & b_2 & c_2 & 0 & \cdots & 0 \\ 0 & a_3 & b_3 & c_3 & 0 & 0 \\ \vdots & \vdots & \vdots & \vdots & \ddots & c_{m-1} \\ 0 & 0 & 0 & 0 & a_m & b_m \end{bmatrix}\begin{bmatrix} h_1 \\ h_2 \\ h_3 \\ \vdots \\ h_m \end{bmatrix} = \begin{bmatrix} d_1 \\ d_2 \\ d_3 \\ \vdots \\ d_m \end{bmatrix} \tag{B.13}$$

Nodes *i*=1 and i=*m* are the boundary conditions (top and bottom respectively). The rest are interior nodes. Both types of node equation are reviewed below.

Interior Nodes

Eq. B.9 can be arranged as follows:

$$\left(\frac{w_{CN}\left(-\lambda-\left(\frac{q_i^n-q_{i-1}^n}{\theta_i^n-\theta_{i-1}^n}\right)\sigma\right)}{2}\right)(h_{i-1}^{n+1}+h_{i-1}^n)+(1+w_{CN}\lambda)(h_i^{n+1}+h_i^n)+$$

$$\left(\frac{w_{CN}\left(\left(\frac{q_i^n-q_{i-1}^n}{\theta_i^n-\theta_{i-1}^n}\right)\sigma-\lambda\right)}{2}\right)(h_{i+1}^{n+1}+h_{i+1}^n)\ +\ S_i^n=0 \qquad \text{(B.14)}$$

Thus, the coefficients $\{a_i,b_i,c_i\}$ for interior nodes *i=2,….m-1* are given by:

$$a_i=\left(\frac{w_{CN}\left(-\lambda-\left(\frac{q_i^n-q_{i-1}^n}{\theta_i^n-\theta_{i-1}^n}\right)\sigma\right)}{2}\right) \qquad \text{(B.15a)}$$

$$b_i=(1+w_{CN}\lambda) \qquad \text{(B.15b)}$$

$$c_i=\left(\frac{w_{CN}\left(-\lambda+\left(\frac{q_i^n-q_{i-1}^n}{\theta_i^n-\theta_{i-1}^n}\right)\sigma\right)}{2}\right) \qquad \text{(B.15c)}$$

From the above expressions, an equation d_i at time *j* can is given as:

$$d_i=h_i^n-\frac{1}{2}(1-w_{CN})\left(\sigma\left(\frac{q_i^n-q_{i-1}^n}{\theta_i^n-\theta_{i-1}^n}\right)(h_{i+1}^n-h_{i-1}^n)-\lambda(h_{i+1}^n-2h_i^n+h_{i-1}^n)\right) \qquad \text{(B.15d)}$$

Boundary nodes

The coefficients $\{a_i,b_i,c_i\}$ for the boundary nodes are detailed below.

Top Node (i=1)

The surface water balance gives the necessary information for the top boundary condition and can be discretized explicitly as:

$$A_{rg}\frac{h_1^{n+1}-h_1^n}{\Delta t}=Q_{Rain}^n(1+1/L)-Q_{Infiltration}^n-A_{rg}\frac{h_1^n-h_d}{\Delta t} \qquad \text{(B.16)}$$

Where $Q_{Infiltration}$ is found through use of the Green-Ampt equation. From the above equation the value of the top node head h_1^{n+1} can be calculated. This is suitable for calculating the upper boundary value when certain conditions apply

- Ponding is present (h_1 is positive)
- h_1 is negative, there is no water input and $h_s < h_{atm}$.

However in cases where h_1 is negative and input is present, a flux boundary condition is more appropriate (with $q_1=Q_{IN}$ in the case of water input or q_1 equal to soil evaporation otherwise). Therefore, the model considers the following two types of boundary condition:

Top Node *(i=1)*

Type 1: head boundary condition (Dirichlet)

In this case h_1, is known and is given by $h_1=h_s$, therefore the coefficients $\{a_i,b_i,c_i\}$ for the uppermost node $i=1$are given by:

$$b_1 = 1 \tag{B.17a}$$

$$c_1 = 0 \tag{B.17b}$$

$$d_1 = h_1 \tag{B.17c}$$

And for the second equation

$$d_2 = d_2 - a_2 h_1 \tag{B.18a}$$

$$a_2 = 0 \tag{B.18b}$$

This preserves the symmetry in the matrix, as $a_2=c_1=0$

Type 2: flux boundary condition (Neuman)

Option 1

For this case, the flux entering node 1 is known and denoted by $q_1 = q_f$, where q_1 is taken as positive in the z-direction; i.e. upwards. For a Neumann Boundary Condition using an upwind approximation:

$$h_1^{n+1} = \frac{1}{M}\frac{\Delta t}{\Delta z} q_f + h_1^n \tag{B.19}$$

Therefore the coefficients $\{a_i,b_i,c_i\}$ for the uppermost node $i=1$are given by:

$$b_1 = 1 \quad \text{(B.20a)}$$

$$c_1 = 0 \quad \text{(B.20b)}$$

$$d_1 = \frac{1}{M}\frac{\Delta t}{\Delta z} q_s + h_1^n \quad \text{(B.20c)}$$

And for the second equation

$$d_2 = d_2 - a_2 d_1 \quad \text{(B.21a)}$$

$$a_2 = 0 \quad \text{(B.21b)}$$

This preserves the symmetry in the matrix, P as $a_2=c_1=0$

Option 2

The above option works well in the majority cases, however depending on soil type sometimes $M\rightarrow\infty$. Therefore another method to calculate the upper boundary condition is needed. The previous soil moisture version of the kinematic wave equation utilises a power function relating relative hydraulic conductivity K_r (cm/s) to effective saturation S (cm^3/cm^3) as its upper boundary condition. This is expressed as (Mualem, 1978):

$$K_r = S^{v_e} \quad \text{(B.22)}$$

Where $S = \frac{\theta-\theta_{res}}{\theta_{sat-\theta_{res}}}$ and v_e (cm/s) is an exponent found to have a lower limit of 2.5 and to have values up to 24.5 for fine-textured soils. For rainfall rate, r (cm/s) less than or equal to K_s flux at the surface is equal to k is equal to r, and a series of waves with saturation S is created by a series of rainfall rates. For rainfall rates larger than K_s, the Green & Ampt Equation predicts infiltration and the soil water ‘’waves’’ will move downwards from the surface with saturated water content for all $r>K_s$.

Bottom Node *(i=m)*

Type 1: head boundary condition (Dirichlet)

In this case h_m is known and is given by $h_m=h_b$ where h_b (cm) is the head at the bottom boundary condition. Therefore, the coefficients $\{a_m,b_m,c_m\}$ are:

$$a_m = 0 \quad \text{(B.23a)}$$

$$b_m = 1 \quad \text{(B.23b)}$$

$$d_m = h_b \quad \text{(B.23c)}$$

And the second-to-last equation:

$$d_{m-1} = d_{m-1} - a_{m-1}h_1 \quad \text{(B.24a)}$$

$$c_{m-1} = 0 \quad \text{(B.24b)}$$

Solution

Following this, coefficients must be formed according to the following pattern, this is the forward sweep

$$e_i = \begin{cases} \frac{c_1}{b_1} & i = 1 \quad \text{(B.25)} \\ \frac{c_i}{b_i - e_{i-1}a_i} & i = 2,3,\ldots\ldots\ldots k-1 \quad \text{(B.26)} \end{cases}$$

And:

$$f_i = \begin{cases} \frac{d_1}{b_1} & i = 1 \quad \text{(B.27)} \\ \frac{d_i - f_{i-1}a_i}{b_i - e_{i-1}a_i} & i = 2,3,\ldots\ldots\ldots k-1 \quad \text{(B.28)} \end{cases}$$

With these new coefficients the matrix may be rewritten as such:

$$\begin{bmatrix} 1 & e_1 & 0 & 0 & \cdots & 0 \\ 0 & 1 & e_2 & 0 & \cdots & 0 \\ 0 & 0 & 1 & e_3 & 0 & 0 \\ \vdots & \vdots & \vdots & \vdots & & e_{k-1} \\ 0 & 0 & 0 & 0 & 0 & 1 \end{bmatrix} \begin{bmatrix} h_1 \\ h_2 \\ h_3 \\ \vdots \\ h_n \end{bmatrix} = \begin{bmatrix} f_1 \\ f_2 \\ f_3 \\ \vdots \\ f_k \end{bmatrix} \quad \text{(B.29)}$$

The final equations are obtained by a back substitution:

$$h_k = f_k, \qquad h_k = f_k - e_k h_{i+1}, \qquad i = k-1, k-2, \ldots., 2, 1 \quad \text{(B.30)}$$

B2. Macropore Kinematic Wave Equation

The solution above can be used to solve the macropore form of the kinematic wave equation:

$$\frac{\partial q}{\partial t} + c_m \frac{\partial q}{\partial z} = 0 \quad \text{(B.31)}$$

Where q (cm/s) is the water flow through the macropore and the macropore celerity c, denotes the one dimensional propogation velocity of a water property and is given by

$$c_m = \frac{dq}{dw} = a_m b_m w^{(a-1)} = a_m {b_m}^{1/a_m} q^{(a_m-1)/a_m} \quad \text{(B.32)}$$

where w (m^3/m^3) is the mobile moisture content, b_m (cm/s) is the conductance and a_m (Dimensionless) is an exponent. In the case of macropore flow diffusion is zero.

Boundary Conditions

The water entering the soil at the surface is modelled as a rectangular wave of flow rate q and duration t_s,(s) leading to the initial and boundary conditions of:

$$t \leq 0, t \geq t_s,\ q(0,t) = w(0,t) = 0 \quad \text{(B.33a)}$$

$$0 \leq t \leq t_s,\ q(0,t) = q,\quad w(0,t) = w_s = \left(\frac{q}{b_m}\right)^{1/a_m} \quad \text{(B.33b)}$$

$$0 \leq z \leq \infty,\ q(z,0) = w(z,0) = 0 \quad \text{(B.33c)}$$

However as stated above, macropore flow is only initiated when ponding occurs, this leads to a slight modification of the boundary layer conditions to:

$$t \leq 0, t \geq t_s,\ q(0,t) = w(0,t) = 0 \quad \text{(B.34a)}$$

$$0 \leq t \leq t_s,\ q(0,t) = \frac{h_s}{\Delta t},\quad w(0,t) = \left(\frac{h_s}{\Delta t b_m}\right)^{1/a_m} \quad \text{(B.34b)}$$

At t=0, a wetting front initiates at the soil surface and moves as a kinematic shock (similar to the model of the sharp wetting front model for the matrix region) with celerity (c_w (cm/s)):

$$c_w = {b_m}^{1/a_m} q^{(a_m-1)/a_m} \quad \text{(B.35)}$$

Thus, the time of arrival of the wetting front at depth z (t_w (s)) can be calculated as:

$$t_w(z) = \frac{z}{{b_m}^{1/a_m} q^{(a_m-1)/a_m}} \quad \text{(B.36)}$$

Following the cessation of infiltration at $t=t_s$, a draining front is initiated at the soil surface travelling with celerity (c_D (cm/s)):

$$c_D = a b^{1/a} q_s^{(a-1)/a} \quad \text{(B.37)}$$

The time of arrival of the drainage front can be calculated by:

$$t_D(z) = t_s + \frac{z}{a_m {b_m}^{1/a_m} q_s^{(a_m-1)/a_m}} \quad \text{(B.38)}$$

B3. Pollution Retention Modelling

Linear

As stated in the **Section 3.5.6** the linear isotherm is the simplest method of examining heavy metal retention when incorporated into the advection-dispersion-adsorption equation (**Eq. 3.13**) using its retardation factor (R (kg/m^3)).

$$R(z,t) = 1 + \frac{\rho}{\theta} K_d \tag{B.39}$$

where ρ (kg/m^3) is bulk density, θ (m^3/m^3) is soil moisture content, K_d (L/kg) is the linear distribution coefficient and *z* (cm) and *t* (s) represent vertical distance and time respectively. The objective of the computer program is to model the heavy metals as both a function of depth so that groundwater contamination can be monitored and time to calculate accumulation. This was achieved by making the dissolved pollutant concentration (C (mg/L)) a function of both time and space (C(z,t)) and employing a simply numerical scheme as detailed below.

The upper boundary condition is:

$$C(0,t) = C_0 \tag{B.40}$$

Where C_0 (mg/L) is the influent pollutant concentration. And the initial boundary condition is:

$$C(z,0) = 0 \tag{B.41}$$

Combining the above with the advection-dispersion-adsorption equation results in the following expression for pollution contamination:

$$C(z,t) = \left(\frac{C_0}{2}\right)\left\{erfc\left[\frac{(R(z,t)z - vt)}{2\sqrt{R(z,t)Dt}}\right] + \exp\left(\frac{vz}{D}\right) erfc\left[\frac{(R(z,t)z + vt)}{2\sqrt{R(z,t)Dt}}\right]\right\}$$

$$0 \le t \le t_s \;\&\; 0 \le x \le \infty \tag{B.42}$$

where D (cm^2/s) is the dispersion coefficient. This was relatively simple as the retardation coefficient is not dependent on pollutant concentration.

The linear isotherm has also been solved using the Thomas Algorithm detailed in **Section B1**, this provides a fast alternative to the above equation and also allows for the possibility of macropore to matrix pollutant transfer in the future.

Langmuir

Unlike the linear isotherm, the Langmuir retardation coefficient is a function of the pollutant concentration:

$$R(z,t) = 1 + \frac{\rho}{\theta(z,t)} \frac{K_L S_{max}}{(1+K_L C(z,t))^2} \quad \text{(B.43)}$$

where K_L (L/kg) is the Langmuir distribution coefficient and S_{max} (mg/kg) is the is the total concentration of sorption sites available. So as the contaminated water moves through the soil, its concentration will diminish and thus have an impact on the retardation factor. This needs to be reflected in the equations used in the programming code.

The boundary and initial conditions for the heavy metal concentration are the same as the linear values above result in the following conditions for the Langmuir retardation coefficient:

The upper boundary value:

$$R(0,t) = 1 + \frac{\rho}{\theta(0,t)} \frac{K_L S_{max}}{(1+K_L C_0)^2} \quad \text{(B.44)}$$

And the initial conditions:

$$R(z,0) = 1 + \frac{\rho}{\theta(z,0)} (K_L S_{max}) \quad \text{(B.45)}$$

Combining the above with the advection-dispersion-adsorption equation results in the following expression for pollution contamination:

$$R(z,t) = 1 + \frac{\rho}{\theta(z,t)} \frac{K_L S_{max}}{(1+K_L C(z-1,t-1))^2} \qquad 0 \le t \le t_s \;\&\; 0 \le x \le \infty \quad \text{(B.46)}$$

$$c(z,t) = \left(\frac{C_0}{2}\right)\left\{erfc\left[\frac{(R(z,t)x-vt)}{2\sqrt{R(z,t)Dt}}\right] + \exp\left(\frac{vz}{D}\right) erfc\left[\frac{(R(z,t)z+vt)}{2\sqrt{R(z,t)Dt}}\right]\right\}$$

$$0 \le t \le t_s \;\&\; 0 \le x \le \infty \quad \text{(B.47)}$$

Freundlich

The Freundlich retardation coefficient is similar to that of Langmuir expression as they are both dependent on the solution phase pollutant concentration. The Freundlich retardation coefficient is expressed as:

$$R(z,t) = 1 + \frac{\rho}{\theta(z,t)} \left(a_f K_F C^{a_f - 1}\right) \quad \text{(B.48)}$$

Where K_F (L/kg) is the Freundlich constant and a_f (Dimensionless) is the Freundlich exponent. Again the boundary and initial conditions for the heavy metal concentration are the same as the linear values above result in the following conditions for the Freundlich retardation coefficient:

The upper boundary value:

$$R(0,t) = 1 + \frac{\rho}{\theta(0,t)}\left(a_F K_F {C_0}^{a_f - 1}\right) \quad \text{(B.49)}$$

And the initial value:

$$R(z,0) = 1 \quad \text{(B.50)}$$

Combining the above with the advection-dispersion-adsorption equation results in the following expression for pollution contamination:

$$R(z,t) = 1 + \frac{\rho}{\theta(z,t)}(a_F K_F C(z-1,t-1)^{a_f - 1}) \qquad 0 \le t \le t_s \;\&\; 0 \le x \le \infty \quad \text{(B.51)}$$

$$C(z,t) = \left(\frac{C_0}{2}\right)\left\{erfc\left[\frac{(R(z,t)z - vt)}{2\sqrt{R(z,t)Dt}}\right] + \exp\left(\frac{vz}{D}\right) erfc\left[\frac{(R(z,t)x + vt)}{2\sqrt{R(z,t)Dt}}\right]\right\}$$

$$0 \le t \le t_s \;\&\; 0 \le x \le \infty \quad \text{(B.52)}$$

Multi-Layered Systems

As a rain garden is a layered system, boundary conditions are needed not only at the soil surface but also at the interface between layers. Thus it is assumed that each layer is homogeneous and part of an effectively semi-infinite system where the concentration in the upper layer is not affected by the lower layer. Solute transport in the lower layer is solved with first type boundary condition at the interface using the outlet concentration of the upper layer as the inlet boundary condition.

Linear Isotherm

This approach results in the following initial and boundary conditions at the surface:

$$t \le 0, t \ge t_s,\ c(0,t) = 0 \quad \text{(B.53)}$$

$$0 \le t \le t_s,\ c(0,t) = C_0, \quad \text{(B.54)}$$

$$0 \le x \le \infty,\ c(x,0) = 0 \quad \text{(B.55)}$$

The boundary conditions at the interface at depth L are:

$$t \leq 0, t \geq t_s,\ c(L,t) = 0 \quad \text{(B.56)}$$

$$0 \leq t \leq t_s,\ c(0,t) = C_e, \quad \text{(B.57)}$$

where C_e is the effluent concentration of the upper layer.

First type boundary conditions were used as these always lead to continuity in the resident concentration between layers (Leij, et al., 1991).

The above technique can be applied to the Langmuir and Freundlich isotherms to achieve the solutions to the initial and upper boundary conditions for a layered system.

C. EXPERIMENTAL DESIGN

C1. Calibration of TDR Probes

In order to properly programme the TDR and gain correct measurements a number of parameters are needed. These are cable length, window length, probe length and probe offset. The cable length and probe length can be measured directly from the sensors. The probe offset can be obtained from literature. However the PCTDR software was required to determine Window Length. **Figure C.1** shows an uncorrected waveform. Here the probe start is at approximately 5.7 m.

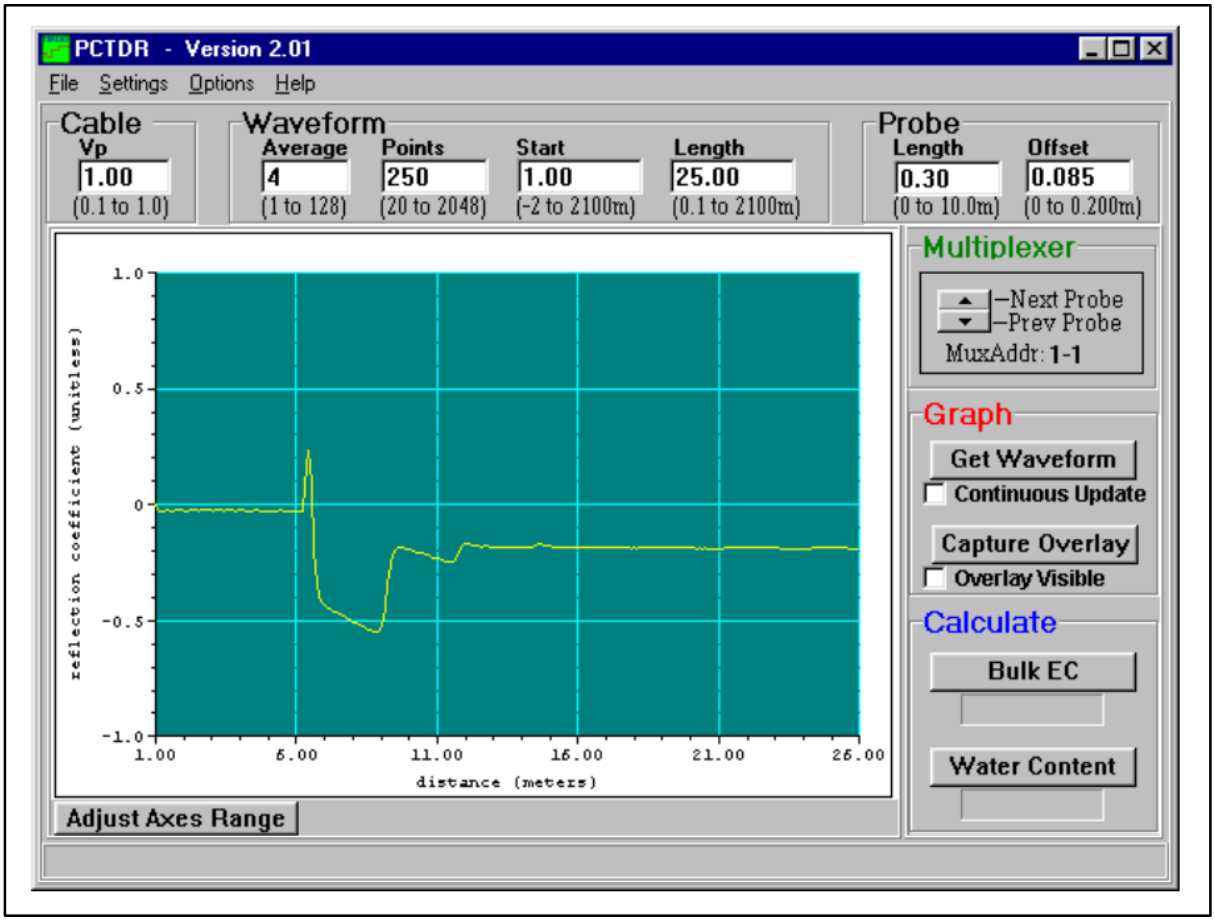

Figure C.1 Waveform of a TDR Probe in Water

Both the start point and length are adjusted until the wave form is contained within the green and red lines see **Figure C.2**, in this case the Waveform Length was given as 5 m. This process was completed for all the TDR probes used. The values obtained are given in **Table C.1**.

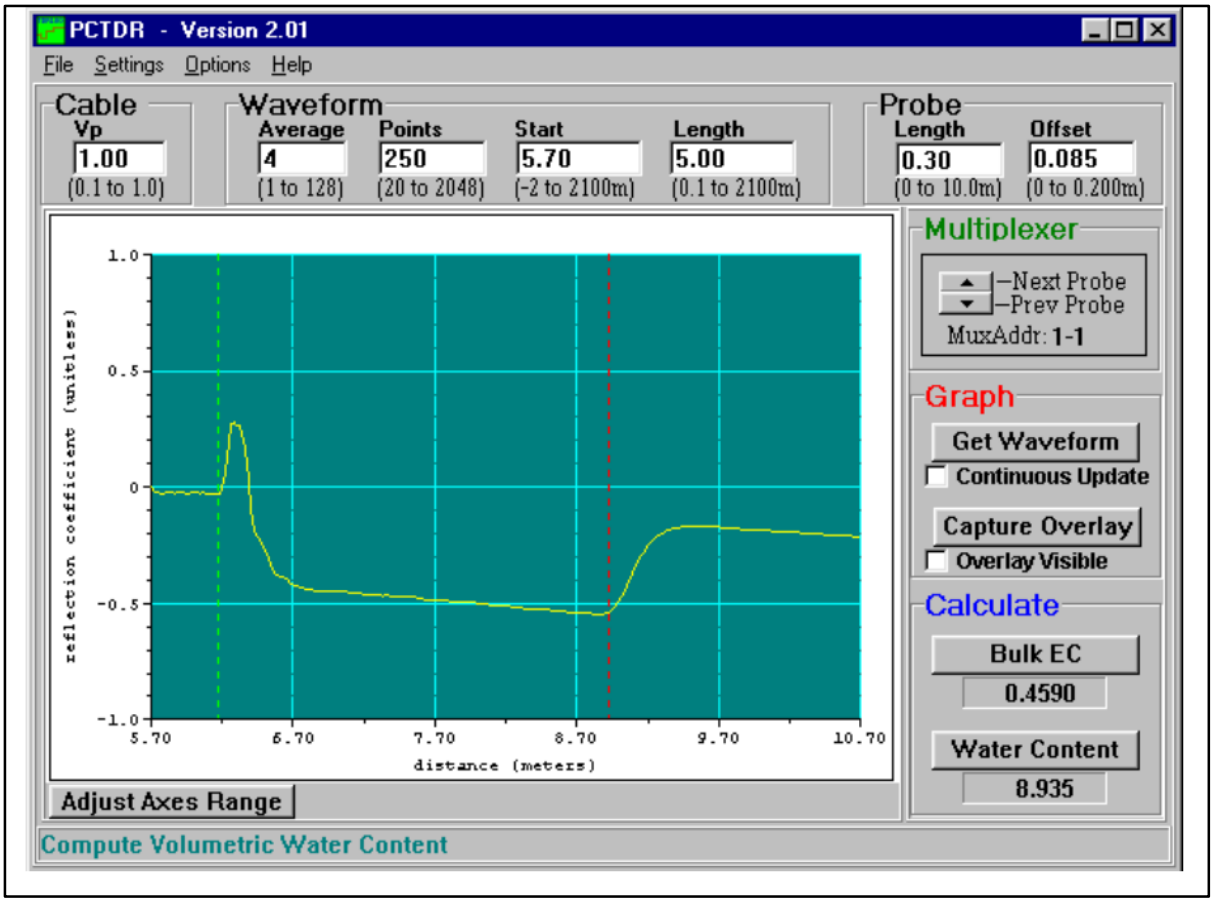

Figure C.2 Waveform of TDR Probe in Water after Changing Start and Length Parameters to Display Relevant Portion of Reflected Signal.

Table C.1 Calibration Parameters for TDR Probes

TDR Probe	Cable Length (m)	Window Length (m)	Probe Length (m)	Probe Offset
1	13.11	3.05	.075	.0325
2	13.11	3		
3	13.2	3.05		
4	13.1	3		
5	13.13	3.1		
6	13.1	2.95		
7	13.11	3		
8	13.2	3.05		

C2. Calibration of WMP Sensors

A detailed description of the principles behind the operation of the 229-L water matric potential sensors is available in Campbell Scientific, Inc. (2009). In the simplest terms the water potential of the soil is determined by a change in temperature of the probes after 30 second of heating. Therefore they do not give a direct measurement of water head only the change in temperature and thus require calibration. As discussed in **Section 5.3.5**, this was achieved by comparing the results of a tensiometer to that of the sensors. This process gives a calibration graph similar to **Figure C.3** below.

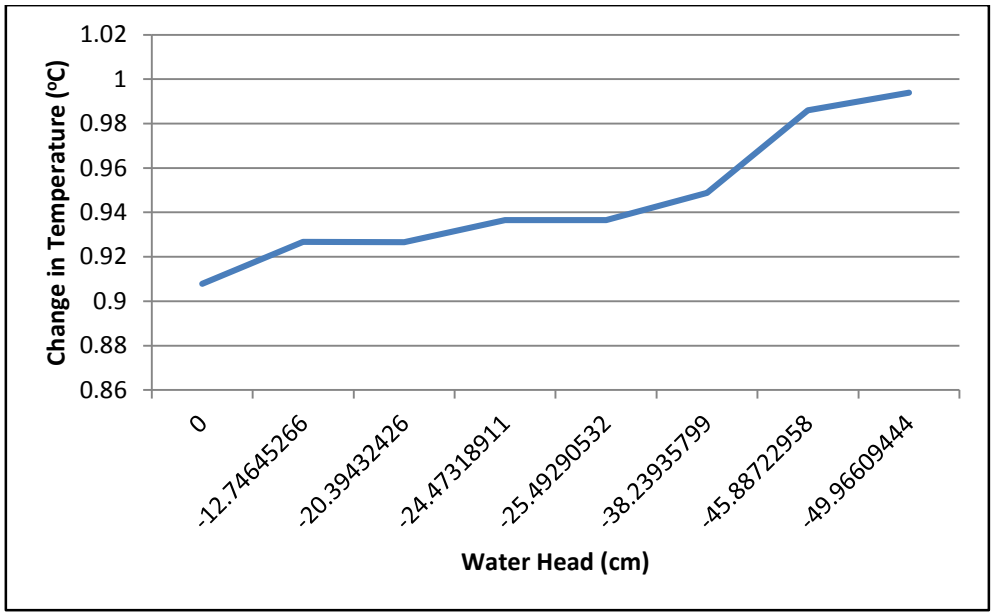

Figure C.3 Calibration Graph for WMP Sensor 1.

C3. Wiring of Sensors

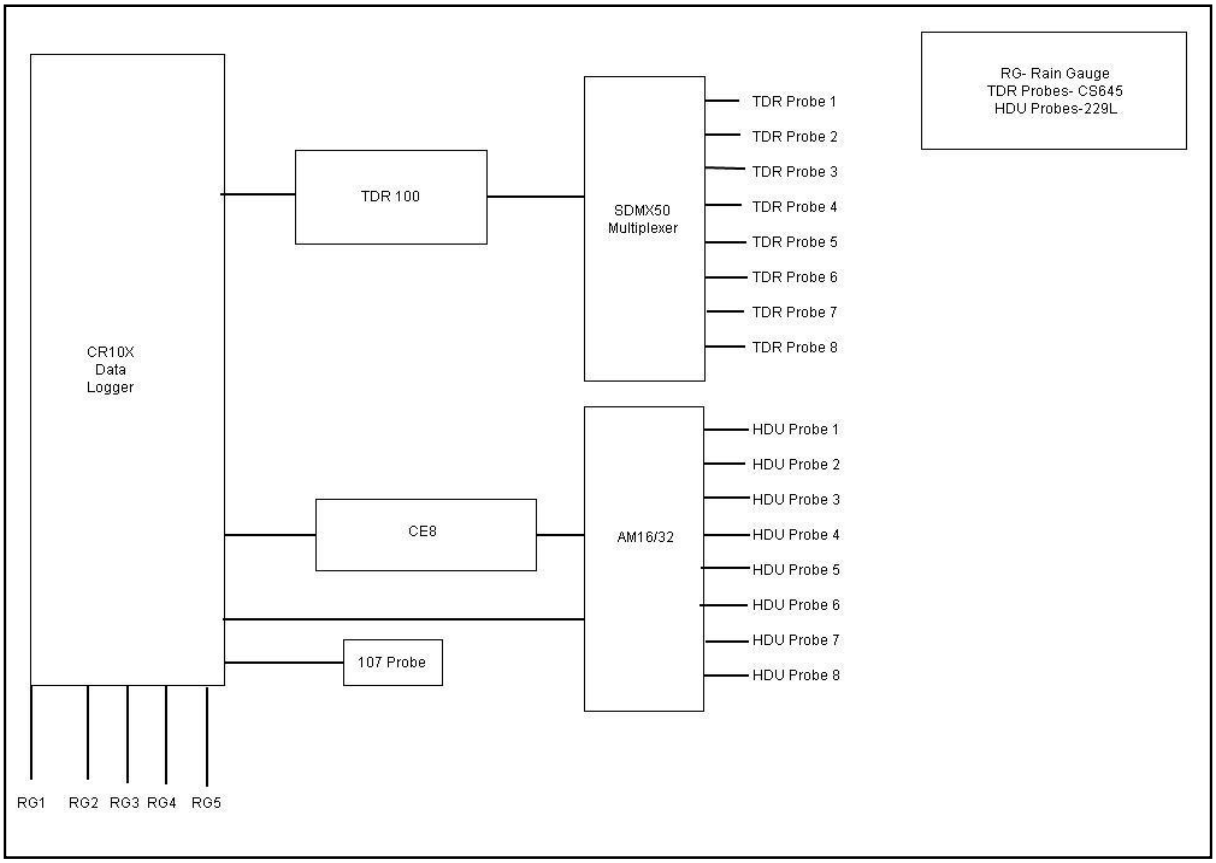

Figure C.4 Laboratory Equipment Layout

C4. Coding for Sensors

1 Define Execution Interval

2 Measure Battery Voltage

Measure TDR Probes

3 Turn on TDR100

4 Take Measurement of TDR Probe 1

5 Square La/L to convert to dialetric constant

6 Multiply dialetric constant by 0.1 to prepare for 3rd order polynomial

7 Polynomial

8 Repeat for 8 Probes

9 Turn off TDR100

10 Stamp and Record TDR measurements

Measure WMP Sensors

11 Turn on AM16/32

12 Measure reference temp of 229 sensor

13 Measure initial temp of HDU 1

14 Turn on CE8

15 Delay excitation for 1 second

16 Read sensor temp after 1 sec

17 Delay 29s more

18 Measure temp after 30s

19 Turn off CE8

20 Calc Temp rise

21 Time stamp and record probe measurement

22 Repeat for other WMP Sensors

Measure Rain Gauge (RG) output

39 Pulse to RG 1

40 Set active storage area

41 Measure Real time

42 Totalize

43 Record Measurements

44 Repeat for RG 2-5

D. EXPERIMENTAL RESULTS

D1. Experimental Setup & Location of Instrumentations

A review of the experimental conditions is given in **Table D.1**.

Table D.1 Summary of Designed Column Experiments

Column No.	Title	Diameter		Upper Boundary Flow Condition	Lower Boundary Flow Condition	Upper Boundary Metal Concentration Condition
		Internal	External			
1	Macropore	0.14 m	0.15 m	Average Flow: 10 cm/h First Flush: 35 cm/h	Free Flow Measured with Rain Gauge	10 mg/L Cu 10 mg/L Pb 30 mg/L Zn
2	Average					
3	Average					
4	Average					
5	Macropore					

As discussed in **Section 5.3.4**, the soil moisture content is measured by TDR probes and the water head is measured by WMP sensors whose positions are given by **Table D.2**.

Table D.2 Position of TDR/HDU Probes

TDR/WMP Sensors	Column	Position
1	5 (Macropore)	15 cm Depth Soil/Sand Upper Layer
2	5 (Macropore)	55 cm Depth Soil/Sand Upper Layer
3	2 (Matrix)	15 cm Depth Soil/Sand Upper Layer
4	2 (Matrix)	55 cm Depth Soil/Sand Upper Layer
5	1 (Macropore)	15 cm Depth Soil/Sand Upper Layer
6	1 (Macropore)	55 cm Depth Soil/Sand Upper Layer
7	5 (Macropore)	75 cm Depth Sand Lower Layer
8	2 (Matrix)	75 cm Depth Sand Lower Layer

D2. Soil Moisture Content

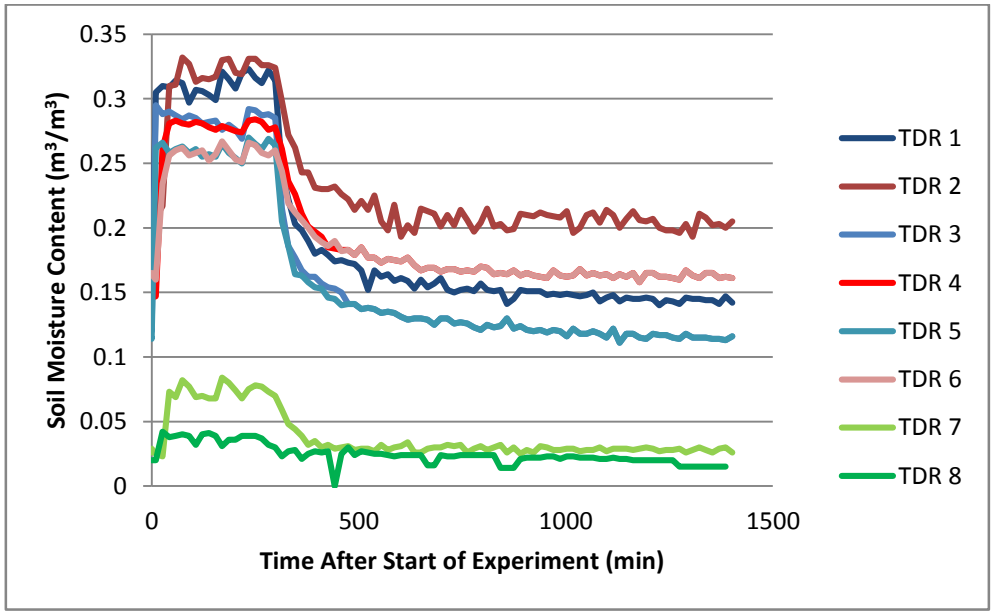

Figure D.1 Soil Moisture Content Results for Run 1 (Average Flow).

(TDR error ∓ 0.01 cm^3/cm^3)

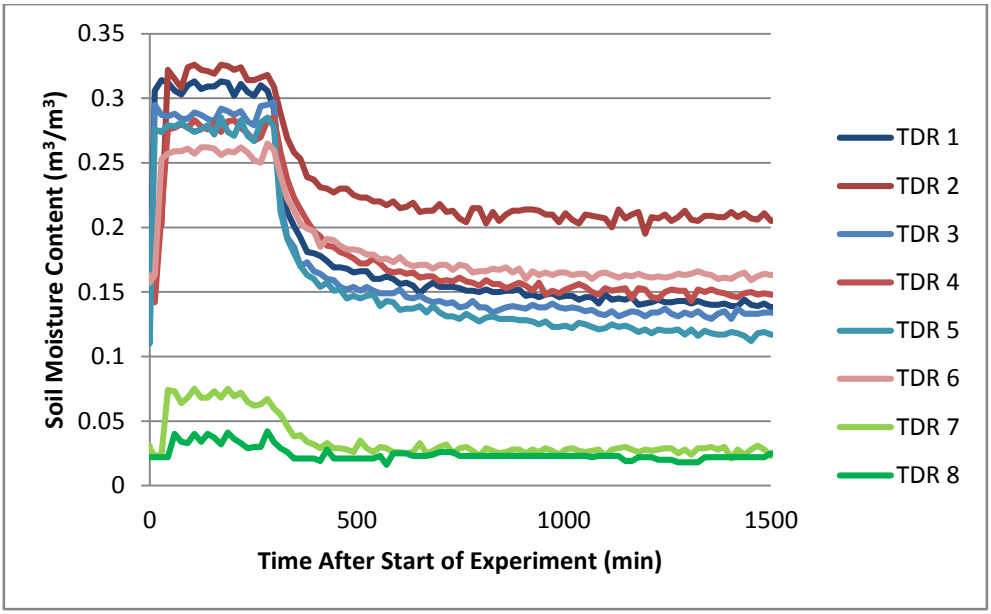

Figure D.2 Soil Moisture Content Results for Run 2 (Average Flow)

(TDR error ∓ 0.01 cm^3/cm^3)

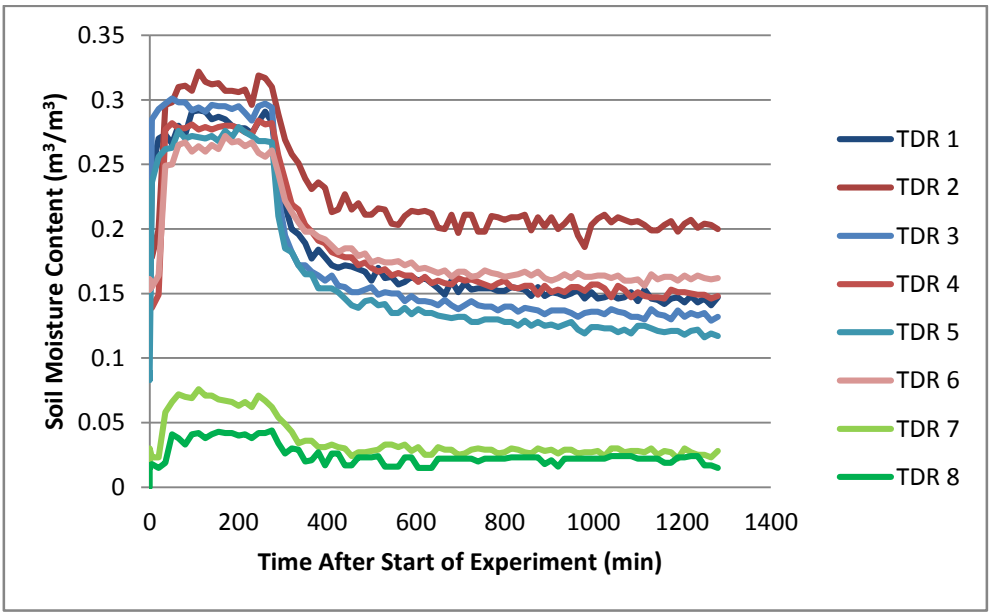

Figure D.3 Soil Moisture Content Results for Run 3 (Average Flow)

(TDR error ∓ 0.01 cm^3/cm^3)

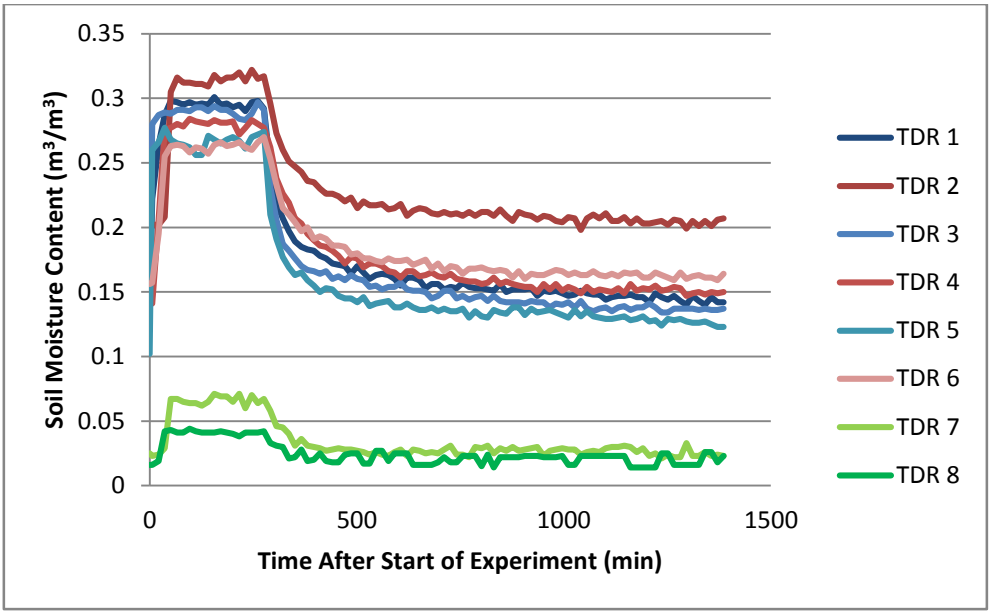

Figure D.4 Soil Moisture Content Results for Run 4 (Average Flow)

(TDR error ∓ 0.01 cm^3/cm^3)

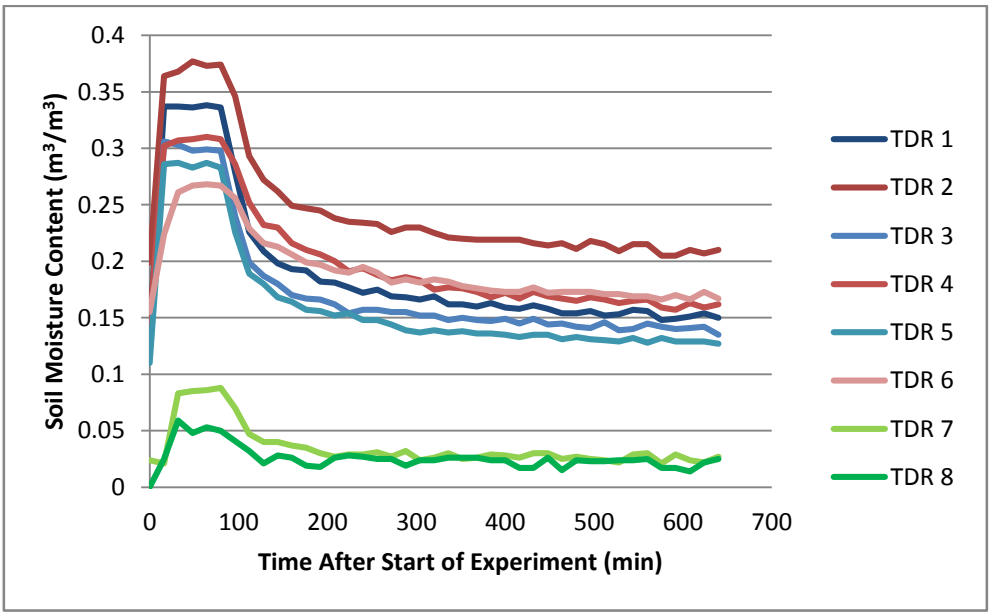

Figure D.5 Soil Moisture Content Results for Run 5 (First Flush)

(TDR error ∓ 0.01 cm^3/cm^3)

D3. Water Head Results

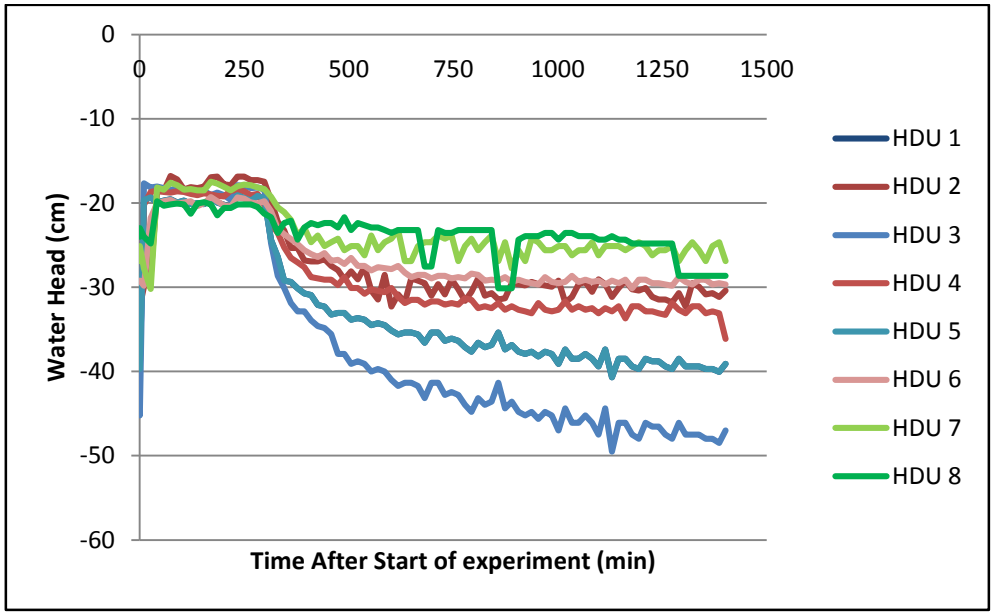

Figure D.6 Water Head Results for Run 1 (Average Flow)

(WMP Sensors error ∓ 2 cm)

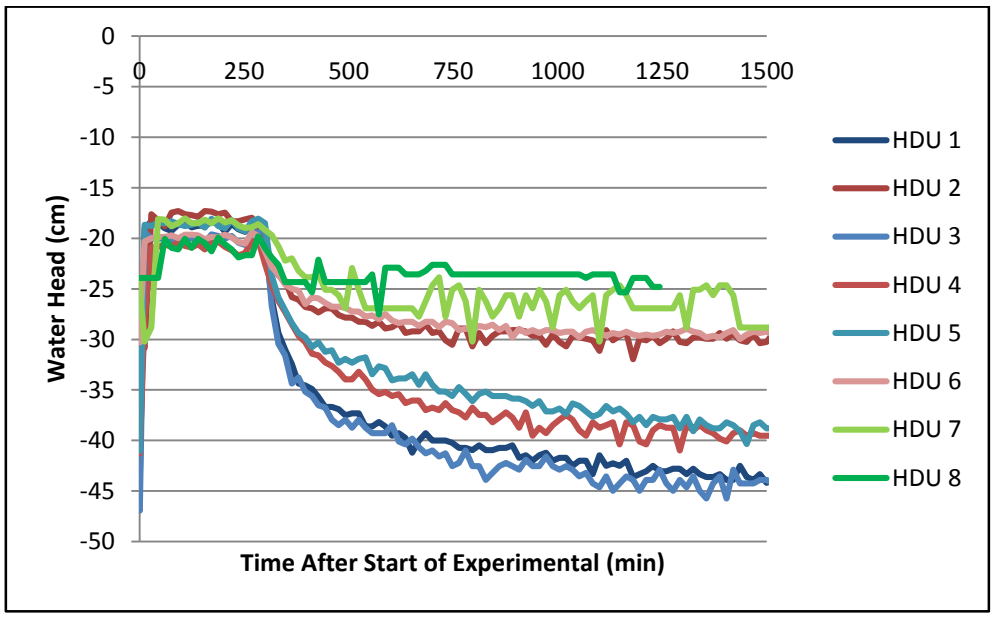

Figure D.7 Water Head Results for Run 2 (Average Flow)

(WMP Sensors ∓ 2 cm)

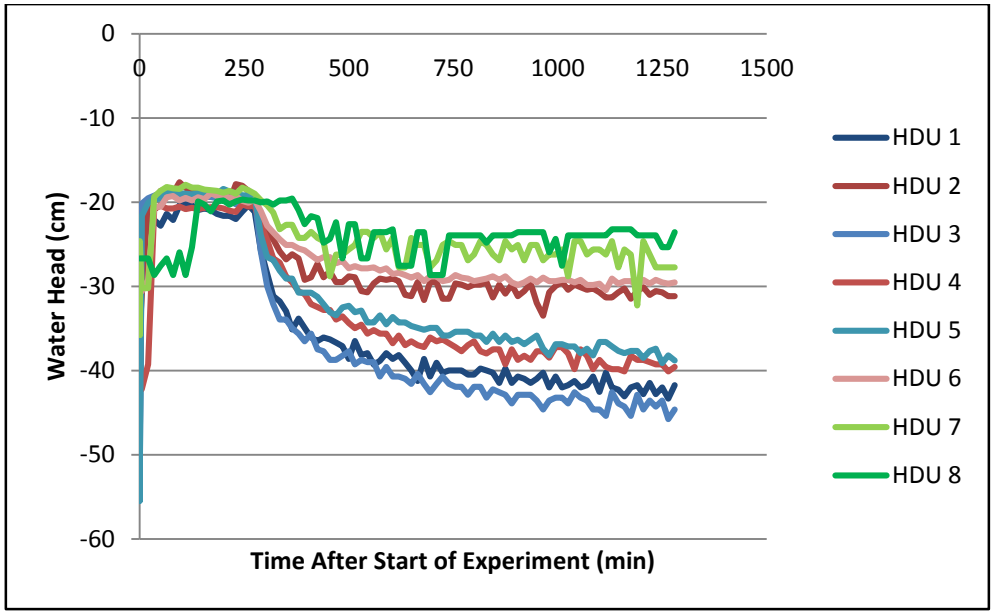

Figure D.8 Water Head Results for Run 3 (Average Flow)

(WMP Sensors ∓ 2 cm)

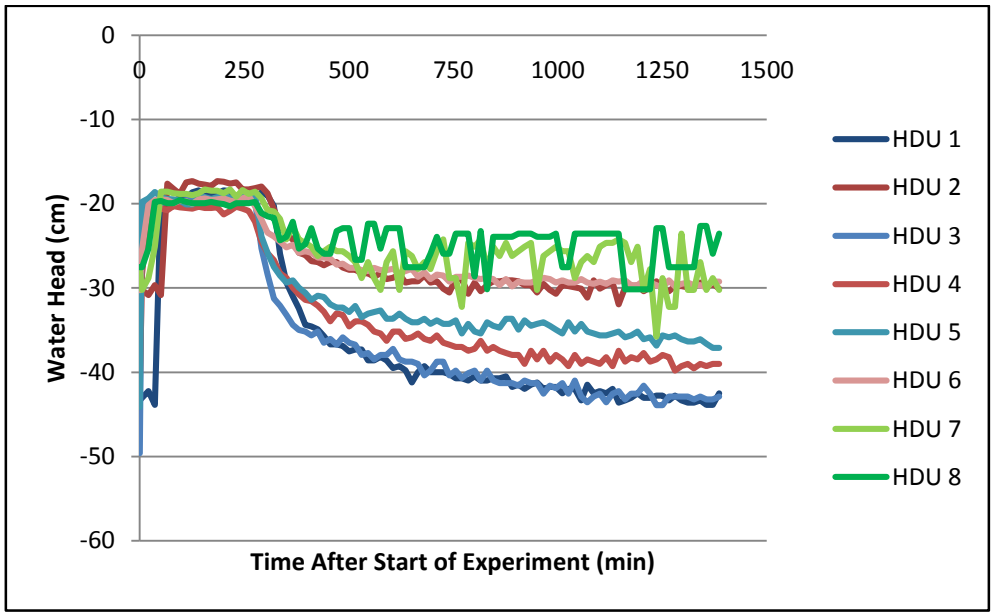

Figure D.9 Water Head Results for Run 4 (Average Flow)

(WMP Sensors ∓ 2 cm)

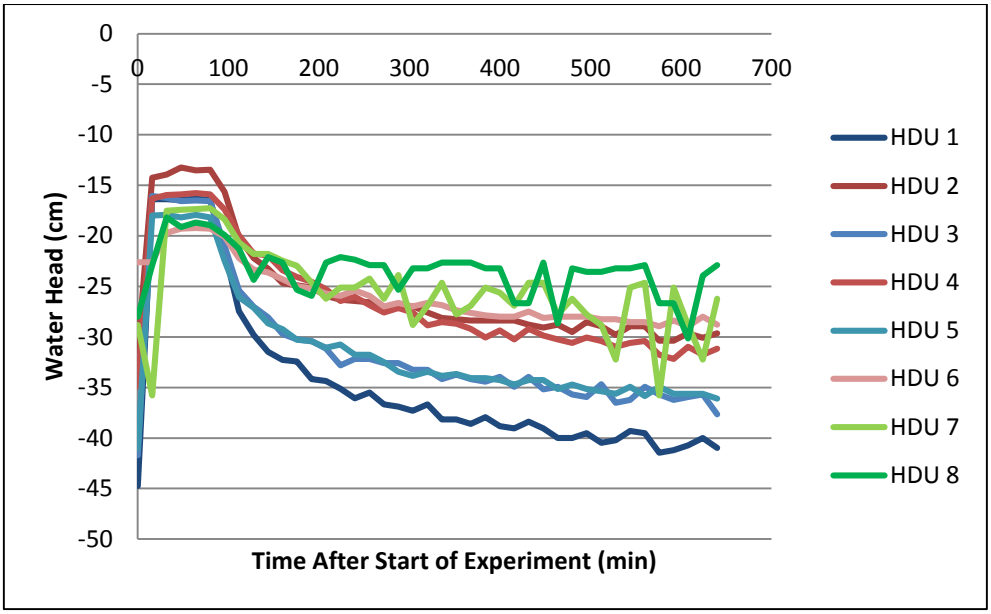

Figure D.10 Water Head Results for Run 5 (First Flush)

(WMP Sensors ∓ 2 cm)

D4. Water Output Results

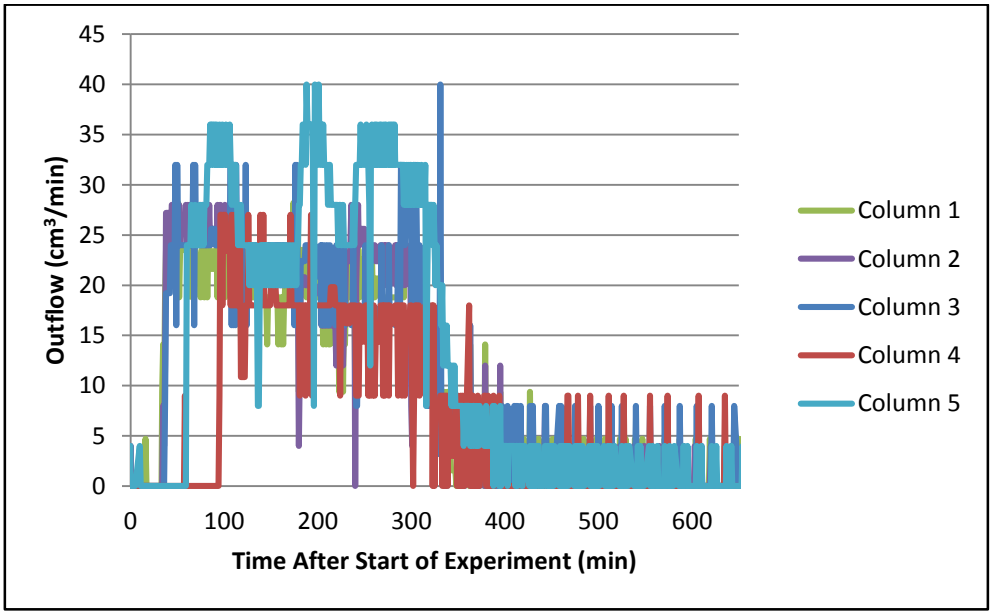

Figure D.11 Water Outflow for Run 1 (Average Flow)

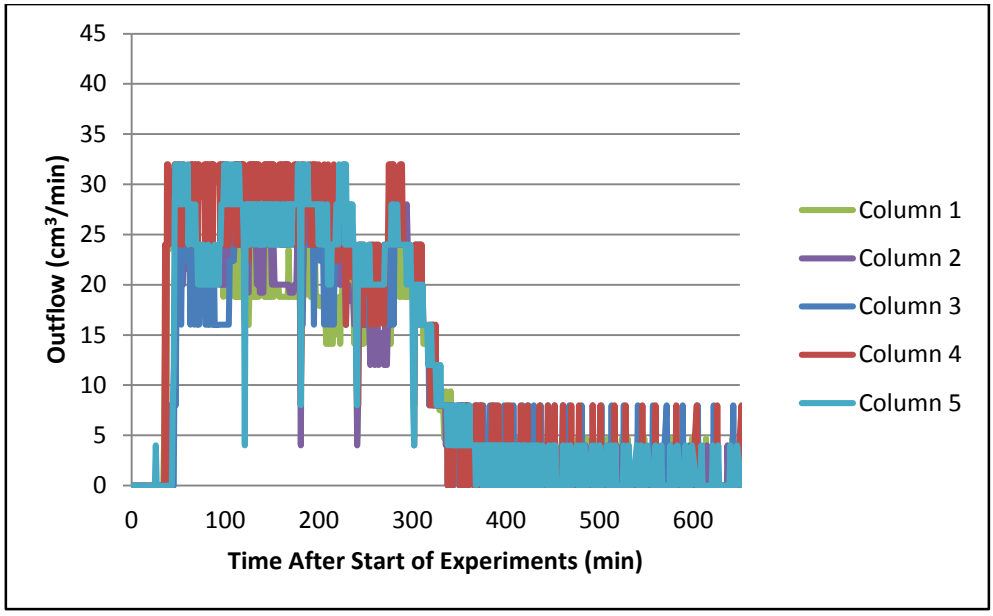

Figure D.12 Water Outflow for Run 2 (Average Flow)

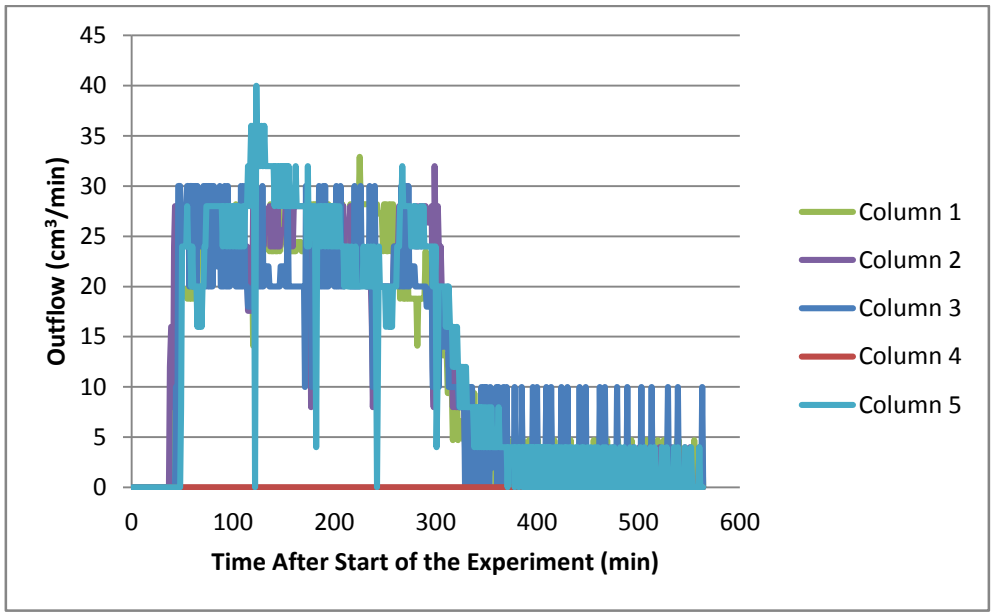

Figure D.13 Water Outflow for Run 3 (Average Flow)

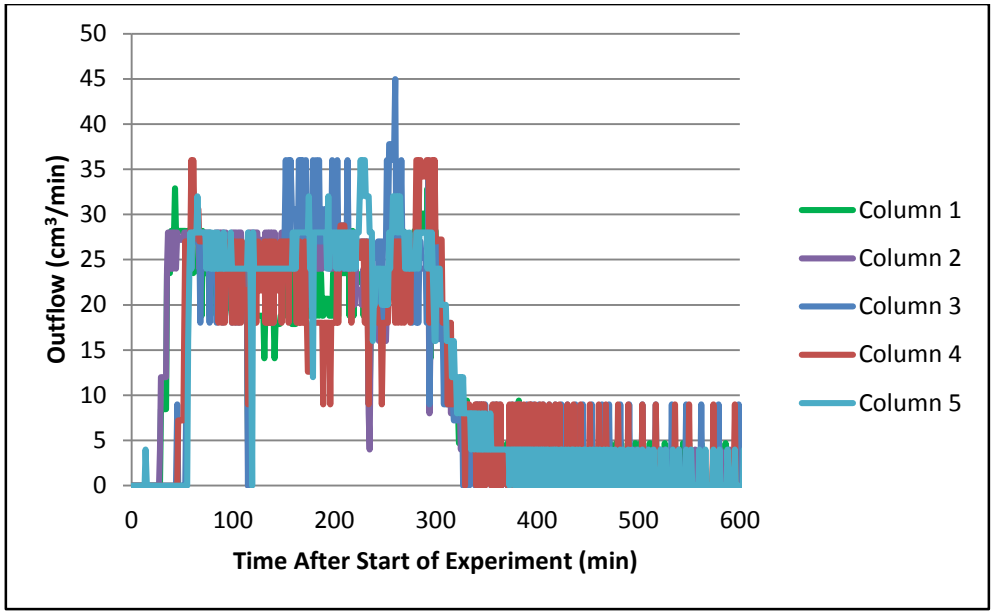

Figure D.13 Water Outflow for Run 4 (Average Flow)

Table D.3 Table of Outflow Values for Run 5 (First Flush). Error ∓ 0.1 cm/h

	18-81min	82-107min	107-1080min
Column 1 (Breakthrough at 18min)	0.49 cm/min (29 cm/h)	0.09 cm/min (5.65 cm/h)	0.003cm/min (.18cm/h)
	19-79 min	82-107 min	107-1080 min
Column 2 (Breakthrough at 19min)	0.46 cm/min (27.71 cm/h)	0.11cm/min (6.34cm/h)	0.003cm/min (.196cm/h)
	22-81 min	82-107min	107-1080min
Column 3 (Breakthrough at 22min)	0.58 cm/min (34.57 cm/h)	0.12 cm/min (7.5 cm/h)	0.004cm/min (.227cm/h)
	21-81 min	82-107min	107-1080min
Column 4 (Breakthrough at 22min)	0.58 cm/min (34.35 cm/h)	0.15 cm/min (8.92 cm/h)	.004 cm/min (.217 cm/h)
	24-81min	82-107min	107-1080min
Column 5 (Breakthrough at 24min)	0.56 cm/min (33.73 cm/h)	0.19 cm/min (11.31 cm/h)	.004 cm/min (.228cm/h)

D5. Blank Samples Results for Heavy Metals for Experimental Sets 2 and 3

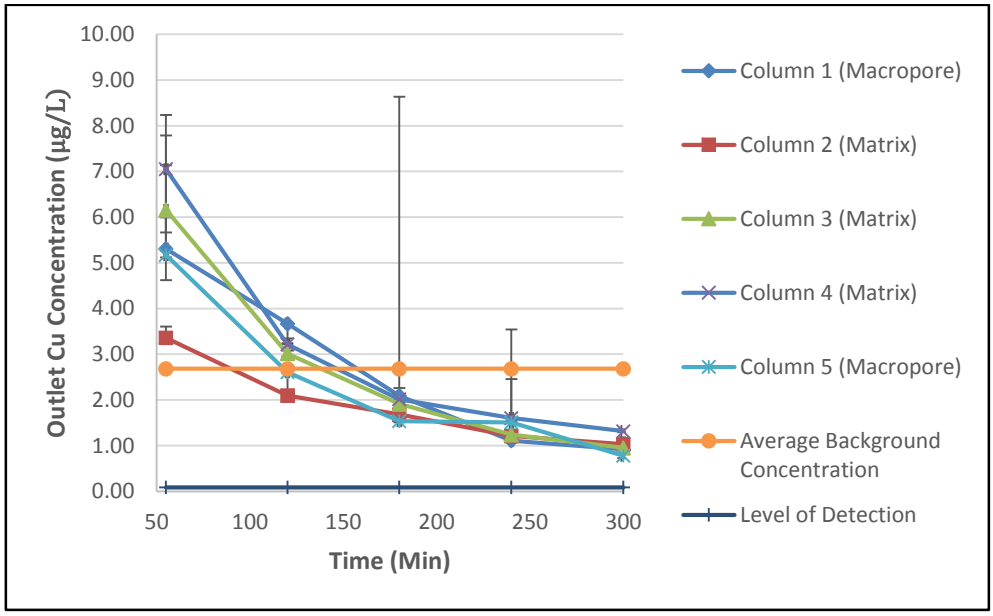

Figure D.14 Blank Cu Outlet Concentration for Experimental Set 2

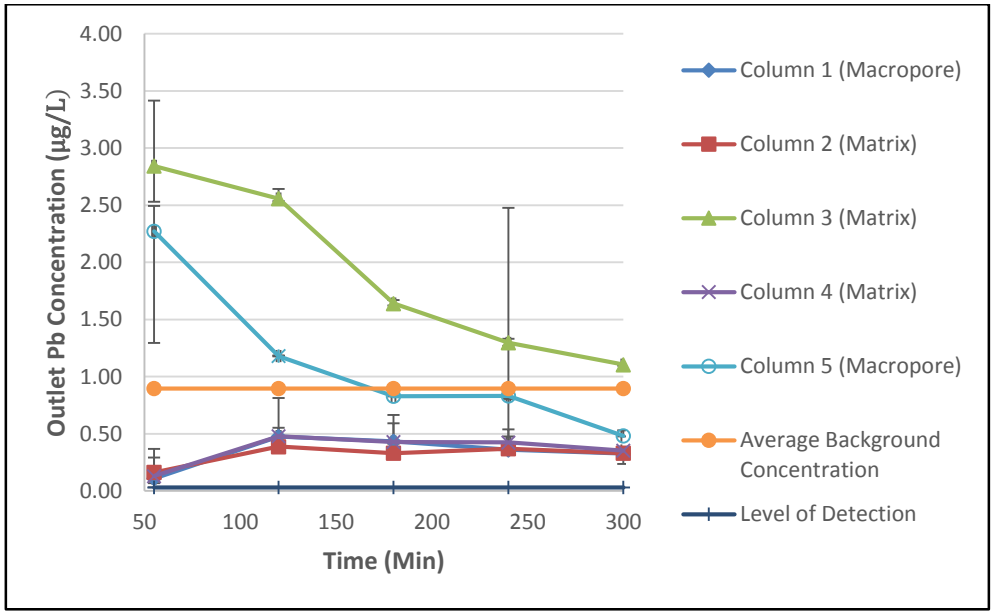

Figure D.15 Blank Pb Outlet Concentration for Experimental Set 2

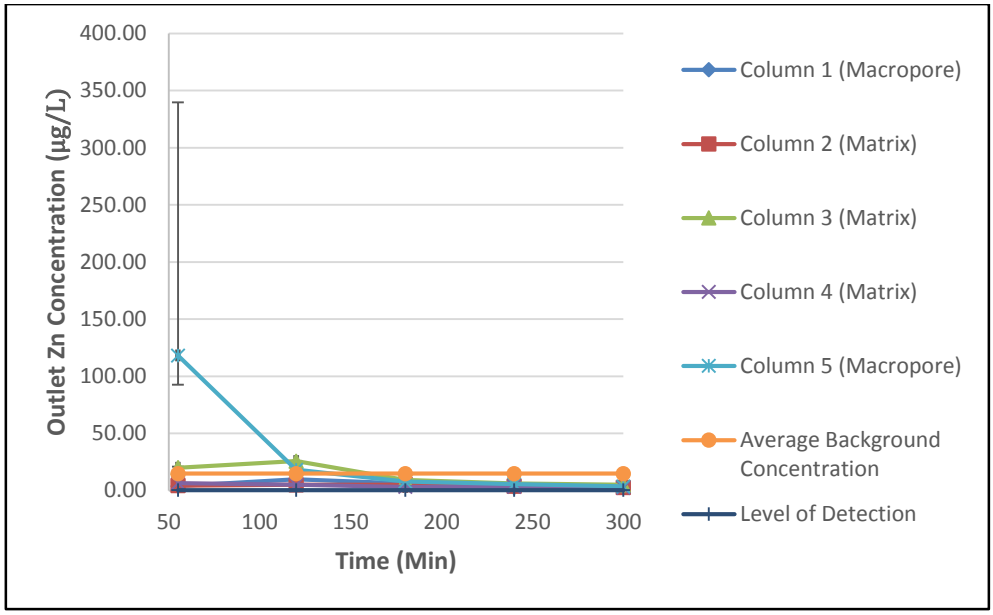

Figure D.16 Blank Zn Outlet Concentration for Experimental Set 2 with Outliers

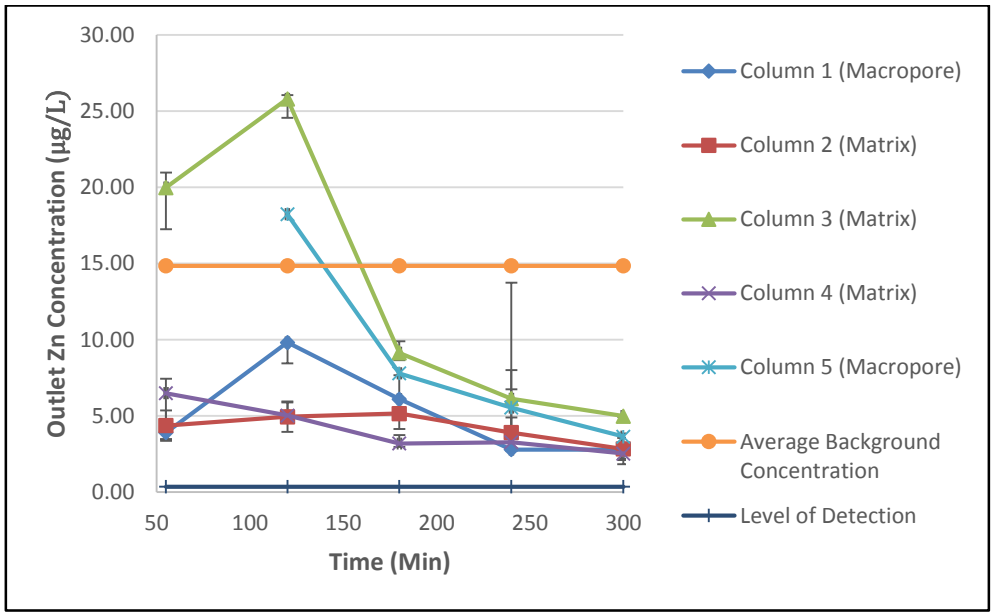

Figure D.17 Blank Zn Outlet Concentration for Experimental Set 2 without Outliers

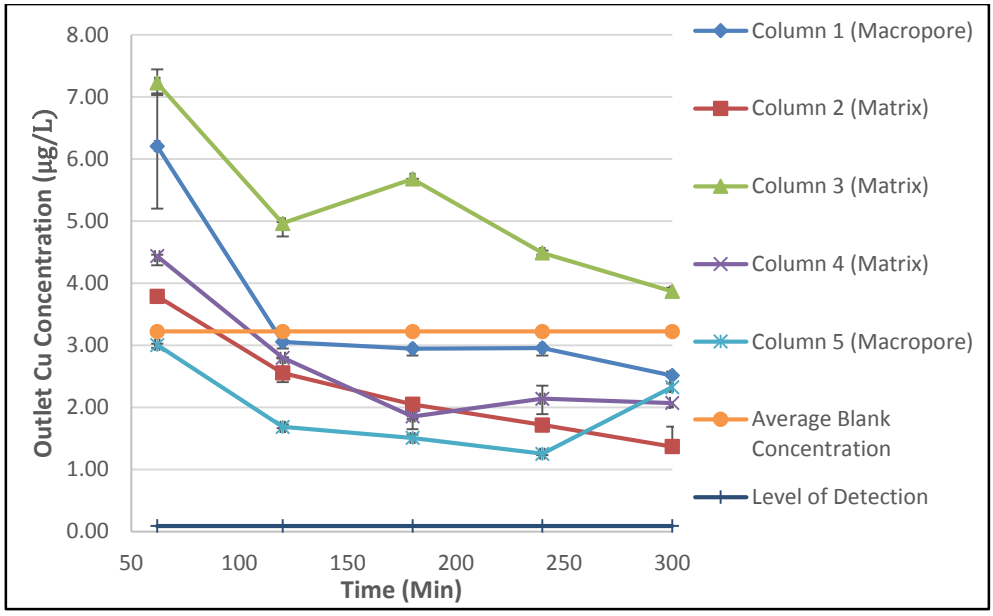

Figure D.18 Blank Cu Outlet Concentration for Experimental Set 3

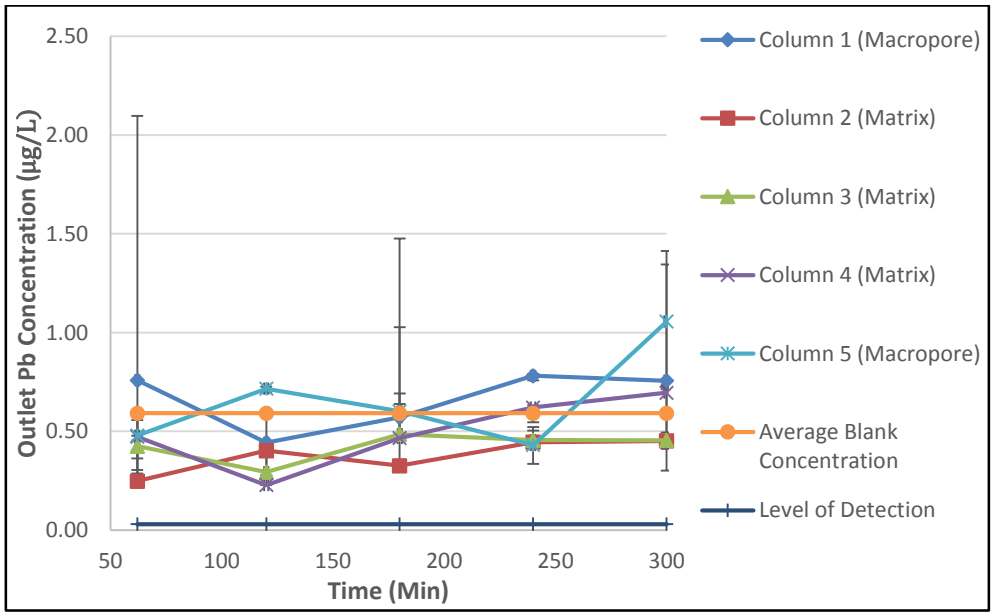

Figure D.19 Blank Pb Outlet Concentration for Experimental Set 3

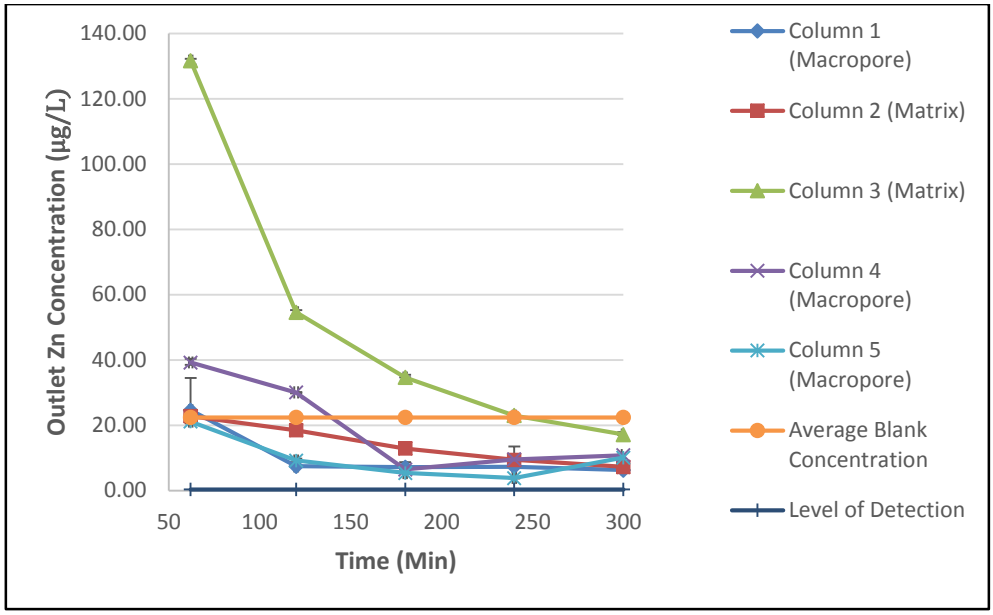

Figure D.20 Blank Zn Outlet Concentration for Experimental Set 3

D6. First Flush Experimental Results

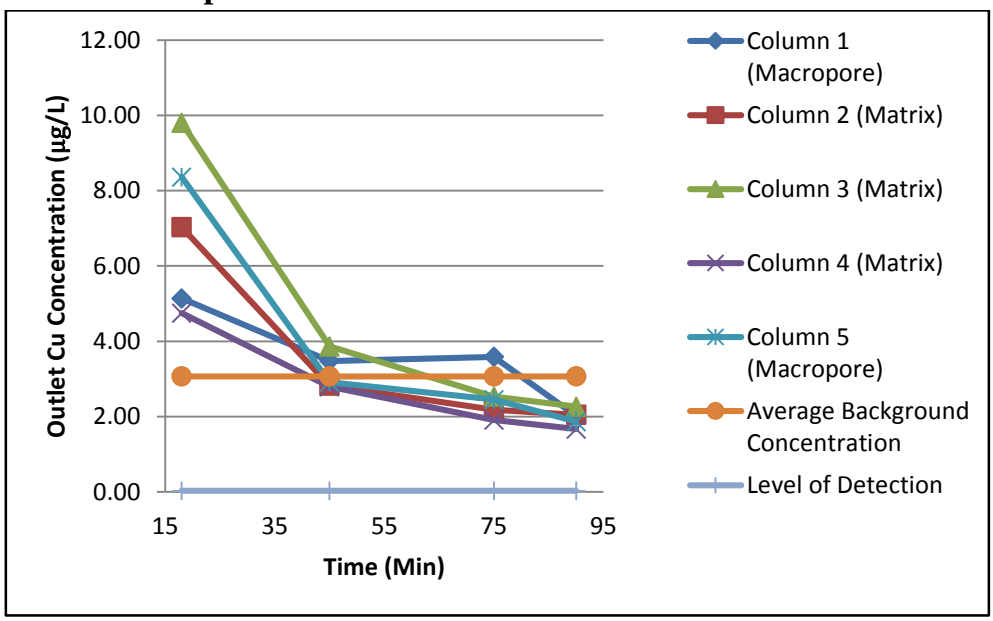

Figure D.21 First Flush Cu Outflow Concentration for Experimental Set 1

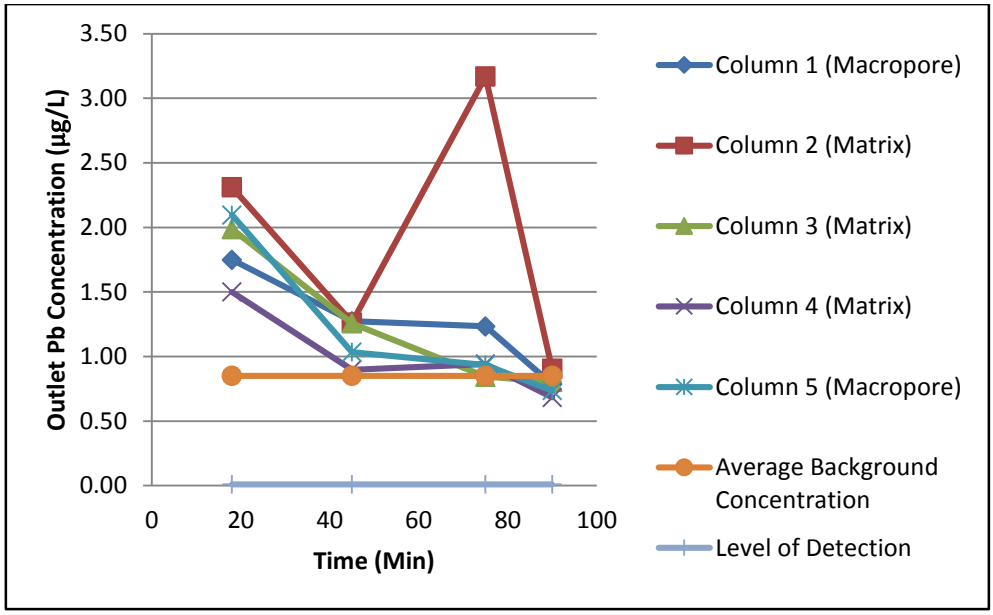

Figure D.22 First Flush Pb Outflow Concentration for Experimental Set 1

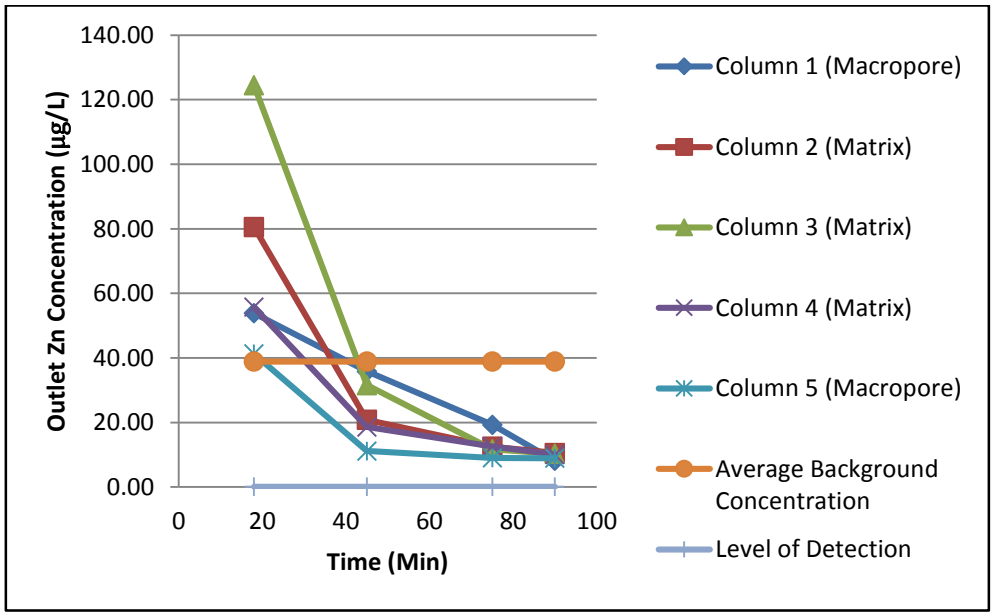

Figure D.23 First Flush Zn Outflow Concentration for Experimental Set 1

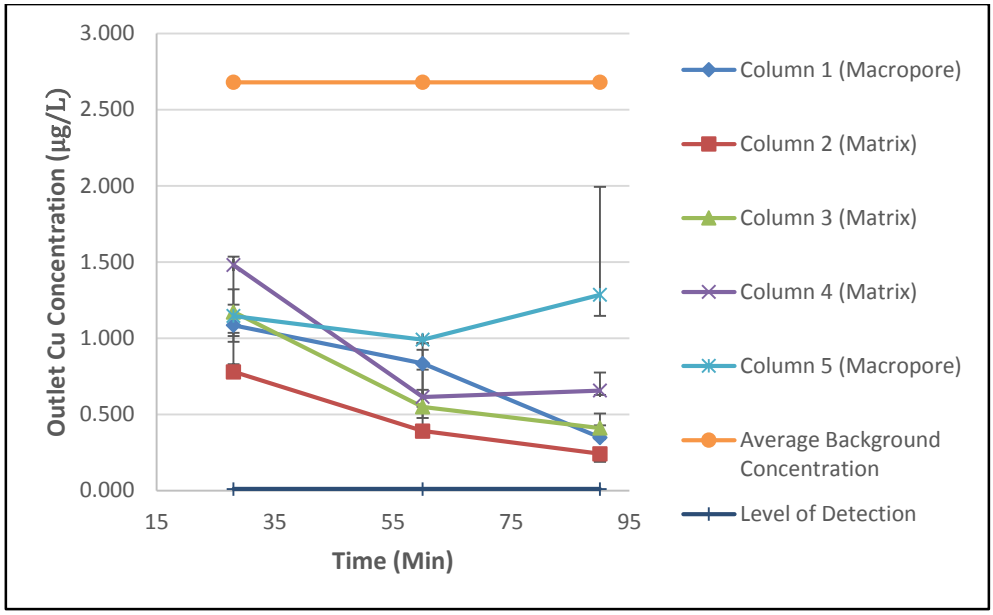

Figure D.24 First Flush Cu Outflow Concentration for Experimental Set 2

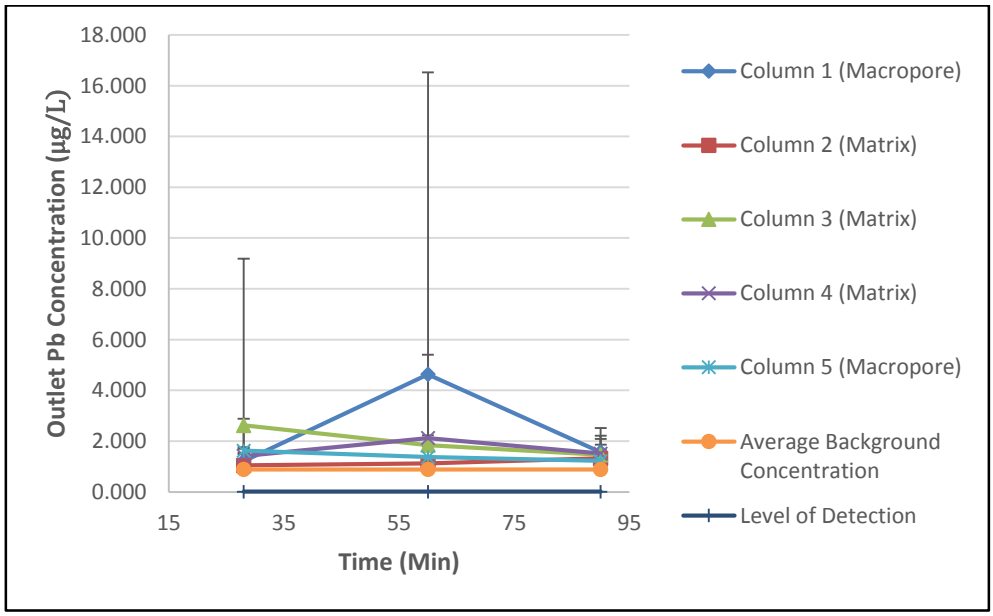

Figure D.25 First Flush Pb Outflow Concentration for Experimental Set 2

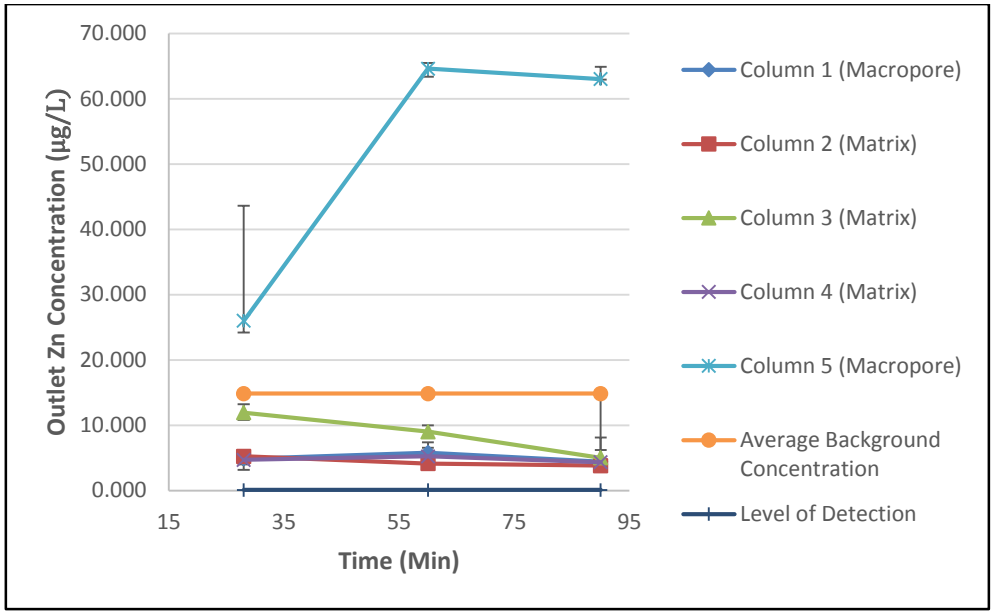

Figure D.26 First Flush Zn Outflow Concentration for Experimental Set 2

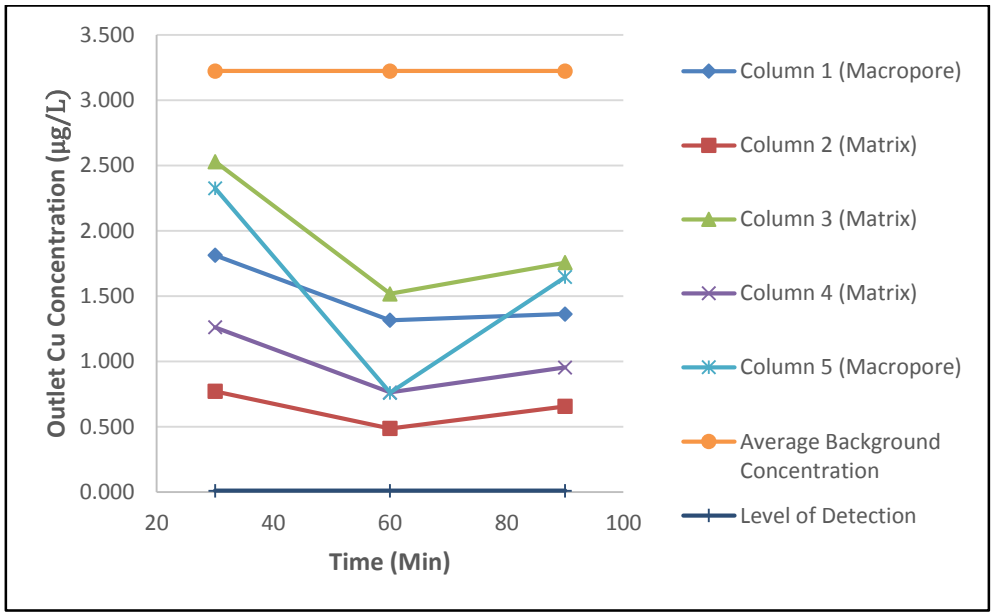

Figure D.27 First Flush Cu Outflow Concentration for Experimental Set 3

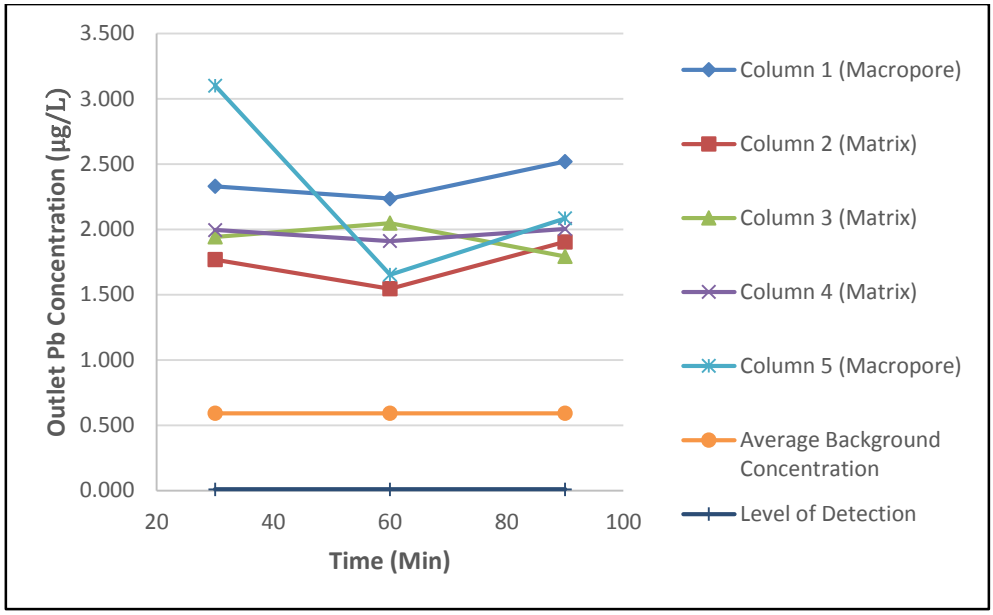

Figure D.28 First Flush Pb Outflow Concentration for Experimental Set 3

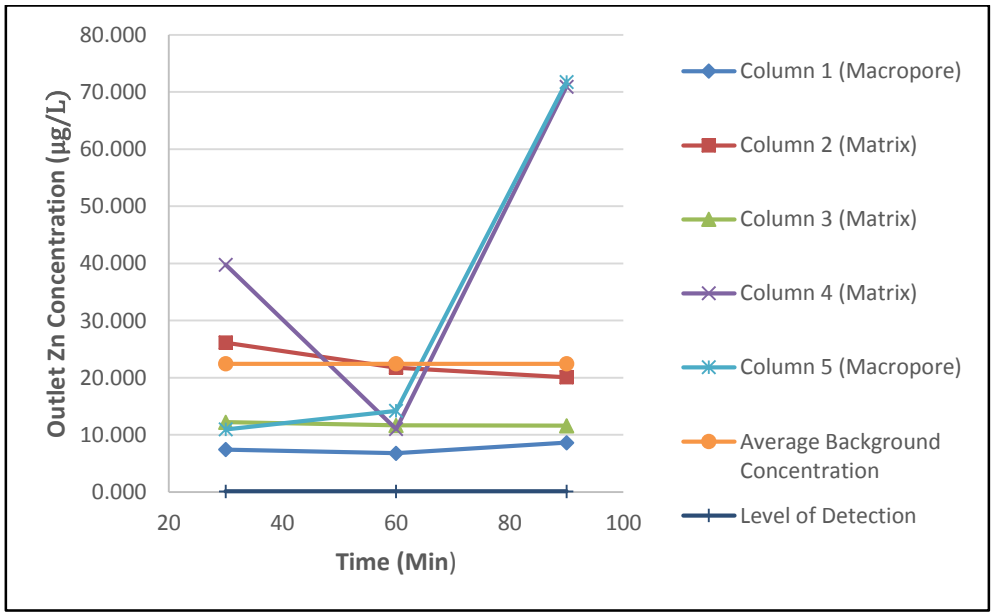

Figure D.29 First Flush Zn Outflow Concentration for Experimental Set 3

D7. Comparison of the Experimental Sets for Average Flow Runs

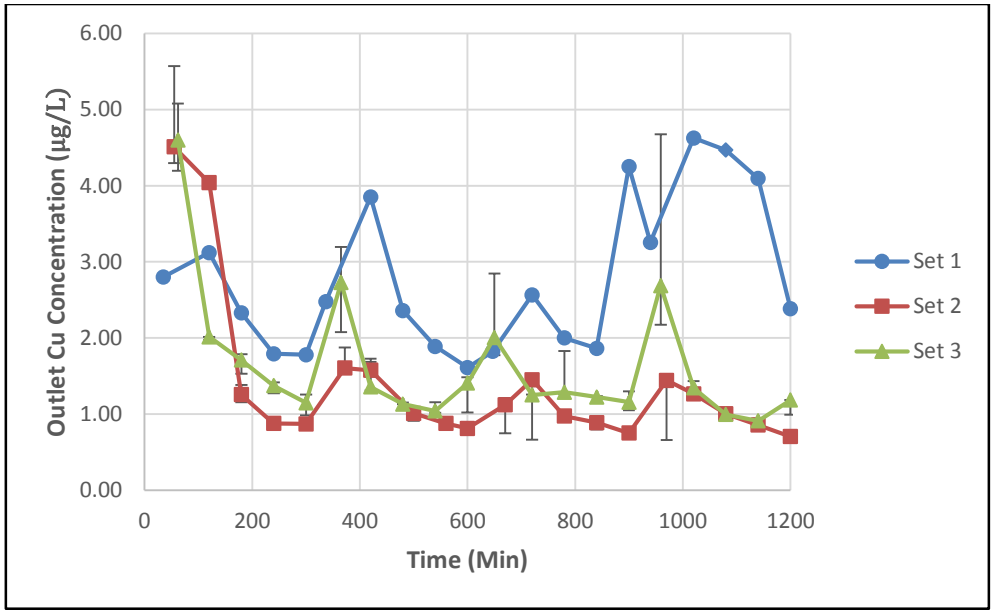

Figure D.30 Comparison of Outflow Cu Concentration in Column 1 for Different Experimental Sets for Average Flow Runs.

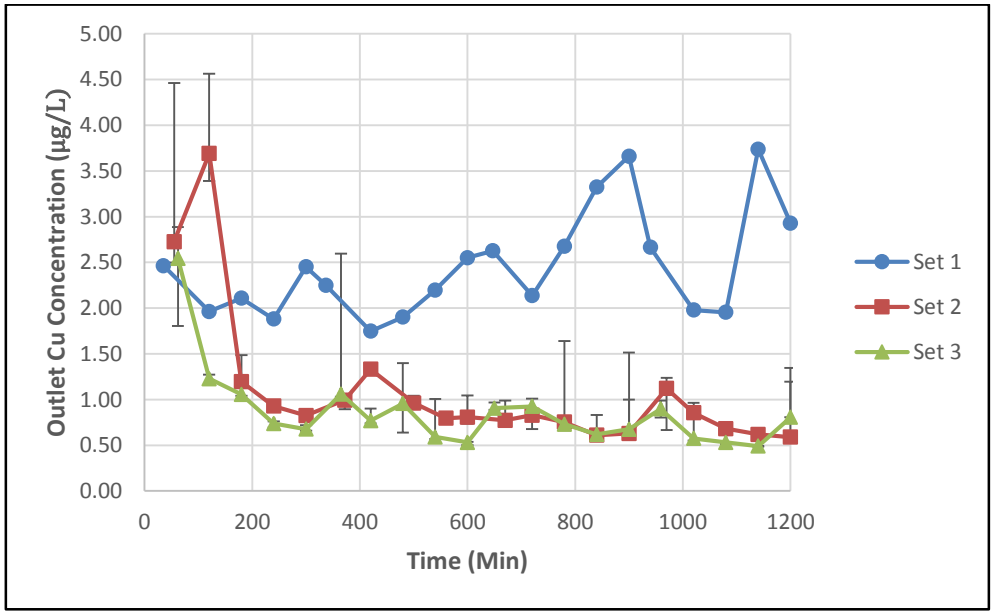

Figure D.31 Comparison of Outflow Cu Concentration in Column 2 for Different Experimental Sets for Average Flow Runs.

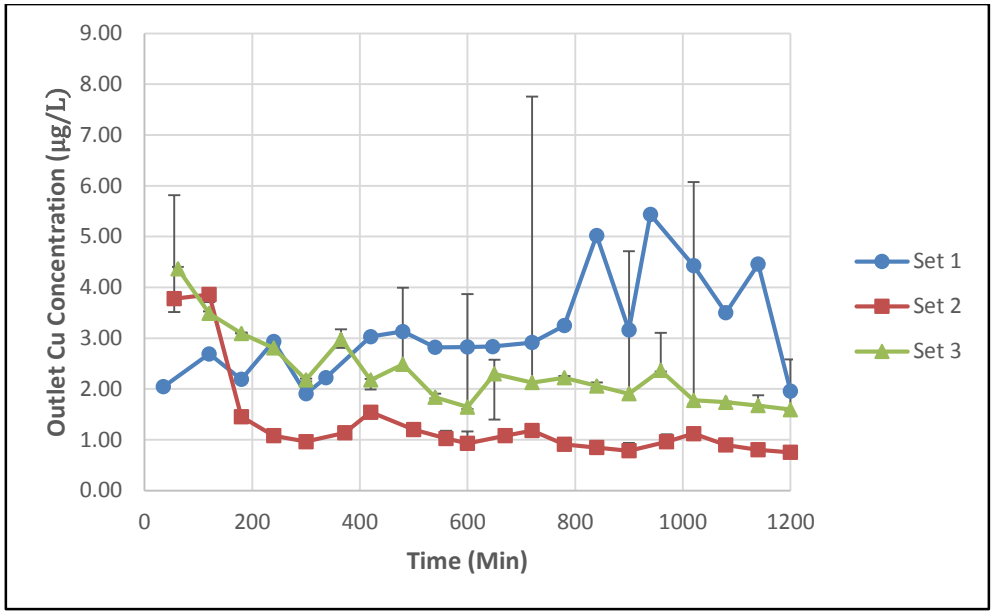

Figure D.32 Comparison of Outflow Cu Concentration in Column 3 for Different Experimental Sets for Average Flow Runs.

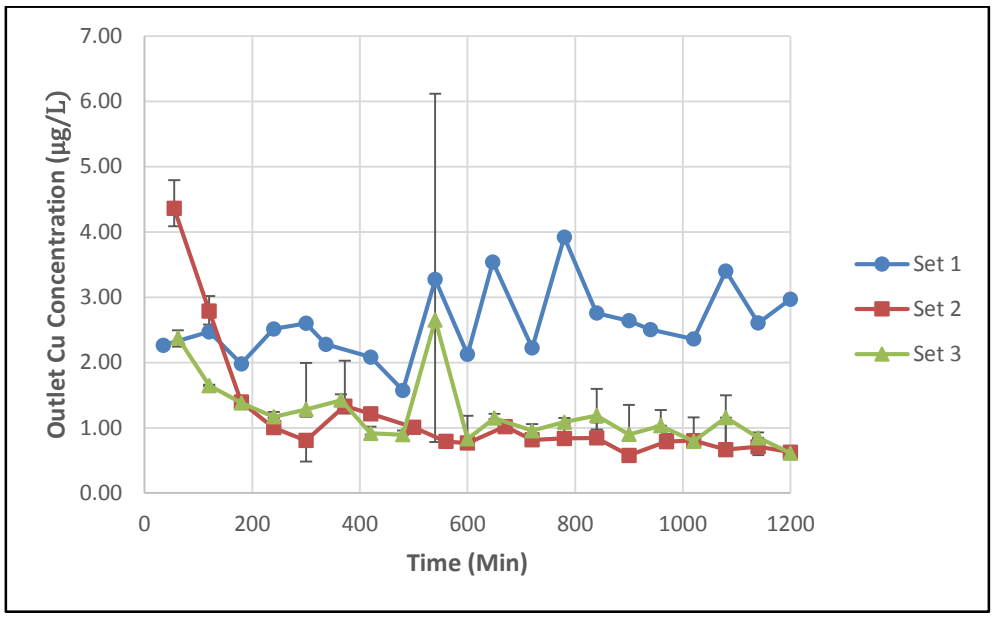

Figure D.33 Comparison of Outflow Cu Concentration in Column 4 for Different Experimental Sets for Average Flow Runs.

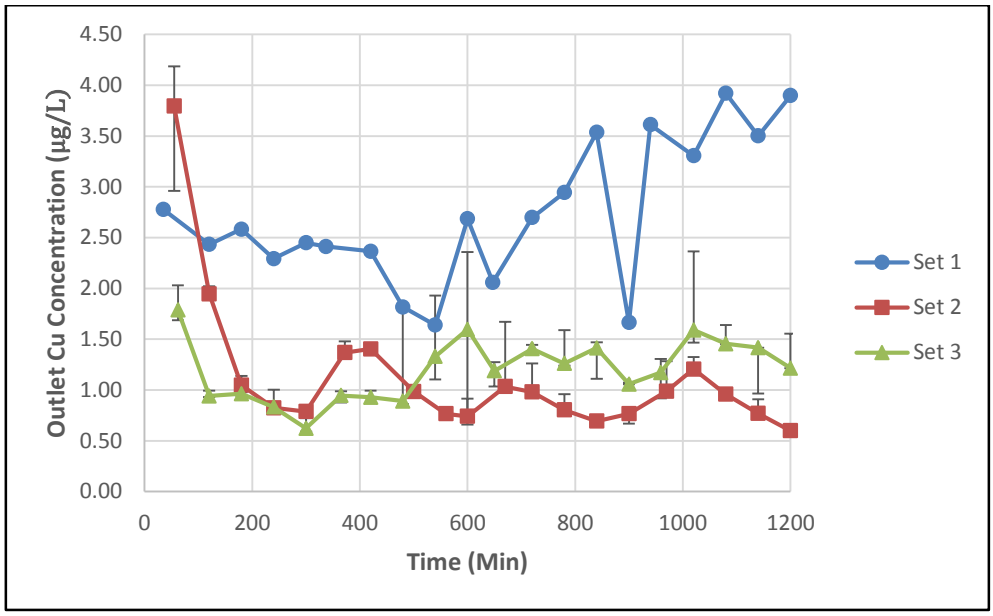

Figure D.34 Comparison of Outflow Cu Concentration in Column 5 for Different Experimental Sets for Average Flow Runs.

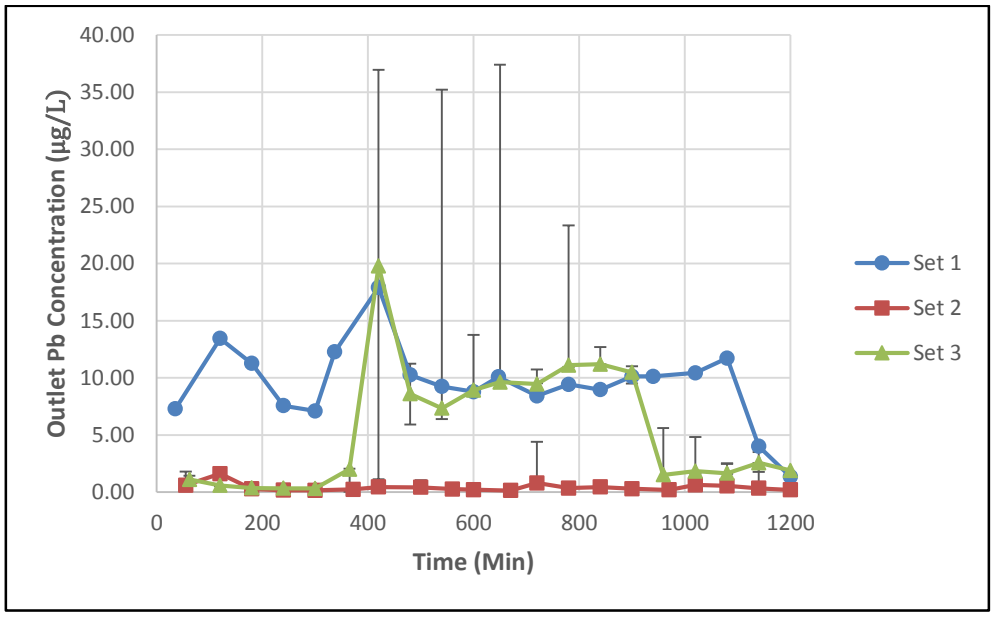

Figure D.35 Comparison of Outflow Pb Concentration in Column 1 for Different Experimental Sets for Average Flow Runs.

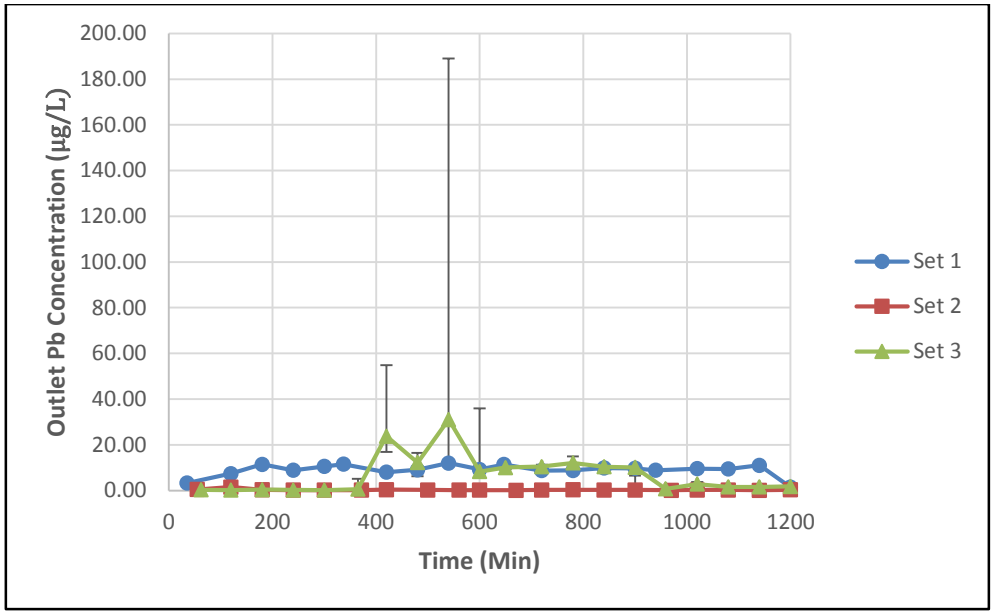

Figure D.36 Comparison of Outflow Pb Concentration in Column 2 for Different Experimental Sets for Average Flow Runs.

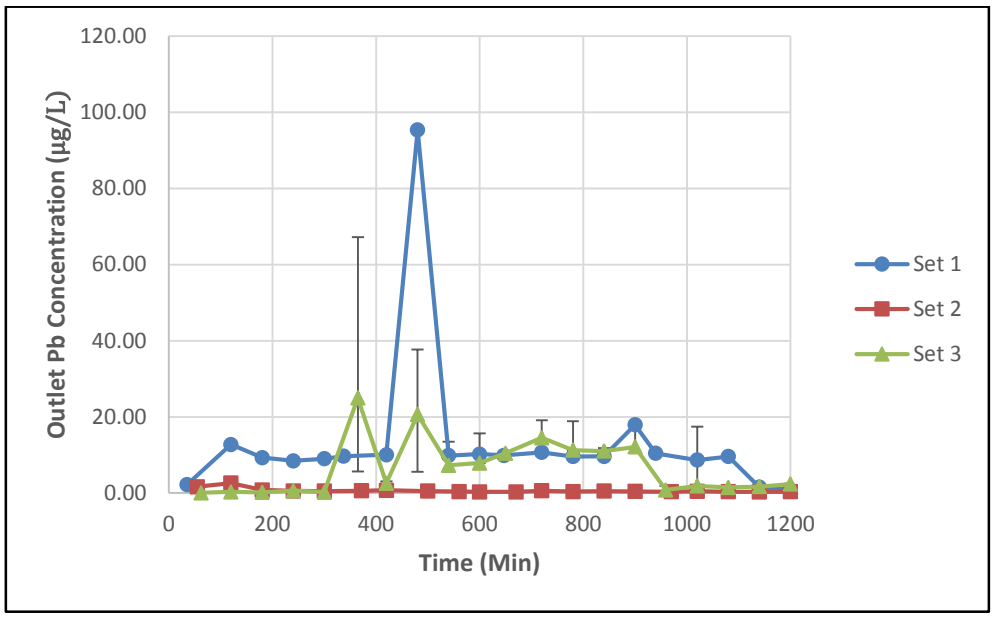

Figure D.36 Comparison of Outflow Pb Concentration in Column 3 for Different Experimental Sets for Average Flow Runs.

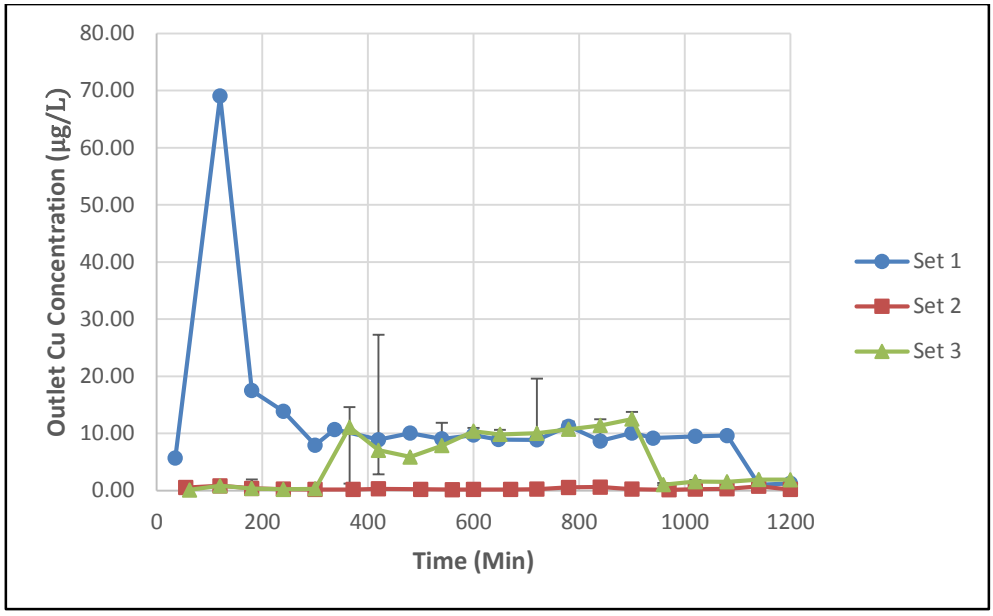

Figure D.37 Comparison of Outflow Pb Concentration in Column 4 for Different Experimental Sets for Average Flow Runs.

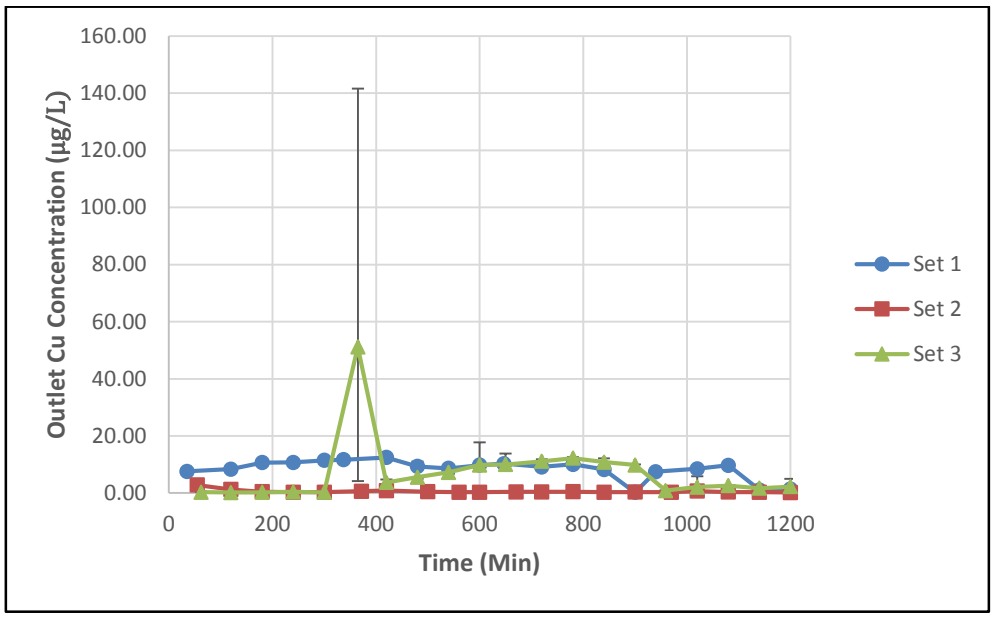

Figure D.38 Comparison of Outflow Pb Concentration in Column 5 for Different Experimental Sets for Average Flow Runs.

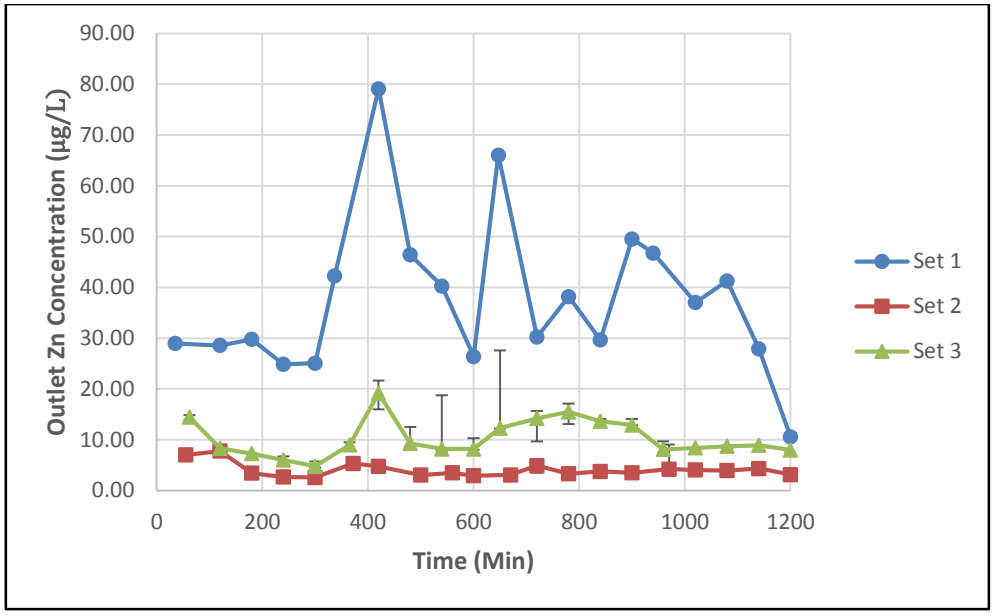

Figure D.39 Comparison of Outflow Zn Concentration in Column 1 for Different Experimental Sets for Average Flow Runs.

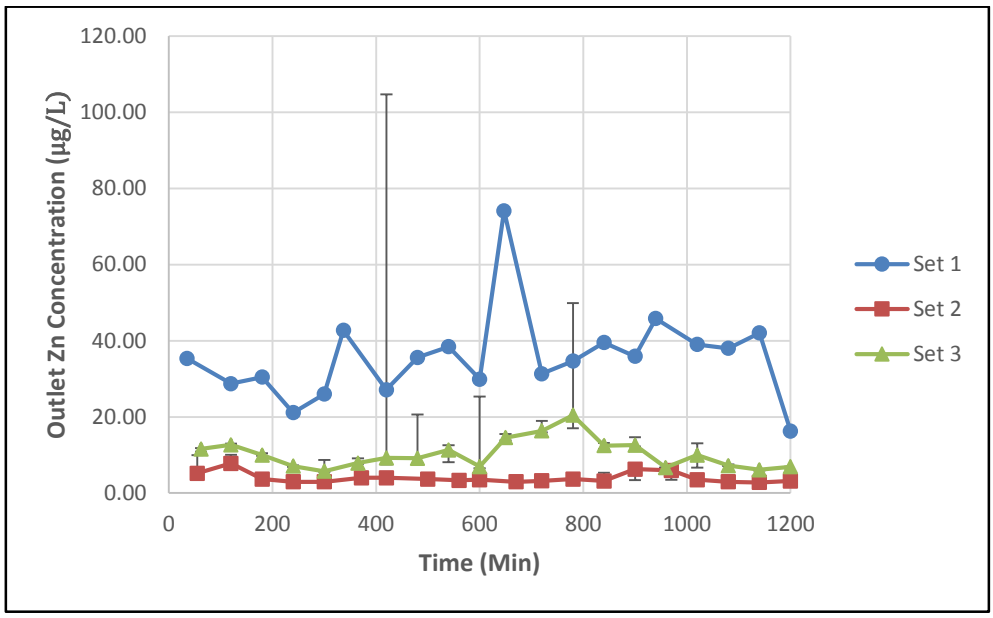

Figure D.40 Comparison of Outflow Zn Concentration in Column 2 for Different Experimental Sets for Average Flow Runs.

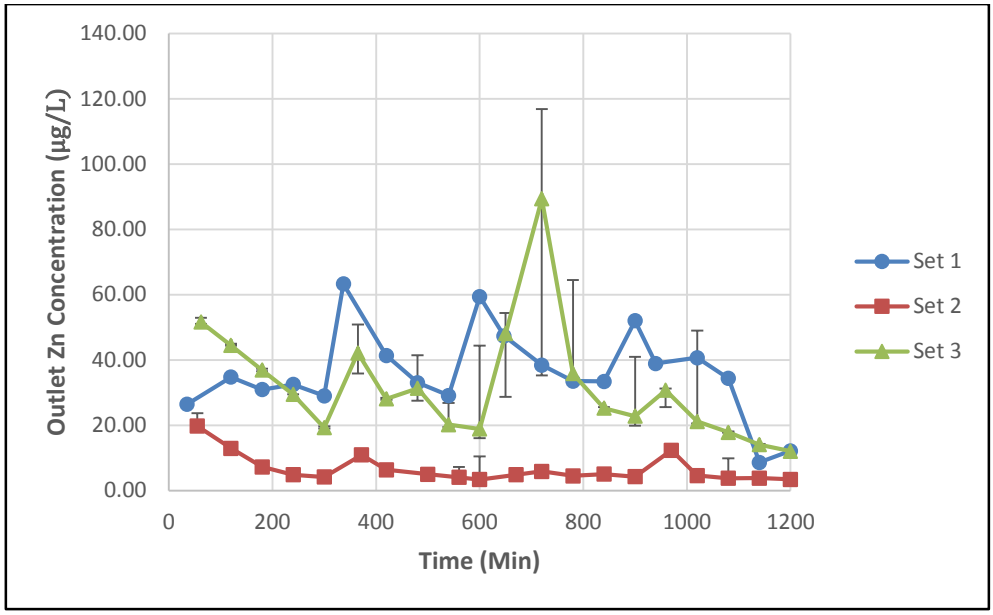

Figure D.41 Comparison of Outflow Zn Concentration in Column 3 for Different Experimental Sets for Average Flow Runs.

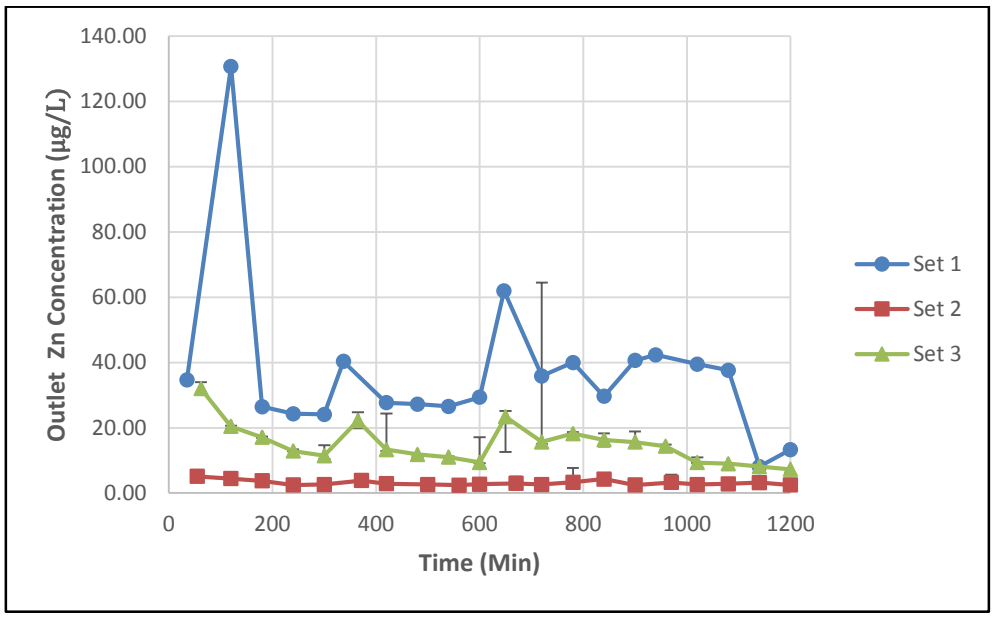

Figure D.42 Comparison of Outflow Zn Concentration in Column 4 for Different Experimental Sets for Average Flow Runs.

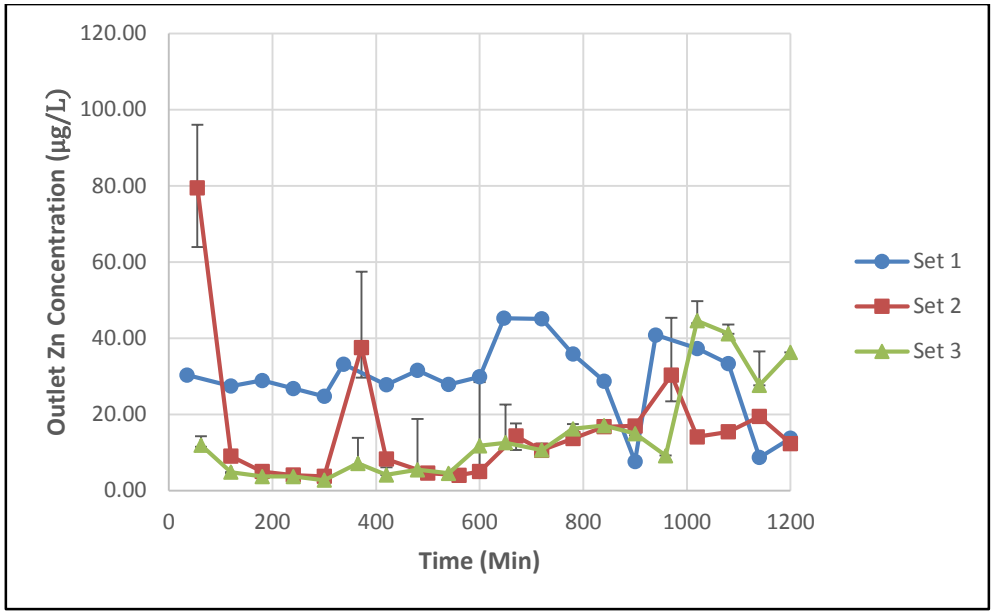

Figure D.42 Comparison of Outflow Zn Concentration in Column 4 for Different Experimental Sets for Average Flow Runs.

D8. Comparison of the Experimental Sets for First Flush Runs

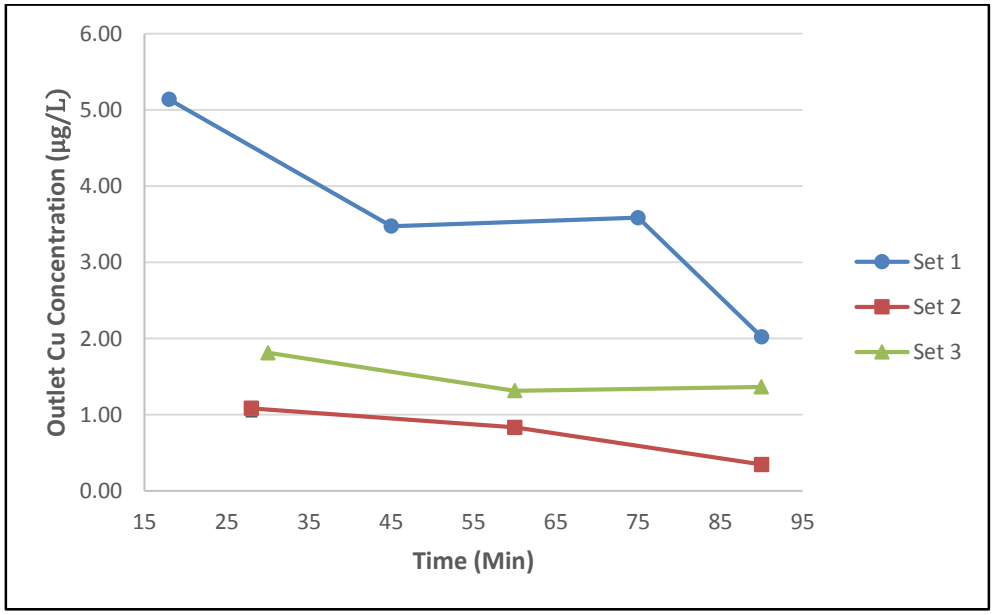

Figure D.43 Comparison of Outflow Cu Concentration in Column 1 for Different Experimental Sets for First Flush Run.

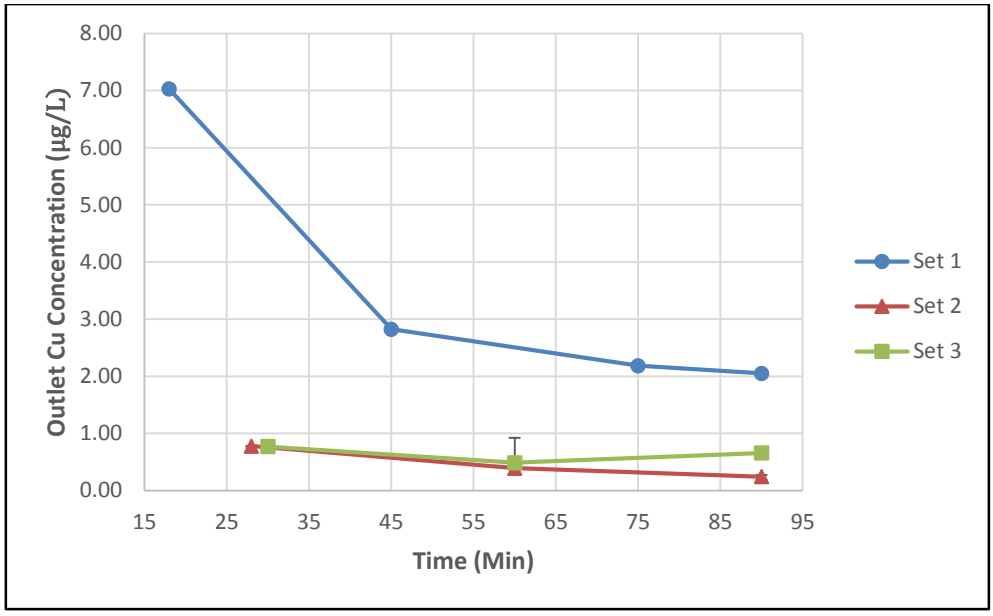

Figure D.44 Comparison of Outflow Cu Concentration in Column 2 for Different Experimental Sets for First Flush Run.

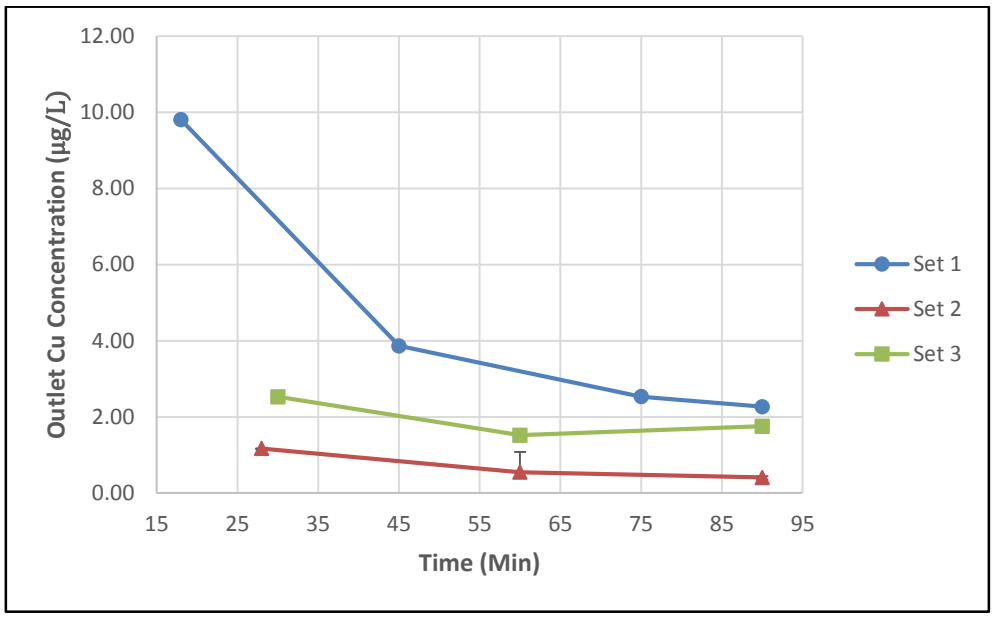

Figure D.45 Comparison of Outflow Cu Concentration in Column 3 for Different Experimental Sets for First Flush Run.

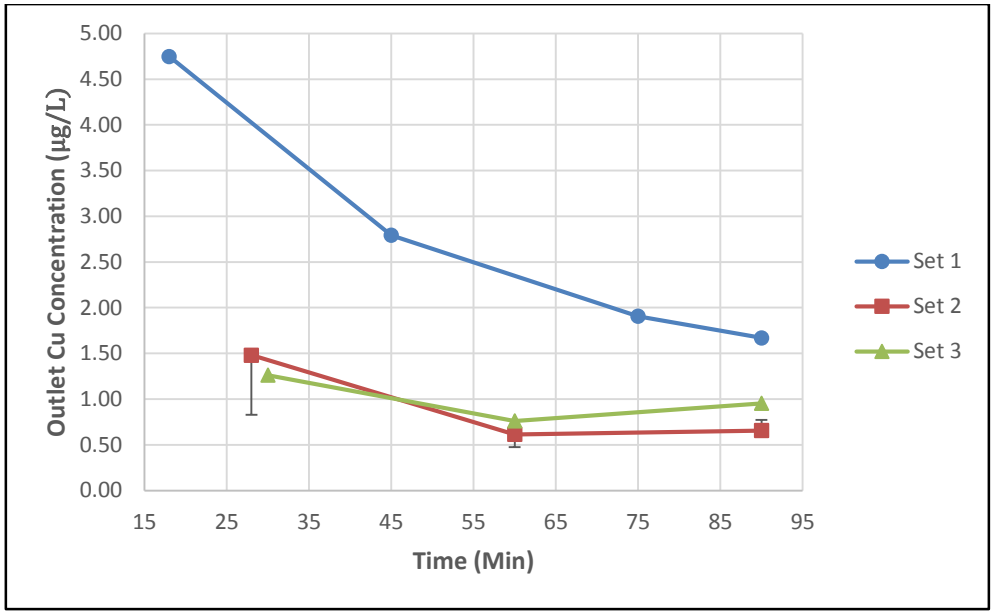

Figure D.46 Comparison of Outflow Cu Concentration in Column 4 for Different Experimental Sets for First Flush Run.

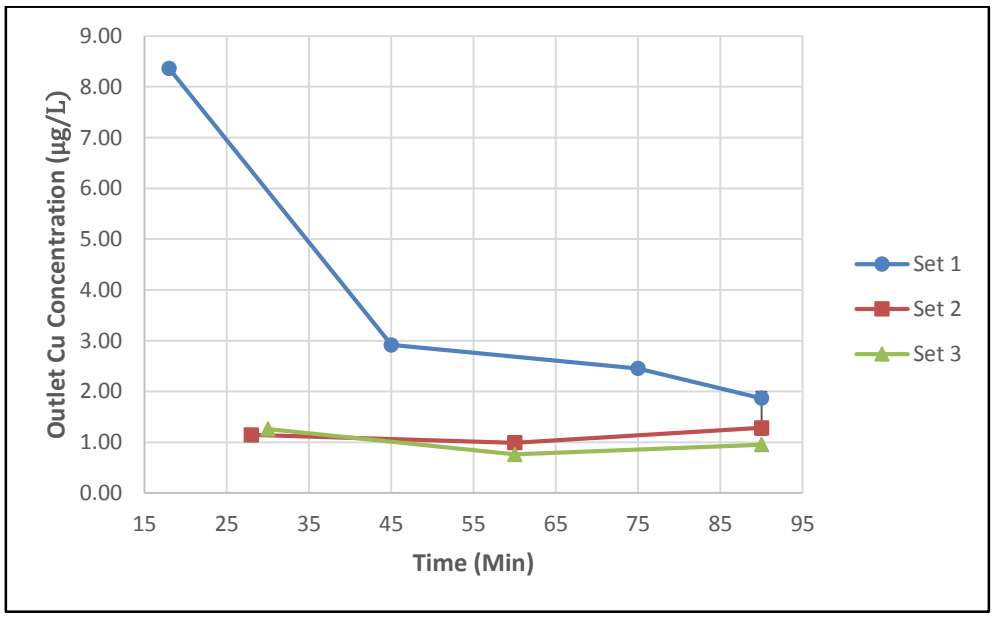

Figure D.47 Comparison of Outflow Cu Concentration in Column 5 for Different Experimental Sets for First Flush Run.

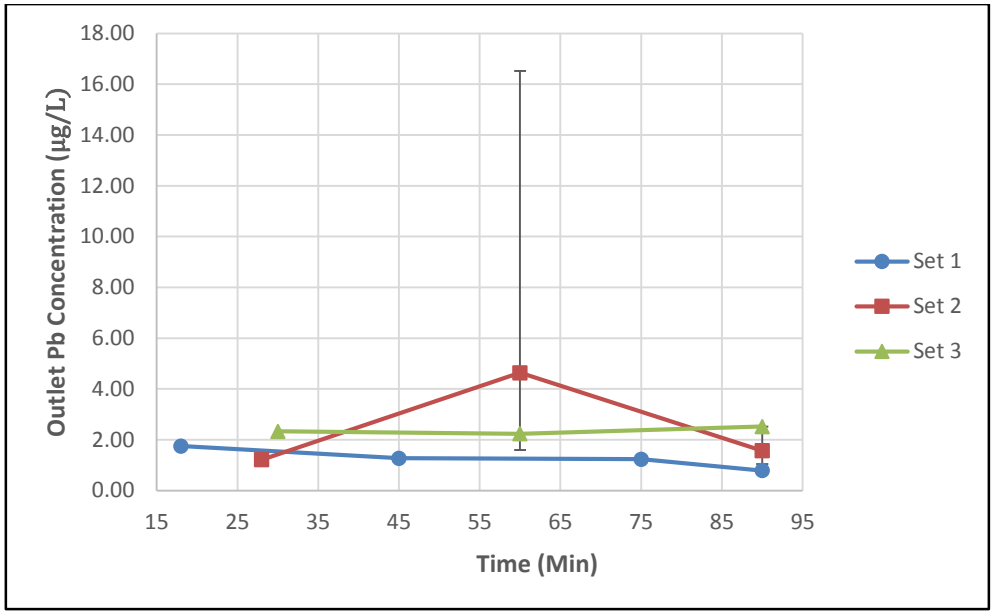

Figure D.48 Comparison of Outflow Pb Concentration in Column 1 for Different Experimental Sets for First Flush Run.

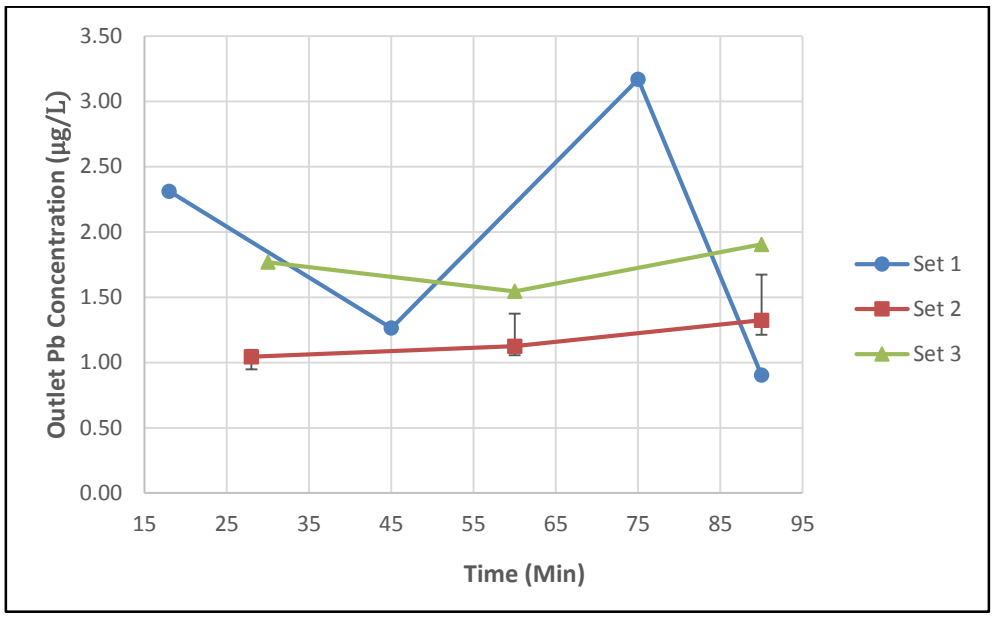

Figure D.49 Comparison of Outflow Pb Concentration in Column 2 for Different Experimental Sets for First Flush Run.

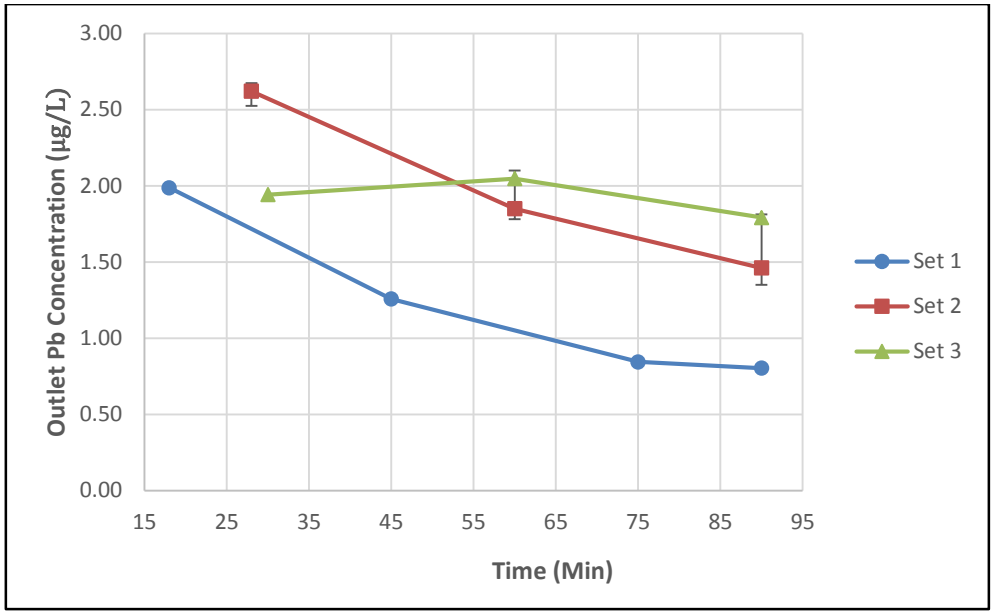

Figure D.50 Comparison of Outflow Pb Concentration in Column 3 for Different Experimental Sets for First Flush Run.

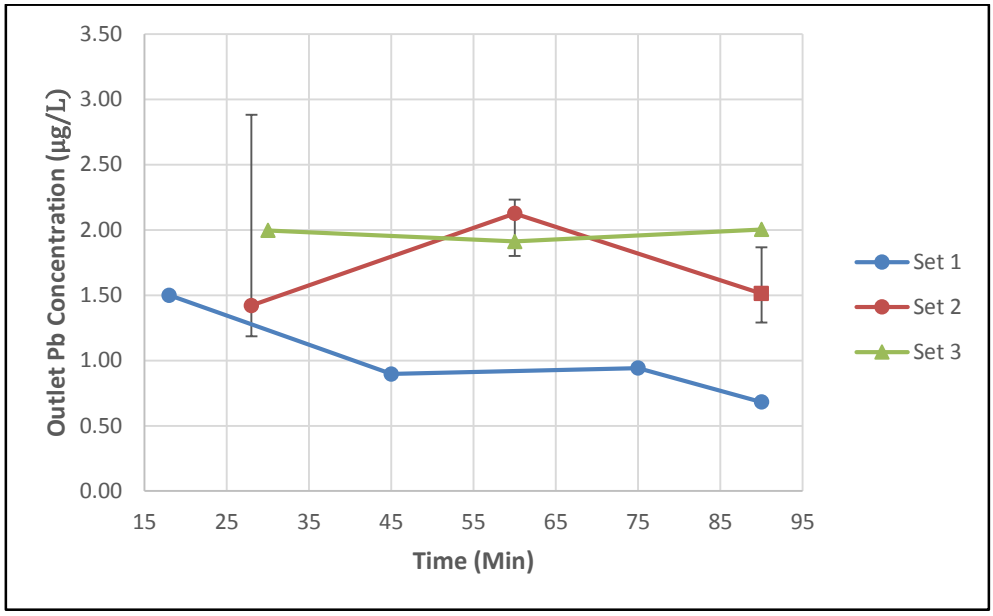

Figure D.51 Comparison of Outflow Pb Concentration in Column 4 for Different Experimental Sets for First Flush Run.

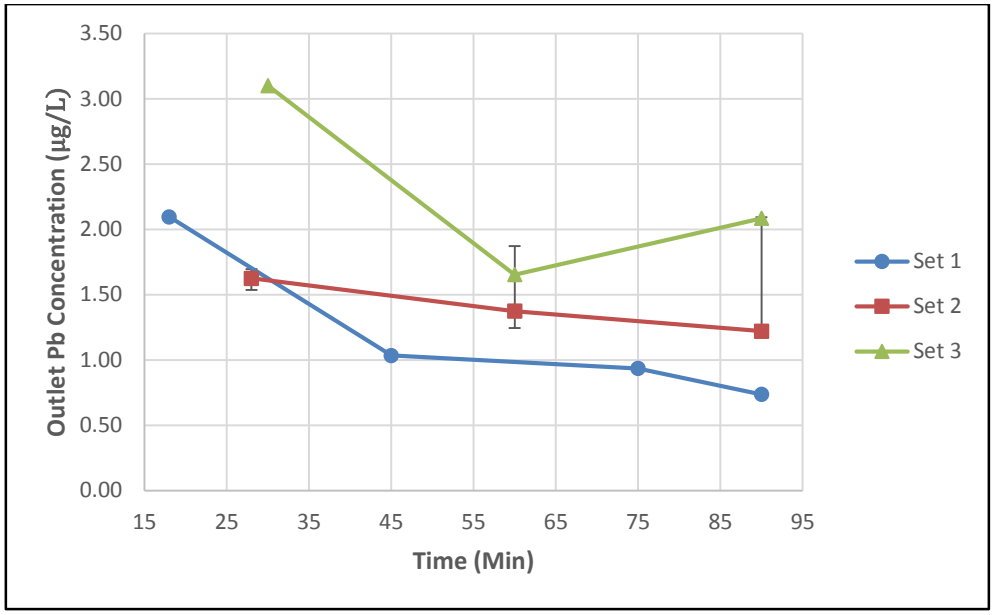

Figure D.52 Comparison of Outflow Pb Concentration in Column 5 for Different Experimental Sets for First Flush Run.

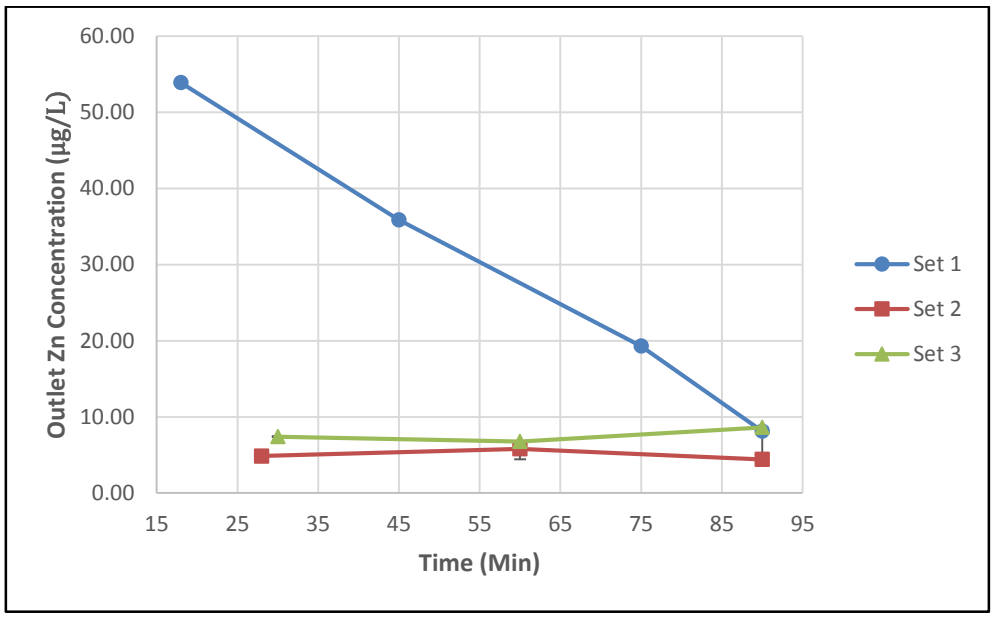

Figure D.53 Comparison of Outflow Zn Concentration in Column 1 for Different Experimental Sets for First Flush Run.

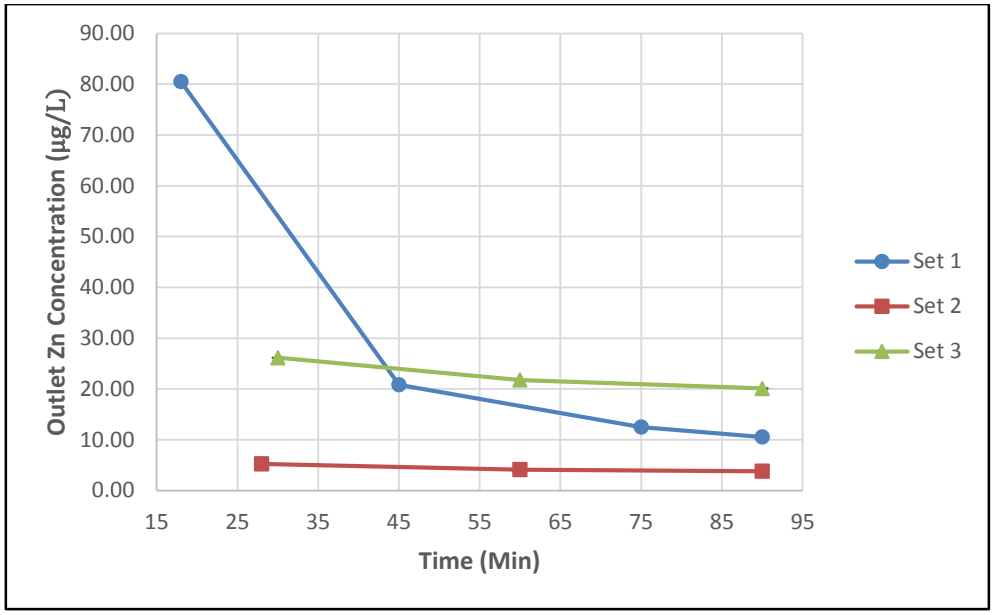

Figure D.54 Comparison of Outflow Zn Concentration in Column 2 for Different Experimental Sets for First Flush Run.

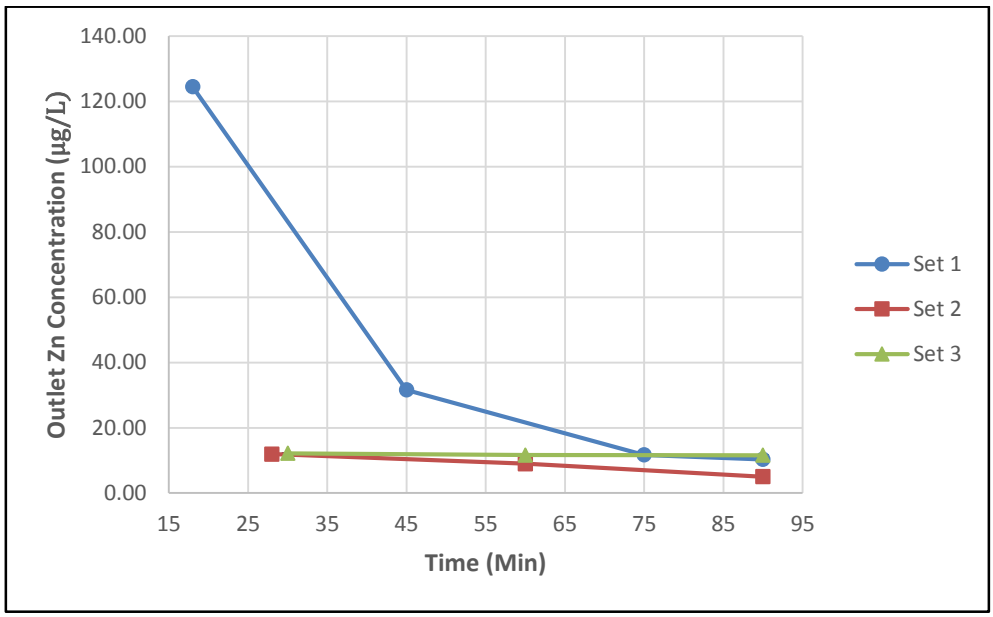

Figure D.55 Comparison of Outflow Zn Concentration in Column 3 for Different Experimental Sets for First Flush Run.

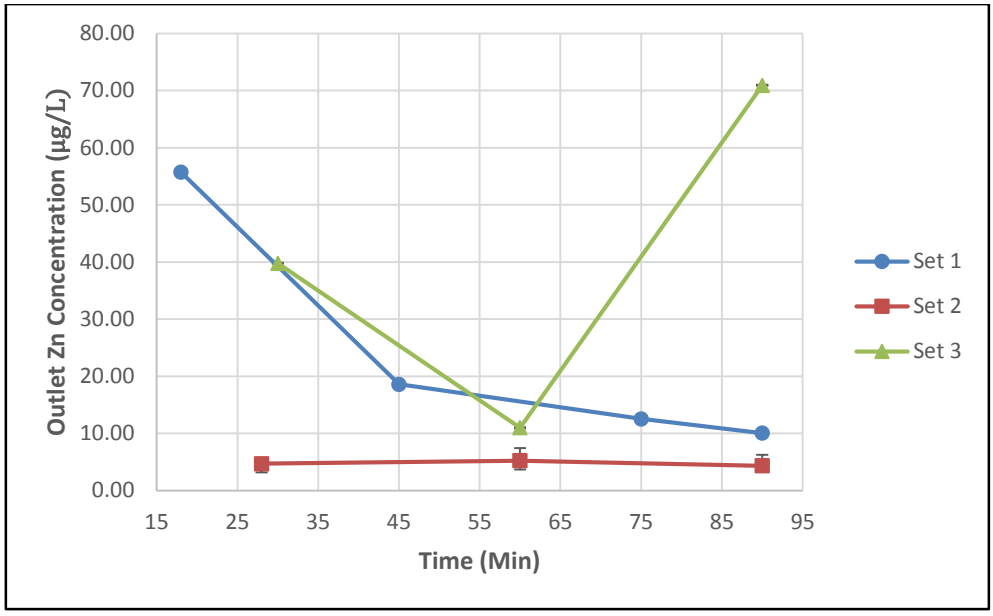

Figure D.56 Comparison of Outflow Zn Concentration in Column 4 for Different Experimental Sets for First Flush Run.

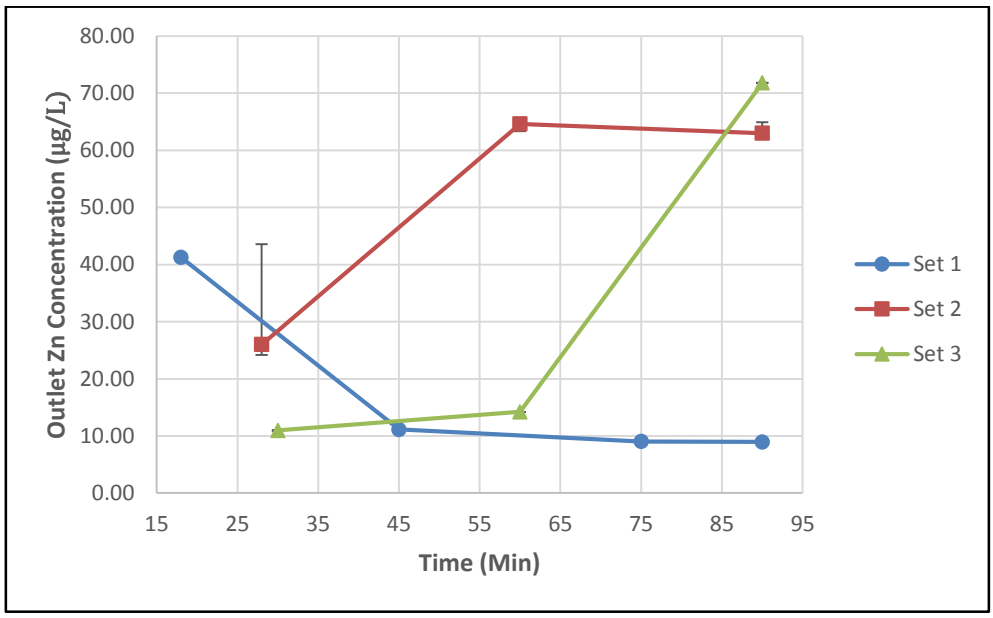

Figure D.56 Comparison of Outflow Zn Concentration in Column 5 for Different Experimental Sets for First Flush Run.

D9. Van Genuchten Parameters

Column 1 (Soil/Sand 10cm)

Table D.4 Van Genuchten Parameters for Column 1 (Soil/Sand 15 cm)

Van Genuchtens Parameters	
θ_{sat} (m^3/m^3)	0.452
θ_{res} (m^3/m^3)	0.05185
Alpha	0.044
n	3.3166
m	0.698486

Column 1 (Soil/Sand 45cm)

Table D.5 Van Genuchten Parameters for Column 1 (Soil/Sand 55 cm)

Van Genuchtens Parameters	
θ_{sat} (m^3/m^3)	0.4799
θ_{res} (m^3/m^3)	0.048581
Alpha	0.050602
n	3.0298
m	0.669945

Column 2 (Soil/Sand 10cm)

Table D.6 Van Genuchten Parameters for Column 2 (Soil/Sand 15 cm)

Van Genuchtens Parameters	
θ_{sat} (m^3/m^3)	0.506
θ_{res} (m^3/m^3)	0.051815
Alpha	0.063814
n	2.6204
m	0.618379

Column 2 (Soil/Sand 45cm)

Table D.7 Van Genuchten Parameters for Column 2 (Soil/Sand 55 cm)

Van Genuchtens Parameters	
θ_{sat} (m^3/m^3)	0.47699
θ_{res} (m^3/m^3)	0.047652
Alpha	0.052005
n	2.9639
m	0.662607

Column 2 (Sand 75cm)

Table D.8 Van Genuchten Parameters for Column 2 (Sand 75cm)

Van Genuchtens Parameters	
θ_{sat} (m^3/m^3)	0.3055
θ_{res} (m^3/m^3)	0.011
Alpha	0.07
n	6.7
m	0.8507

Column 5 (Soil/Sand 10cm)

Table D.9 Van Genuchten Parameters for Column 5 (Soil/Sand 15 cm)

Van Genuchtens Parameters	
θ_{sat} (m^3/m^3)	0.482
θ_{res} (m^3/m^3)	0.047819
Alpha	0.055673
n	2.8943
m	0.654493

Column 5 (Soil/Sand 45cm)

Table D.10 Van Genuchten Parameters for Column 5 (Soil/Sand 55 cm)

Van Genuchtens Parameters	
θ_{sat} (m^3/m^3)	0.452
θ_{res} (m^3/m^3)	0.051815
Alpha	0.044
n	3.3166
m	0.698486

Column 5 (Sand 75cm)

Table D.11 Van Genuchten Parameters for Column 5 (Sand 75 cm)

Van Genuchtens Parameters	
θ_{sat} (m^3/m^3)	0.34312
θ_{res} (m^3/m^3)	0.019755
Alpha	0.074234
n	6.691
m	0.85

E. PUBLICATIONS AND CONFERENCES

Quinn, R. and Dussaillant A. Predicting pollutant retention in SUDS, with a rain garden application. 2012. *BHS National Symposium*. 3-6 July. DOI: 0.7558/bhs.2012.ns45

Quinn, R. and Dussaillant A. Predicting heavy metal retention in Sustainable Urban Drainage Systems. 2012. *SUDSnet International Conference.* 4-5 September.

Quinn, R. and Dussaillant A. 2014. Heavy metal retention and bypass in Sustainable Drainage Systems: application to bioretention facilities. *Clean.* 42(2), pp.160-168.

Quinn, R. and Dussaillant, A. 2014. Predicting infiltration pollutant retention in bioretention sustainable drainage systems: model development and validation. *Hydrology Research*, 45 (6), pp. 855-867.